

Physiological and genetic dissection of rice tolerance to water-deficit stress



Niteen Narharirao Kadam

Propositions

1. Phenotypic plasticity of above and below ground organs is less synergistic to tolerate water-deficit in rice than in wheat.
(this thesis)
2. The development of a crop ideotype through QTL-based ecophysiological modeling is still in its infancy.
(this thesis)
3. The natural evolution of any stress tolerance mechanism is a random phenomenon and requires extensive scientific endeavors to detect and use in crop improvements.
4. Science should always be both theory and problem oriented.
5. Communication between plant breeders and ecophysiologicalists is complicated.
6. Maintaining a proper balance between professional work and personal life is extremely challenging in the sandwich PhD programme of Wageningen University & Research.
7. No matter how intelligent an early career researcher is, (s)he needs some mental support during the initial scientific journey.

Propositions belonging to the thesis, entitled

“Physiological and genetic dissection of rice tolerance to water-deficit stress”

Niteen Narharirao Kadam

Wageningen, 20th February 2018

**Physiological and genetic dissection of rice
tolerance to water-deficit stress**

Niteen Narharirao Kadam

Thesis committee

Promotor

Prof. Dr Paul C. Struik
Professor of Crop Physiology
Wageningen University & Research

Co-promotors

Dr Xinyou Yin
Senior Scientist, Centre for Crop Systems Analysis
Wageningen University & Research

Dr Krishna S.V. Jagadish
Associate Professor, Department of Agronomy
Kansas State University, Manhattan, Kansas, USA

Other members

Prof. Dr L.F.M. Marcelis, Wageningen University and Research
Prof. Dr H. Stützel, Leibniz University of Hannover, Germany
Prof. Dr C.S. Testerink, Wageningen University and Research
Prof. Dr E. Jacobsen, Wageningen University and Research

This research was conducted under the auspices of the C.T. de Wit Graduate School for Production Ecology and Resource Conservation (PE & RC).

Physiological and genetic dissection of rice tolerance to water-deficit stress

Niteen Narharirao Kadam

Thesis

submitted in fulfilment of the requirements for the degree of doctor
at Wageningen University
by the authority of the rector Magnificus,
Prof. Dr A.P.J. Mol,
in the presence of the
Thesis Committee appointed by the Academic Board
to be defended in public
on Tuesday 20 February 2018
at 1.30 p.m. in the Aula.

Niteen Narharirao Kadam

Physiological and genetic dissection of rice tolerance to water-deficit stress, 242 pages.

PhD thesis, Wageningen University, Wageningen, the Netherlands (2018)

With references, with summary in English

ISBN: 978-94-6343-740-0

DOI: 10.18174/431721

Abstract

Niteen N. Kadam (2018) “*Physiological and genetic dissection of rice tolerance to water-deficit stress*”. PhD thesis, Wageningen University & Research, Wageningen, The Netherlands. 242 pp.

Rice (*Oryza sativa* L.) is the world's most important staple food crop, especially in Asia. As a semi-aquatic crop species, water-scarcity and increasing severity of water-deficit stress owing to climate change, are a major threat to sustaining irrigated rice production. Improving the rice adaptation to water-deficit is, therefore, a primary breeding target. The main goal of this dissertation is to study the morphological, anatomical, physiological and genetic basis for responses of a rice plant to water-deficit stress.

To give leads into how water-deficit tolerant rice should behave, a comparative study was conducted, whereby representative rice genotypes was compared at the same moisture stress during the vegetative stage with genotypes of wheat, a dryland cereal wheat (*Triticum aestivum* L.) known to be more tolerant to water-deficit than rice. Under-water-deficit, rice genotypes (IR64 & Apo) developed thinner roots allowing rapid water-acquisition, whereas wheat followed a water-conserving strategy through developing thicker leaves and roots, and moderate tillering. Root anatomy such as root diameter, xylem and stele diameter and xylem number were more plastic in wheat than in rice under-water-deficit.

The methodology and findings from those representative genotypes were then projected to a diverse panel of nearly 300 rice genotypes. Such a panel was previously constructed by the International Rice Research Institute as a potential means of discovery of novel beneficial alleles for diverse phenotypic traits and their plasticity, with 46K high-quality single nucleotide polymorphisms (SNPs). A genome-wide association study (GWAS) was undertaken to identify the genomic regions regulating the morphological, physiological and root anatomical traits in rice, based on a large-scale greenhouse phenotyping of these traits. The genetic basis of these traits was different in control and water-deficit stress (strong quantitative trait loci [QTL] × environment interaction), in line with novel loci detected for the plasticity of traits. Key *a priori* candidate genes near to these genetic loci were also identified.

Rice grain yield is strongly affected by water-deficit stress coinciding with sensitive reproductive stage. Strong genotypic variability for grain yield as well as yield components and related traits were observed in the same rice *indica* diversity panel, under control and reproductive stage water-deficit stress in field conditions across two years. The GWAS analysis

identified the core loci of rice genome governing the grain yield and related traits. Most of the genomic loci were specific to treatment and year, indicating strong QTL \times environment interactions.

To enable GWAS findings to be used for better designing of genotypes by breeding, an existing process-based crop model GECROS was used in a case study, where grain yield of the same *indica* diversity panel (267 rice genotypes) from the control treatment in one season was dissected into eight physiological parameters. Some parameters had a stronger effect on grain yield than other parameters. Using these parameters, the model showed the ability to predict the genotypic variation of rice diversity panel for grain yield under different field conditions. Further, the GWAS analysis was extended to model-input parameters on randomly chosen 213 genotypes as a training dataset. The SNP-based estimates of parameter values calculated from the additive allelic effect of the loci were used as input to the crop model GECROS. Although the SNP-based modelling approach demonstrated the ability to predict the genotypic variation in training datasets under different environments, the prediction accuracy was lower in the remaining 54 genotypes used as a testing dataset. In addition, the prediction accuracy of grain yield was also lower using either parameter or SNP-based GECROS model in completely new season. However, the model-based sensitivity analysis effectively identified the different SNPs between control and water-deficit environments. Virtual ideotypes designed based on pyramiding the SNPs identified by modelling had a higher yield than those based on SNPs for yield *per se*.

Keywords: water-deficit stress, rice, wheat, root anatomy, root diameter, stele diameter, *Oryza sativa* L., *Triticum aestivum* L., eco-physiological crop modelling, GECROS, single nucleotide polymorphism, genome-wide association study quantitative trait loci, training dataset, testing dataset.

Table of Contents

	Abstract	
Chapter 1	General introduction	1
Chapter 2	Does morphological and anatomical plasticity during the vegetative stage make wheat more tolerant of water-deficit stress than rice?	15
Chapter 3	Genetic control of plasticity in root morphology and anatomy of rice in response to water-deficit	47
Chapter 4	Genome wide association reveals genetic basis of rice grain yield and its component traits under water-deficit stress during the reproductive stage	111
Chapter 5	Linking eco-physiological modelling with genome wide association mapping to design crop ideotypes: A case study on rice under water-deficit conditions	157
Chapter 6	General discussion	189
	References	203
	Summary	229
	Acknowledgements	233
	List of publications	237
	PE&RC Training and Education statement	239
	Curriculum vitae	241
	Funding	242

CHAPTER 1

General introduction

Background on general response of cereals to abiotic stress

During the 1960s, breeding efforts to enhance grain yield created improved cultivars responsive to increased input resources and improved agronomic practices that resulted in the Green Revolution in rice and wheat. Breeding and agronomic improvement during the Green Revolution had a tremendous impact on grain production. This yield increase allowed maintaining better balance between food supply and demand to feed the global population. However, there is serious challenge to maintain the same balance with steady increases in global population, which will reach 8.5-10 billion in 2050 (Tester and Langridge, 2010). To meet the needs of this projected future population, grain production needs to be increased at least by 50% compared to current production, and by 110% relative to that of the production obtained during 2006 (Tilman et al., 2011). The current crop breeding or genetic gain (Fischer and Edmeades, 2010) and agronomic interventions (Zorrilla et al., 2012) have not been able to increase the production enough to keep pace with the growing population. Hence, in the future, achieving sustainable increases in grain production would need substantial changes in crop breeding and cultural practices. Further, there is continuous reduction in availability of water resources for agriculture due to the growing population, increasing industrial demand and climate change effect (Kang et al., 2009). Therefore, achieving increased production would be challenging in stable environments, but undoubtedly even more challenging under changing global climate conditions. The current global climate change has already displayed damaging effects on crop yield, and is expected to have a more severe impact on grain production in future climate scenarios (IPCC, 2013).

The gradual increase in atmospheric carbon dioxide concentration [CO_2] is the major driver of global climate change. The CO_2 level has increased approximately from the pre-industrial level of 280 to the current average of 405 $\mu\text{mol mol}^{-1}$ (August 2017; <https://www.co2.earth/annual-co2>; last visited October 10, 2017), and is projected to reach 700 $\mu\text{mol mol}^{-1}$ by the end of the twenty-first century (Pearson and Palmer, 2000; Prentice, 2001; Leakey et al., 2009). The potential effects of gradually rising [CO_2] include occurrence of abiotic stresses such as high temperature, water-deficit and flooding stress (Wassmann et al., 2009). Current models predict a mean increase in temperature of 1.0-3.7 °C, and a wide spread of severe water-deficit stress by the end of the twenty-first century (IPCC, 2013). The impact of increasing temperature and water-deficit stress, owing to climate change, is region specific, severely affecting crop productivity and socio-economic conditions (Figure 1). The individual effects of high temperatures and water-deficit stress were extensively studied in cereals.

However, under real field conditions these two major abiotic stresses strongly interact with each other (Jagadish et al., 2012) and are often considered as a commonly occurring companion stress (Mittler, 2006). In addition, recent studies demonstrated the occurrence of high temperature and water-deficit stress in many parts of the world (Asia, Europe, the USA and Africa), which threatens crop productivity (Ciais et al., 2005; Wassmann et al., 2009; Olesen et al., 2011; Lobell et al., 2011; Bindi and Olesen, 2011; Zhang and Huang, 2012). Wassman et al. (2009) demonstrated the occurrence of water-deficit and high temperature stress during critical flowering and early grain-filling stages in major rice growing areas of Asia. Crop plants display both unique and similar responses to a combined effect of water-deficit and high temperature stress at whole plant to cellular level. In addition, combined effects strongly depend upon many factors such as intensity and duration of stress, crop species (Araus et al., 2002), crop genotype (Ristic and Cass, 1992; Acevedo et al., 1999), developmental stage of the organ, and cellular compartments (Ristic and Cass, 1992; Barnabás et al., 2008). Together, such complex responses make water-deficit and high-temperature stresses complex traits. The individual and combined effects of water-deficit and high-temperature stress in interaction with elevated CO₂ on agronomic and physiological traits in major cereals were systematically summarized in detail by my review paper published as Kadam et al. (2014).

Water scarcity: a growing concern for rice productivity

Water scarcity is one of the major threats to rice (*Oryza sativa* L.) production because rice has a semi-aquatic origin and is mostly cultivated in lowland conditions. Rice alone consumes 30% of water used for agriculture, while other dryland cereals require 2-3 times less water than rice (Peng et al., 2006). However, approximately 15-20 million hectares of rice growing area will most likely become affected by water scarcity by the year 2025 (<http://irri.org/our-work/research/rice-and-the-environment/coping-with-water-scarcity>). Exploring alternative solutions to reduce water requirement of rice cultivation will, therefore, have a greater significant impact on sustaining rice production in a water scarce world (Molden et al., 2010). To reduce rice water requirement, several water saving technologies have been developed such as alternate wetting and drying (Yao et al., 2012), the system of rice intensification (Stoop et al., 2002) and aerobic rice (Bouman et al., 2005). While these new technologies each have their own benefits, there are several associated risk factors including a strong yield penalty. The latter might be overcome by breeding for stress tolerant cultivars. Hence, combining these water saving technologies with breeding genotypes for a better tolerance to water-deficit stress would

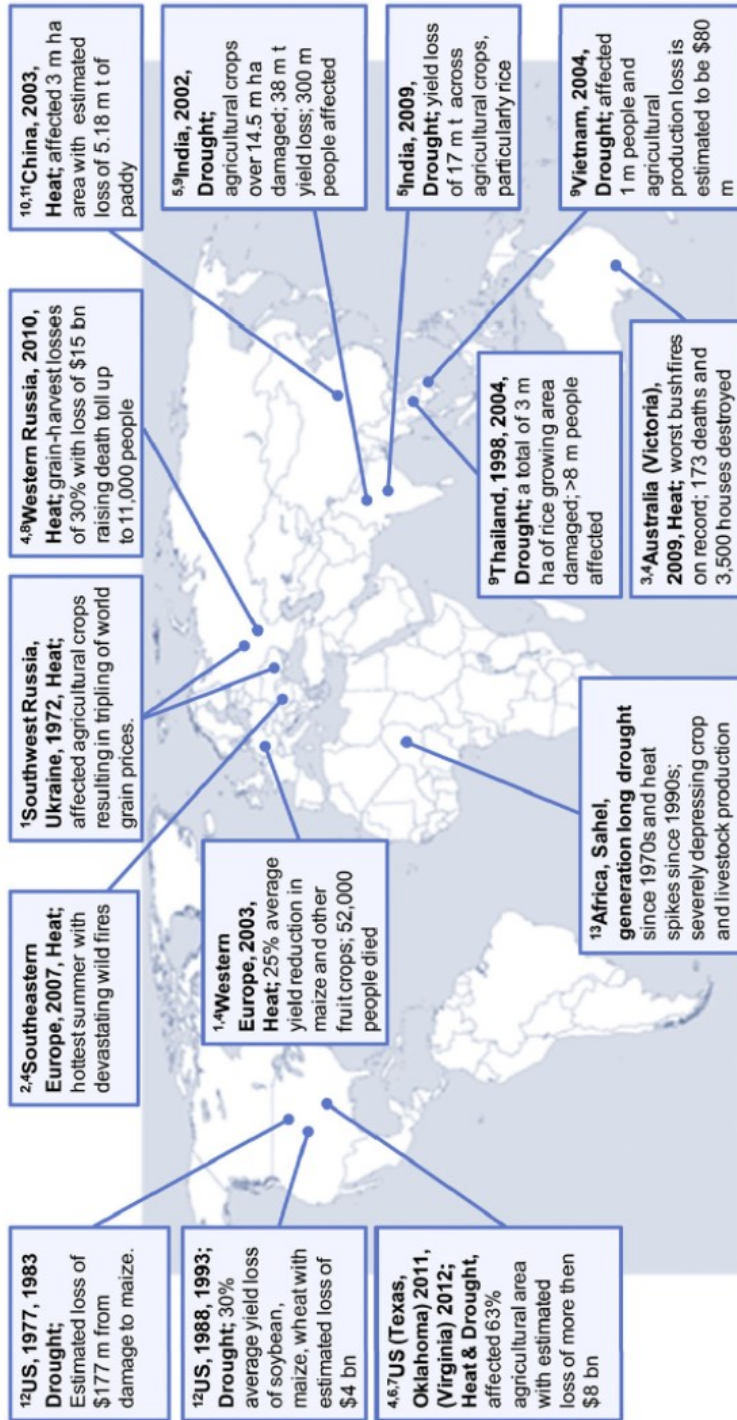


Figure 1: Major water-deficit and high-temperature stress events across the globe with catastrophic impact on agriculture and socio-economic conditions (Kadam et al., 2014).

be a more viable approach to address water scarcity in rice production (Bouman et al., 2006).

There are clear morphological differences between rice varieties adapted to upland and flooded conditions. Upland rice varieties generally have more roots and probably less shoot biomass under dry conditions, which could be one of the main reasons for overcoming water-deficit stress (De Datta *et al.* 1975). Adachi et al. (2010) documented that high hydraulic conductance due to large root surface area had significantly helped to maintain a higher rate of leaf photosynthesis in rice. However, precise information on physiological and morphological plasticity of root and shoot traits in response to water-deficit conditions is limited. Rice is highly sensitive to water-deficit during its reproductive stage and efforts have been devoted in understanding and improving rice stress resilience (Lanceras et al., 2004; Yue et al., 2006; Bernier et al., 2007; Vikram et al., 2011; Swamy et al., 2011). Nevertheless, water-deficit stress also occurs during the vegetative stage in major rainfed rice growing areas. For instance, vegetative stage water-deficit stress is more common in the Mekong region of Cambodia, where rainfall follows a bimodal pattern-decreasing during the early-middle part of the rainy season (Kamoshita et al., 2008).

Water-deficit stress striking during the vegetative stage reduces shoot elongation rate, leaf area and tillering due to decreased CO₂ assimilation because of lower stomatal conductance, transpiration and lower relative water content (Barnabás et al., 2008; Lipiec et al., 2013; Aslam et al., 2013). In contrast, stress occurring during young microspore development and anthesis (reproductive stage) leads to pollen and spikelet abortion, induces poor anther dehiscence, and restricts panicle exertion, thereby strongly reducing grain yield in major cereals (Kato et al., 2008; Lobell et al., 2011), including rice. A mild water-deficit stress during the pre-anthesis period showed 70% reduction in secondary branches of panicles and 45% decrease in spikelets per panicle in rice (Kato et al., 2008). The higher pollen abortion in rice and other cereals under water-deficit stress was mostly associated with accumulation of abscisic acid (ABA) that suppresses the supply of sucrose (Powell et al., 2012). In addition, stress coinciding during the grain filling (terminal water-deficit stress) in rice and other cereals results in early senescence with shorter grain-filling period that strongly reduces the 1000-grain weight and total grain yield (Samarah, 2005; Foulkes et al., 2007). For these reasons, rice genotypes should possess a range of characteristics to become adapted to varying levels of stress intensity at any given time during the growing period. Therefore, a fundamental understanding of the physiological and morphological traits contributing to stress tolerance with underlying genetic control is essential for designing rice-breeding strategies under water-deficit stress.

General response and adaptive strategies of plants to tolerate water-deficit stress

In general, plants have developed or acquired several strategies to mitigate water-deficit stress such as escape (phenological plasticity, i.e. early maturing), avoidance (maintaining high tissue water status), tolerance (physiologically active at low leaf tissue water status), and recovery (ability of plants to recover completely after water-deficit stress). These strategies are not mutually exclusive and can operate in combination under water-deficit stress (Ludlow and Muchow, 1990). Water-deficit stress induces a complex network of interactions between different morphological, physiological and biochemical processes at the whole plant as well as organ and cellular level. Roots are capable to first perceive stress and synthesize the chemical compound (phytohormone ABA) that communicates the stress signal to the shoot. This indeed allows the shoot and root to respond rapidly to the stress conditions. The molecular mechanism underlying these processes consists of stress signalling genes that trigger downstream genes leading to the activation of the stress tolerance pathway (Chaves et al., 2003). In the longer term, these responses can lead to fine-tuning of root biomass (increased root to shoot ratio), and alteration of morphology and anatomy of root and shoot. These adjustments help plants to avoid and tolerate stress conditions. Together, such a network, involving both short-term responses and long-term adaptive adjustments, makes water-deficit stress tolerance complex; identifying the key determinants is therefore always challenging.

To better understand the plant responses to water-deficit stress, Kamoshita et al. (2008) classified water-deficit responsive traits into primary, secondary, integrative, and phenology and plant type traits (Table 1). Primary traits are further grouped into constitutive traits (i.e. also expressed under non-stress conditions, e.g. root depth, cuticle thickness) and induced traits (i.e. expressed under stress, e.g. osmotic adjustment). These traits are highly interactive, for example, constitutive root traits under water-deficit stress may help to extract water from deeper layers of soil. This influences the expression of induced and secondary traits such as maintenance of plant water status and canopy temperature. Better performance of these secondary traits strongly influences the grain yield component traits (also called integrative traits; Figure 2). For instance, better water uptake by roots maintains cooler canopy, which reduces water-deficit induced spikelet sterility and ultimately grain yield (Kobata et al., 1994). Phenology (flowering time) and plant-type (plant height and tillering) traits play a major role in stress adaptation, and strongly affect the expression of secondary and integrative traits and thereby grain yield. Further, compared to other traits, plant-type and phenology traits are

genetically less complex with higher heritability; hence they have extensively been used in traditional crop breeding (Cooper et al., 1999a; Cooper et al., 1999b). In contrast, grain yield and its component traits are genetically more complex traits controlled by many genes/quantitative trait loci (QTL) compared to the traits belonging to other categories in Table 1.

Rice root development and function: Present status and future challenges

Roots, because of their primary role in water and nutrient uptake, have historically gained much more attention than shoot development in improving water-deficit stress tolerance. Rice has a well-described fibrous root system, and mainly exhibits nodal and lateral roots although it also has active seminal roots during the first two weeks of seedling growth (Yoshida and Hasegawa, 1982). Significant genotypic variation for root morphological and anatomical traits, and their functional relevance in stress tolerance have been reported in rice [for details see the review by Gowda et al. (2011)]. A deeper root system is generally viewed as a desirable trait (Gowda et al., 2011), which improves rice grain yield in water-deficit stress (Uga et al., 2013). In addition, direct selection of grain yield as a criterion under water-deficit stress resulted in the tolerant genotypes (Lanceras et al., 2004; Yue et al., 2006; Bernier et al., 2007; Vikram et al., 2011). Further studies also proved the role of root morphology and anatomy in improving grain yield under stress (Henry et al., 2012). In summary, rice root research is already in an advanced stage, and much of the knowledge is generated allowing to design the root ideotype to improve stress adaptation. Despite this fundamental progress and knowledge in root research, rice cultivars are more stress susceptible than genotypes of other dryland species (wheat, maize and sorghum). Rice developed several different root characteristics compared to dryland species, such as root aerenchyma that allows adapting to lowland/flooded conditions. In addition, we hypothesize that rice possesses a narrower xylem diameter than dryland cereals. Thus overall water transport in rice will be slower because the transport rate depends on the overall cross-sectional area of the xylem (Niklas, 1985). Although such differences are obvious, the direct comparison of physiology and rooting plasticity between cereals under stress conditions is lacking. A recent study demonstrated that rice and wheat responses can be compared at the same moisture conditions (Praba et al., 2009). We assume that such direct comparison of rice with other dryland species will help to understand why rice cannot perform like other cereals in terms of its ability to tolerate stress. It will also allow identifying the key root mechanisms / traits that can be prioritized in genetic mapping to understand the molecular pathway (potential QTLs/

Table 1. Generic classification of water-deficit stress adaptive traits (Kamoshita et al., 2008).

	Primary traits		Secondary traits	Integrative traits	Phenology and plant type traits
	Constitutive	Induced			
Roots		Osmolytes, osmotic adjustment	Relative water content	Harvest index	Plant height
Epicuticular waxes	Cell viability		Canopy temperature	Spikelet sterility	Tillering
Stomatal frequency and index	Membrane integrity		Leaf rolling/ folding	1000 grain weight	Days to flowering
Water use efficiency	Chlorophyll stability		Leaf senescence	Biomass	
Specific leaf area	Reactive oxygen species		Stay green	Grain number per panicle	
Pigments	Chlorophyll fluorescence			Drought susceptibility index	
Ash content	Lipid peroxidation			Grain yield	
	Gas exchange				
	Leaf maintenance respiration				
	Plant hormones				

genes) underlying rice adaptation to water-deficit conditions.

Genetic dissection of complex water-deficit stress tolerance in rice through a genome-wide association study

Water-deficit stress tolerance is a complex trait controlled by many genes/QTLs (Fleury et al., 2010; Ravi et al., 2011). Recent advances in genotyping coupled with precise phenotyping can potentially help to dissect the genetic architecture and regulatory pathways that confer adaptation of rice to water-deficit stress. So far, the use of genotypic variation to identify markers/genes for water-deficit traits has been typically conducted using a population resulting from a bi-parental cross. Gu et al. (2012), for example, recently identified QTLs for highly environmentally sensitive and difficult-to-measure photosynthetic parameters in rice under field water-deficit condition. In addition, several QTLs were identified for water-deficit stress tolerant traits such as root traits [for more details see the review by Mai et al. (2014)], grain yield and yield component traits (Lanceras et al., 2004; Bernier et al., 2007; Kumar et al., 2007; Venuprasad et al., 2009b; Vikram et al., 2011). Although the bi-parental QTL approach has been extensively used in rice for mining QTLs linked to several traits (Mir et al., 2012), one major limitation is the use of only two parents and hence limited genetic variation. It is unlikely that a wide range of traits that can potentially confer water-deficit stress tolerance (Table 1) can be identified in bi-parental populations since the two parents used are unlikely to substantially contrast for so many traits of interest. Further, a bi-parental population includes insufficient recombination events, hence identified QTLs often localize in a large genomic segment. Thus, a bi-parental linkage approach lacks the potential to exploit the vast genomic variability and tremendous phenotypic plasticity housed within the 120,000 rice accessions in public germplasm repositories (Zhao et al., 2011).

To overcome the constraints of conventional QTL mapping, genome wide association studies (GWAS) or linkage disequilibrium (LD) mapping, in which statistical associations between genotype and phenotype are assessed in large panels of germplasm, are now emerging as a viable strategy to identify QTLs/genes underlying quantitative variation of traits (Rafalski, 2010). In general, a GWAS consists of six steps namely: (1) germplasm selection with wide coverage of genetic diversity, (2) genotyping a population with available markers, (3) phenotypic measurement of traits of interest, (4) quantification of extent of LD in the population using marker data, (5) determining population structure (level of genetic differentiation among groups within the population) and kinship (coefficient of relatedness between pairs of each

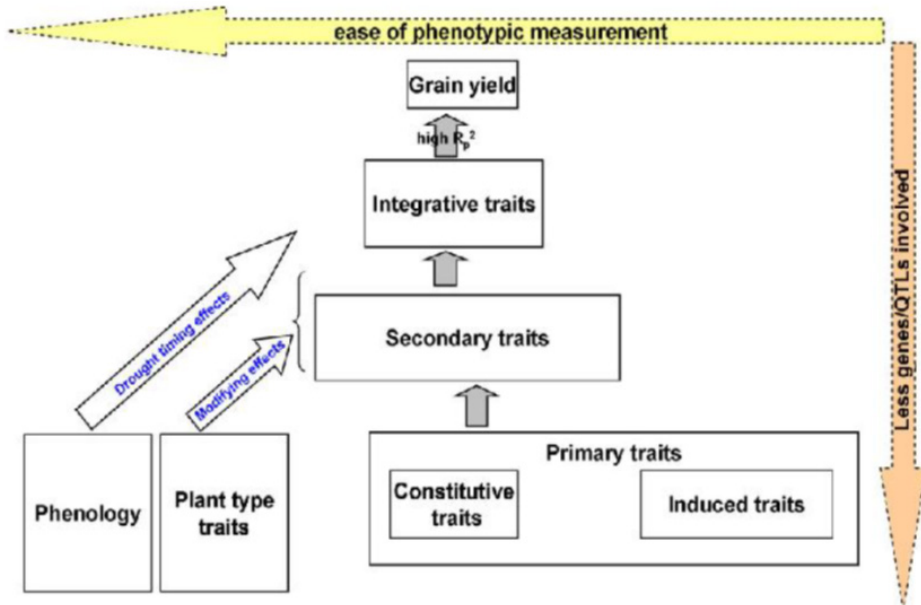


Figure 2: Relationship between water-deficit stress tolerance traits classified by Kamoshita et al. (2008). High R_p^2 indicates the strength of correlation between grain yield and integrative traits.

individual within the population), and (6) construction of a high-density haplotype map of the genome and association of phenotypic traits (Abdurakhmonov and Abdugarimov, 2008). This approach fits perfectly with rice due to the availability of a reference genome sequence and genome wide single nucleotide polymorphisms (SNPs) dataset for a large number of accessions at the International Rice Research Institute (IRRI), which will enhance the analytical power of the GWAS.

Linking eco-physiological crop modelling with genome-wide association mapping to design ideotypes for improved grain yield

A common challenge for both geneticists and physiologists is to predict the effect of genomic regions/genes identified in one environment on trait phenotypes in another environment. Crop modelling provides an option in this regard. Recent case studies on integration of crop eco-physiological models with traditional genetic mapping (QTL-based eco-physiological modelling) extended the scope of modelling to determine the QTL–trait phenotype relationships and genotype-environment interactions, in which QTL-based parameter values are used to calibrate the eco-physiological model. The QTL-based modelling was first used in barley to

predict grain yield by (Yin et al., 1999; Yin et al., 2000) and subsequently, with more success, applied to simpler crop traits such as leaf elongation rate in maize (Reymond et al., 2003), flowering time in barley (Xu et al., 2005; Yin et al., 2005) and in rice (Nakagawa et al., 2005). There is evidence to demonstrate that such a linking of genetic mapping and eco-physiological modelling can help to transform QTL mapping into more efficient marker-assisted breeding strategies (Hammer et al., 2006). Recently, it was shown that a rice ideotype designed using this approach by pyramiding the alleles of yield component traits shows higher grain yield than the ideotype based on alleles for grain yield *per se* (Gu et al., 2014). However, it remains to be seen whether this approach can be extended to link the process-based eco-physiological model with QTLs identified by GWAS analysis for design of the virtual grain yield ideotype.

Major objectives of this study

Although there have been several independent studies conducted to understand the water-deficit stress tolerance in rice, studies integrating various aspects to better understand the water-deficit stress tolerance are limited. In this study, I tried to use a multidisciplinary approach, covering physiology, genetics and crop modelling, to understand the rice water-deficit stress tolerance. This study has multiple key objectives:

- 1) Quantify physiological, morphological and root anatomical traits plasticity of rice and wheat to vegetative stage water-deficit conditions;
- 2) Investigate the genetic control of physiological, morphological and root anatomical traits plasticity through GWAS under vegetative stage water-deficit stress;
- 3) Investigate the genetic control of grain yield and yield components variation through GWAS under water-deficit stress during the sensitive reproductive stage;
- 4) Examine the ability of an existing process-based eco-physiological “GECROS” model to quantify the grain yield differences in rice association mapping panel;
- 5) Model the proportional contribution of the identified SNPs or QTLs to grain yield increase under water-deficit conditions;
- 6) Pyramiding the genetic effects of the SNPs or QTLs to design the virtual grain yield ideotype using modelling approach.

I surmise that addressing these above key objectives will help to establish a new platform for identification and selection of key traits for breeding stable high-yielding rice varieties for water

-deficit stress.

Methodological framework

To achieve the above objectives, I studied underlying mechanisms of rice water-deficit stress tolerance through a multidisciplinary approach of integrating physiology, genetics and crop growth modelling. The general methodological framework is summarized in four steps. In the first step, I characterized the physiological, morphological (shoot and root) and root anatomical response of rice and wheat under well watered and water-deficit stress conditions to create meaningful knowledge and insight useful for designing the genetic mapping study. In the second step, I scaled down the finding of the first study on a large set of rice genotypes to identify the phenotypic and genetic variation in physiological, morphological and anatomical traits. In the third step, I screened the same set of genotypes under field conditions to quantify the variation in grain yield and yield components under reproductive stage water-deficit stress. Further, I conducted a genetic analysis to link these phenotypic variations with genomic regions (high-density SNP markers) to identify the QTLs/genes with their possible environmental interaction. In the last step, I tried to incorporate the effect of QTLs detected for grain yield-influencing parameters into a process-based “GECROS” crop model to design the virtual grain yield ideotype, with the hope to assist the traditional breeding for improved rice stress tolerance. I hypothesize that such an integrated multidisciplinary approach can lead to new insights into water-deficit stress tolerance, providing the breeder with more knowledge that can improve the selection efficiency to increase the grain yield under changing climate.

Outline of this thesis

This dissertation consists of six chapters including this chapter as general introduction (**Chapter 1**). The general content and key message of Chapters 2-6 are summarized below.

In **Chapter 2**, I describe the key findings from an experiment conducted to test the physiological, morphological and root anatomical response of rice and wheat to vegetative-stage water-deficit stress. The results show that wheat has stronger morphological and root anatomical plasticity in response to water-deficit stress than rice.

In **Chapter 3**, I scale the key findings from Chapter 2 up to a rice association mapping panel and quantify the quantitative genotypic variation of phenotypic plasticity for physiological, morphological and root anatomical responses under vegetative stage water-deficit stress.

Significant genotypic variation is found for phenotypic plasticity. Genome-wide association analysis identifies several genomic regions associated with phenotypic plasticity that upon validation can be used for marker-assisted selection (MAS). In addition, key *a priori* candidate genes are identified near to these genomic regions, which can be used for further molecular validation.

In **Chapter 4**, I describe the field experiment to investigate the variation in grain yield as well as in yield components under control and reproductive-stage water-deficit stress conditions across two independent growing seasons. Significant genotypic variation and genotype-by-environment interaction are observed for grain yield and yield components. Genome-wide association analysis identifies genomic regions regulating the grain yield, yield components, and demonstrates strong interactions with environment. Key *a priori* candidate genes are identified.

In **Chapter 5**, I describe a case study to link the process-based “GECROS” model with genome-wide association mapping to design a virtual grain yield ideotype. Using the model input parameters derived from an experiment as described in Chapter 4, I calibrate the “GECROS” model to quantify the grain yield differences in a rice association mapping panel under control. I also extrapolate this calibrated “GECROS” model to predict the grain yield difference under water-deficit stress and in completely new environments. A model based-sensitivity analysis identifies the key grain yield determining SNPs marker that breeder can prioritize. By pyramiding the alleles of SNPs detected for model input traits, a virtual grain yield ideotype is designed.

In **Chapter 6**, I summarize the key conclusions of this thesis; discuss their potential implications and limitations in improving the rice water-deficit stress tolerance. In addition, I also discuss future potential avenues to improve rice adaption to water-deficit stress.

CHAPTER 2

Does morphological and anatomical plasticity during the vegetative stage make wheat more tolerant of water-deficit stress than rice?

Niteen N. Kadam^{1,2}, Xinyou Yin², Prem S. Bindraban³, Paul C. Struik²,
Krishna S.V. Jagadish¹

¹International Rice Research Institute, DAPO Box 7777, Metro Manila, Philippines

²Centre for Crop Systems Analysis, Wageningen University and Research Centre, PO Box
430, 6700 AK Wageningen, The Netherlands

³Virtual Fertilizer Research Center, Washington, D.C. 20005, USA

Abstract

Water scarcity and the increasing severity of water-deficit stress are major challenges to sustaining irrigated rice (*Oryza sativa* L.) production. Despite the technologies developed to reduce the water requirement, rice growth is seriously constrained under water-deficit stress compared with other dryland cereals such as wheat (*Triticum aestivum* L.). We exposed rice cultivars with contrasting responses to water-deficit stress and wheat cultivars well adapted to water-limited conditions, to the same moisture stress during vegetative growth to unravel the whole-plant (shoot and root morphology) and organ/tissue (root anatomy) responses. Wheat cultivars followed a water-conserving strategy by reducing specific leaf area and developing thicker roots and moderate tillering. In contrast, rice 'IR64' and 'Apo' adopted a rapid water acquisition strategy through thinner roots under water-deficit stress. Root diameter, stele and xylem diameter, and xylem number were more responsive and varied with different positions along the nodal root under water-deficit stress in wheat, whereas they were relatively conserved in rice cultivars. Increased metaxylem diameter and lower metaxylem number near the root tips and exactly the opposite phenomena at the root-shoot junction facilitated the efficient use of available soil moisture in wheat. Tolerant rice 'Nagina 22' had an advantage in root morphological and anatomical attributes over cultivars IR64 and Apo but lacked plasticity, unlike wheat cultivars exposed to water-deficit stress. The key traits determining the adaptation of wheat to dryland conditions have been summarized and discussed.

Keywords: rice, nodal root anatomy, root diameter, stele diameter, water-deficit stress, water use efficiency, wheat, root-shoot junction.

Abbreviations

$\Delta^{13}\text{C}$: carbon isotope discrimination, g_s : stomatal conductance, LMXD: late metaxylem diameter, LMXN: late metaxylem number, LWR: leaf weight ratio, LPr: radial hydraulic conductance, MRL: maximum root length, RA: root apex, RB: root biomass, RLD: root length density, RSJ: root-shoot junction, RV: root volume, RWR: root weight ratio, SD:RD: stele diameter in proportion to root diameter, SLA: specific leaf area, SRL: specific root length, SWR: stem weight ratio, TRL: total root length, WUE: water use efficiency.

Introduction

Among cereals, rice (*Oryza sativa* L.) and wheat (*Triticum aestivum* L.) are the most important staple food crops and they belong to the family *Poaceae*. These two cereals share a common ancestor and diverged about 65 million years ago (Sorrells et al., 2003). Rice eventually developed strong adaptation potential for fully flooded conditions across tropical to temperate environments, while wheat became well adapted to aerobic conditions mostly restricted to temperate environments. Rice, with a semi-aquatic behavior, consumes about 30% of the total fresh water available for agricultural crops worldwide, which equates to a 2-3-fold higher consumption than other cereals such as wheat and maize [*Zea mays* L.] (Peng et al., 2006). Despite significantly lower water requirement, the potential yield of wheat in a favorable environment (9 t ha⁻¹) is comparable with the yield of fully flooded rice (9 t ha⁻¹) in the dry season at the International Rice Research Institute (IRRI; Fischer and Edmeades, 2010). Hence, rice records very low water productivity compared with wheat and other dry-land cereals. Because of growing concerns about water scarcity and increased frequency and magnitude of water-deficit stress events under current and future climates, increasing or even sustaining rice yield under fully flooded conditions is highly challenging. To minimize the total water requirement for cultivating rice, several water-saving technologies have been developed such as direct-seeded aerobic rice cultivation (Bindraban et al., 2006). These water-saving technologies increased water productivity substantially compared with flooded conditions, but were invariably associated with a yield penalty. A major challenge that water-saving technologies including aerobic rice currently face is the lack of mechanistic understanding for further genetic improvement.

Rice, by virtue of its wider adaptation to a range of edaphic conditions, is considered to possess the diversity to adapt to upland or aerobic scenarios extending into water-deficit conditions (Khush et al., 1997). Genetic differences in rice root biomass and rooting depth and variation in root morphology with water-deficit stress exposure are well documented (Kato et al., 2006, 2007; Henry et al., 2011; Kano et al., 2011). But, the underlying mechanisms differing across diverse germplasm that influence water uptake under water-deficit stress are not fully understood (Gowda et al., 2011). A recent report has documented water-deficit-tolerant genotypes recording a lower bleeding rate and narrow xylem diameter under stress (Henry et al., 2012). Contrastingly, a higher root hydraulic conductivity helped to maintain a higher photosynthetic rate (Adachi et al., 2010), with tolerant cultivars maintaining greater root hydraulic conductivity than susceptible cultivars (Matsuo et al., 2009). Further, upland rice

cultivars with deeper roots outperformed lowland cultivars possessing a shallow root system when encountering water-deficit stress (Uga et al., 2013). Additionally, major-effect grain yield MQTL (meta-quantitative trait loci) under water-deficit stress identified in rice were found to co-localize on the genomes of other dry-land cereals such as wheat, maize, and pearl millet [*Pennisetum glaucum* L.] (Swamy et al., 2011), indicating a possible common evolutionary pathway for water-deficit adaptation across cereals. Despite these achievements and the relatedness among cereals, rice does not respond in a way like other dry-land cereals to water-deficit stress conditions. To bring in a revolutionary change in future breeding strategies for upland/aerobic and water-deficit tolerance in rice, there is a need for a fundamental understanding and identification of the key traits that determine water-deficit stress response in well-adapted dry-land cereals. Hence, comparing whole-plant responses (shoot and root) of rice with those of other dry-land cereals such as wheat is essential. A comparative study between two C₃ cereals (rice and wheat) will help identify the core adaptive mechanisms and/or a suite of traits that render wheat to grow with less water and more tolerant of water-deficit stress. Such comparative analysis should target key morphological, physiological, anatomical and agronomic traits throughout the crop growth cycle, as water-deficit stress occurs at both early (vegetative stage) and late (reproductive stage) season in rice (Pandey et al., 2007). Extensive research efforts are currently ongoing to reduce the impact of water-deficit stress during the reproductive stage in rice (Venuprasad et al., 2008; Verulkar et al., 2010; Vikram et al., 2011; Kumar et al., 2014) and in wheat (Oliveras-Villegas et al., 2007; Lopes and Reynolds, 2010; Pinto et al., 2010). Therefore, our study focused on stress during the vegetative stage, to identify key checkpoints that determine whole-plant responses of representative rice cultivars adapted to lowland, upland/aerobic, or water-deficit conditions and of wheat cultivars with moderate to high water-deficit tolerance. Cultivars from both species, were exposed to moisture levels that resembles aerobic conditions and water-deficit stress during the vegetative stage. Our study follows a previous report that has successfully demonstrated the approach to expose rice and wheat to the same moisture stress conditions (Praba et al., 2009) and is designed to address the following specific objectives—(1) to quantify the adaptive plasticity in shoot and root morphology and biomass partitioning among different plant parts (leaves, stem, and root); (2) to estimate the key supportive physiological mechanisms such as whole-plant water use efficiency and leaf-level carbon isotope discrimination; and (3) to dissect root anatomical plasticity across different key zones in both rice and wheat roots exposed to water-deficit stress. Finally, novel traits that benefit dry-land adaptation in wheat compared with rice cultivars

requiring more water are highlighted.

Materials and Methods

Plant materials and growth conditions

Greenhouse and controlled-environment experiments were conducted to compare the vegetative-stage water-deficit stress response of rice and wheat with emphasis on root morphological and anatomical plasticity. Three rice cultivars, rice ‘IR64’ (susceptible to water-deficit stress), rice ‘Apo’ (aerobic/water-deficit tolerant), and rice ‘N22’ (water-deficit and high-temperature tolerant), were chosen for our study based on previous reports (Liu et al., 2006; Jagadish et al., 2011; Rang et al., 2011; Venuprasad et al., 2012). The two wheat cultivars selected were wheat ‘Serim82,’ which is moderately susceptible (Pfeiffer, 1988) to tolerant of water-limited conditions (Villareal et al., 1995), and wheat ‘Weebill4,’ a highly drought-tolerant check cultivar (Reynolds et al., 2007; Praba et al., 2009). Dormancy of rice seeds was broken after exposure to 50°C for 3 days, and pre-germinated seeds were sown in white-painted pots (55 cm long and 15 cm diameter) as recommended by Poorter et al. (2012) to minimize the confounding effects of increasing temperature of pot surface and soil. The pots were filled with 11 kg of clay loam soil and maintained under natural greenhouse conditions at the IRRI during the 2012 wet season (i.e. during the season when temperature in the greenhouse and pot can be controlled best). Each pot was drilled with holes on either side at the bottom for imposing controlled water-deficit stress and lined with polythene covers to facilitate easier separation of roots from soil at the end of the treatment. Simultaneously, wheat seeds were directly sown in pots with the same dimensions and maintained in controlled-environment large walk-in chambers (10.6-m² area), built as an extension to the greenhouse where the rice plants were maintained. The chambers were maintained at day/night temperatures of 21°C/18°C, 60% to 70% relative humidity, 16h/ 8h light/dark cycle, and light at 650 mmol m⁻² s⁻¹, following Praba et al. (2009). Across both cereals and the treatments imposed, three replications were maintained and placed in a completely randomized design.

Water-deficit stress imposition, cumulative water transpiration, and whole-plant WUE

Both rice and wheat plants were maintained at two moisture regimes: control at 100% field capacity (FC) that is the maximum soil moisture content after drainage of excess water-resembling an aerobic condition and water-deficit stress at 55 to 60% FC. Water-deficit stress was imposed after seedling establishment, that is, 15 days after seedling emergence, before

which all the pots were maintained uniformly at 100% FC. Pots with the control treatment were maintained at 100% FC throughout the experiment while water-deficit stress was imposed by unplugging the stoppers at the bottom of the pots. A standardized gravimetric approach of daily pot weighing (Raju et al., 2014) was followed to gradually attain 55 to 60% FC and thereafter maintained at the same level until the end of the experiment (for details, see Supplementary Figure S1). Once the target stress level was reached, daily consumed water due to transpiration was replenished by adding an exact amount of water to bring back the moisture content to the desired target in each pot. The soil surface was covered with a circular polythene sheet to protect from direct evaporative loss of water and a slit across the radius of the polythene sheet prevented heat buildup on the soil surface. In addition, a set of filled pots without a plant was also maintained to correct for evaporative loss of water from the opening created by the slit in the circular-shaped polythene sheet. Daily pot weights recorded for 30 consecutive days of stress period were used to calculate the daily evapo-transpiration. After correcting for evaporative loss from empty pots, actual transpiration was calculated. Finally, daily actual transpiration was summed for the 30-day period to calculate cumulative water transpired. Whole-plant water use efficiency (g kg^{-1}) was calculated as the ratio of total biomass (root and shoot) to cumulative water transpired.

Shoot morphology and leaf $\Delta^{13}\text{C}$

Following 30 days of stress, plants were harvested 45 days after sowing and tiller numbers were counted, and total leaf area was estimated by a leaf area meter (LI-3000, LI-COR, Lincoln, NE, USA). Leaves and stems were separately oven-dried at 70 °C for 72 h to compute specific leaf area and shoot biomass. Top-most fully expanded leaves from 4-5 tillers per plant were collected from control and from water-deficit-stressed pots immediately before relieving stress separately for three replications and oven-dried and ground to fine powder. Samples were analyzed for carbon isotope composition ($\delta^{13}\text{C}$) by a stable isotope ratio mass spectrometer (IRMS) facility available in the analytical service laboratory of IRRI (<http://asl.irri.org/lims/>). The analytical precision of the samples was within 0.1%. Further, carbon isotope discrimination ($\Delta^{13}\text{C}$) value was calculated relative to the atmospheric ^{13}C isotopic composition ($\delta^{13}\text{C}$) as follows (Farquhar et al., 1989).

$$\Delta^{13}\text{C} = \frac{\delta^{13}\text{C}_a - \delta^{13}\text{C}_p}{1 + \delta^{13}\text{C}_p/1000}$$

where $\delta^{13}\text{C}_a$ and $\delta^{13}\text{C}_p$ denote the carbon isotope compositions of atmosphere (-8‰) and leaf

sample, respectively.

Root sample processing

The entire column of soil along with the roots was placed on a 1 mm sieve and meticulously washed using a gentle stream of water to minimize the loss of small roots and root hairs. Rice root system is mainly composed of nodal roots and only one radicle or seminal root (primary root), with the latter growing to a maximum length of 15 cm and being viable until the 7-leaf stage. On the contrary, wheat develops and maintains several seminal roots until maturity (Yoshida and Hasegawa, 1982). To make meaningful comparison between rice and wheat, nodal root was investigated in our study. Across both rice and wheat cultivars, three replicate root sections (2-3 cm) were collected from three different positions along the nodal root for root anatomy study: (1) near the root-shoot junction (RSJ), (2) ~15 cm from the root apex (RA) from water-deficit-stressed samples and ~10 cm from RA on control samples following Henry et al. (2012), and (3) at 6 cm from RA in both treatments (Fig. 1A). Collected samples were stored in 40% alcohol to study root anatomy. The remaining whole-plant root samples were placed in 20% alcohol and stored at 4 °C for root scanning and image analysis.

Root image acquisition and root morphology traits

Root samples stored in 20% alcohol were cut meticulously to fit the scanner tray and aligned vertically in plates to avoid overlapping. An 8-bit gray-scale image was acquired by scanning with an EPSON perfection 7000 scanner at 600 dots-per-inch resolution next to a ruler. After capturing the image, root samples were oven-dried at 70 °C for 72 h to record the total root biomass. Morphological attributes such as total root length, average root thickness, and root volume were computed by analyzing images with WinRHIZO Reg 2012b software (http://www.regent.qc.ca/assets/winrhizo_software.html). To avoid underestimation of fine root lengths during image processing, the threshold pixel was adjusted to automatic mode (Kato et al., 2010; Kato and Okami, 2011).

Derived shoot and root growth parameters

Leaf weight ratio (LWR), stem weight ratio (SWR), and root weight ratio (RWR) were calculated as a ratio of leaf, stem, and root weight to total biomass. Average specific leaf area was calculated as the ratio of total leaf area to leaf dry weight. Root length density was calculated as the ratio of total root length to the volume of soil in the pot, and total root weight

density was calculated as the ratio of root length density to root biomass. Specific root length was calculated as the ratio of total root length to root biomass.

Root anatomy and theoretically calculated axial conductance

To investigate root anatomical features, samples stored in 40% ethanol obtained from three different positions along the root (Fig. 1A) were hand-sectioned with a razor blade under a dissecting microscope. Root sections were stained with 0.5% w/w phloroglucinol in water followed by 20% (V/V) hydrochloric acid (Jensen, 1962) for lignin staining. Images of the root sections were acquired with a Zeiss axioplan 2 compound microscope (Zeiss, Germany) with 50× and 100× magnification. At least 3-5 root images per replicate and tissue position were considered for measuring anatomical traits such as root cross-section diameter, stele diameter, late metaxylem diameter, and sclerenchyma with image J software (for details, see Abramoff et al., 2004). A schematic sketch of the different root anatomical traits measured using image J is provided in Fig. 1B.

If the number of xylem vessels is n , their overall theoretical axial conductance (K_h ; $\text{mg m MPa}^{-1} \text{s}^{-1}$) was calculated with the modified Hagen-Poiseuille's law described by Tyree and Ewers (1991) and Tombesi et al. (2010).

$$K_h = \frac{\pi\rho}{128\eta} \sum_{i=1}^n d_i^4$$

where d_i is the radius of the i^{th} vessel in meters, ρ is the fluid density (assumed to be $1 \times 10^9 \text{ mg m}^{-3}$), and η is the viscosity (assumed to be $1 \times 10^{-9} \text{ MPa}\cdot\text{s}$).

Statistical analysis

The shoot and root morphological data were analyzed to check the significance level through analysis of variance (ANOVA) in Genstat release13 (<https://www.vsni.co.uk/genstat>), with cultivar and treatment as a main factor. But for root anatomy data, root tissue position was included in analysis as a factor along with cultivar and treatment.

Results

Shoot morphology and whole-plant and leaf-level WUE

A significant reduction in total leaf area, total biomass, and cumulative water transpiration was recorded under water-deficit stress in rice cultivars with a stronger reduction in the tolerant N22 ($P < 0.001$) and in both wheat cultivars ($P < 0.01$ to $P < 0.001$; Supplementary Table S1). Specific

leaf area and tiller number decreased under water-deficit stress only in wheat cultivars ($P < 0.001$; Fig. 2A and Supplementary Table S1). Whole-plant water use efficiency (WUE) increased in response to water-deficit stress in two out of three rice cultivars (IR64: 32%; Apo: 16%) and in both wheat cultivars (~40%). The tolerant rice cultivar N22 recorded higher WUE than the other two cultivars in the absence of stress and was not altered by water-deficit stress; hence, significant cultivar and treatment interaction ($P < 0.01$; Fig. 2B) was observed. Carbon isotope discrimination ($\Delta^{13}\text{C}$) of leaf is often used as a proxy to measure WUE (lower $\Delta^{13}\text{C}$ means higher WUE; Impa et al., 2005). In both species, water-deficit stress had a strong effect on $\Delta^{13}\text{C}$ ($P < 0.001$), but there were no cultivar differences ($P > 0.05$). On average, $\Delta^{13}\text{C}$ decreased by 6.3% in rice cultivars and by 8% in wheat cultivars. The absolute value of $\Delta^{13}\text{C}$ was higher in wheat cultivars than in rice cultivars (Fig. 2C).

Biomass partitioning among leaf, stem, and root

In general, both species recorded higher biomass partitioning to leaf (LWR) and stem (SWR) than to root (RWR), with a higher proportion of biomass partitioned to roots in wheat than in rice (Supplementary Table S1). Leaf weight ratio (LWR) and stem weight ratio (SWR) varied only in rice cultivars ($P < 0.01$), with a significant effect of water-deficit stress ($P < 0.05$ to $P < 0.01$). The susceptible IR64 had 16% lower LWR and 24% higher SWR with water-deficit stress. The tolerant N22 had lower LWR and higher SWR than other cultivars and was not altered by water-deficit stress. In both species, root weight ratio (RWR) did not differ significantly among cultivars and treatments ($P > 0.05$), but an increasing trend was observed with tolerant rice cultivar N22 and both wheat cultivars in water-deficit stress.

Root morphology

Root morphological traits such as maximum root length (MRL), total root length (TRL) and root length density (RLD) did not differ with either cultivars or stress treatments in rice ($P > 0.05$), but root volume (RV) and root biomass (RB) differed with both cultivars and treatments ($P < 0.05$ to $P < 0.01$; Supplementary Table S2). Conversely, in both wheat cultivars, the water-deficit stress treatment effect was highly significant for all the above-mentioned traits ($P < 0.05$ to $P < 0.001$), but there were no cultivar differences. The MRL of the two wheat cultivars was increased in response to water-deficit stress compared with control conditions (Supplementary Table S2).

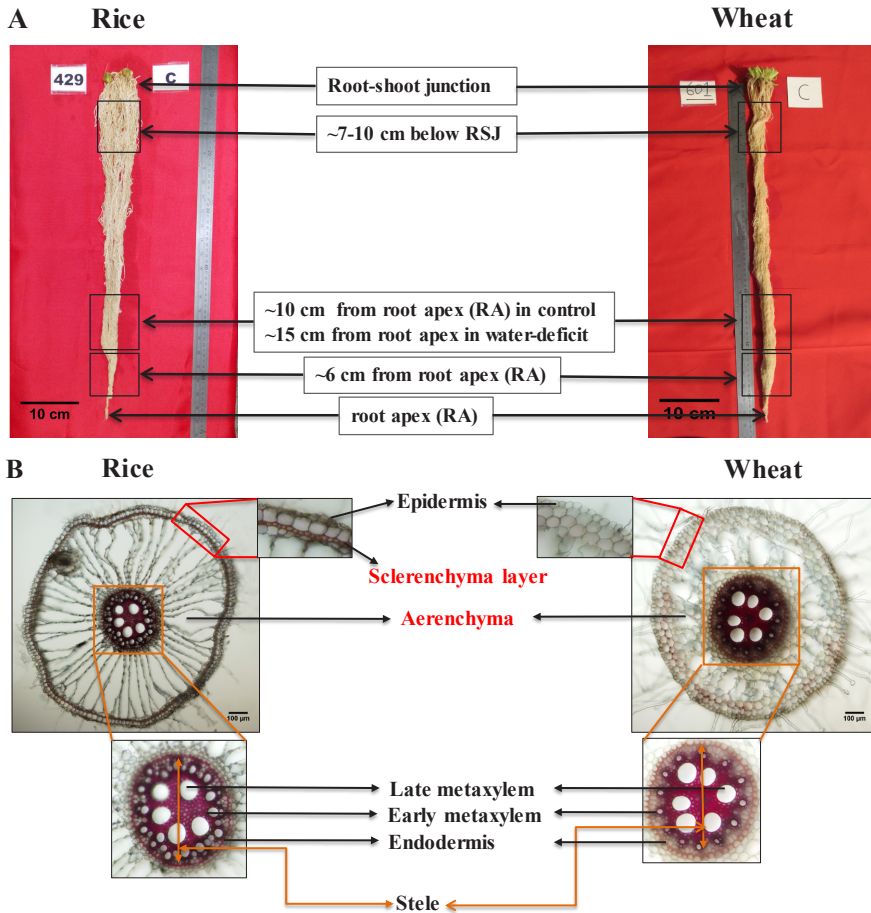


Figure 1. Root samples were collected in three different zones on nodal roots for anatomy study (**Panel A**). Radial root cross sections showing anatomical variation in rice and wheat (**Panel B**). Scale bars on root image = 10 cm (**Panel A**) and 100 μm (**Panel B**).

Specific root length, average root thickness, and total root weight density

Specific root length (SRL), expressed as the ratio of root length to root biomass, is a key indicator of root thickness. In response to water-deficit stress, SRL increased significantly in two of the three rice cultivars (IR64: 59%; Apo: 28%), but decreased in both wheat cultivars by $\sim 40\%$ (Fig. 3A). The SRL is independently controlled by two other components, root thickness and root weight density (Ostonen et al., 2007). Our results support this, with an increased SRL in rice cultivar IR64 determined mainly by reduced total root weight density (42%), while in Apo this was due to a reduction in both average root thickness (15%) and total root weight density (18%). On average, the lower SRL in the wheat cultivars was due to a

greater increase in total root weight density (68.5%) than average root thickness (29%; Fig. 3B-C).

Radial root anatomy

To further confirm the observed variation in root morphology, we investigated root anatomical variables at three different locations along the root length (Fig. 1A-B). Note that root cross-sections were stained with phloroglucinol to assess the secondary cell-wall thickening and lignin deposition under water-deficit stress. While it appears that there were changes in the staining pattern (e.g. Weebill4 under water-deficit treatment; Fig. 4), results were not consistent across replications in both the species and thus we will avoid discussing such changes.

Root diameter

Variation in root diameter is due to change in number and size/width of cortical cells and in stele diameter. In both species, root diameter varied significantly with cultivar ($P < 0.05$ to < 0.001) and position along the root ($P < 0.001$). A significant effect of water-deficit stress on root diameter was documented with rice cultivars ($P < 0.01$; Supplementary Table S3). Root diameter at the root-shoot junction (RSJ; see Fig. 1A) decreased with stress exposure in rice cultivar IR64 (25%), with no change in the aerobic Apo and tolerant N22 (Fig. 4A). A clear pattern was not observed at 10 to 15 cm from the root apex (RA; Fig. 4B). However, an opposite response was observed at 6 cm from the RA, where the tolerant cultivars showed lower root diameter (N22: 19%; Apo: 20%), with no change in IR64 (Fig. 4C). Unlike in rice cultivars, root diameter at the RSJ increased significantly in both wheat cultivars (Serim82: 42%; Weebill4: 30%), but at other two positions a decreasing trend was observed (i.e. 10 to 15 cm from RA and 6 cm from RA; Fig. 4).

Stele diameter and stele diameter in proportion to root diameter (SD:RD)

Stele is the central part of the root system that contains vascular tissue (i.e. xylem and phloem; Fig. 1B). Both cereals recorded a strong cultivar and spatial (different positions along the root) variation ($P < 0.001$) for stele diameter (Supplementary Table S3). Stele diameter at the RSJ did not differ in any of the rice cultivars (Fig. 5A), but the tolerant N22 maintained a higher stele diameter at 10 to 15 cm from RA and at 6 cm from RA (Fig. 5B-C). Additionally, stele diameter was more stable and was not affected by water-deficit stress in rice ($P > 0.05$). Unlike in rice, stele diameter increased significantly under water-deficit stress at the RSJ in wheat cultivars,

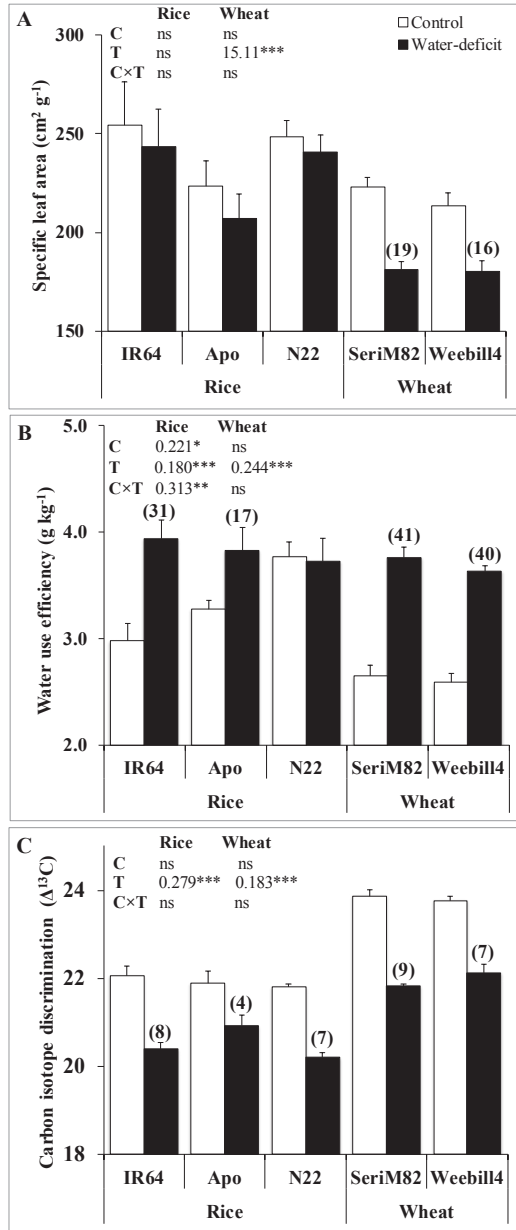


Figure 2: Specific leaf area (**Panel A**), whole-plant water use efficiency (**Panel B**), and carbon isotope discrimination ($\Delta^{13}\text{C}$; **Panel C**) of rice and wheat. In the figure, the white column represents control and dark water-deficit stress. Values in parentheses represent the significant percentage change (increase or decrease) over the control. The analysis of variance results with least significant difference (LSD) value are given on panel for cultivar (C), treatment (T), and C×T interaction. Significance level: * $P < 0.05$, ** $P < 0.01$, *** $P < 0.001$.

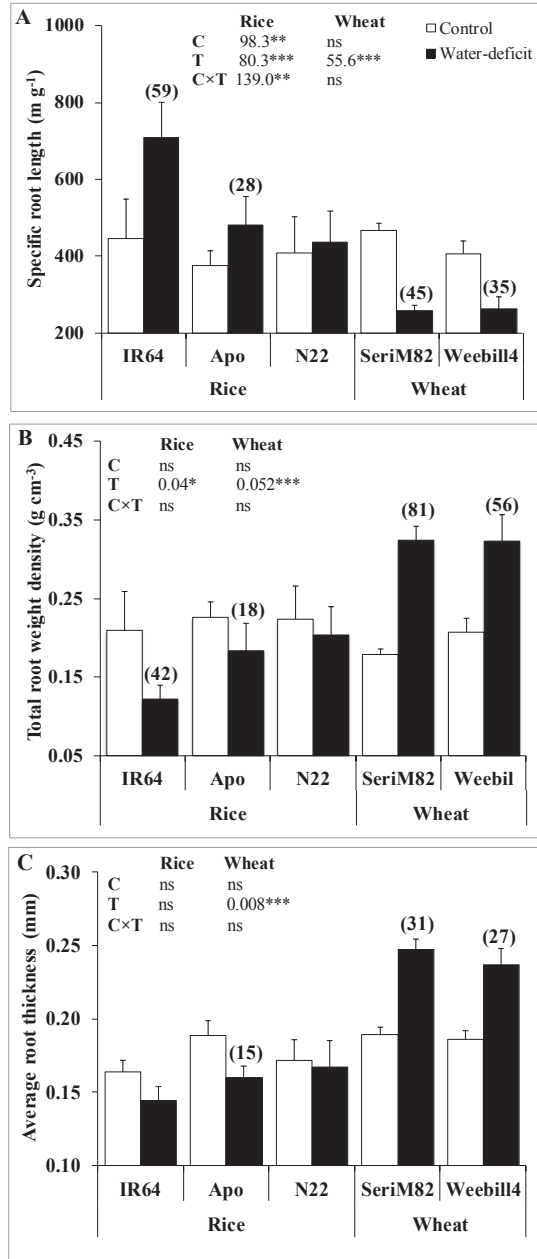


Figure 3: Specific root length (**Panel A**), total root weight density (**Panel B**), and average root thickness (**Panel C**) of rice and wheat. In the figure, the white column represents control and dark water-deficit stress. Values in parentheses represent the significant percentage change (increase or decrease) over the control. The analysis of variance results with least significant difference (LSD) value are given on panel for cultivar (C), treatment (T), and C×T interaction. Significance level: * $P < 0.05$, ** $P < 0.01$, *** $P < 0.001$.

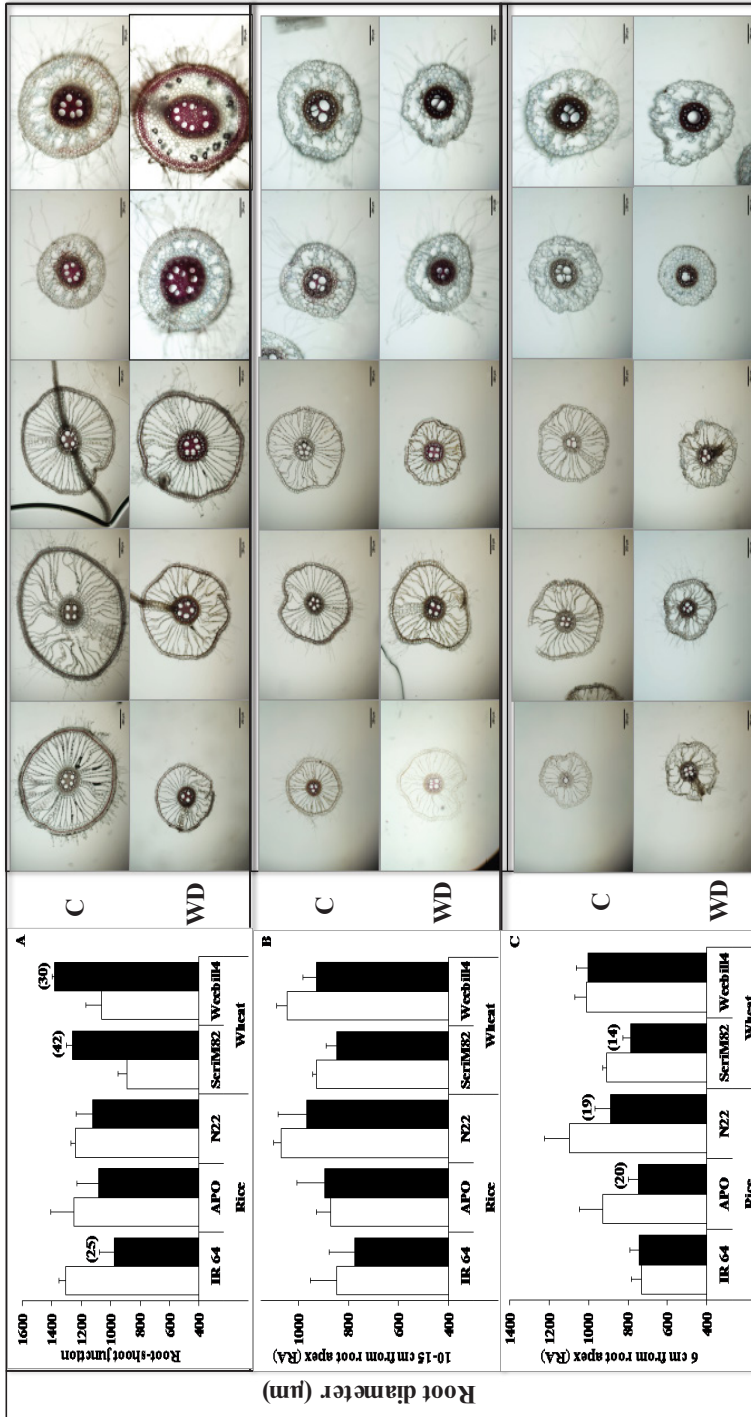


Figure 4: Root diameter at root-shoot junction (RSJ; **Panel A**), 10 to 15 cm from root apex (RA, **Panel B**), and 6 cm from RA (**Panel C**) on nodal roots of rice and wheat cultivars. In the figure, the white column represents control (C) and dark water-deficit stress (WD). Values in parentheses represent the significant percent change (increase or decrease) over the control value. Scale bar on each image=200µm.

with SeriM82 (52%) showing a greater increase than Weebill4 (33%; Fig. 5A). Stele diameter responded in an opposite manner with a strong reduction at two other positions on roots (10 to 15 cm and 6 cm from the root apex) in SeriM82 and at 10 to 15 cm from RA only for Weebill4 (Fig. 5B-C).

Stele diameter in proportion to root diameter (SD:RD) was strongly affected by water-deficit stress in rice ($P<0.001$) and lacked cultivar and tissue position variation on nodal roots. By contrast, wheat cultivars documented a significant variation along the root tissue position ($P<0.001$) and its interaction with treatment ($P<0.05$; Supplementary Table S3). Wheat cultivars maintained higher SD:RD (~35 to 40%) than rice cultivars (~20 to 25%) across three root positions sectioned (Fig. 6). An increasing trend with SD:RD was observed in response to water-deficit stress in all three rice cultivars (Fig. 6), but this was least affected by water-deficit stress in wheat, except for a noticeable reduction at 10 to 15 cm from RA for SeriM82 (Fig. 6B).

Late metaxylem diameter and number

Late metaxylem diameter (LMXD) remained relatively constant in rice cultivars across different root tissue positions under both control and water-deficit stress, with a narrow variation ($P<0.05$) recorded among cultivars (Supplementary Table S3). The effect of water-deficit stress on LMXD was not significant, but a decreasing trend was observed across all three rice cultivars near the RSJ (Fig. 7A). Late metaxylem number (LMXN) varied significantly with root tissue position ($P<0.01$), cultivar, and treatment ($P<0.05$) in rice. Among rice cultivars, lowland-adapted IR64 had lower LMXN at 6 cm from RA in non-stress conditions, but, upon exposure to stress, LMXN increased significantly and was like that of other cultivars (Fig. 7F). Unlike in rice, LMXD varied with cultivar and tissue position and their interaction in wheat ($P<0.001$; Supplementary Table S3). In both control and water-deficit stress, wheat cultivars maintained higher LMXD at 10 to 15 cm from RA and at 6 cm from RA compared with RSJ, except for SeriM82 recording a 28% lower LMXD at 10 to 15 cm from RA under water-deficit stress (Fig. 7B). LMXD increased greatly in both wheat cultivars at 6 cm from RA under water-deficit stress exposure, with the increase being higher in Weebill4 (51%) than in SeriM82 (30%; Fig. 7C). Additionally, LMXN displayed strong interaction between treatment and tissue position ($P<0.001$). Exposure to water-deficit stress resulted in an increase in LMXN at RSJ in wheat cultivars (Fig. 7D), but this decreased at two other positions, with a highly significant reduction observed at 6 cm from RA (Fig. 7E-F). According to Hagen-

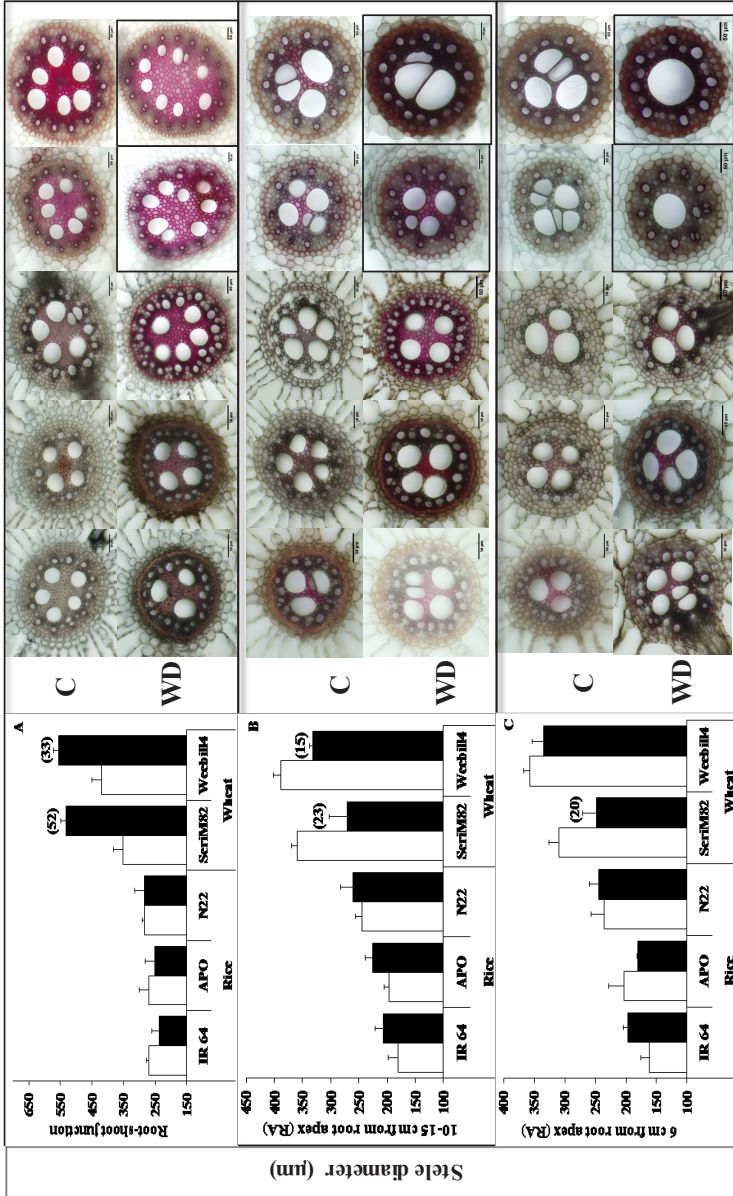


Figure 5: Stile diameter at root-shoot junction (**Panel A**), 10 to 15 cm from root apex (**RA**, **Panel B**), and 6 cm from RA (**Panel C**) on nodal roots of rice and wheat. In the figure, the white column represents control (**C**) and dark water-deficit stress (**WD**). Values in parentheses represent the significant percentage change (increase or decrease) over the control value. Scale bar in each image=50µm.

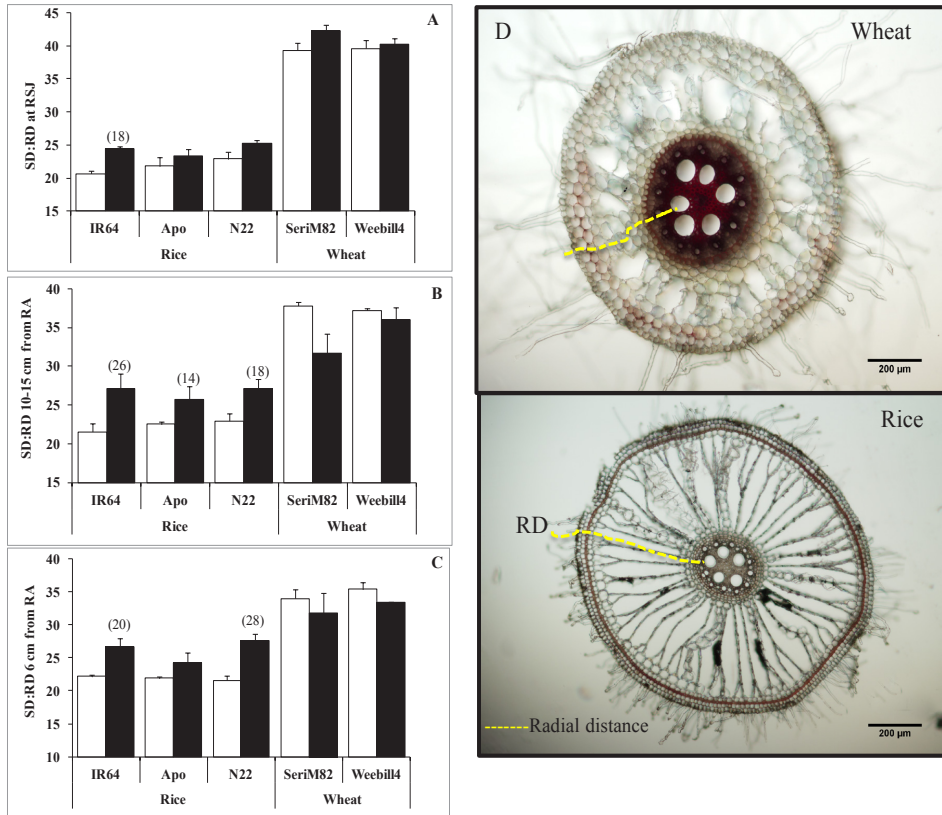


Figure 6: Stele diameter in proportion to root diameter (%) (SD:RD) at root-shoot junction (RSJ, **Panel A**), 10 to 15 cm from root apex (RA, **Panel B**), and 6 cm from RA (**Panel C**) on nodal roots of rice and wheat. In the figure, the white column represents control and dark water-deficit stress. A pictorial representation of radial distance in rice and wheat (**Panel D**). Values in parentheses represent the significant percentage change (increase or decrease) over the control value. Scale bar in image=200μm.

Poiseuille's law, the flow of water in any given conduit is the fourth power of the radius of the conduit. Theoretically calculated axial conductance by modified Hagen-Poiseuille's law also followed a pattern like that of LMXD across three different positions on nodal roots in both species (Fig. 8).

Discussion

We compared rice and wheat for their adaptive responses in root morphology and anatomy to water-deficit stress. Findings from our study are discussed below.

Reduced specific leaf area is a determining factor for increased water use efficiency under stress in wheat

Reducing SLA in response to water-deficit stress to conserve water has been documented across crop species (Rao and Wight, 1994; Araus et al., 1997; Craufurd et al., 1999; Nautiyal et al., 2002), and the same was observed with wheat cultivars (Fig. 2A). Increased WUE under water-deficit conditions is well known (Blum, 2009). Our results also documented increased WUE with cultivars of both species except for rice cultivar N22 under water-deficit stress; in wheat, this increased WUE (Fig. 2B) could be due to reduced SLA. Variation in $\Delta^{13}\text{C}$ is determined by the balance between stomatal conductance (g_s) and carboxylation efficiency (Farquhar et al., 1989). Both species had a comparable reduction in $\Delta^{13}\text{C}$ in water-deficit stress (Fig. 2C), but possibly for different reasons. Lower SLA leads to higher carboxylation rate, but under water-deficit condition limitation of g_s also reduces photosynthesis. Therefore, reduced $\Delta^{13}\text{C}$ under water-deficit stress in wheat could be due to both lower g_s and higher carboxylation rate (cf. Condon et al., 1990), but in rice due to lower g_s only.

Specific root length displays opposing responses among rice and wheat cultivars under water-deficit stress

SRL captures the overall effect of both root thickness and root weight density (Fitter, 2002). In our study, SRL increased under water-deficit stress in rice cultivars (IR64 and Apo) because of reduced average root thickness, while lower SRL in wheat cultivars resulted from increased average root thickness and total root weight density (Fig. 3). Our results suggest that rice cultivars (except for N22) aimed for rapid water acquisition strategy, since thinner roots (higher SRL) increase overall root hydraulic conductance by exploring more soil volume for water and enabling rapid uptake of water (Reich et al., 1998; Eissenstat and Achor, 1999; Solari et al., 2006, Hernandez et al., 2010). This strategy could lead to higher susceptibility to water-deficit stress due to quicker water depletion (Ryser, 2006). On the other hand, the two wheat cultivars employed a conservative strategy by developing thicker roots and exploring less soil volume for water by reducing root length density. Thicker roots enhance soil penetrating ability to access deeper layers in drying soil conditions (Davis and Bacon, 2003). This can be substantiated by our results on maximum root length. Although full potential to express maximum root length of wheat could be influenced by limited pot size in our study, it however increased in response to water-deficit stress in wheat, while this was not the case with rice (Supplementary Table S2; Supplementary Figure S2). Among the rice cultivars, tolerant N22

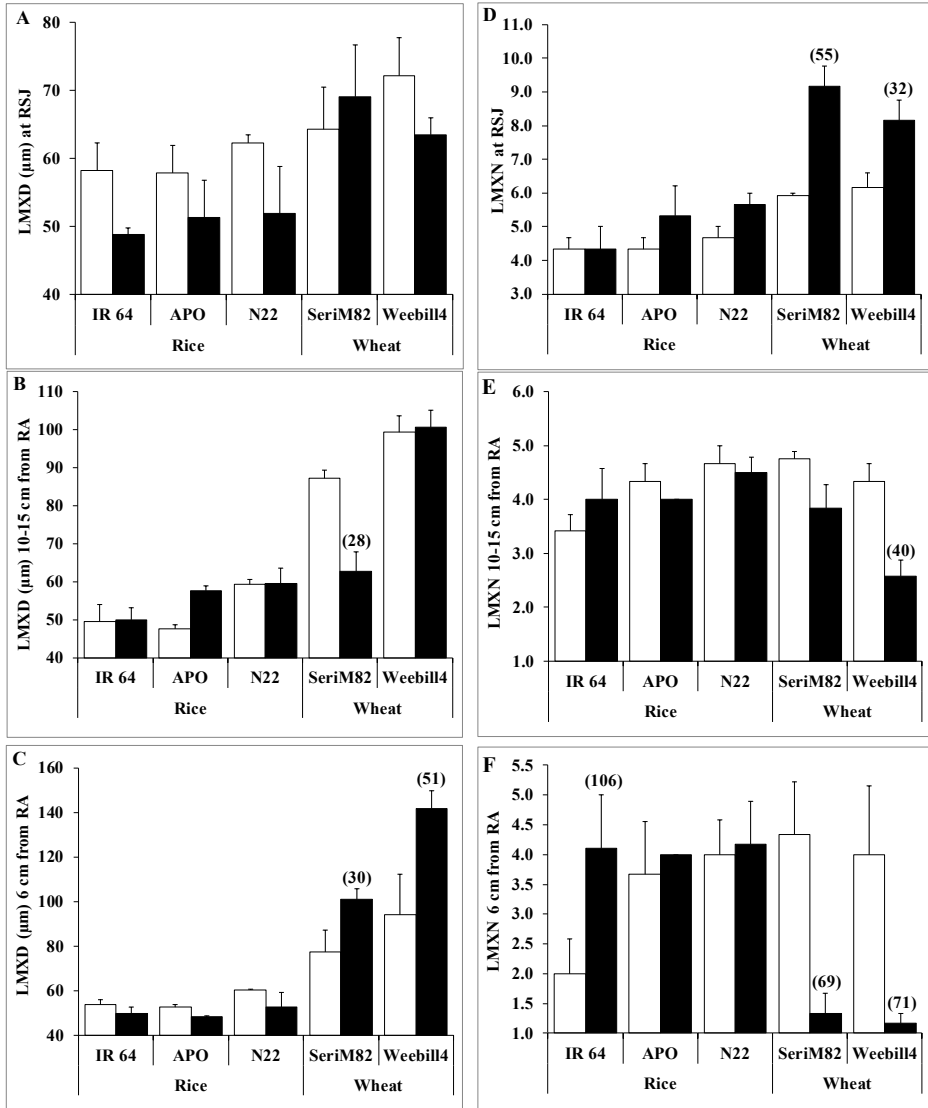


Figure 7: LMXD and LMXN at RSJ (Panels A & D), 10 to 15 cm from root apex (RA, **Panels B & E**), and 6 cm from RA (**Panels C & F**) on nodal roots of rice and wheat (mean \pm SE). White column represents control and dark water-deficit stress. Values in parenthesis represent the significant percentage change (increase or decrease) over the control value.

followed a conservative strategy by reducing root length density (Supplementary Table S2), but, unlike wheat, it lacked plasticity in SRL, average root thickness, and total root weight density (Fig. 3).

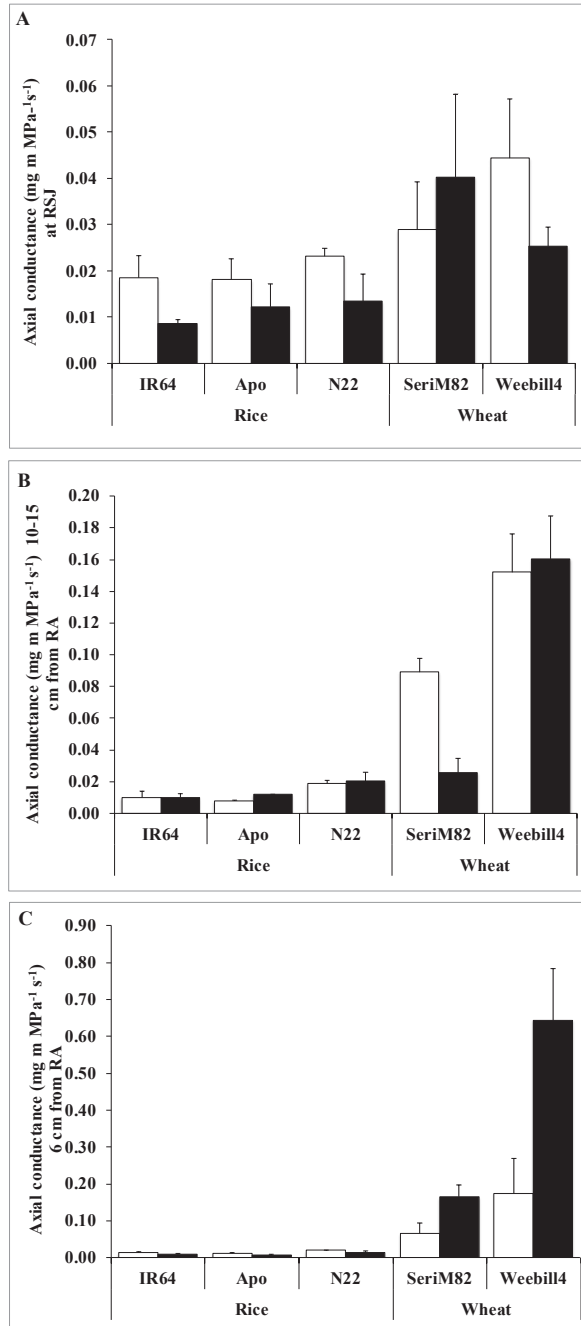


Figure 8: Theoretically calculated axial hydraulic conductance at root-shoot junction (RSJ) (**Panel A**), 10 to 15 cm from root apex (RA, **Panel B**), and 6 cm from RA (**Panel C**) on nodal roots of rice and wheat cultivars. In the figure, the white column represents control and dark water-deficit stress.

Stele diameter was more responsive to water-deficit stress in wheat than in rice

The proportion of stele diameter to root diameter (SD:RD) provides an indirect measure of cortex tissue area/width. The stele size and SD:RD are lower in wetland than in dry-land plants (McDonald et al., 2002), and our result confirms this difference between rice and wheat (Figs. 5-6). This anatomical feature in wetland species aims to optimize the consumption of O₂ under water-logging (Armstrong and Becket, 1987; Armstrong et al., 1991; Aguilar, 1998). A distinct sclerenchyma layer as an apoplastic barrier to impede radial oxygen loss was observed in rice, even in the absence of water-logging (Supplementary Figure S3). These root anatomical features in rice have an advantage under flooded conditions, but could affect root water uptake. An inverse relationship between overall radial hydraulic conductance and cortex width has been documented (Rieger and Litvin, 1999). Radial hydraulic conductance is lower in rice than in other cereals (Miyamoto et al., 2001), possibly because of larger aerenchyma in the cortex (Ranathunge et al., 2003). There was a significant position effect on the stele tissue, with higher stele diameter at the RSJ than at the other two positions (10 to 15 cm and 6 cm from RA) in both species but more conspicuously with wheat (Figs. 5-6). Although the exact eco-physiological significance of such gradient in stele tissue is unclear, it could play an important role in maintaining water uptake by improving internal aeration of roots, particularly near the root tip. The availability of O₂ is known to decrease with increasing depth of the soil and smaller stele tissue tends to prevent O₂ deficiency to support uninterrupted xylem transport (Gibbs et al., 1998). Further, water uptake by a region close to the root tip appears to be a predominant feature of all cereal roots (Greacen et al., 1976). An increased stele diameter near the RSJ in wheat may play a supportive role in water transport rather than in direct water uptake, but smaller stele diameter at the other two positions near the root apex (Fig. 5) could help in maintaining water uptake under stress. Contrary to this, stele diameter did not differ significantly under water-deficit in rice, but increasing trends of SD:RD were documented across all three positions along the root (Fig. 6). A similar increased SD:RD under water-deficit stress was previously identified in rice (Henry et al., 2012). The above response demonstrates the attempt of rice to reduce radial distance under water-deficit stress by decreasing cortex width (i.e. an increase in SD:RD without changing stele diameter) to improve radial hydraulic conductance (see Fig. 6D, pictorial representation of radial distance in rice & wheat). Together, the observed variation in root diameter under water-deficit in wheat was mostly due to a change in stele diameter, but in rice it was due to variation in cortex width (Fig. 4). Both wheat cultivars and the tolerant rice cultivar N22 maintained higher stele diameter, substantiating its role in

water-deficit stress adaptation.

Xylem developmental plasticity was more responsive to water-deficit stress in wheat than in rice

The development of late metaxylem diameter (LMXD) and number (LMXN) varied strongly along the root length in wheat, with lower xylem diameter but a higher number near the RSJ and higher diameter but a lower number at 10 to 15 cm from RA and 6 cm from RA. Unlike in wheat, xylem diameter and number were least affected by either water-deficit stress or along the three different positions in rice roots (Fig. 7). Bulk flow of water or axial conductance is known to be closely related to the cross-sectional area or diameter of xylem vessels (Niklas, 1985). Hence, wheat cultivars would have higher water uptake than rice cultivars because of higher xylem diameter (Fig. 7), which was confirmed with calculated axial conductance (Fig. 8). Recently, it has been hypothesized that combining low axial conductance (narrow xylem diameter) at the base of the root system (i.e. closer to the RSJ) with higher axial conductivity (higher xylem diameter) near the root tips in deeper soil facilitates effective water use until flowering and grain development (Wasson et al., 2012). This is a pilot report, showing such a developmental gradient in xylem diameter along the root length in both wheat cultivars and it was confirmed with calculated axial hydraulic conductance. A large proportion of the lateral roots are generally developed towards the RSJ part compared to the root tip (Bramley et al., 2009). Therefore, under water-deficit stress increase in LMXN near the RSJ can help increase uptake of water by lateral roots from the top soil layers, but a strong decrease at the root tip (6 cm from RA) to conserve moisture in lower soil profiles. In summary, the response of xylem diameter and number to water-deficit stress in wheat was a novel finding and this provides additional mechanistic understanding of wheat root plasticity toward adapting to water-deficit stress.

Conclusion

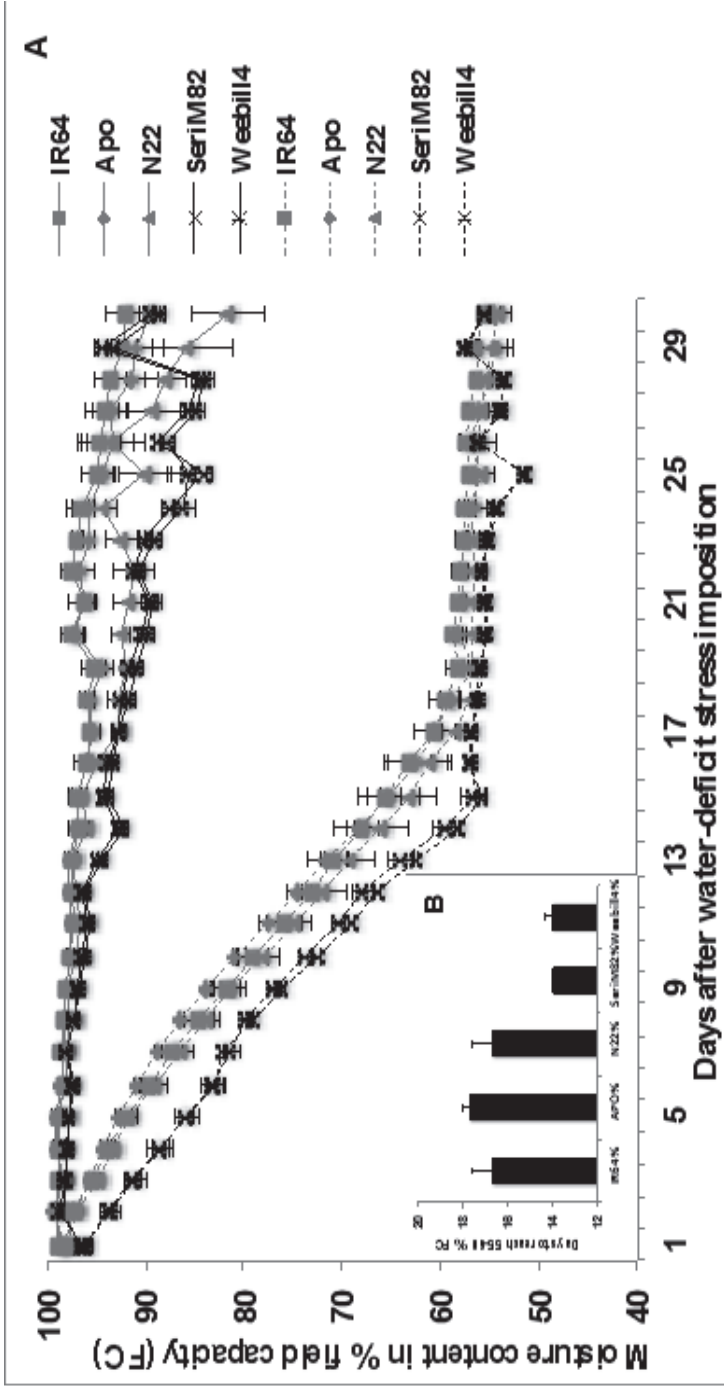
A comprehensive analysis of two diverged species, one adapted to flooded conditions and the other to aerobic conditions, allowed us to demonstrate the functional role of organ/tissue plasticity for adapting to water-deficit stress. Both wheat cultivars had thicker leaves and roots and moderate tillering that help conserve soil moisture during vegetative-stage water-deficit stress (see summarized responses in Table 1). Plasticity in stele and xylem diameter, and xylem number along the root length in wheat cultivars facilitates efficient use of available moisture

under water-deficit stress. Therefore, future studies should aim towards establishing the relationship between root morphology, anatomy with yield and yield components under water-deficit conditions.

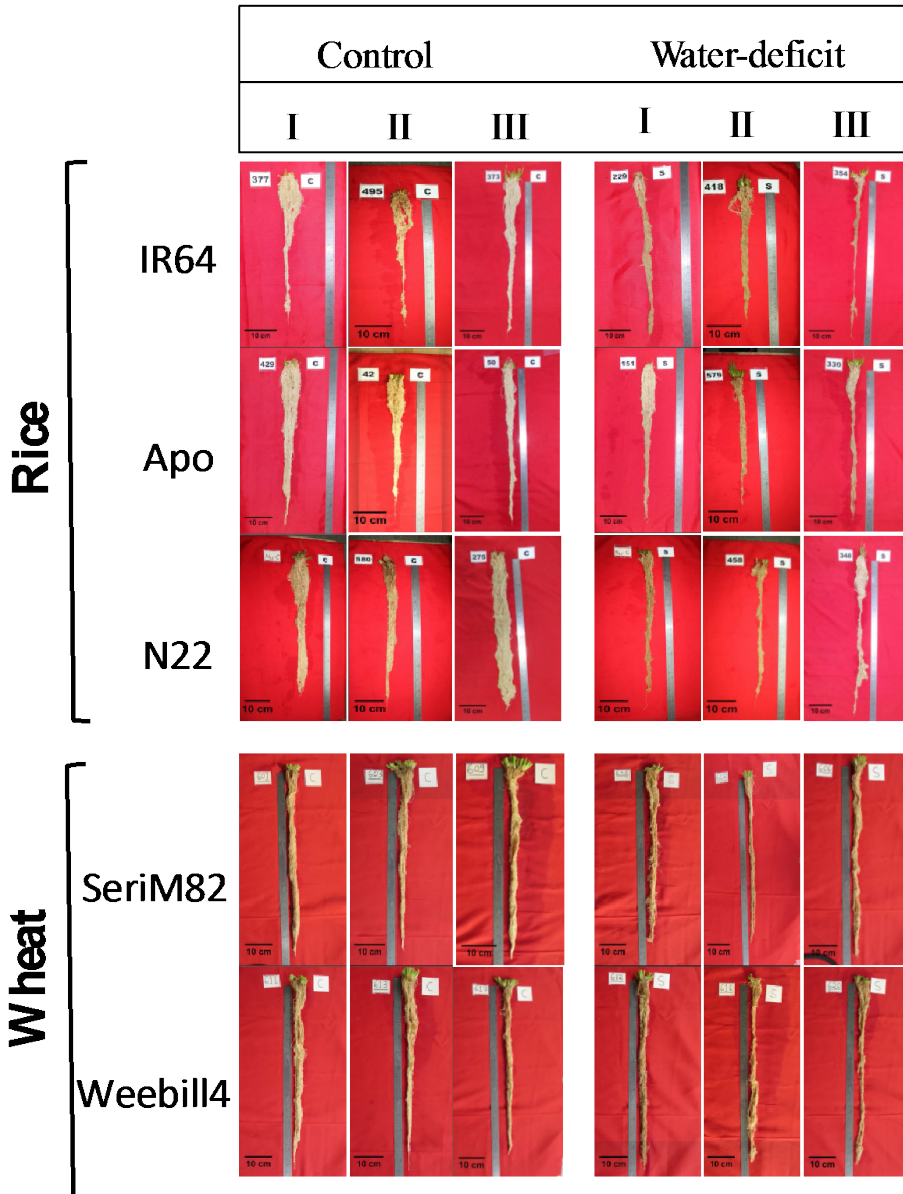
Table 1: Summary of adaptive changes in key morphological, physiological, and root anatomical traits in response to water-deficit stress of tolerant rice and wheat cultivars. (Signs: =: no change, +: increase, -: reduction in water-deficit), (+/- : <10%, +/- : >10 to 20%, +++/--- : >20 to 35%, ++++/---- : >35 to >50%).

	Rice				Wheat	
	Apo	N22	SeriM82	Weebill4		
Morphology						
Water deficit adaptive traits						
Shoot						
Tiller number	=	=	---	---		
Specific leaf area	=	=	---	---		
Root						
Root length density	=	---	---	---		
Specific root length	+++	=	---	---		
Average root thickness	--	=	+++	+++		
Total root weight density	--	=	+++	+++		
Physiology						
Whole-plant water use efficiency	++	=	+++	+++		
$\Delta^{13}C$	-	-	-	-		
Nodal root anatomy						
	Root tissue position					
Stele diameter						
	RSJ	=	=	+++		+++
	10-15 cm from RA	=	=	---		---
	6 cm from RA	=	=	---		---
Late metaxylem diameter						
	RSJ	=	=	=		=
	10-15 cm from RA	=	=	---		---
	6 cm from RA	=	=	+++		+++
Late metaxylem number						
	RSJ	+++	+++	+++		+++
	10-15 cm from RA	=	=	---		---
	6 cm from RA	=	=	---		---

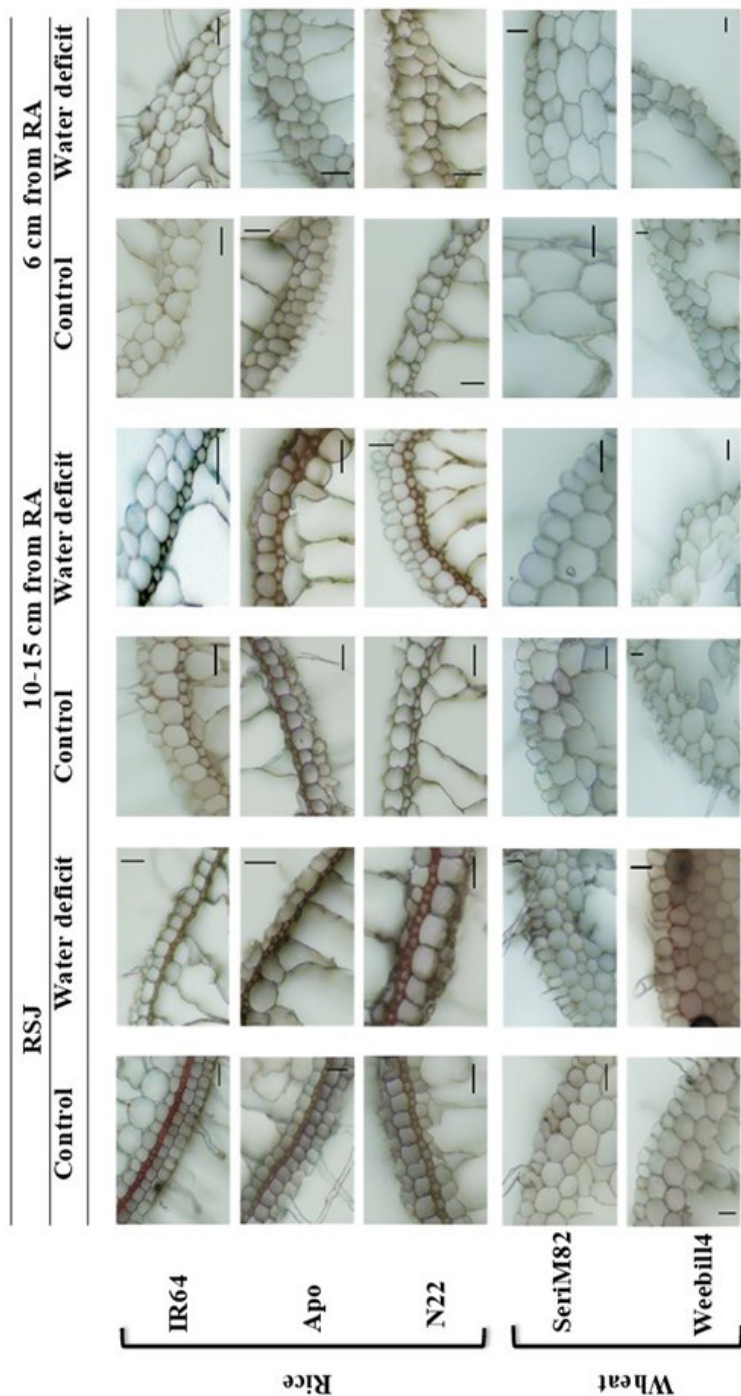
Supplementary information in Chapter 2



Supplementary Figure S1: rate of water depletion calculated based on pot weighing data for both rice (IR64, Apo, and N22) and wheat (SeriM82 and Weebil4) cultivars and expressed as moisture content in % field capacity (A). Number of days taken after stress imposition to reach the desired water-deficit stress expressed in % field capacity (FC) for both rice and wheat cultivars (B). Compared to rice, wheat cultivars reached the target-water-deficit stress (55-60 % FC) 3 days earlier but no cultivar differences were observed in either species.



Supplementary Figure S2: Maximum root length (MRL) of rice (IR64, Apo, and N22) and wheat (SeriM82 and Weebill4) cultivars under control and water-deficit stress. Figure consists of replicated images (n=3). Scale bar on each image represents=10 cm.



Supplementary Figure S3: Variation in sclerenchyma layer in different root zones of rice and wheat in control and water-deficit conditions. Scale bar on each image represents=30µm.

Supplementary Table S1: Tiller number, total biomass, cumulative water transpiration, and biomass partitioning to various organs (leaf, stem, and root) of rice and wheat cultivars in control and water-deficit conditions. Values in table represent mean±SE and analysis of variance result with least significant difference (LSD) for each trait.

Species	Cultivar	Treatment	TLA	TN	TB	CWT	LWR	SWR	RWR
Rice	IR64	Control	1282±178	19.67±4.48	10.50±1.98	3.49±0.60	0.495±0.008	0.408±0.015	0.097±0.010
	IR64	Water-deficit	855±149	18.67±1.45	8.36±1.06	2.15±0.35	0.416±0.012	0.505±0.010	0.079±0.002
	N22	Control	2544±347	21.00±2.52	23.78±2.83	6.35±0.92	0.431±0.027	0.473±0.023	0.096±0.012
	N22	Water-deficit	1120±238	16.67±1.86	10.94±1.90	2.89±0.39	0.423±0.027	0.465±0.011	0.111±0.016
	APO	Control	1451±106	14.33±1.86	13.24±2.00	4.02±0.55	0.502±0.016	0.401±0.009	0.098±0.008
	APO	Water-deficit	1007±188	13.33±1.20	10.02±1.44	2.65±0.47	0.481±0.017	0.433±0.012	0.085±0.007
Wheat	SeriM82	Control	2005±254	34.67±2.19	18.45±1.41	6.94±0.36	0.488±0.048	0.364±0.033	0.147±0.016
	SeriM82	Water-deficit	1077±68	23.67±2.33	12.50±0.01	3.32±0.10	0.475±0.016	0.365±0.013	0.160±0.004
	Weebil4	Control	2261±26	29.67±1.20	19.55±0.84	7.55±0.55	0.543±0.016	0.313±0.006	0.143±0.010
	Weebil4	Water-deficit	1085±121	18.33±2.40	12.03±1.04	3.30±0.26	0.499±0.008	0.347±0.006	0.155±0.014
LSD ($P < 0.05$)									
Rice	Cultivar (C)		297.0 ^{***}	4.417 [*]	2.721 ^{***}	0.838 ^{**}	0.031 ^{**}	0.028 ^{**}	0.018 ^{ns}
	Treatment (T)		242.5 ^{***}	3.606 ^{ns}	2.222 ^{***}	0.684 ^{***}	0.026 [*]	0.023 ^{**}	0.015 ^{ns}
	C×T		420.0 ^{**}	6.246 ^{ns}	3.849 ^{**}	1.185 [*]	0.045 ^{ns}	0.040 ^{**}	0.026 ^{ns}
Wheat	Cultivar (C)		380.1 ^{ns}	5.840 ^{ns}	1.681 ^{ns}	0.690 ^{ns}	0.067 ^{ns}	0.047 ^{ns}	0.026 ^{ns}
	Treatment (T)		380.1 ^{**}	5.840 ^{**}	1.681 ^{***}	0.690 ^{***}	0.067 ^{ns}	0.047 ^{ns}	0.026 ^{ns}
	C×T		537.5 ^{ns}	8.260 ^{ns}	2.377 ^{ns}	0.976 ^{ns}	0.095 ^{ns}	0.067 ^{ns}	0.036 ^{ns}

TLA=total leaf area (cm² plant⁻¹), TN=tiller number per plant, TB=total biomass (g plant⁻¹), CWT=cumulative water transpiration (kg plant⁻¹), ¹³C=carbon isotope discrimination, LWR=leaf weight ratio [g (leaf) g⁻¹ (plant)], SWR=stem weight ratio [g (stem) g⁻¹ (plant)], RWR=root weight ratio [g (root) g⁻¹ (plant)]. **Significance level:** * $P < 0.05$, ** $P < 0.01$, *** $P < 0.001$, ns=non-significant, SE=standard error.

Supplementary Table S2: Root morphological attributes of rice and wheat in control and water-deficit conditions. Values in table represent mean±SE and analysis of variance result with least significant difference (LSD) for each trait.

Species	Cultivar	Treatment	MRL	TRL	RLD	RV	RB
Rice	IR64	Control	46.83±6.93	0.49±0.19	5.85±2.27	10.46±4.07	1.00±0.19
	IR64	Water-deficit	51.72±6.83	0.46±0.06	5.48±0.69	7.51±0.38	0.66±0.10
	N22	Control	53.3±1.21	0.97±0.31	11.7±3.78	22.94±5.37	2.35±0.53
	N22	Water-deficit	55.03±3.49	0.57±0.22	6.83±2.70	11.98±3.01	1.24±0.31
APO	Control	52.6±5.83	0.49±0.10	5.95±1.20	15.47±2.48	1.31±0.23	
	Water-deficit	51.73±2.61	0.42±0.11	5.12±1.36	8.64±1.88	0.85±0.14	
Wheat	SeriM82	Control	55.67±3.18	1.26±0.14	15.11±1.63	37.41±4.37	2.72±0.38
	SeriM82	Water-deficit	64.33±0.88	0.52±0.03	06.21±0.35	26.15±2.75	2.00±0.04
	Weebill4	Control	61±2.08	1.12±0.05	13.52±0.62	33.35±2.55	2.81±0.32
	Weebill4	Water-deficit	64±2.65	0.48±0.04	05.78±0.46	22.27±2.11	1.86±0.24
LSD ($P<0.05$)							
Rice	Cultivar (C)		6.60 ^{ns}	0.286 ^{ns}	3.440 ^{ns}	5.052 [*]	0.486 ^{**}
	Treatment (T)		5.39 ^{ns}	0.233 ^{ns}	2.809 ^{ns}	4.125 ^{**}	0.397 ^{**}
	C×T		9.34 ^{ns}	0.404 ^{ns}	4.865 ^{ns}	7.144 ^{ns}	0.687 ^{ns}
Wheat	Cultivar (C)		5.12 ^{ns}	0.172 ^{ns}	2.065 ^{ns}	5.550 ^{ns}	0.472 ^{ns}
	Treatment (T)		5.12 [*]	0.172 ^{***}	2.065 ^{***}	5.550 ^{**}	0.472 ^{**}
	C×T		7.24 ^{ns}	0.243 ^{ns}	2.920 ^{ns}	7.840 ^{ns}	0.667 ^{ns}

MRL=maximum root length (cm), TRL=total root length (km plant⁻¹), RLD=root length density (cm cm⁻³), RV=root volume (cm³), RB=root biomass (g plant⁻¹). **Significance level:** * $P<0.05$, ** $P<0.01$, *** $P<0.001$, ns=non-significant, SE=standard error.

Supplementary Table S3: Analysis of variance results for nodal root anatomical traits in rice and wheat. Values in table represent least significant difference (LSD) for each trait.

Rice	RD	SD	LMXD	LMXN	SD:RD	AC
Cultivar	108.3*	21.11***	4.239*	0.647*	1.262 ^{ns}	0.0040**
Treatment	088.5**	17.24 ^{ns}	3.461 ^{ns}	0.528*	1.030***	0.0033*
Tissue position	108.3***	21.11***	4.239 ^{ns}	0.647**	1.262 ^{ns}	0.0040
Cultivar×Treatment	153.2 ^{ns}	29.86 ^{ns}	5.995 ^{ns}	0.914 ^{ns}	1.785 ^{ns}	0.0057
Cultivar×Tissue position	187.6 ^{ns}	36.57 ^{ns}	7.342 ^{ns}	1.120 ^{ns}	2.186 ^{ns}	0.007
Treatment×Tissue position	153.2 ^{ns}	29.86 ^{ns}	5.995 ^{ns}	0.914 ^{ns}	1.785 ^{ns}	0.0057*
Cultivar×Treatment×Tissue position	265.4 ^{ns}	51.72 ^{ns}	10.383 ^{ns}	1.584 ^{ns}	3.091 ^{ns}	0.0099
Wheat						
Cultivar	066.5***	22.20***	8.92***	0.664 ^{ns}	2.122 ^{ns}	0.062***
Treatment	066.5 ^{ns}	22.20 ^{ns}	8.92 ^{ns}	0.664 ^{ns}	2.122 ^{ns}	0.062**
Tissue position	081.4***	27.18***	10.93***	0.814***	2.599***	0.0759***
Cultivar×Treatment	094.0 ^{ns}	31.39 ^{ns}	12.62 ^{ns}	0.940 ^{ns}	3.001 ^{ns}	0.0877*
Cultivar×Tissue position	115.1 ^{ns}	38.44 ^{ns}	15.45*	1.151 ^{ns}	3.675 ^{ns}	0.0074**
Treatment×Tissue position	115.1***	38.44***	15.45***	1.151***	3.675*	0.107***
Cultivar×Treatment×Tissue position	162.0 ^{ns}	54.37 ^{ns}	21.85 ^{ns}	1.627 ^{ns}	5.197 ^{ns}	0.152*

RD=root diameter (µm), SD=stele diameter (µm), LMXD=late metaxylem diameter (µm), LMXN=late metaxylem number, SD:RD=stele diameter in proportion to root diameter (%), AC=axial conductance (mg m MPa⁻¹ s⁻¹). **Significance level:** *P<0.05, **P<0.01, ***P<0.001, ns= non-significant.

Genetic control of plasticity in root morphology and anatomy of rice in response to water-deficit

Niteen N. Kadam^{1,2}, Anandhan Tamilselvan^{1,3}, Lovely M. F. Lawas¹, Cheryl Quinones¹,
Rajeev N. Bahuguna¹, Michael J. Thomson^{1,4}, Michael Dingkuhn¹, Raveendran Muthurajan³,
Paul C. Struik², Xinyou Yin², Krishna S.V. Jagadish^{1,5}

¹International Rice Research Institute (IRRI), DAPO, Box 7777, Metro Manila, Philippines

²Centre for Crop Systems Analysis, Department of Plant Sciences, Wageningen University &
Research, PO Box 430, 6700 AK Wageningen, The Netherlands

³Tamil Nadu Agricultural University, Coimbatore, Tamil Nadu, India

⁴Department of Soil and Crop Sciences, Texas A & M University, Texas, USA

⁵Department of Agronomy, Kansas State University, Manhattan, USA

Abstract

Elucidating the genetic control of rooting behaviour under water-deficit stress is essential to breed climate-robust rice (*Oryza sativa* L.) cultivars. Using a diverse panel of 274 *indica* genotypes grown under control and water-deficit conditions during vegetative growth, we phenotyped 35 traits, mostly related to root morphology and anatomy, involving ~45,000 root scanning images and nearly ~25,000 cross-sections from the root-shoot junction. Phenotypic plasticity of these traits was quantified as the relative change in trait value under water-deficit compared to control conditions. We then carried out a genome-wide association analysis on these traits and their plasticity, using 45,608 high quality single-nucleotide polymorphisms. One hundred four significant loci were detected for these traits under control condition, 106 were detected under water-deficit stress, and 76 were detected for trait plasticity. We predicted 296 (control), 284 (water-deficit stress) and 233 (plasticity) *a priori* candidate genes within linkage disequilibrium (LD) blocks for these loci. We identified key *a priori* candidate genes regulating root growth and development and relevant alleles that upon validation can help improve rice adaptation to water-deficit stress.

Keywords: *Oryza sativa* L., root plasticity, linkage disequilibrium, loci, *a priori* candidate genes, multi-locus analysis.

Introduction

Increasing water scarcity, caused by global climate change and increasing competition for available water resources, is a major constraint for crop production and global food security (Rosegrant et al., 2009). Rice (*Oryza sativa* L.) is the most important staple cereal. It requires two-three times more water than dryland cereals, as it is grown predominately under flooded paddy cultivation. Improving rice adaptation to water-deficit conditions could support developing dryland rice production systems, thereby reducing the dependence of rice on large volumes of water. Therefore, current rice breeding programmes are striving to develop cultivars that are productive under water-deficit conditions (Bernier et al., 2009; Kumar et al., 2014; Sandhu et al., 2014). This will require a suite of morphological, anatomical and physiological adjustments of shoot and root traits (Kadam et al., 2015; Sandhu et al., 2016). Interactions among these traits in response to water-deficit are complex, rendering effective knowledge-intensive breeding strategies.

To adapt to water-deficit stress, rice needs to be plastic. Phenotypic plasticity is a characteristic of a given genotype to produce a distinct phenotype in response to changing environments (Nicotra et al., 2010). Mostly, the plasticity of traits is desirable for better stress adaptation. Both natural and human selection have created many rice types that are sensitive and tolerant to water scarcity and have different levels of (desired or undesirable) plasticity. Climate change and increased water scarcity demand a new compromise among stress resistance, stress escape or avoidance, and potential productivity through phenotypic plasticity. Previous studies have shown the role of root trait plasticity in improving water-deficit stress adaptation. For instance, the plasticity of root-length density in water-deficit stress contributes to rice grain yield stability (Sandhu et al., 2016). Similarly, the comparative analysis between water-deficit tolerant rice and wheat (*Triticum aestivum* L.) has demonstrated the functional relevance of plasticity in shoot and root traits to better adapt to water-deficit stress (Kadam et al., 2015). However, phenotypic traits that express constitutively with no plasticity could also provide stress adaptation. For example, changes in the root angle during early development resulted in constitutive expression of deep root architecture that helps in later stages to increase rice grain yield under water-deficit (Uga et al., 2013).

Although phenotypic plasticity is heritable (Nicotra and Davidson, 2010), plasticity *per se* is usually not targeted when breeding rice for water-deficit conditions. Breeding for plasticity in traits other than yield would offer alternative routes to enhance resilience to stress conditions (Sambatti and Caylor, 2007) and to tap into a larger rice genetic diversity pool for adapting to

stressful environments (McCouch et al., 2013). The plasticity of traits is controlled by key environment-sensing genes (Juenger, 2013). Yet, no study has been undertaken to comprehensively demonstrate the quantitative variation in root and shoot plasticity and the underlying genetic control using diverse rice genotypes grown under water-deficit stress.

We report here a genome-wide association study (GWAS) in rice to unravel the genetic control of phenotypic traits in control and water-deficit stress and their plasticity. Given our diverse *indica* rice panel, which incorporates more evolutionary recombination events compared with biparental mapping populations (Ingvarsson and Street, 2011), we expect to detect phenotype associations with narrow genomic regions or even nearby/within causal genes. Specific objectives were (1) to assess natural genetic variability in root and shoot morphological and anatomical traits in control and water-deficit conditions and their plasticity as a relative change, (2) to associate genetic variation in root and shoot phenotypic plasticity with adaptive significance under water-deficit stress, and (3) to elucidate the genetic architecture of phenotypic traits and their plasticity by identifying the genomic loci with underlying *a priori* candidate genes.

Materials and Methods

Plant materials

For our GWAS study, we used a diverse collection of 274 genotypes covering traditional and improved *indica* rice sub-species, originating from major rice growing countries of tropical regions (Supplementary Figure S1 and Supplementary Data Set S1). This panel was carefully assembled at the International Rice Research Institute (IRRI) for the Phenomics of Rice Adaptation and Yield potential (PRAY) project for use in GWAS studies (Al-Tamimi et al., 2016; Rebolledo et al., 2016; Kikuchi et al., 2017) in the context of the GRiSP Global Rice Phenotyping Network (<http://ricephenonetwork.irri.org/>).

Stress imposition and plant growth conditions

A pot experiment was carried out in natural greenhouse conditions at the International Rice Research Institute (IRRI), for phenotyping root and shoot traits under two moisture regimes: (1) control, i.e., 100% field capacity (FC), which is defined as the maximum soil moisture content after draining excess water, and (2) water-deficit stress at 55 to 60% FC. The experiment was laid out in a randomized complete block design and replicated over three different time periods, due to space and labour constraints, during 2012 and 2013

(Supplementary Figure S2A). Before sowing, rice seeds were exposed to 50 °C for 3 days to break dormancy and pregerminated seeds were sown in white-coloured painted pots (55 cm long and 15 cm diameter) to minimize confounding effects of increasing temperature of pot surface and soil (Poorter et al., 2012). The pots were lined with polythene bags on the inside, filled with 11 kg of clay loam soil, and care was taken to avoid over compaction of the soil. Each pot had two holes at the bottom for imposing controlled stress. Water-deficit stress was imposed 15 days after seedling emergence (after ensuring healthy seedling establishment) and until then all pots were maintained at 100% FC (Supplementary Figure S2B). A standardized gravimetric approach of daily pot weighing (Kadam et al., 2015) was followed on 1649 (5 pots were empty to measure evaporation) pots to gradually attain 55 to 60% FC and thereafter maintained at the same level until the end of the experiment (Supplementary Figure S2C). Once the target stress level was reached, daily water loss due to evapotranspiration was replenished by adding back an exact amount of water to bring back the moisture content to the desired target in each pot. The soil surface was covered with a circular polythene sheet to protect direct evaporative loss of water and a slit across the radius of the polythene prevented heat build-up on the soil surface. Additionally, a set of soil-filled pots without a plant was also maintained to correct for evaporative loss of water from the opening created by slit in the circular shaped polythene sheet. Daily pot weights recorded for 30 consecutive days of stress period were used to calculate the daily evapotranspiration. After correcting for evaporative loss obtained from empty pots, actual transpiration was calculated. Finally, daily actual transpiration was summed for the 30-day period to calculate cumulative water transpired. Whole plant water use efficiency (g kg^{-1}) was calculated as a ratio of total weight (root and shoot) to cumulative water transpired. Air temperature and humidity were constantly measured at 10-minute intervals by sensors installed in the greenhouse. The average daily temperature (day and night) and air humidity were recorded (Supplementary Figure S2D).

Shoot and root harvesting

After 30 days of water-deficit stress exposure, plants were harvested at 45 days after sowing and tiller numbers were counted and total leaf area was estimated by a leaf area meter (Li-3000, LI-COR, Lincoln, NE, USA). Leaves and stems were separately oven-dried at 70 °C for 72 h to compute the specific leaf area and shoot weight. The entire column of soil along with the roots was placed on a large 1 mm sieve and meticulously washed using a gentle stream of water to minimize the loss of small roots and root hairs.

A strong plasticity in wheat root anatomy primarily near root-shoot junction (RSJ) and root tips under water-deficit stress has been confirmed following a similar approach (Kadam et al., 2015). Hence, three replicate root sections were collected near the RSJ (~7-10 cm) from control ($274 \times 3 = 822$) and water-deficit stressed ($274 \times 3 = 822$) samples (1644 samples). Collected samples were stored in 40% (v/v) alcohol to assess root anatomy. The remaining whole-plant root samples were placed in 20% (v/v) alcohol and stored at 4 °C for root scanning and image analysis.

Root image acquisition and processing in WinRHIZO

Root samples stored in 20% (v/v) alcohol were cut to smaller segments to fit the scanner tray and aligned vertically on scanning plates to avoid overlapping (Supplementary Figure S3). An eight-bit greyscale image was acquired by scanning with an Epson Perfection 7000 scanner at a resolution of 600 dots per inch next to a ruler. After capturing the images, root samples were oven dried at 70 °C for 72 h to record the root weight. In total, we captured ~45, 000 images from 274 genotypes across treatments and replications. The root morphological attributes such as total root length, average root thickness, root length classified based on root thickness, root volume, root surface area was computed by analysing images with WinRHIZO Reg 2012b (Supplementary Figure S3) software (http://regent.qc.ca/assets/winrhizo_about.html). To avoid underestimation of fine root lengths during image processing, the threshold that separates the roots and background was adjusted to automatic mode (Bouma et al., 2000).

Root anatomical study

To study the root anatomical parameters near root-shoot junction (~7-10 cm; Supplementary Figure S4), samples stored in 40% alcohol were hand sectioned with a razor blade under the dissection microscope. Images of root sections were acquired with Zeiss Axioplan 2 compound microscope (Zeiss, Germany) with 50× and 100× magnification. At least three to five root images per replicate were considered for measuring anatomical parameters such as root cross-section diameter, stele diameter and late meta xylem diameter, with image J software (Schneider et al., 2012).

Derived shoot, root and water uptake parameters

Average specific leaf area was calculated as the ratio of total leaf area to leaf dry weight. Ratios of leaf weight, stem weight and root weight to total weight were also calculated. Root length

density was calculated as the ratio of total root length to the soil volume in pot, and total root weight density was calculated as the ratio of root weight to root length density. Specific root length was calculated as the ratio of total root length to root weight. Root length per unit leaf area was calculated as the ratio of total root length to leaf area.

Calculation of phenotypic plasticity

The phenotypic plasticity of all traits was calculated as a relative change in water-deficit stress compared with control conditions, using the following formula (Sandhu et al., 2016).

$$\text{Phenotypic plasticity} = \frac{\text{stress} - \text{control}}{\text{control}}$$

To distinguish trait plasticity from the trait *per se*, all acronyms for plasticity starts with lowercase letter “r” (Table 1).

Statistical data analysis

The observed variation in a phenotypic trait can be partitioned to a source of variation in genotype (G), treatment (T) and their interaction (G×T). The analysis of variance was performed using mixed linear model (MLM) for each phenotypic trait in Genstat release 17.1, as defined by

$$y_{ijk} = \mu + G_i + T_j + (G \times T)_{ij} + r_{k(j)} + e_{ijk}$$

where y_{ijk} is the measured trait, μ is the overall mean, G_i is the effect of i^{th} genotype, T_j is the effect of j^{th} treatment, $(G \times T)_{ij}$ is the interaction between i^{th} genotype and j^{th} treatment, $r_{k(j)}$ is the effect of replication k within the j^{th} treatment and e_{ijk} is the random error. Genotypic and treatment effects were considered as fixed effect with their interaction (G×T term) in the model, and replications were treated as random effect. The best linear unbiased estimator (BLUE) value of each phenotypic trait was computed separately across treatments by MLM. The BLUE value of traits was later used for histograms, box plots, principal component analysis (PCA) and Pearson’s correlation analysis. The PCA analysis was performed in XLSTAT and correlation heat maps were compiled using the R package “corrplot” in R studio. The P values of correlation coefficient were calculated by two-sided t-test using the `cor.mtest` function in R and only significant ($P < 0.05$) correlation was plotted on the heat maps.

SNPs genotyping data

The studied panel is a large subset of 329 *indica* genotypes that were genotyped using the genotype-by-sequencing (GBS) protocol (Elshire et al., 2011) at Cornell University, USA. The reads were demultiplexed and aligned to the rice reference genome (Os-Nipponbare-Reference-IRGSP-1.0; Kawahara et al., 2013), and variants were identified using the NGSEP pipeline (Duitama et al., 2014). Missing data were imputed with the implementation of the Fast Phase Hidden Markov Model (Scheet and Stephens, 2006).

Two different datasets with different missing SNPs imputation from GBS data were recently used in GWAS analysis for this panel, i.e., the 90K SNPs dataset with 22.8% missing imputation by (Rebolledo et al., 2016) and the 45K SNPs dataset with 8.75% missing imputation by (Kikuchi et al., 2017). In addition, this panel was also genotyped with a 700K SNPs dataset and recently used in a GWAS (Al-Tamimi et al., 2016). However, only 240 out of 274 genotypes used in our study were overlapped with quality SNPs. Thus, we used the 45K SNPs data set with 8.75% missing imputation that was more precise than the 90K SNPs dataset with higher percentage of missing imputation. The original dataset contains 46,999 SNPs with minor allele frequency (MAF) ≥ 0.05 and 8.75% missing data for 329 genotypes. We selected the SNP data for 274 genotypes phenotyped in our study with another round of MAF (≥ 0.05) filtering resulting in the final dataset containing 45,608 SNPs. MAF ≥ 0.05 was used to reduce the spurious association caused by rare variants.

Single-locus genome-wide association analysis

The single-locus GWAS analysis was performed on 45,608 SNPs and phenotypic traits by compressed mixed linear model (CMLM; Zhang et al., 2010) in the Genomic Association and Prediction Integrated Tool (GAPIT; Lipka et al., 2012). We incorporated population structure (Q matrix as a PCA component) matrix (Supplementary Figure S5A-B) and family kinships (K) matrix (Supplementary Figure S6) calculated with 45,608 SNPs:

$$Y = X\alpha + P\beta + K\mu + e$$

where Y and X represent the vector of phenotype (BLUE) and genotype (SNP) respectively, P is the PCA matrix and K is the relative kinship matrix. $X\alpha$ and $P\beta$ are the fixed effects, and $K\mu$ is the random effect and e represents the random error. The P and K terms were introduced to correct for false-positive association. Although correction for the population structure substantially reduces false positives, it sometimes eliminates the true-positive association due to overcorrection (Zhao et al., 2011). Therefore, the optimal number of PCs were determined

for each trait before incorporating into CMLM, based on forward model selection using the Bayesian information criterion. Such statistical methods help to control both false positive and false negative associations effectively although they cannot eliminate both completely. Most of the root traits are complex polygenic in nature and we expected that the effect of the individual underlying loci would be small. Therefore, we chose a suggestive threshold of the probability P value $\leq 1.00E-04$ to detect significant associations, as followed recently for the same population (Rebolledo et al., 2016) and in many other rice GWAS studies (Zhao et al., 2011; Norton et al., 2014; Dimkpa et al., 2016). The similar threshold was also used in another GWAS study for rice root traits (Courtois et al., 2013).

Broad-sense and narrow-sense heritability

Phenotypic variance can be decomposed into variance caused by genetic and environmental factors. The broad sense heritability (H^2) is the proportion of phenotypic variance that is due to genetic variance. Genetic variance can be a result of additive, dominance or epistatic effects. The broad-sense heritability (H^2) of traits was calculated across each treatment using following equation.

$$H^2 = \frac{\sigma_G^2}{\sigma_G^2 + \frac{\sigma_E^2}{r}}$$

where σ_G^2 and σ_E^2 are the genotypic and residual variance respectively and r is the number of replications. The restricted maximum likelihood estimate was used to calculate the variance components in Genstat 17.1. The narrow-sense heritability is the proportion of phenotypic variance that is due to additive genetic variance. The marker-based narrow sense heritability (h^2) was obtained from above mentioned CMLM equation and was calculated using following equation in GAPIT.

$$h^2 = \frac{\sigma_a^2}{\sigma_a^2 + \sigma_e^2}$$

where σ_a^2 is the additive genetic variance and σ_e^2 is the residual variance.

Multi-locus genome wide association analysis

In addition to correcting the confounding effect of population structure (first three PCA components) and family kinships (K) matrix, multi-locus linear mixed model (MLMM) corrects the confounding effect of background loci may be present due to LD in the genome (Segura et al., 2012). This was done by explicitly using loci as cofactors in the statistical model,

similar to standard composite interval mapping of biparental analysis (Jansen and Stam, 1994). The multi-locus GWAS was implemented in the modified version of MLM in R studio (R script for `mlmm.cof.r` available at <https://cynin.gmi.oeaw.ac.at/home/resources/mlmm>). First, we ran the complete model as recommended with stepwise forward inclusion of the strongest significant markers as a cofactor until the heritability reached close to zero, and after that backward elimination of the least significant markers from the model was carried out with estimating the variance components and P values at each step (Segura et al., 2012). In the second step we checked the optimal model selection using the available criteria in MLM: (1) extended Bayesian information and (2) the multiple Bonferroni. However, both these criteria were too conservative to identify loci for most of the traits in our study and identified significant loci for very few traits (LMXN, RS, SW and SWR) only in water-deficit stress condition. Therefore, we checked the P value of markers at first step (similar to single locus GWAS analysis with no cofactor in the model) before including them as a cofactor and continued the model with inclusion of markers as a cofactor on an arbitrary cut-off significance threshold P value $\leq 1.00E-04$ as used in the single-locus GWAS analysis. The model was stopped when no significant loci appeared above the cut-off threshold P value and all significant cofactors with this approach were considered as significant genetic loci.

Linkage disequilibrium (LD) analysis

The pair wise LD was calculated for the whole panel using the correlation coefficient (r^2) between pairs of SNPs on each chromosome by setting the sliding window at 100 in TASSEL 5.0 (Bradbury et al., 2007). A total of 45,608 SNPs with $MAF \geq 0.05$ were considered for LD analysis. To investigate the LD decay rate, the r^2 values of the chromosome and average across the chromosomes representing the whole genome LD pattern were plotted against the physical distance (kb) among the markers. The LD decay rate was measured as the physical distance (kb) at which r^2 value drops to half of its initial value.

***A priori* candidate gene selections**

The variation in recombination rates (an essential determinant of LD structure) could have broken the chromosome into a series of discrete haplotype LD blocks that determined the actual resolution of association mapping. The upper limit of LD decay rate is ~ 500 kb in rice (Mather et al., 2007). Therefore, we selected ~ 0.5 to 0.6 Mb (total ~ 1.1 Mb) region on each side of the significant SNPs identified through GWAS analysis, to investigate the local LD pattern near to

the significant SNPs (Huang et al., 2010). The Haploview 4.2 program was used to calculate LD structure near the significant SNPs (Barrett et al., 2005) and visualize the discrete haplotype block in ~ 1.1 Mb region. The LD haplotype block harbouring the significant SNP or more than one significant SNPs was identified and considered as a unique significant locus. The known genes (genes with known annotation) located within LD blocks were collected. The closest Arabidopsis (*Arabidopsis thaliana* L.) orthologue genes were obtained from the MSU7 Rice genome database (<http://rice.plantbiology.msu.edu/cgi-bin/gbrowse/rice/>). All the genes described as a transposon and retro transposon were not selected and genes described as an expressed protein (EP) were considered only when there was relevant information available from Arabidopsis orthologue.

Results and Discussion

Genotypic variation in phenotypic traits and their interrelations

Rice exhibits large functional diversity due to strong natural and human selection pressure, which underlies evolutionary variation in traits inducing stress adaptation (McCouch et al., 2013). A set of 274 rice *indica* genotypes assembled from major rice growing regions across the world was evaluated to assess the variation in phenotypic traits (Supplementary Figure S1 and Supplementary Data Set S1). In total, 35 phenotypic traits, broadly classified into five categories (shoot morphology, whole-plant physiology, root morphology, root anatomy, and dry matter production), were evaluated on plants grown in control and water-deficit stress conditions during the vegetative phase (Table 1).

Genotypic variation observed in all traits across treatments was strong ($P \leq 0.001$), except in root length classes RL3035 and RL35 (Supplementary Table S1). The broad-sense heritability (H^2) ranged from 0.10 to 0.89 in the control and from 0.03 to 0.88 under water-deficit stress (Supplementary Table S2). A principal component analysis (PCA) identified eight significant principal components (PCs) with eigenvalue >1 , cumulatively explaining $> 80\%$ of the total variation for the 35 traits across the panel in each treatment (Supplementary Figure S7). The first PC, explaining more than 35% of the total variation, was associated with genotypic variation in most morphological (shoot and root), dry matter and cumulative water transpiration (CWT) traits in both treatments (Fig. 1A-B) and with substantial correlations among these traits (Supplementary Figure S8A-B). The second PC, explaining more than 12% of the total variation, was mainly associated with root anatomical traits but a portion of the variation was also accounted for by root morphological traits such as specific root length (SRL)

Table 1. The list of measured and derived phenotypic traits broadly classified into five categories (A-E) with trait acronyms and units.

Traits	Trait acronym	Unit	Phenotypic plasticity acronym
(A) Shoot morphological traits			
Plant height	PHT	cm	rPHT
Tiller number	TN	plant ⁻¹	rTN
Total leaf area	TLA	m ² plant ⁻¹	rTLA
Specific leaf area	SLA	m ² g ⁻¹	rSLA
(B) Physiological traits			
Cumulative water transpiration	CWT	kg plant ⁻¹	rCWT
Water use efficiency	WUE	g kg ⁻¹	rWUE
(C) Root morphological traits			
Total root length	TRL	m plant ⁻¹	rTRL
Root length (RL) with diameter (mm) class			
RL_0-0.5	RL005	m plant ⁻¹	rRL005
RL_0.5-1.0	RL0510	m plant ⁻¹	rRL0510
RL_1.0-1.5	RL1015	m plant ⁻¹	rRL1015
RL_1.5-2.0	RL1520	m plant ⁻¹	rRL1520
RL_2.0-2.5	RL2025	m plant ⁻¹	rRL2025
RL_2.5-3.0	RL2530	m plant ⁻¹	rRL2530
RL_3.0-3.5	RL3035	m plant ⁻¹	rRL3035
RL_3.5	RL35	m plant ⁻¹	rRL35
Maximum root length	MRL	cm	rMRL
Surface area	SA	cm ² plant ⁻¹	rSA
Root volume	RV	cm ³ plant ⁻¹	rRV
Average root thickness	ART	mm	rART
Specific root length	SRL	m g ⁻¹	rSRL
Total root weight density	TRWD	g cm ⁻³	rTRWD
Root length per unit leaf area	RLLA	m m ⁻²	rRLLA
(D) Root anatomical traits			
Root diameter	RD	μm	rRD
Cortex diameter	CD	μm	rCD
Stele diameter	SD	μm	rSD
Late metaxylem diameter	LMXD	μm	rLMXD
Late metaxylem number	LMXN	μm	rLMXN
Stele diameter in proportion of root diameter	SD:RD	%	rSDRD
(E) Dry matter traits			
Leaf weight	LW	g plant ⁻¹	rLW
Stem weight	SW	g plant ⁻¹	rSW
Root weight	RW	g plant ⁻¹	rRW
Total weight	TW	g plant ⁻¹	rTW
Root: shoot ratio	RS	-	rRS
Leaf weight ratio	LWR	-	rLWR
Stem weight ratio	SWR	-	rSWR

and two of its components: total root weight density (TRWD) and average root thickness (ART; Fig. 1A-B). Moreover, these root anatomical and morphological traits were correlated with each other. For instance, SRL showed a negative correlation with TRWD (on average $r = -0.87$), ART ($r = -0.73$), and all root anatomical traits ($r = \text{ca } -0.30$) in both treatments, except with late metaxylem number (LMXN) in control and stele diameter in proportion of root diameter

(SD:RD) in both control and stress (Supplementary Figure S8A-B). These results clearly indicate, that an increase in SRL could result in reducing the root thickness, stele diameter (SD) and late metaxylem diameter (LMXD). The first two components in control and water-deficit stress explained many of these complex relationships for most of the traits in this study (Fig. 1). In general, such relationships among traits might be due to pleiotropic or tightly linked genetic loci or gene, although that cannot be inferred directly from their positive and negative relationships.

High degree of trait variability in response to water-deficit stress underlies phenotypic plasticity

Phenotypic plasticity can have adaptive significance, while in some cases it can be an inevitable response under resource limitations (Nicotra et al., 2010). Significant treatment effects ($P < 0.001$) on all traits indicate expression of phenotypic plasticity under water-deficit stress. For most traits water-deficit stress resulted in lower values than observed for the control, with reductions ranging from 2 to 66%. Most of the root traits showed significant reductions. However, SRL, SD:RD, stem weight ratio (SWR), root length per unit leaf area (RLLA) and water use efficiency (WUE) were increased for plants grown under water-deficit stress than for plants under control conditions (Supplementary Table S1). Roots were thinner under water-deficit stress than under control conditions as indicated by SRL (22% increase over control) and two of its components TRWD (20% decrease) and ART (11% decrease; Fig. 2A-C).

The rice root anatomy is adapted to semiaquatic conditions with characteristic outer sclerenchymatous layer, large cortex diameter, small stele and xylem (Coudert et al., 2010; Kadam et al., 2015). However, to what extent natural and human selection has shaped root anatomical plasticity in response to water-deficit stress remains to be elucidated. In this study, all root anatomical traits showed phenotypic plasticity to stress treatment (T: $P < 0.001$) but lacked genotypic variability for plasticity (G×T: $P \geq 0.05$) (Supplementary Table S1 and Fig. 2D-I). Cortex diameter (CD) showed a strong response (18% decrease; Fig. 2E) with low level of plasticity for stele diameter (SD; 4% decrease, Fig. 2F), LMXD (7% decrease; Fig. 2H) and LMXN (2 % decrease; Fig. 2I). These results are in agreement with a recent study involving three rice genotypes (Kadam et al., 2015). The reduced CD increases the relative area Constituted by the stele (increased SD:RD; Fig. 2G) in roots, decreases radial distance, and improves radial hydraulic conductivity. The reduced CD could also significantly reduce the roots metabolic cost of soil exploration, thereby improving the water and nutrient acquisition

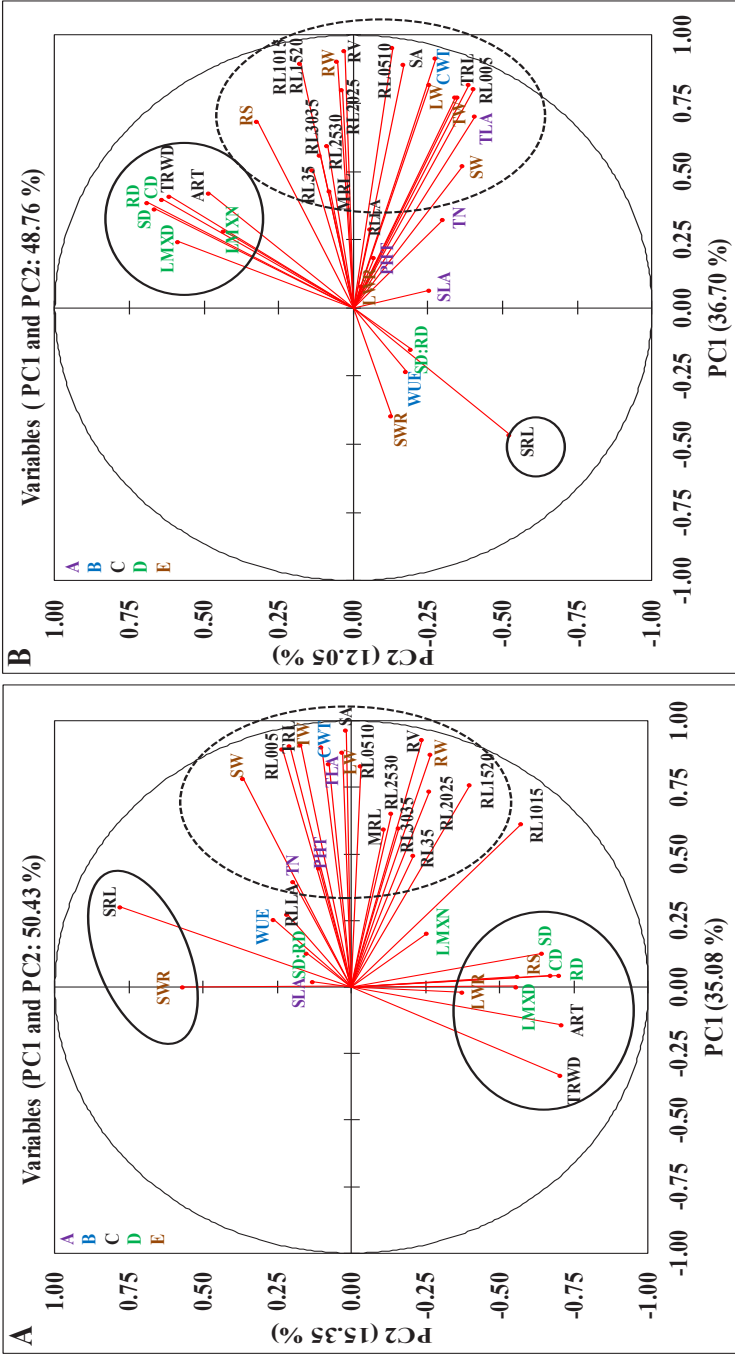


Figure 1. Principal component analysis of the 35 traits with first two components showing variation in control (**Panel A**), and water-deficit stress (**Panel B**) conditions. The traits marked by dashed ellipses contributing more to the variation explained by the PC1 and marked by solid circle/ellipses to PC2. Trait labels coloured differently according to category (uppercase letter in each panel) in Table 1; acronyms are given in the Table 1 as well.

in water-deficit and nutrient stress (Chimungu et al., 2014; Vejchasarn et al., 2016). However, reduced CD reduces the root thickness (Fig. 2D) and thereby mechanical strength of the root, which is a key to penetrating soil hardening under water-deficit stress (Yoshida and Hasegawa, 1982).

Population structure and whole-genome linkage disequilibrium

A balanced population structure and an optimal amount of linkage disequilibrium (LD) are important prerequisites for a successful GWAS, because the former corrects any confounding effect to avoid spurious associations whereas the LD is critical to infer the results (Mackay and Powell, 2007). The PCA with 46K SNPs ($MAF \geq 0.05$) revealed continuous distribution with no deep substructure in the 274 rice *indica* genotypes as, indicated by the limited amount of genetic variation (only 19%) explained by the first four PCs (Supplementary Figure S5A-B). Likewise, the LD on average across chromosomes dropped to half of its initial value at ~55 to 65 kb and to the background levels ($r^2 \leq 0.1$) at around ~600 kb to 1 Mb (Supplementary Figure S10). The observed LD decay distance was significantly shorter than previously observed values in rice *indica* subgroups at ~100-125 kb (Huang et al., 2010; Zhao et al., 2011), indicating more historical recombination events in our studied population likely due to the diverse sampling of a wide range of landraces and breeding lines with a low degree of genetic relatedness. Hence, a higher resolution can be expected from the mapping efforts, although it would also depend on the local LD pattern near the significant peaks.

Single-locus and multi-locus mapping identifying core regions of rice genome associated with phenotypic traits

To elucidate the genetic architecture, we conducted GWAS on 33 traits (excluding two traits [RL3035 & RL35] that lacked genotypic variation) across treatments and of their plasticity with 46K, SNPs ($MAF \geq 0.05$) using a single-locus compressed mixed linear model (CMLM) and a multi-locus mixed model (MLMM; more details in Materials and Methods). Table 2 provides a summary of GWAS for 33 traits from five categories. In total, we detected a nearly equal number of associations in control (104) and the water-deficit stress (106), although the significant loci varied across and within trait categories and treatments. Furthermore, 22 out of 104 associations in control and 10 out of 106 in water-deficit conditions were linked with more than one trait, possibly due to tight linkages or pleiotropic effects of loci or genes. For plasticity of traits, we identified 76 associations (Table 2 and Supplementary Tables S3-S5), of which

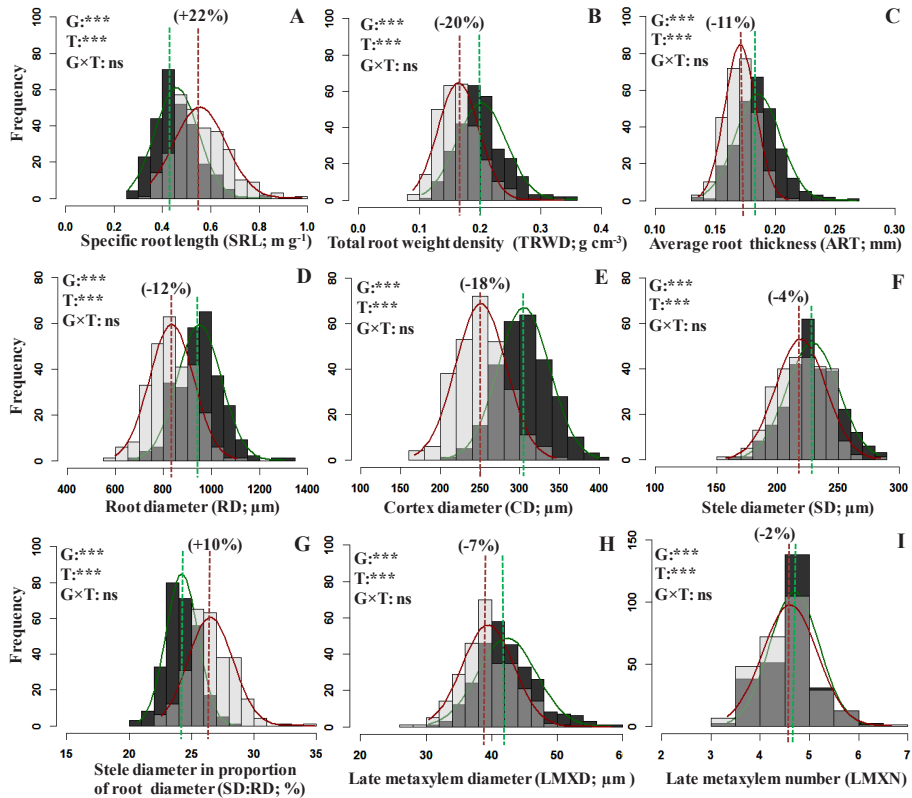


Figure 2. Overlying histograms with normal distribution curves (control: green line, dark grey bars; water-deficit stress: red line, light grey bars; intermediate grey: overlap for the treatment with the lower frequency value) showing the phenotypic distribution of root morphological (**Panel A-C**) and anatomical (**Panel D-I**) traits. The vertical lines in the histograms show population mean values in control (green) and water-deficit stress (red) conditions and values in parentheses represent the significant percentage change (+: increase or -: decrease) in water-deficit stress conditions over the control. Levels of significance for Genotype (G), Treatment (T) and their interaction (G×T) effects from ANOVA are given in the histograms (***, $P < 0.001$; ns, not significant).

nine were linked with more than one trait (Supplementary Table S6). Of the total loci, 22% in control, 33% in water-deficit stress and 27% for plasticity of the traits were detected commonly by both approaches, with statistically improved power (lower P value) for most of the loci using the MLM approach. In addition, MLM identified additional novel loci in both treatments and for trait plasticity. In particular, MLM identified significant loci for some traits where CMLM failed to identify any loci, and the identified loci was mostly novel, although in a few cases, they were already found to be associated with other traits in this study. For instance, we

identified four and three loci for total root length (TRL) in control, and water-deficit stress conditions, respectively, only with MLMM, and one locus on chromosome 4 under stress was associated with root weight (RW) and root: shoot ratio (RS; Supplementary Figures S11-S12). Similarly, we identified three loci for CWT and four for WUE in water-deficit condition only through MLMM (Supplementary Figure S13). Thus, MLMM approach proved to be valuable in dissecting the genetic architecture of complex traits by identifying additional novel loci (Segura et al., 2012). The detailed GWAS results through CMLM and MLMM approach are given in Supplementary Tables S3-S5.

Quantitative variation of root morphology in two moisture regimes and their plasticity provides insights into a complex genetic pattern

The genetic architecture of root traits is complex; determined by multiple small effect loci and studied extensively on mapping populations of rice representing the narrow genotypic base (Courtois et al., 2009). The genetic variations of root traits are relatively less characterized in diverse rice genotypes (Courtois et al., 2013; Phung et al., 2016; Biscarini et al., 2016) and can be a potential source for evolutionary beneficial alleles. Further, most of these studies have characterized the genetic variations in single isolated environments and not considered the two moisture regimes simultaneously, typically due to difficulty in the root phenotyping (space, time and cost). In this study, we carefully phenotyped the root traits in two moisture regimes and extracted the root morphology in various hierarchies by automated digital image analysis tool WinRHIZO (Table 1; Materials and Methods for root phenotyping). Through GWAS analysis, we detected 34 loci for 11 morphological, one for RW and three for RS in control and 52 loci for 12 morphological, four for RW and four for RS ratio under water-deficit (Table 2 and Supplementary Tables S3-S4). The SRL is one of the important root morphological traits and often used as a proxy for root thickness. We observed three and eight loci for SRL in control and stress conditions through CMLM and MLMM (Fig. 3 and Supplementary Tables S3-S4). The mean narrow-sense heritability (h^2) of root traits that showed significantly associated loci varied between 0.20 and 0.89 in control and between 0.32 and 0.78 in stress conditions (Supplementary Table S2). In addition, we identified 33 loci for 12 root morphological plasticity traits, one locus for rRW and four loci for rRS ratio, with mean $h^2=0.40$ for traits that showed significant associations (Table 2; Supplementary Tables S2 and S5). Above results clearly illustrate that variation in root plasticity is heritable and determined by the genetic factors.

Table 2. Summary of significant loci identified by GWAS analysis using two approaches (comprised mixed linear model (CMLM) and multi-locus mixed model (MLMM) for 35 traits across five categories (A-E) in control (C) and water-deficit (WD) conditions and for phenotypic plasticity (PP) of traits as a relative measure

Trait classification	C	WD	PP
(A) Shoot morphological traits	6	11	8
(B) Physiological traits	16	6	6
(C) Root morphological traits	34	52	33
(D) Root anatomical traits	14	17	15
(E) Dry matter traits	34	20	14
Total loci	104 (22)	106 (10)	76 (9)
Loci detected by CMLM approach	39 [32%]	26 [24%]	19 [25%]
Loci detected by MLMM approach	42 [40%]	45 [42%]	36 [47%]
Loci detected by both approaches	23 [22%]	35 [33%]	21 [27%]
Total predicted <i>a priori</i> genes	296	284	233
Genes responsive to abiotic stress stimulus	48	61	38

The values in parenthesis are loci associated with more than one trait (see Supplementary Table S6) and values in square brackets are the percentages of loci out of total loci detected by CMLM, MLMM and both the approaches. The total *a priori* genes are predicted in expected LD block of peak SNP/SNPs.

Dividing a trait into multiple component traits unravels the underlying inherited complexity (Yin et al., 2002). We detected an increased number of genetic loci for root length classified on root thickness than for TRL across treatments (Supplementary Tables S3, S4 and S7). For instance, we identified four loci in control and three loci in water-deficit stress for TRL. Mapping with root length traits of different root thickness classes resulted in identifying the additional 10 loci in control and 18 loci under water-deficit stress that were not detected by TRL *per se* (Supplementary Table S7). Similar result was observed for total weight (TW) and for its three component traits namely leaf weight (LW), stem weight (SW) and RW (Supplementary Tables S3-S4). These results clearly suggested that separating the complex trait into component traits improves the power to detect significant associations, perhaps by minimizing the variance between raw value, thereby increases the chance to detect variation in its component traits in agreement with a previous study (Crowell et al., 2016). However, for plasticity, we identified only five loci for root length of different root thickness classes, of which one was common with rTRL and four were novel loci (Supplementary Table S7). This lower number of loci for plasticity could also be due to the fact that plasticity is the trait ratio estimated from measurements across two treatments. Nevertheless, our ability to identify these distinct genetic loci when mapping the component traits might be capturing the key causal genetic regulator controlling the various aspects of root morphology. Moreover, there were no common loci detected either for TRL or its component traits across treatments, and this suggests

that genetic control of root morphology is different across moisture regimes and strongly influenced by water-deficit. This could be further substantiated by all the novel loci identified for plasticity in the above traits, which might be a specific stress responsive genetic loci determining the plastic response.

Colocalization of root morphology loci explains underlying genetics and physiology

Many of the root traits and other traits result from complex combination of biological mechanisms controlling the expression in coordination, as explained by their correlation. This correlation between traits could result from pleiotropic action of genetic loci on different traits or due to tight linkage between genetic loci. The root system supports the aboveground shoot growth through absorption of water and nutrients. In this study, one locus on chromosome 5 (7131196) was commonly associated with root morphology (root volume [RV], RL1015, RL1520), RW, CWT and TW in control condition (Supplementary Table S6). All these traits showed a positive ($r \approx 0.65$) correlation with CWT in control condition (Supplementary Figure S8A). In water-deficit stress, one locus on chromosome 1 (a different SNP but falls within same LD block) was commonly associated with CWT (23207640) and SRL (23218344) and both these traits were negatively correlated ($r = -0.34$; Supplementary Figure S8B). Similarly, for plasticity, one locus on chromosome 7 (9463744) was commonly associated with r_{TRL} , r_{SA} (9463899; different SNP but falls within same LD block), r_{TLA} and r_{CWT} (Supplementary Table S6). To comprehend, these results clearly illustrate the common genetic control of root morphology and water transpiration possibly to maintain the balanced hydraulic continuum between water uptake and transpiring organ. One locus on chromosome 9 (14829621) was commonly associated with RV, leaf weight ratio (LWR) and stem weight ratio (SWR), in water-deficit (Fig. 4). The minor allele at this locus had a positive effect on SWR and negative on RV and LWR (Supplementary Table S4). This further elucidates the negative correlation of SWR with RV and LWR (Supplementary Figure S8B). The same locus was associated with root length 0.5 to 1.0 mm diameter class (RL0510) and surface area (SA) in water-deficit stress (Supplementary Table S6). The ratio of root to shoot is more often used as an index of water-deficit stress tolerance and surrogate for root morphology. One locus on chromosome 4 (29111186) was commonly associated with r_{TRL} , RL005, RW and RS in water-deficit. The minor allele of this locus had a positive effect on all these traits (Supplementary Table S4). Furthermore, one of the significant loci was commonly detected in both the moisture regimes; associated with maximum root length (MRL) in control and SRL in water-deficit stress

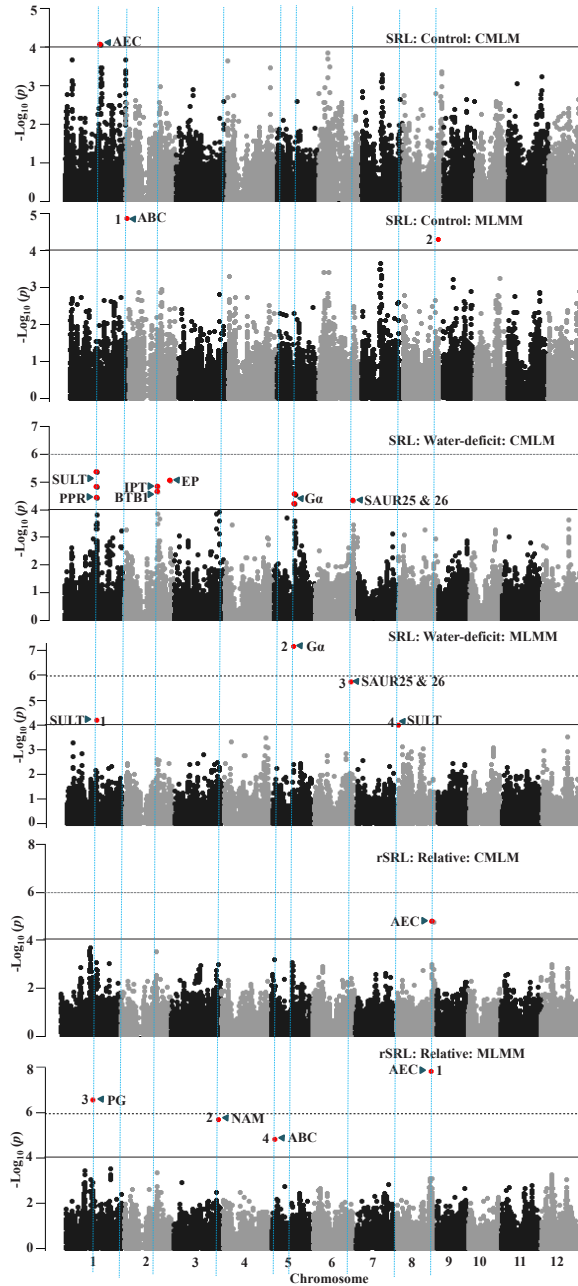


Figure 3. GWAS results through the compressed mixed linear model (CMLM) and the multi locus mixed model (MLMM) approaches for specific root length (SRL) in control (the two upper panels) and water-deficit conditions (the two middle panels) and the trait plasticity calculated as the relative value of the water-deficit stress conditions over the control (the two bottom panels). Significant SNPs (coloured red in the Manhattan plots) are distinguished by

Figure 3. (Continued)

threshold P value lines (solid black= $[-\text{Log}_{10} P > 4]$ and dotted black= Bonferroni-corrected threshold). Significant SNPs in MLM Manhatten plots are numbered in the order that they were included in the model as a cofactor. *A priori* candidate genes (Supplementary Tables S9S11) are indicated near to peak SNP/SNPs in the Manhattan plot. **AEC**: auxin efflux carrier; **ABC**: ATP-binding cassette transporters; **SULT**: Sulfate transporter; **PPR**: Pentatricopeptide; **IPT**: Inorganic phosphate transporter; **BTB1**: Brick-Brack, Tramtrack, Broad Complex BTB; **EP**: Expressed protein; **Gα**: G-protein alpha subunit; **SAUR**: Small auxin UP-RNA; **PG**: Polygalacturonase; **NAM**: No apical meristem.

(Supplementary Tables S3-S4). We also identified locus on chromosome 12 (25006932) commonly associated with plasticity of root morphology traits (rTRL, rRL005, rSA, rRV, rRTN and rRLD) and rTN (Supplementary Table S6). These identified loci influencing multiple traits could be a potential marker for the marker assisted selection after validating in the elite genetic background.

Genetic basis of radial root anatomy

The functioning of roots is strongly depending on radial organization of root anatomy, which is regulated by the asymmetric cell division. The genetic control of radial root organization is less studied in rice, with largely unknown underlying genetic mechanisms. Understanding the genetic control of radial root anatomy is more challenging in rice because the complexity and size of the fibrous root system presented several phenotyping challenges. To date, only one study in rice has identified the genomic regions for radial root anatomy (Uga et al., 2008). Through GWAS analyses, we identified 14 significant loci for five anatomical traits in control; 17 loci for four anatomical traits in water-deficit and 15 loci for the plasticity of four anatomical traits (Table 2 and Supplementary Tables S3-S5). Root diameter (RD; anatomical) of the adventitious root and ART (morphological) of the complete root system are positively correlated (control: $r=0.22$ and water-deficit: $r=0.25$) and a locus on chromosome 1 (1099857/1111294; different marker but fall within same LD block) was commonly associated in control condition (Supplementary Table S6). Both these traits are measures of root thickness, thus illustrate that measuring the RD at one position (near root-shoot junction) to some extent, was able to capture genetic variation of complete root system thickness. Three anatomical traits, namely RD, CD and SD:RD, were highly correlated with each other in control (Supplementary Figure S8A), and we found one common locus (21266079) associated with them on chromosome 7 (Supplementary Table S6). Stele tissue is the central part of the root enclosing the vascular cylinder (xylem and phloem), and one locus on chromosome 9 (13788883) and 5

(3057869) was commonly associated with SD and LMXD in stress (Supplementary Table S6). However, no locus was commonly detected across moisture regimes clearly suggest that genetic control of radial root anatomy is strongly influenced by stress. For anatomical plasticity, we observed two loci (11038867 and 11596350) on chromosome 1 common to rRD, rCD and rSD (Supplementary Figure S14) and plasticity of these traits was positively correlated with each other (Supplementary Figure S9). Hence, relative change in these traits in response to the water-deficit is partly under similar genetic control because they also have another independently associated genetic loci.

***A priori* candidate genes underlying the genetic loci of phenotypic traits**

A lower LD decay rate results in larger LD block and lower mapping resolution, which makes the GWAS not straightforward in identifying the causal genes. On average across genome LD decay rate was 55 to 65 kb in the studied population but then again, the association resolution varied with loci due to local LD pattern. Hence, we have calculated the LD pattern near to all the significant loci identified in this study (See Materials and Method). In total, we have collected a list of 296, 284, and 233 *a priori* candidate gene within the expected LD block in control, water-deficit and for their plasticity, respectively. Of the total *a priori* candidate genes, 48 (control), 61 (water-deficit) and 38 (plasticity) genes were responsive to abiotic stress stimulus (Table 2 and Supplementary Data Sets S2-S4). Furthermore, we have identified the list of 70 *a priori* genes close to significant loci for shoot morphological, physiological, dry matter traits in control (32 genes), water-deficit (21 genes) and for their plasticity (17 genes; Supplementary Table S8). For instance, one locus on chromosome 6 (13412649) for CWT and one on chromosome 9 (15426362) for WUE under stress was near to AQUAPORIN (AQP; 4 kb) and the WAX2 (66 kb) genes, respectively (Supplementary Figure S13 and Supplementary Table S8). The AQP gene is known to maintain root hydraulic conductivity, cell turgor, mesophyll conductance, water transpiration and thereby growth (Flexas et al., 2006; Henry et al., 2012), whereas WAX2 gene regulates epicuticular wax production, maintains cellular water status and improves the WUE (Premachandra et al., 1994; Chen et al., 2003). Similarly, one locus on chromosome 2 (31650233) for tiller number (TN) in control was within ethylene-responsive transcription factor (ERFTF) gene and homologue of this gene was known to regulate rice tillering (Qi et al., 2011). Likewise, for all the root traits (root morphology and anatomy, RW and RS), we have identified a list of 40, 57 and 41 *a priori* candidate genes in control, water-deficit and for their plasticity, respectively, with a role in root growth and

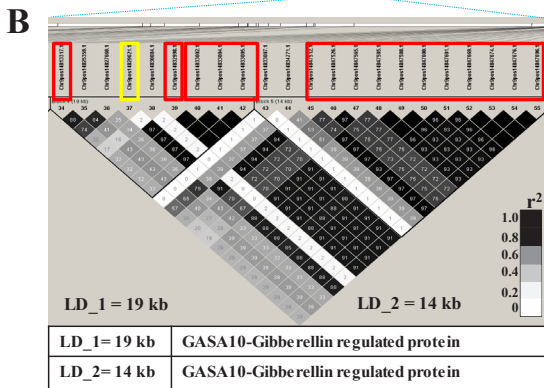
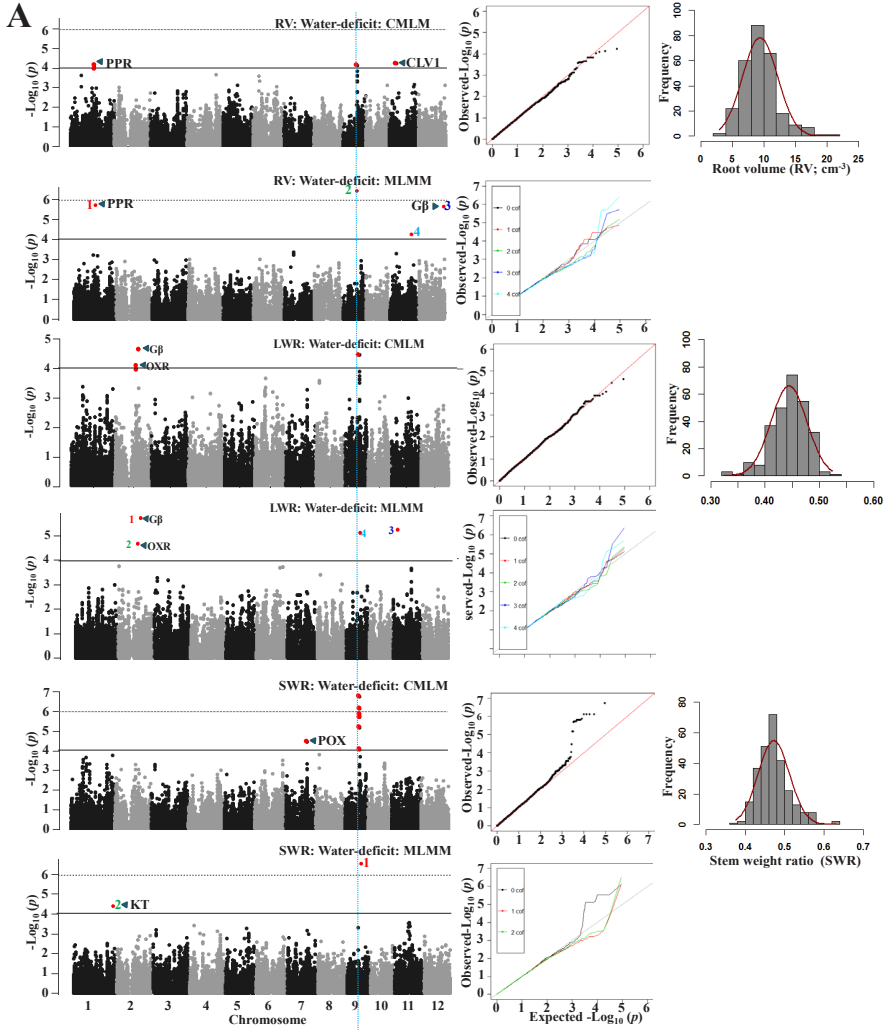


Figure 4. GWAS results through compressed mixed linear model (CMLM) and multi-locus mixed model (MLMM) approaches (Manhattan and Quantile-Quantile plots) for root volume (RV), leaf weight ratio (LWR) and stem weight ratio (SWR) in water-deficit stress. Significant SNPs (coloured red in the Manhattan plots) are distinguished by threshold P value lines (solid black= $[-\text{Log}_{10} P > 4]$ and dotted black= Bonferroni-corrected significance threshold) and coloured red in the Manhattan plots (**Panel A**). Significant SNPs on MLMM Manhattan plots are numbered in the order that they were included in the model as a cofactor. Identified LD blocks based on pairwise r^2 values between SNPs on chromosome 9 (**Panel B**) with *a priori* candidate gene in the underneath table (for more details see Supplementary Tables S8 and S10). The colour intensity of the box corresponds with r^2 value (multiplied by 100) according to the legend. Significant SNP (“**14829621**”) marked in yellow rectangle was commonly associated with RV, LWR and SWR (Panel B). **PPR**: Pentatricopeptide, **CLV1**: CLAVATA1; **Gβ**: G-protein beta subunit; **OXR**: Oxidoreductase; **POX**: Peroxidase; **KT**: Potassium transporter.

development (Supplementary Tables S9-S11). Several genes were regulating root growth and development through phytohormone transport and signalling (Auxin, ABA, GA, ethylene and brassinosteroid); cell division and differentiation; cellular redox homeostasis; molecular chaperone; water and nutrient transporter; cellular component organization and cell wall remodelling. For instance, one locus on chromosome 6 (366330) for RL0510 in control (Supplementary Table S9) was within the SCARECROW (SCR) gene that regulates radial root and shoot anatomy and root hair tip growth through cell division and differentiation (Gao et al., 2004). One locus on chromosome 1 (40526762) for RV in control was within the OsSAUR3 gene, an early auxin responsive gene that regulates root elongation (Markakis et al., 2013). The two homologues of this gene were close (OsSAUR25=11 kb and OsSAUR26=42 kb) to the locus on chromosome 6 (27819933) for MRL in control (Supplementary Table S9). Likewise, in water-deficit conditions, a locus on chromosome 9 (14829621) was commonly associated with RV, RL0510, SA, LWR and SWR and was found within the GASA10 gene (Supplementary Table S10). The GASA10 gene is known to participate in phytohormone crosstalk leading to redox homeostasis, and regulates root, stem and other organs growth (Nahirñak et al., 2012). For plasticity, one locus on chromosome 8 (26362631) for rSRL was near (30 kb) to an auxin efflux carrier component protein (AEC; Supplementary Table S11) and this gene is known to regulate auxin transport with mutant showing defective root development (Grieneisen et al., 2007).

Three interesting *a priori* candidate genes were recognized for radial root anatomy loci in this study. A locus on chromosome 11 (2838776) for LMXN in control was near (7 kb) to bHLH (basic helix-loop helix protein). The Arabidopsis orthologue LONESOME HIGHWAY having sequence similarity to bHLH, regulates the stele and xylem development (Supplementary Table S9). Similarly, a locus on chromosome 11 (28871551) for LMXD in

stress was within SCR (3 homologous copies in LD block), a gene that regulate radial anatomy of root and shoot (Supplementary Table S10); its homologue was associated with root morphology traits as discussed earlier. The LONESOME HIGHWAY gene regulates vascular tissue differentiation and number with involvement of auxin in Arabidopsis (Ohashi-Ito et al., 2013), while SCR is an auxin responsive gene regulating radial patterning in both root and shoot in Arabidopsis (Gao et al., 2004). Likewise, one of the locus on chromosome 9 (13788883) commonly associated with SD and LMXD in stress (Supplementary Table S10). This locus was near (24 kb) KANADI gene that regulates root development (Hawker and Bowman, 2004), and expressed during vascular tissue development (Zhao et al., 2005). In summary, many *a priori* candidate gene regulating the root morphology and radial root anatomy has been identified in this study.

Conclusions

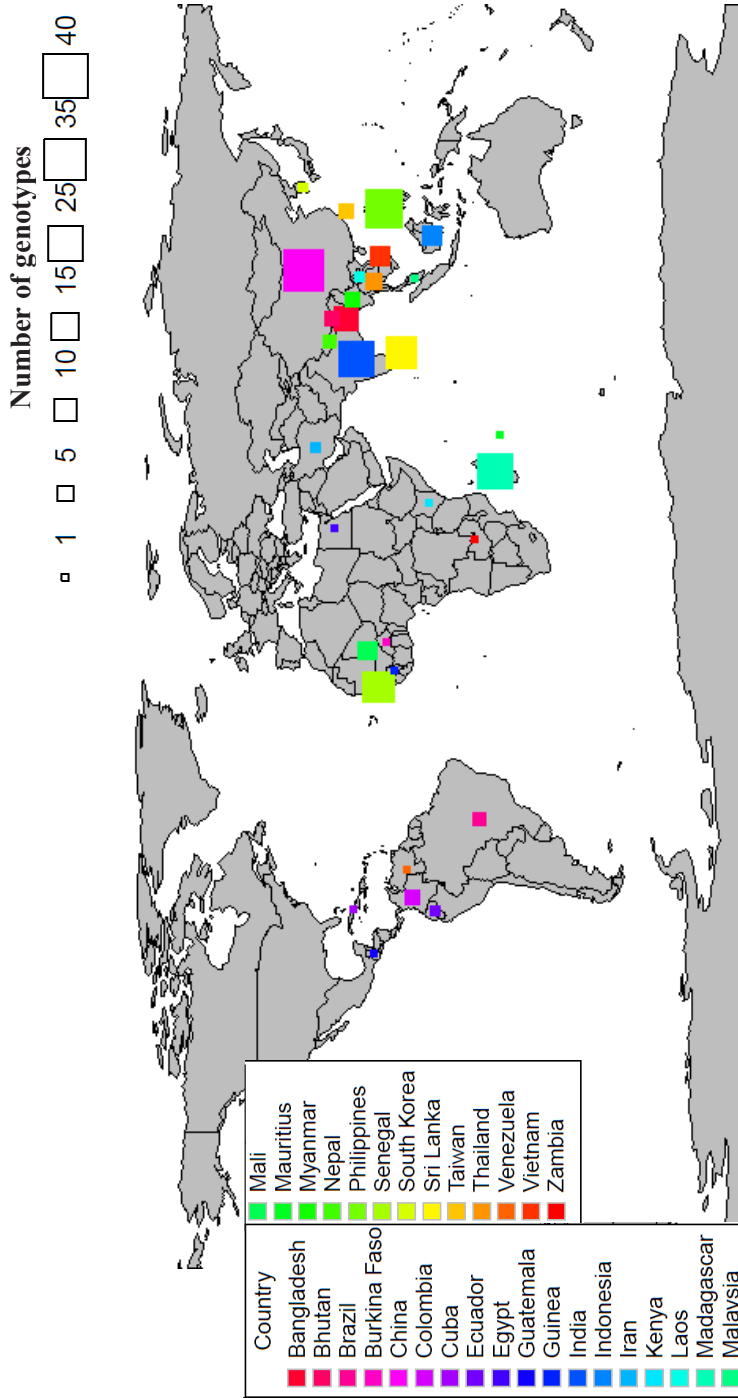
In the past mainly root morphological differences have been extensively (phenotypically and genetically) characterized with very little attention to radial root anatomy in rice. To our knowledge, for the first time, we have characterized phenotypic variation for root morphological traits through powerful and intensive image-based systems and anatomical traits through microscopic dissection of root in a diverse set of rice *indica* genotypes across two moisture regimes. The single-locus and multi-locus GWAS analyses provided novel genetic insights that can help explain the observed genotypic variation of root morphological and anatomical traits across two moisture regimes. The phenotypic plasticity of the root morphology and anatomy was moderately heritable and had sufficient genetic control that resulted in identifying key core regions of rice genome. Thus, variation in root traits is valuable resources that can result in identifying the potential novel genetic loci. Favourable alleles of these identified loci could after validation be directly used for marker-assisted selection. Many of these loci were either close to known genes or within genes themselves that play a role in root growth and development. For example, several phytohormone genes influencing transport and signalling were found close to our identified loci, confirming well-known dominant role of these genes in root growth and development. The cloning and characterization of these genes can provide additional checkpoints in rice root growth and development. A further holistic approach of root system genetics is needed to be complemented with GWAS studies to understand the complexity of gene networks in controlling root growth and development. Future studies should also aim for more efficient high-throughput root phenotyping approaches

both in field and control glasshouse conditions, to help advance root genetics.

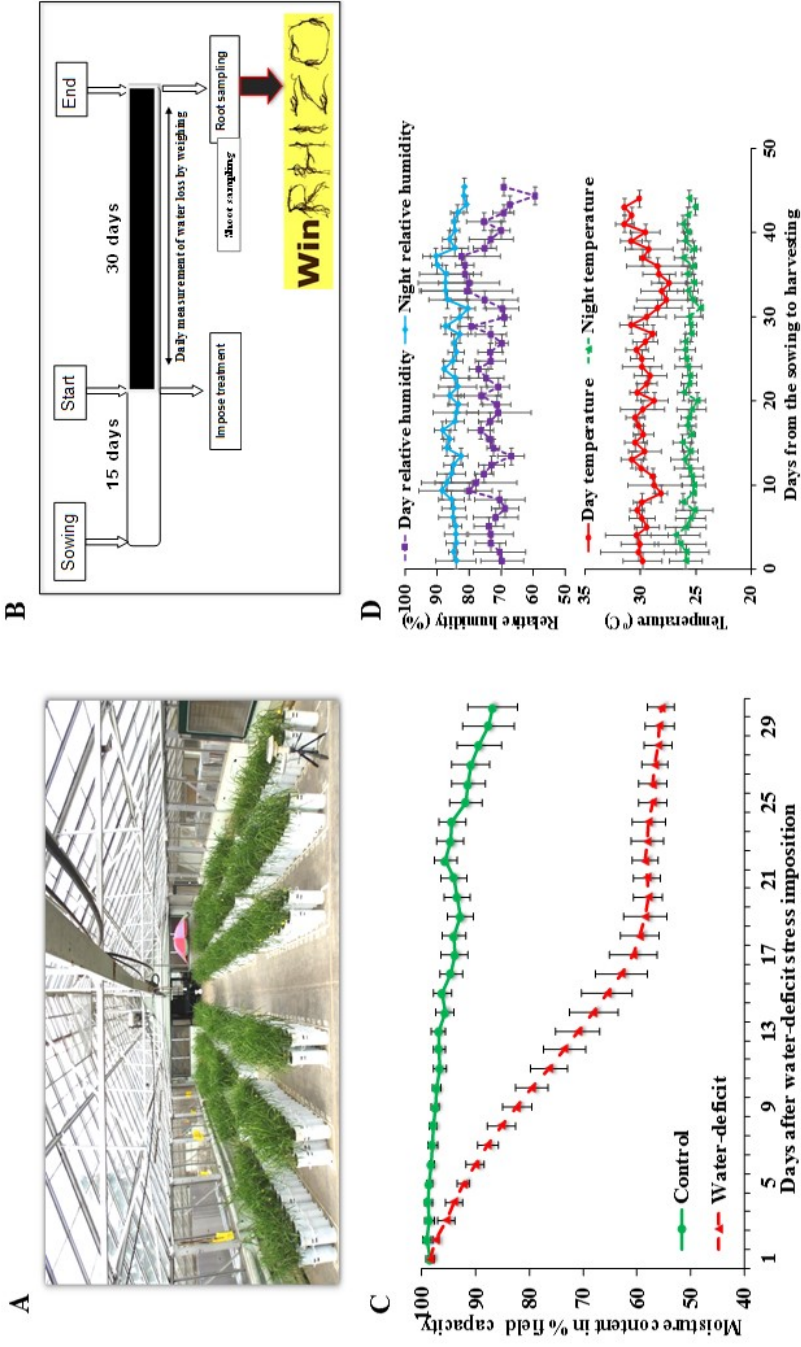
URLs.

WinRHIZO root image analysis, http://regent.qc.ca/assets/winrhizo_about.html/; R version of MLMM, <https://cynin.gmi.oeaw.ac.at/home/resources/mlmm/>; Michigan State University (MSU) Genome Browser, <http://rice.plantbiology.msu.edu/cgi-bin/gbrowse/rice/>.

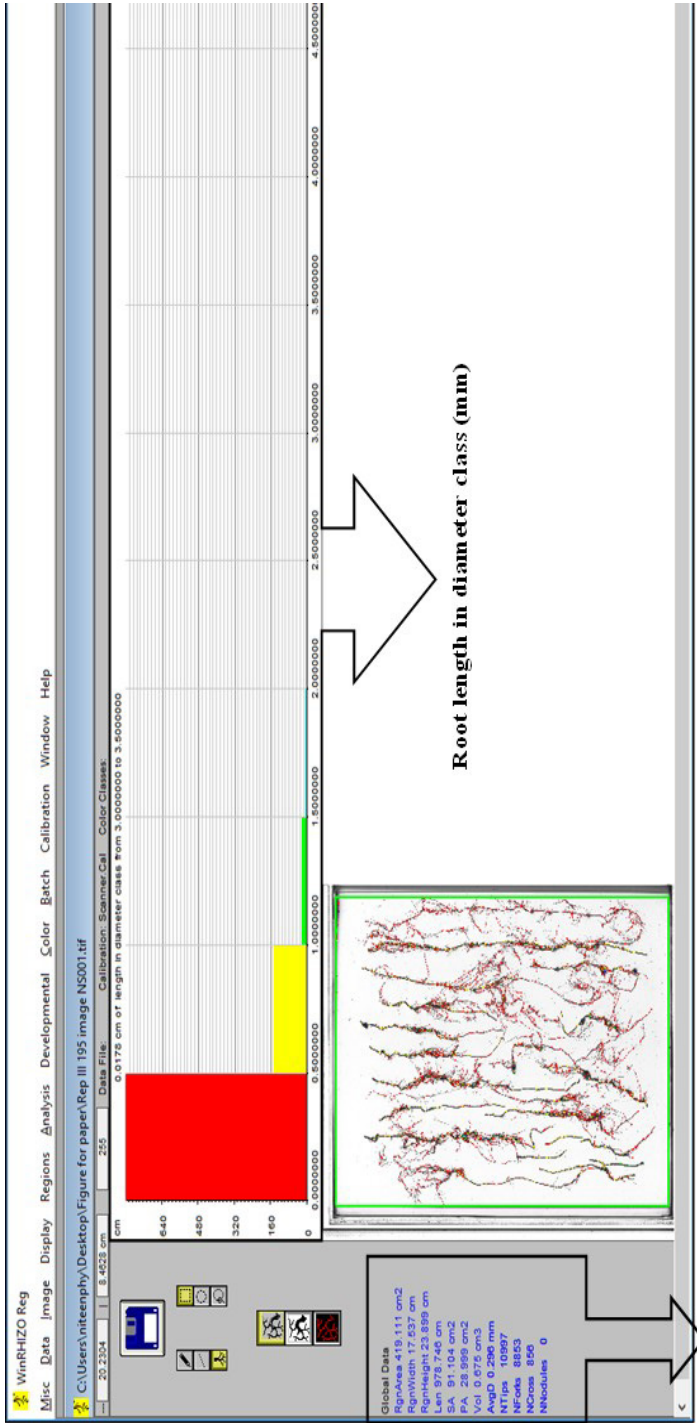
Supplementary information in Chapter 3



Supplementary Figure S1. Geographical origin of 273 rice *indica* genotypes grown in tropical regions of the world and one genotype without available information. The size of the symbol on the world map corresponds to the number of genotypes.

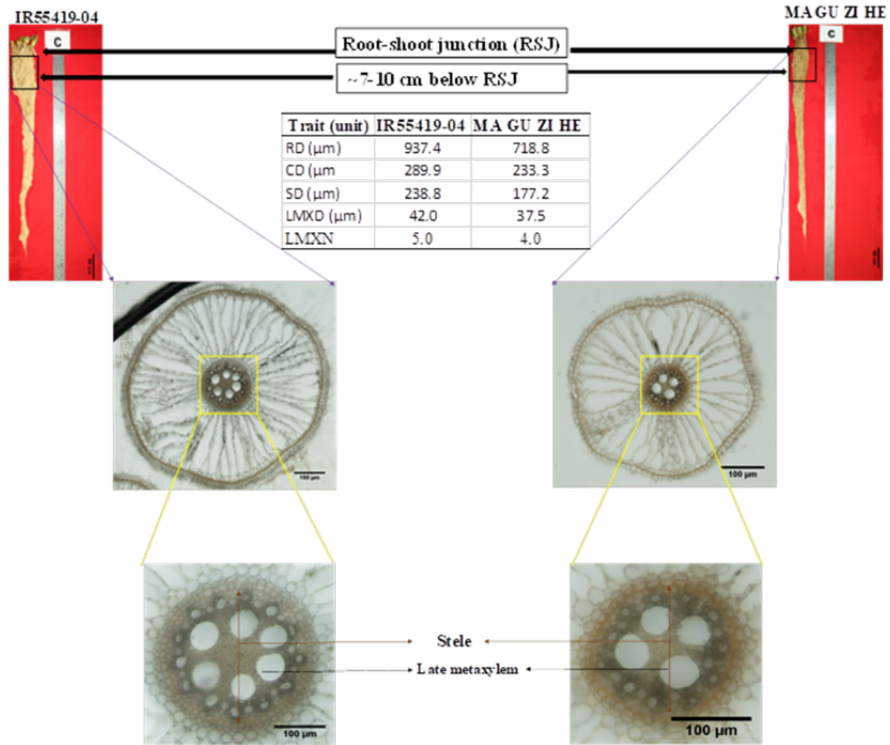


Supplementary Figure S2. The experimental setup for phenotyping a diverse set of 274 rice genotypes under greenhouse experiment for phenotypic traits (**Panel A**). The procedure followed to set up the experiment and to maintain two moisture regimes (**Panel B**). The rate of water depletion from the soil was calculated for each genotype based on the pot weighing data and expressed in moisture content in % field capacity (**Panel C**). Average daily day and night temperature and relative humidity during the growing period across the three independent replications (**Panel D**). Bars in panels C and D are the standard error of the mean.

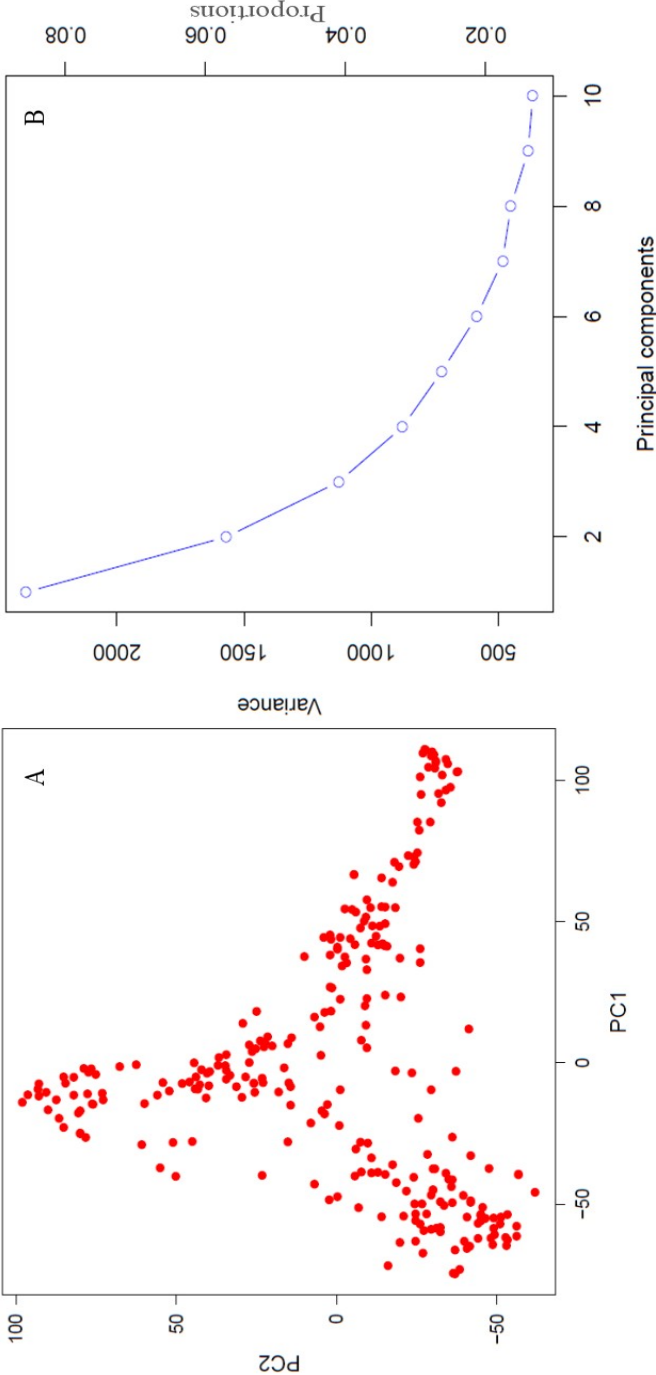


Root morphological data

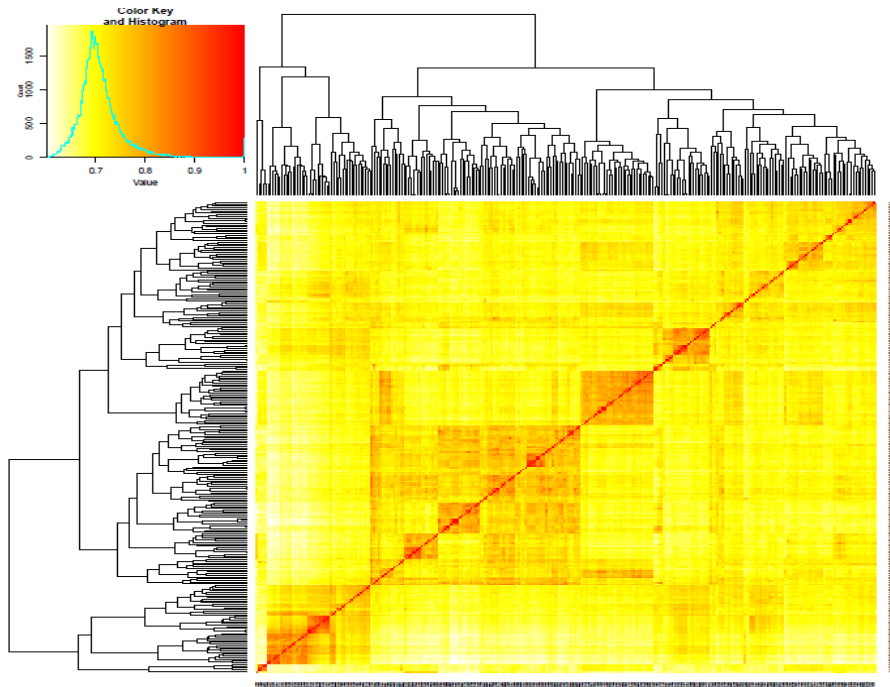
Supplementary Figure S3: Illustrative root image analysis with WinRHIZO programme displaying the measurement of root morphological traits. The dissimilar colour for roots indicates the different root length diameter class. For instance, red colour indicates the root length in 0.0-0.5 mm diameter class. The left side on images shows the measurement of root morphological traits such as **Len**= root length (cm); **SA**=surface area (cm²); **Vol**= root volume (cm³); **AvgD**=average diameter (mm) that we renamed to average thickness to avoid misperception with measured root anatomical diameter.



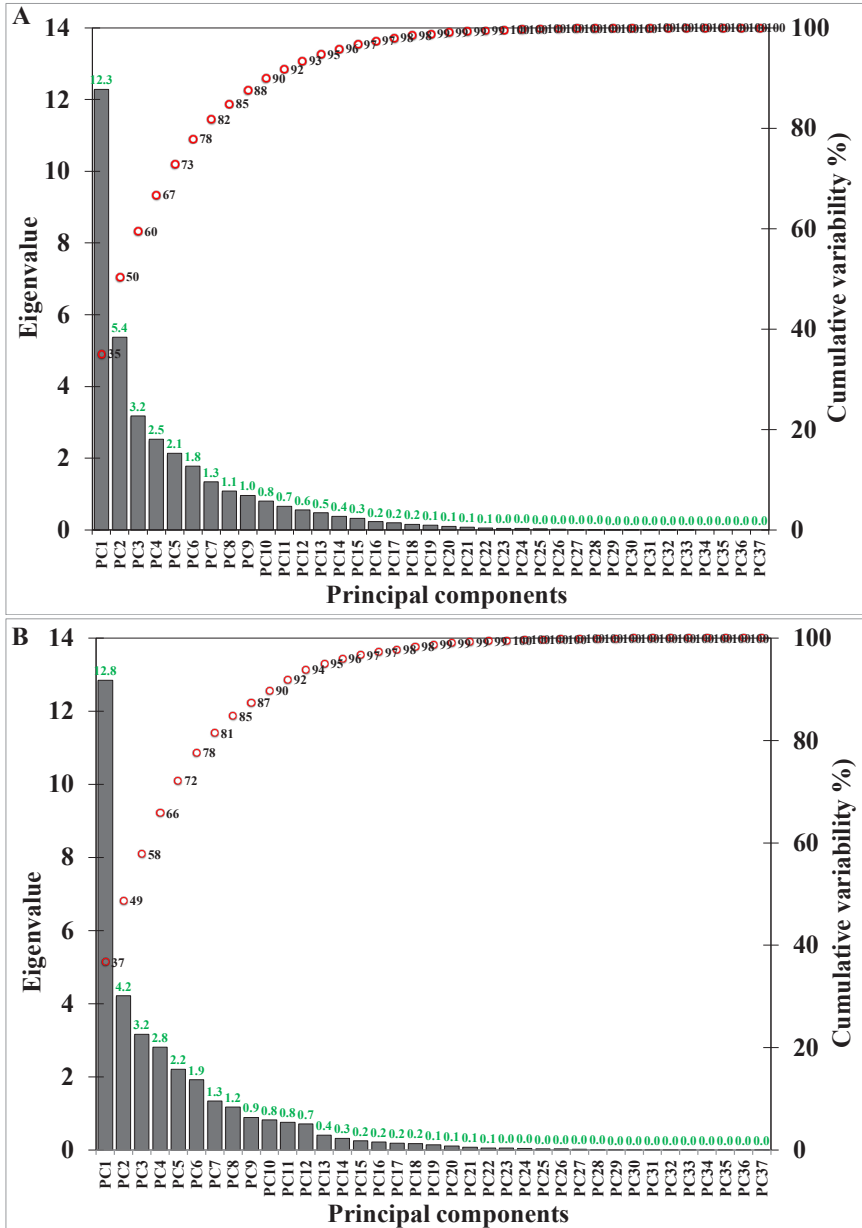
Supplementary Figure S4: The root anatomical trait variation of two rice genotypes near root-shoot junction in control conditions. **RD**: root diameter, **CD**: cortex diameter, **SD**: stele diameter, **LMXD**: late metaxylem diameter and **LMXN**: late metaxylem number. Scale bar on root morphology image is 50 cm and on root anatomy is 100 μm . The table on image displays mean root anatomical variation measured across three replications.



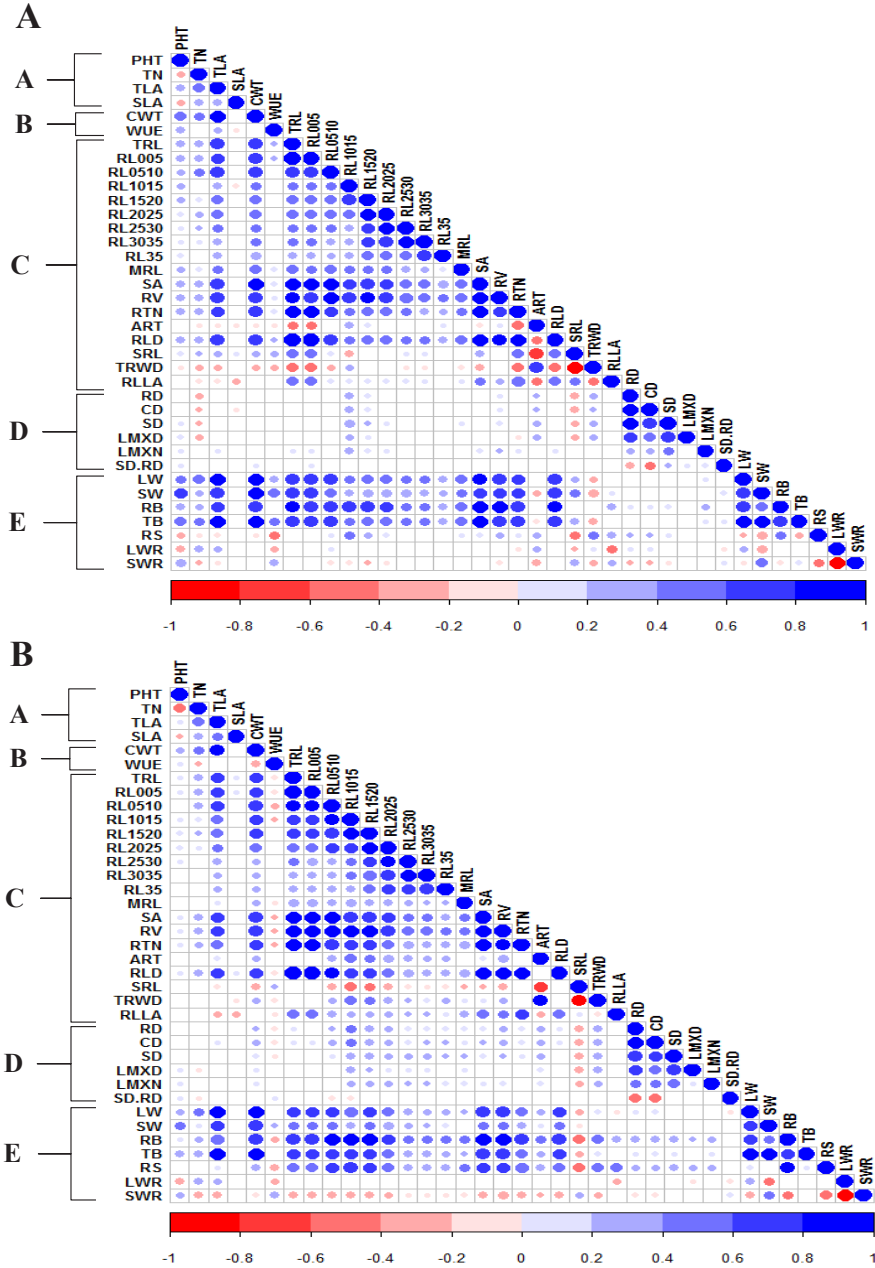
Supplementary Figure S5. The Principal Component analysis constructed on 46K SNPs ($MAF \geq 0.05$) across 274 genotypes with first two components depicting the population structure (**Panel A**). The scree plot shows the variation explained by each principal component in proportion (**Panel B**).



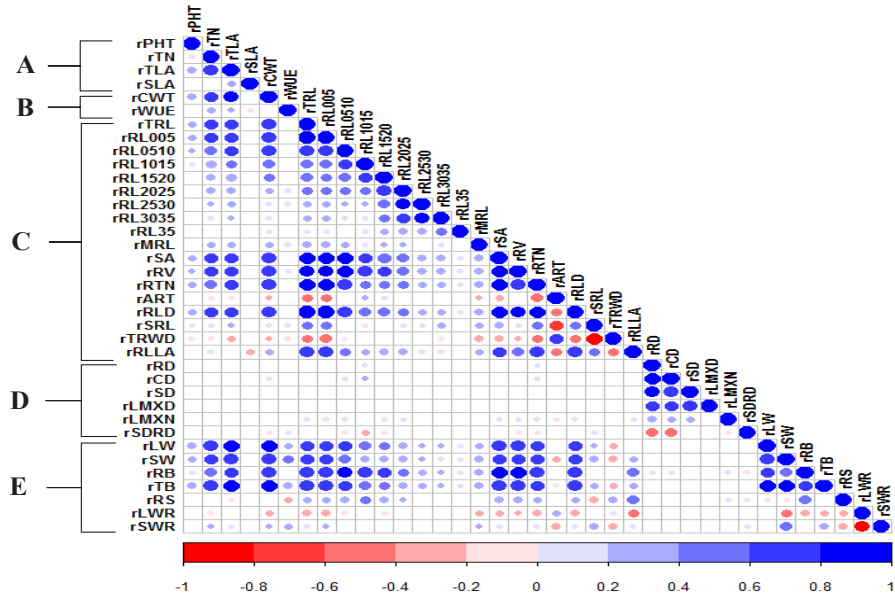
Supplementary Figure S6. The heat map of kinship matrix defining genetic relatedness across 274 genotypes with red and yellow colour indicates the highest and lowest correlation between pairs of the genotypes respectively. A hierarchical clustering between genotypes is based on kinship values.



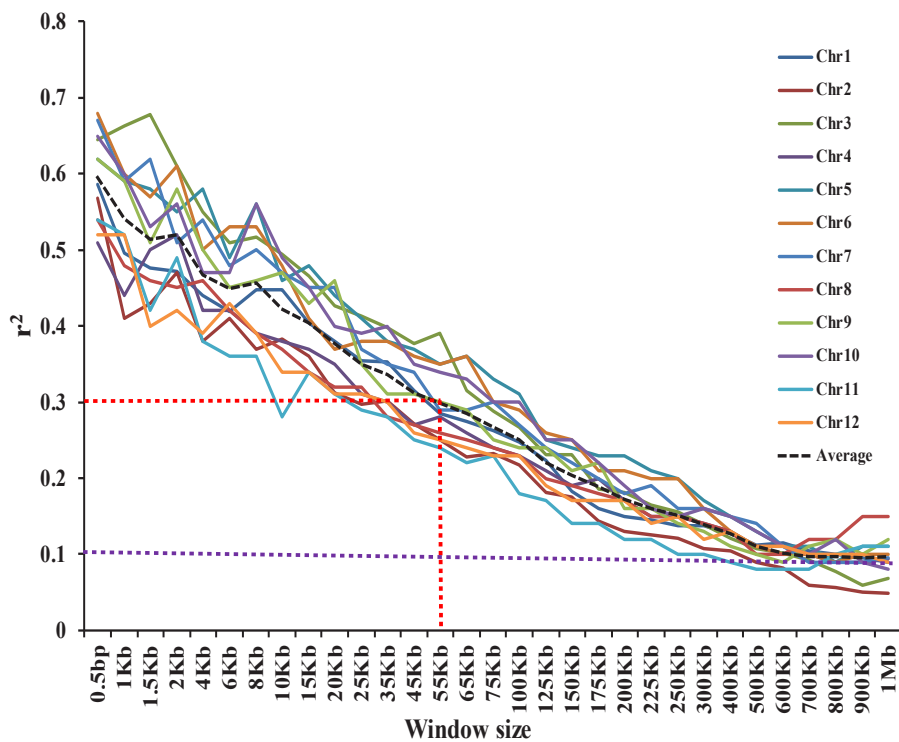
Supplementary Figure S7. The Principal Component Analysis scree plot of 35 phenotypic traits across 274 genotypes depicting the variation explained by each component (PC) in control (**Panel A**) or water-deficit stress (**Panel B**) conditions. The PC1 to PC8 with eigenvalues greater than 1.0 (green value above bars) were considered significant and cumulatively explained >80 % total variation.



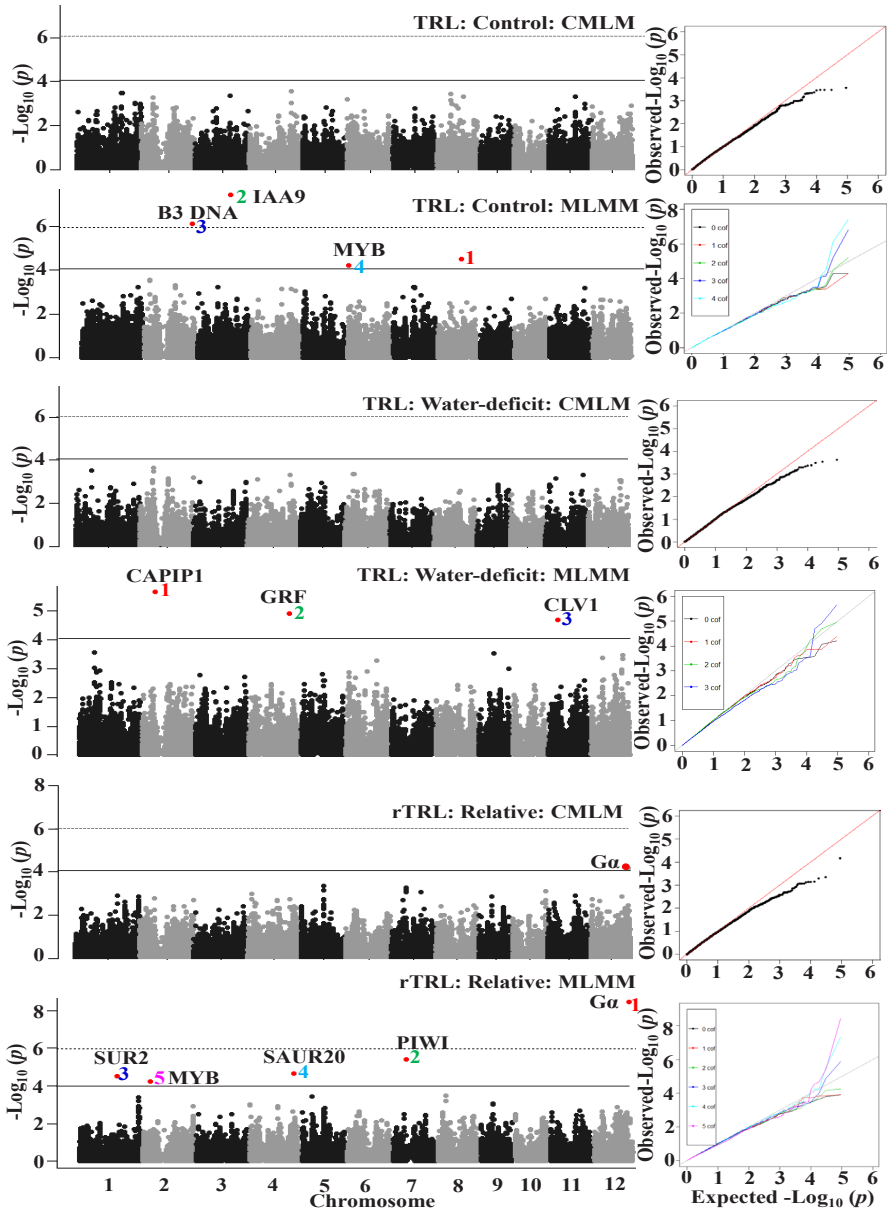
Supplementary Figure S8. Pearson correlation coefficients between 35 phenotypic traits in control (**Panel A**) and water-deficit stress (**Panel B**) conditions. The blue and red colours indicate positive and negative correlations, respectively. Colour intensity and size of the circle are proportional to the strength of correlation coefficients between the pair of traits. Uppercase letters on the left panels of the figure correspond with trait classifications as in Table 1; for trait acronyms and units see the Table 1.



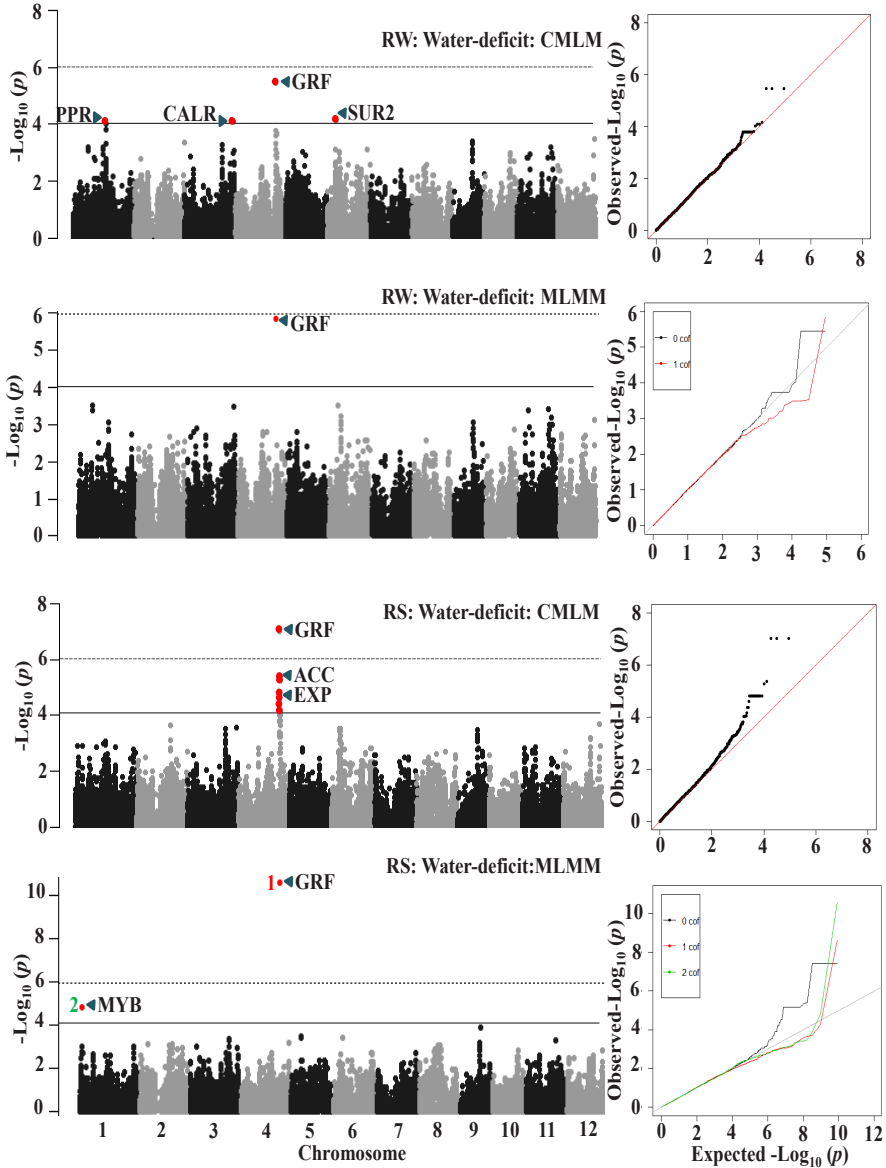
Supplementary Figure S9. Pearson correlation coefficients for the plasticity of 35 phenotypic traits (**Panel C**). The blue and red colours indicate positive and negative correlations, respectively. Colour intensity and size of the circle are proportional to the strength of correlation coefficients between the pair of traits. Uppercase letters on the left panels of the figure correspond with trait classifications as in Table 1; for trait acronyms and units see the Table 1.



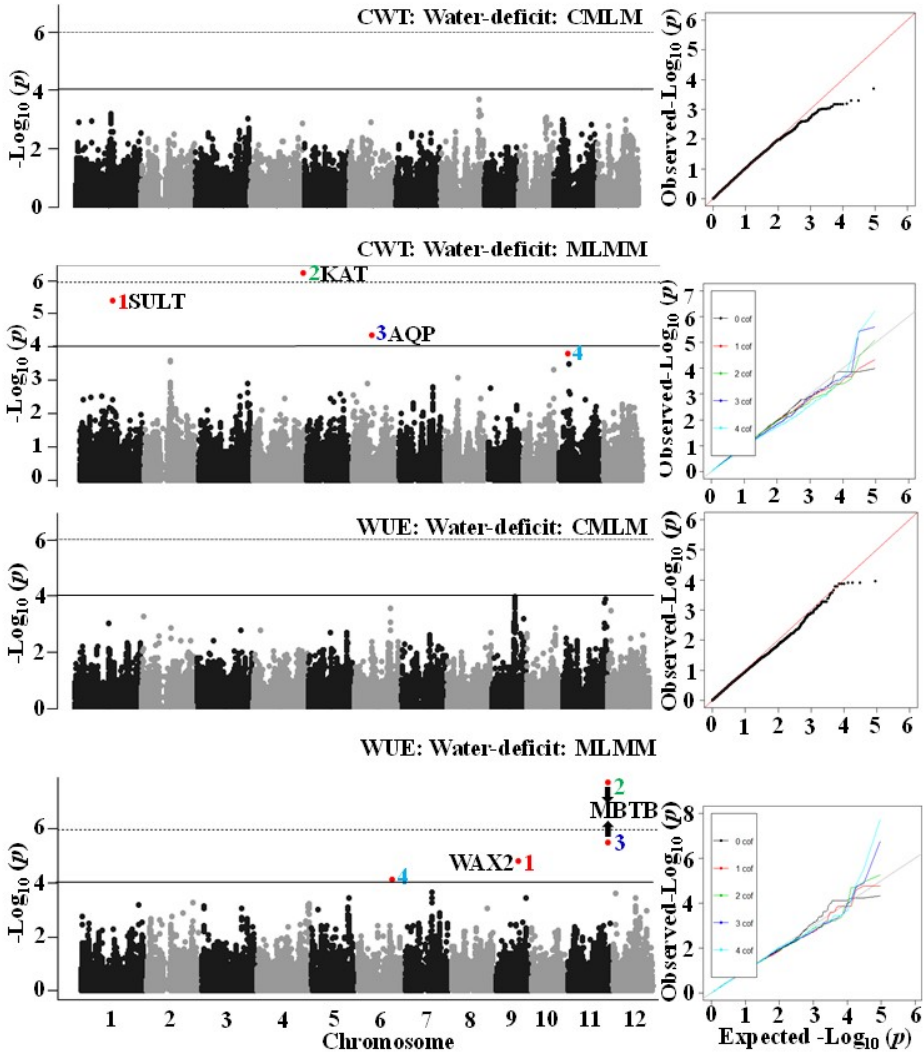
Supplementary Figure S10. Individual chromosome and average genome wide linkage disequilibrium decay as a measure of r^2 between the pairs of SNPs over the physical distance on the genome. The r^2 was calculated using the 100 bp sliding window in the TASSEL 5 programme.



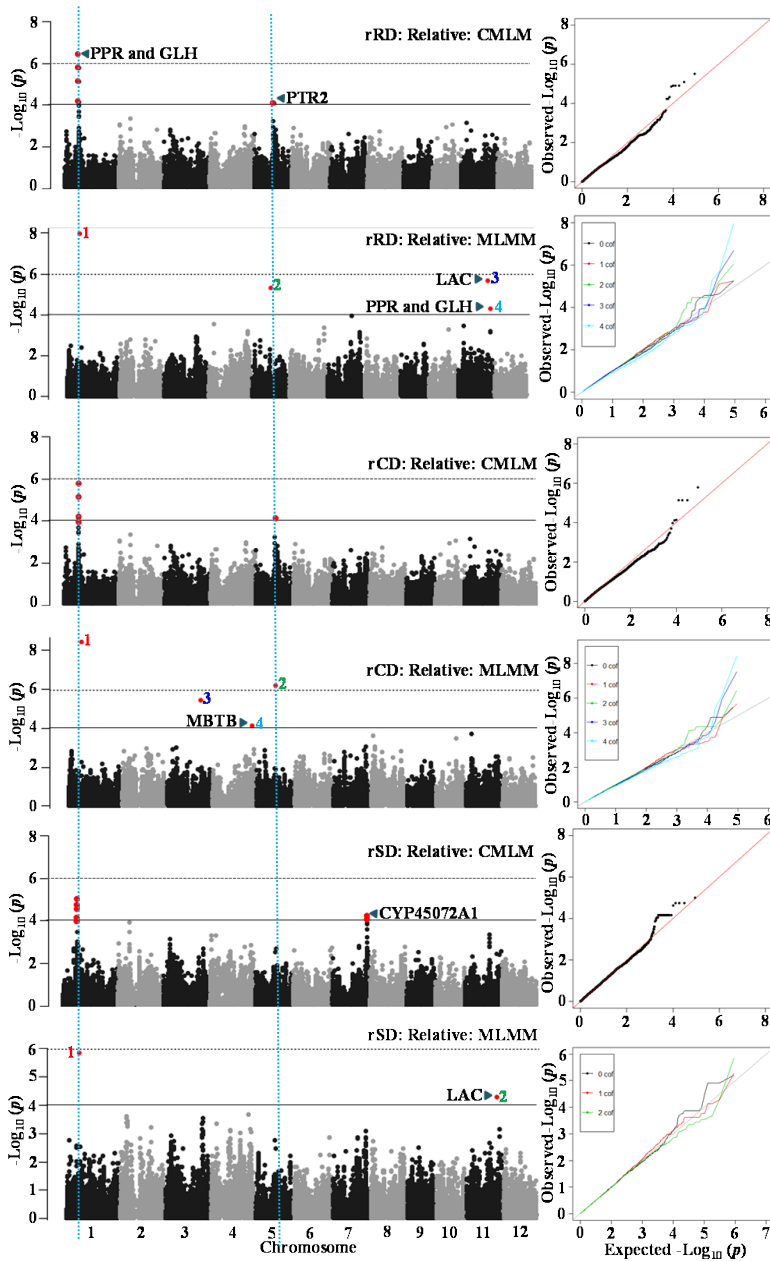
Supplementary Figure S11. The GWAS result through the compressed mixed linear model (CMLM) and the multi-locus mixed model (MLMM) approaches for total root length (TRL) in control and water-deficit stress conditions and for its plasticity as a relative measure. Significant SNPs (coloured red in the Manhattan plots) are distinguished by a threshold P value lines (solid black= $-\text{Log}_{10} P > 4$) and dotted black=Bonferroni-corrected significance threshold). Significant SNP on MLMM Manhattan plots are numbered in the order that they were included in the model as a cofactor (cof in Quantile-Quantile plot is for cofactor). *A priori* candidate genes (see the Supplementary Tables S9-S11) are indicated near to peak SNP in the Manhattan plot.



Supplementary Figure S12. The GWAS result through the compressed mixed linear model (CMLM) and multi-locus mixed model (MLMM) approaches for root weight (RW) and root: shoot ratio (RS) in water-deficit stress condition. Significant SNPs (coloured red in the Manhattan plots) are distinguished by a threshold P value lines (solid black= $[-\text{Log}_{10} P > 4]$ and dotted black=Bonferroni-corrected significance threshold). Significant SNP on MLMM Manhattan plots are numbered in the order that they were included in the model as a cofactor (cof in Quantile-Quantile plot is for cofactor). *A Priori* candidate gene (see the Supplementary Table S10) are indicated near to peak SNP/SNPs in the Manhattan plot.



Supplementary Figure S13. The GWAS result through the compressed mixed linear model (CMLM) and multi-locus mixed model (MLMM) approaches for cumulative water transpiration (CWT) and water use efficiency (WUE) in water-deficit stress condition. Significant SNPs (coloured red in the Manhattan plots) are distinguished by a threshold P value lines (solid black= $-\text{Log}_{10} P > 4$) and dotted black=Bonferroni-corrected significance). Significant SNP on MLMM Manhattan plots are numbered in the order that they were included in the model as a cofactor (cof in Quantile-Quantile plot is for cofactor). *A priori* candidate genes (see the Supplementary Table S8) are indicated near to peak SNP/SNPs in the Manhattan plot.



Supplementary Figure S14. The GWAS result through the compressed mixed linear model (CMLM) and multi-locus mixed model (MLMM) approaches for plasticity as the relative value of the water-deficit stress over the control conditions for root diameter (rRD), cortex diameter (rCD) and stele diameter (rSD). Significant SNPs (coloured red in the Manhattan plots) are distinguished by a threshold P value lines (solid black= $-\text{Log}_{10} P > 4$] and dotted black=Bonferroni-corrected significance). Significant SNP on MLMM Manhattan plots are numbered in the order that they were included in the model as a cofactor (cof in Quantile-Quantile plot is for cofactor). *A priori* candidate genes (see the Supplementary Table S11) are indicated near to peak SNP in the Manhattan plot.

Supplementary Table S1. Descriptive statistics and the significance of *P* (Wald test summary) value based on a linear mixed model for genotype (G), treatment (T) and their interactions (G×T). For more details on trait acronyms and units see the Table 1.

Traits	Control (C)			Water-deficit (WD)			<i>P</i> value (Wald test)			
	Mean±SD	Min	Max	Mean±SD	Min	Max	% C	G	T	G×T
(A) Shoot morphological traits										
PHT	107.00±16.40	63.47	150.10	84.40±13.60	51.70	120.40	-21	<0.001	<0.001	0.027
TN	19.10±6.03	7.67	38.70	14.70±4.14	6.00	28.00	-23	<0.001	<0.001	0.133
TLA	0.19±0.05	0.06	0.37	0.09±0.02	0.04	0.18	-53	<0.001	<0.001	<0.001
SLA	0.02±0.002	0.02	0.03	0.02±0.002	0.02	0.03	-2	<0.001	<0.001	0.131
(B) Physiological traits										
CWT	5.57±1.30	1.72	8.90	2.40±0.49	1.30	4.09	-56	<0.001	<0.001	<0.001
WUE	3.24±0.27	2.40	4.06	4.00±0.44	2.90	6.60	+23	<0.001	<0.001	0.038
(C) Root morphological traits										
TRL	0.76±0.25	0.19	1.67	0.40±0.11	0.15	0.88	-47	<0.001	<0.001	0.004
RL005	0.71±0.24	0.17	1.60	0.39±0.10	0.15	0.84	-45	<0.001	<0.001	0.005
RL0510	41.70±11.15	13.64	87.40	16.80±5.45	5.19	39.00	-60	<0.001	<0.001	<0.001
RL1015	8.27±3.90	1.64	29.30	2.80±1.23	0.48	7.54	-66	<0.001	<0.001	<0.001
RL1520	1.20±0.46	0.33	3.55	0.68±0.28	0.11	1.90	-43	<0.001	<0.001	0.043
RL2025	0.51±0.24	0.11	2.02	0.31±0.14	0.04	0.88	-39	<0.001	<0.001	0.235
RL2530	0.27±0.15	0.04	0.96	0.16±0.08	0.01	0.50	-41	0.004	<0.001	0.411
RL3035	0.12±0.08	0.01	0.48	0.07±0.04	0.004	0.23	-42	0.116	<0.001	0.657
RL35	10.80±10.30	0.41	94.70	7.04±4.70	0.28	30.20	-35	0.711	<0.001	0.922
MRL	58.10±5.60	41.8	73.90	55.50±5.60	37.80	69.40	-4	<0.001	<0.001	0.262
SA	0.40±0.12	0.11	0.94	0.21±0.06	0.07	0.47	-48	<0.001	<0.001	0.006
RV	19.00±5.70	5.85	45.48	9.43±2.80	2.91	21.70	-50	<0.001	<0.001	0.002
ART	0.19±0.02	0.14	0.27	0.17±0.01	0.14	0.21	-11	<0.001	<0.001	0.026
SRL	0.46±0.09	0.26	0.85	0.56±0.13	0.35	1.71	+22	<0.001	<0.001	0.612
TRWD	0.20±0.04	0.10	0.36	0.16±0.03	0.09	0.34	-20	<0.001	<0.001	0.832
RLLA	3.94±0.92	2.04	7.40	4.40±0.98	2.00	8.50	+12	<0.001	<0.001	0.359
(D) Root anatomical traits										
RD	949.50±92	668.10	1305.90	834.17±91.60	597.60	1106.40	-12	<0.001	<0.001	0.507
CD	305.01±32.60	202.00	401.00	250.80±31.70	167.10	345.60	-18	<0.001	<0.001	0.545
SD	228.90±21.22	166.90	283.40	219.18±20.60	157.70	284.40	-4	<0.001	<0.001	0.490
LMXD	42.36±4.50	30.40	58.20	39.46±3.90	27.82	51.38	-7	<0.001	<0.001	0.454
LMXN	4.70±0.50	3.33	6.33	4.60±0.56	3.33	6.67	-2	<0.001	<0.001	0.361
SD:RD	24.20±1.30	20.70	28.30	26.52±1.80	22.57	34.87	+10	<0.001	<0.001	0.648
(E) Dry matter and dry matter partitioning traits										
LW	8.40±2.21	2.57	14.97	4.15±0.82	1.87	6.93	-51	<0.001	<0.001	<0.001
SW	8.01±2.30	2.33	14.73	4.46±0.93	2.00	7.53	-44	<0.001	<0.001	0.002
RW	1.60±0.46	0.54	3.72	0.79±0.25	0.23	1.93	-51	<0.001	<0.001	0.007
TW	18.09±4.55	5.44	31.55	9.39±0.75	4.84	14.81	-48	<0.001	<0.001	<0.001
RS	0.10±0.02	0.05	0.22	0.09±0.02	0.03	0.18	-10	<0.001	<0.001	0.019
LWR	0.47±0.04	0.30	0.55	0.44±0.03	0.32	0.52	-6	<0.001	<0.001	0.055
SWR	0.44±0.05	0.35	0.64	0.47±0.04	0.38	0.63	+7	<0.001	<0.001	0.002

Bold *P* values are not statistically significant ($P \geq 0.05$). % C: % change (+: increase or -: decrease) over control condition.

Supplementary Table S2. Broad-sense (H^2) heritability for 35 phenotypic traits classified in 5 (A-E) categories in control (C) and water-deficit stress (WD) conditions. The narrow-sense (h^2) heritability of 35 phenotypic traits in C, and WD conditions and for their phenotypic plasticity (PP). The details on trait acronyms and units are given in the Table 1.

Trait acronym	H^2		h^2		
	C	WD	C	WD	PP
(A) Shoot morphological traits					
PHT (rPHT)	0.89	0.88	0.84	0.86	0.46
TN (rTN)	0.70	0.77	0.86	0.86	0.46
TLA (rTLA)	0.61	0.58	0.84	0.65	0.57
SLA (rSLA)	0.63	0.52	0.73	0.64	0.34
(B) Physiological traits					
CWT (rCWT)	0.53	0.42	0.70	0.39	0.56
WUE (rWUE)	0.48	0.22	0.59	0.68	0.58
(C) Root morphological traits					
TRL (rTRL)	0.46	0.45	0.82	0.56	0.48
RL005 (rRL005)	0.46	0.44	0.82	0.55	0.49
RL0510 (rRL0510)	0.47	0.47	0.81	0.32	0.34
RL1015 (rRL1015)	0.71	0.6	0.89	0.48	0.51
RL1520 (rRL1520)	0.46	0.45	0.52	0.48	0.08
RL2025 (rRL2025)	0.28	0.30	0.20	0.55	0.21
RL2530 (rRL2530)	0.10	0.08	0.47	0.60	0.30
RL3035 (rRL3035)	-	0.08	-	-	-
RL35 (rRL35)	-	0.04	-	-	-
MRL (rMRL)	0.34	0.13	0.52	0.52	0.28
SA (rSA)	0.49	0.5	0.80	0.52	0.35
RV (rRV)	0.54	0.52	0.79	0.47	0.56
ART (rART)	0.58	0.03	0.57	0.57	0.64
SRL (rSRL)	0.57	0.36	0.78	0.57	0.61
TRWD (rTRWD)	0.44	0.42	0.60	0.58	0.49
RLLA (rRLLA)	0.25	0.40	0.71	0.69	0.17
(D) Root anatomical traits					
RD (rRD)	0.38	0.36	0.70	0.59	0.29
CD (rCD)	0.31	0.33	0.76	0.54	0.31
SD (rSD)	0.47	0.44	0.80	0.72	0.26
LMXD (rLMXD)	0.56	0.46	0.71	0.72	0.33
LMXN (rLMXN)	0.27	0.46	0.56	0.78	0.50
SD:RD (rSDRD)	0.31	0.43	0.75	0.41	0.24
(E) Dry matter traits					
LW (rLW)	0.57	0.57	0.72	0.69	0.63
SW (rSW)	0.51	0.42	0.72	0.33	0.77
RW (rRW)	0.57	0.58	0.78	0.53	0.35
TW (rTW)	0.51	0.47	0.78	0.40	0.63
RS (rRS)	0.44	0.64	0.71	0.71	0.43
LWR (rLWR)	0.25	0.65	0.77	0.65	0.61
SWR (rSWR)	0.82	0.71	0.76	0.45	0.65

Supplementary Table S3. Summary of identified genome-wide significant association loci for phenotypic traits in control condition using compressed mixed linear model (CMLM) and multi-locus mixed model (MLMM) approaches. The loci commonly detected through both the approaches were marked by an asterisk sign (*) and those detected through only MLMM were marked by a hashtag sign (#). All the other unmarked loci were detected only through the CMLM approach. Trait acronyms are given in the Table 1.

Traits	Chr	Position	Allele	MAF	P value _{CMLM}	P value _{MLMM}	RAE	LD block		Size (kb)
								From	To	
(A) Shoot morphological traits										
PHT	5	2173057	A:G	0.201	1.22E-05	-	0.036	2102183	2197641	95
	1*	38286772	G:A	0.288	0.0001	1.23E-05	-0.051	38178239	38437530	259
TN	2*	31650233	A:G	0.307	1.75E-05	4.83E-08	0.095	31624655	31770057	145
	5#	16091302	C:T	0.106	-	4.94E-07	0.241	15933499	16151637	218
	12#	22528624	A:G	0.088	-	5.48E-05	0.246	22511727	22544593	32
SLA	11*	19707755	A:G	0.493	3.08E-05	1.56E-05	-0.030	19695820	19762199	66
(B) Physiological traits										
CWT	1	29132939	G:A	0.062	1.36E-05	-	0.111	29124263	29250090	125
	1*	29441428	A:T	0.066	5.17E-07	1.75E-06	0.127	29394012	29470779	76
	1	29575437	A:G	0.058	1.40E-06	-	0.127	29483935	29597597	113
	1	29600620	C:T	0.058	1.40E-06	-	0.127	29597627	29606402	8
	1	29620240	T:C	0.058	1.40E-06	-	0.127	29606625	29918762	312
	1	29981149	T:G	0.055	3.73E-06	-	0.129	29935443	29999692	64
	1	30060278	G:A	0.055	3.73E-06	-	0.129	30027570	30172920	145
	2	22518040	T:C	0.062	2.60E-05	-	0.113	22518040	22554488	36
	5	7131196	A:G	0.091	7.95E-05	-	0.093	7021512	7216325	194
	11	24219301	C:A	0.124	9.73E-05	-	-0.072	24219246	24244335	25
	11#	7124411	T:C	0.091	-	1.28E-05	0.252	7095402	7124411	29
WUE	4	3707267	G:A	0.128	4.65E-05	-	0.031	3707245	3798274	91
	3	26299468	A:G	0.378	8.03E-05	-	0.023	26078859	26333221	254
	8	20079154	A:G	0.066	9.82E-05	-	0.040	20021659	20091332	69
	7#	20000202	C:T	0.191	-	6.20E-06	-0.026	19968125	20085468	117
	12#	22169193	T:G	0.310	-	1.91E-05	0.031	22161720	22194001	32
(C) Root morphological traits										
TRL	8#	17150092	C:A	0.098	-	3.20E-05	-0.055	17032320	17158399	126
	3#	23497636	T:C	0.084	-	3.74E-08	-0.186	23497636	23514021	16
	2#	34358656	C:A	0.153	-	7.87E-07	0.174	34337530	34358688	21
	6#	416782	T:C	0.271	-	6.20E-05	0.217	397816	457474	59
RL005	8#	17150092	C:A	0.098	-	3.13E-05	-0.052	17032320	17158399	126
	3#	23497636	T:C	0.084	-	3.42E-08	0.192	23497636	23514021	16
	2#	34358656	C:A	0.153	-	6.36E-07	0.180	34337530	34358688	21
RL05100	8#	9082010	C:T	0.084	-	1.44E-06	0.200	9049321	9090378	41
	6#	366330	A:G	0.449	-	4.25E-05	0.168	132127	366436	234
RL1015	5*	7131196	A:G	0.091	5.97E-05	5.05E-09	0.213	7021512	7216325	194
	5	16517488	T:C	0.234	-	7.19E-07	0.165	16218476	16580411	361
	7	6865357	A:G	0.062	-	7.06E-09	0.444	6705724	6865357	159
RL1520	2	24961280	T:A	0.062	-	2.27E-06	-0.156	24937103	24981552	44
	5*	7131196	A:G	0.091	1.46E-05	5.05E-09	0.192	7021512	7216325	194
RL2025	2	25265958	G:T	0.055	4.65E-05	-	0.208	25125170	25265958	140
	2*	25265958	G:T	0.055	3.61E-05	4.30E-06	0.235	25125170	25265958	140
	8#	17321714	A:T	0.474	-	1.93E-06	-0.124	17254709	17338132	83
	1#	28515026	C:G	0.109	-	2.69E-06	0.394	28449249	28917868	468
MRL	2#	24210664	G:A	0.161	-	7.83E-05	-0.194	24210664	24225612	14
	6*	27819933	T:C	0.062	4.14E-05	5.93E-07	-0.049	27819933	27872692	52

Supplementary Table S3. (Continued)

RV	5*	7131196	A:G	0.091	3.66E-05	-	0.140	7021512	7216325	194
	7#	6865357	A:G	0.062	-	1.23E-11	0.327	6705724	6865357	159
	5#	16517488	T:C	0.234	-	1.42E-06	0.127	16218476	16580411	361
	2#	24961280	T:A	0.062	-	8.18E-06	-0.062	24937103	24981552	44
	1#	40526762	T:G	0.288	-	1.55E-05	-0.025	40526762	40614822	88
	11#	24219246	C:T	0.124	-	4.01E-05	-0.098	24219246	24244335	25
ART	11*	28808353	G:C	0.489	1.34E-05	1.76E-05	0.026	28808219	28839108	30
	1	10998576	G:T	0.190	0.0001	-	0.037	10947296	11220396	273
	1	34378789	C:G	0.255	-	1.08E-04	0.041	34378789	34396661	17
SRL	1	25773127	C:A	0.069	8.93E-05	-	0.091	25666408	26101392	434
	1#	43108024	G:C	0.277	-	1.37E-05	-0.057	43065133	43245089	179
	8#	27104372	A:G	0.388	-	4.97E-05	0.354	27104372	27142568	38
RLLA	2*	10134429	G:A	0.343	9.63E-05	4.57E-05	0.069	10134419	10188662	54
	8#	24892309	G:A	0.241	-	7.03E-05	-0.002	24831278	24907343	76
(D) Root anatomical traits										
RD	7*	21266079	C:T	0.099	2.02E-05	2.18E-12	-0.044	21245869	21290877	45
	1*	11112944	C:T	0.175	0.0001	2.68E-07	-0.032	10947296	11220396	273
	3#	4913579	A:G	0.372	-	1.57E-06	-0.033	4882848	5008438	125
	3#	29686521	G:T	0.350	-	1.69E-06	0.032	29614230	29742101	127
	5#	28880728	A:C	0.408	-	3.86E-05	0.018	28862506	28957228	94
CD	7*	21266079	C:T	0.099	9.86E-06	3.12E-06	-0.052	21245869	21290877	45
LMXD	4*	29450620	A:G	0.095	4.58E-05	4.91E-06	0.046	29398010	29526672	128
	4	29606053	A:C	0.168	7.88E-05	-	0.043	29531026	29621778	90
	1#	19177575	A:G	0.190	-	4.32E-06	0.108	19174820	19262944	88
	12#	22371182	C:T	0.377	-	5.49E-05	-0.013	22194036	22425011	230
LMXN	11#	2838776	G:T	0.297	-	6.59E-06	0.046	2723682	2942360	218
	1#	39902281	T:C	0.190	-	2.66E-05	-0.035	39886933	40061573	174
SD:RD	7	21266079	C:T	0.099	7.28E-05	-	0.020	21245869	21290877	45
	4#	31749561	G:T	0.095	-	5.29E-05	-0.052	31728015	31778051	50
(E) Dry matter traits										
SW	1	29132939	G:A	0.062	6.42E-05	-	0.140	29124263	29250090	125
	1*	29441428	A:T	0.066	7.82E-06	5.53E-06	0.150	29394012	29470779	76
	1	29575437	A:G	0.058	1.50E-05	-	0.154	29483935	29597597	113
	1	29600620	C:T	0.058	1.50E-05	-	0.154	29597627	29606402	8
	1	29620240	T:C	0.058	1.50E-05	-	0.154	29606625	29918762	312
	1	29981149	T:G	0.055	5.15E-05	-	0.149	29935443	29999692	64
	1	30060278	G:A	0.055	5.15E-05	-	0.149	30027570	30172920	145
	5	7131196	A:G	0.091	2.59E-05	-	0.127	7021512	7216325	194
LW	6	366330	G:A	0.449	7.71E-05	-	0.067	132127	366436	234
	5	7131196	A:G	0.091	8.85E-05	-	0.114	7021512	7216325	194
	11*	7124411	T:C	0.091	9.18E-05	1.77E-05	0.108	7095402	7149638	54
	7#	15930391	G:A	0.285	-	5.63E-05	-0.020	15930391	16109354	178
RW	5*	7131196	A:G	0.091	6.78E-05	4.05E-05	0.138	7021512	7216325	194
TW	1*	29441428	A:T	0.066	7.57E-05	3.39E-05	0.127	29394012	29470779	76
	1	39058787	T:G	0.248	9.20E-05	-	0.072	39047133	39165647	118
	5#	7131196	A:G	0.091	-	5.03E-05	0.213	7021512	7216325	194
RS	1*	39255482	C:T	0.350	2.24E-05	1.28E-06	0.100	39225855	39394856	169
	12*	25497648	C:A	0.232	7.25E-05	5.70E-06	0.080	25482817	25632919	150
	1#	1562911	A:C	0.365	-	1.07E-07	-0.160	1532281	1562911	30
LWR	8*	3265446	C:T	0.084	6.54E-06	5.28E-07	-0.043	3248294	3318437	70
	9	14127114	C:T	0.193	3.56E-05	-	-0.026	14053172	14127114	73
	1	14788199	C:T	0.069	3.99E-05	-	-0.040	14749963	14788222	38
	3	32750373	A:C	0.223	9.26E-05	-	-0.023	32637987	32847633	209
	7#	21266079	C:T	0.096	-	6.12E-06	-0.087	21245869	21290877	45
	5#	23606267	C:T	0.124	-	1.03E-05	0.047	23606267	23623230	16
SWR	1*	14788199	C:T	0.069	1.54E-06	2.07E-09	0.059	14749963	14788222	38

Supplementary Table S3. (Continued)

8	3265446	C:T	0.084	4.29E-06	-	0.052	3248294	3318437	70
9	14127114	C:T	0.193	8.13E-05	-	0.030	14053172	14127114	73
12	5829054	G:T	0.197	8.34E-05	-	0.036	5829054	5839553	10
9	14829621	G:A	0.142	9.20E-05	-	0.036	14813317	14833005	19
6 [#]	6744100	G:A	0.387	-	2.91E-05	0.048	6684474	6769503	85
12 [#]	141599	G:A	0.124	-	6.14E-06	0.080	141599	148272	6
11 [#]	18947620	T:C	0.179	-	1.14E-05	0.052	18922273	18954436	32
11 [#]	22302172	G:A	0.051	-	7.45E-05	0.120	22274274	22302172	27

Chr: chromosome, MAF: minor allele frequency, RAE: relative allelic effect calculated as a ratio of minor allele effect trait value to population average trait value, LD: linkage disequilibrium

Supplementary Table S4. Summary of identified genome-wide significant association loci for phenotypic traits in water-deficit condition using compressed mixed linear model (CMLM) and multi-locus mixed model (MLMM) approaches. The loci commonly detected through both the approaches were marked by an asterisk sign (*) and those detected through only MLMM were marked by a hashtag sign (#). All the other unmarked loci were detected only through the CMLM approach. Trait acronyms are given in the Table 1.

Traits	Chr	Position	Allele	MAF	P value _{CMLM}	P value _{MLMM}	RAE	LD block		Size (kb)	
								From	To		
(A) Shoot morphological traits											
PHT	1*	38286772	G:A	0.288	8.88E-06	3.14E-07	-0.065	38178239	38437530	259	
	3*	30407838	C:G	0.297	2.75E-05	5.32E-06	-0.039	30407838	30499464	91	
	5*	2173057	A:G	0.201	2.81E-05	3.88E-06	0.040	2102183	2197641	95	
	6#	22909435	A:G	0.051	-	5.95E-06	0.213	22850994	22969216	118	
TN	3*	9995472	C:T	0.265	5.80E-06	1.03E-06	0.089	9967155	10106317	139	
	2	25053043	C:T	0.398	2.58E-05	-	0.059	25044454	25109632	65	
	8	4505925	C:A	0.058	3.68E-05	-	0.173	4505925	4629870	123	
	1*	24821998	T:A	0.401	7.61E-05	1.69E-05	0.071	24792895	24869656	76	
TLA	8*	25121944	C:T	0.077	5.42E-05	2.47E-06	0.111	25091497	25238735	147	
	3#	29050414	C:T	0.088	-	1.22E-05	0.178	29018521	29050414	33	
	3#	11725360	C:A	0.172	-	7.85E-05	0.189	11693492	11725360	31	
(B) Physiological traits											
CWT	1#	23207640	G:A	0.066	-	8.30E-06	-0.147	23095746	23298172	202	
	4#	34640918	C:A	0.175	-	3.59E-05	0.047	34608671	34640918	32	
	6#	13412649	G:C	0.077	-	4.33E-05	-0.078	13360689	13465974	105	
WUE	9#	15426362	T:G	0.263	-	1.49E-05	0.074	15394548	15559339	164	
	11#	27574096	C:T	0.08	-	1.92E-08	0.112	27478419	27603835	125	
	6#	23297154	A:G	0.336	-	7.41E-05	0.047	23243062	23338253	95	
(C) Root morphological traits											
TRL	2#	8835096	G:T	0.149	-	2.20E-06	0.145	8769237	8874697	105	
	4#	29111186	T:C	0.084	-	1.20E-05	0.235	28701604	29126558	424	
	11#	7124411	T:C	0.091	-	2.04E-05	0.228	7095402	7124411	29	
RL005	2#	8835096	G:T	0.149	-	1.56E-06	0.144	8769237	8874697	105	
	4#	29111186	T:C	0.084	-	1.34E-05	0.228	28701604	29126558	424	
	11#	7124411	T:C	0.091	-	2.50E-05	0.215	7095402	7124411	29	
RL0510	11	24625645	T:C	0.069	2.24E-05	-	0.165	24423060	24639658	216	
	11	25317141	G:C	0.235	9.42E-05	-	0.092	25317141	25426798	109	
	1*	23079331	A:G	0.113	9.51E-05	2.50E-06	-0.122	22992632	23095676	103	
	12#	26195748	A:G	0.080	-	2.34E-05	0.263	26124690	26202838	78	
	9#	14829621	G:A	0.142	-	1.18E-04	-0.211	14813317	14833005	19	
RL1015	1*	23044334	T:C	0.113	6.18E-05	6.53E-05	-0.175	22992632	23095676	103	
RL2025	1*	4421833	G:A	0.217	9.36E-06	6.77E-08	0.174	4421833	4438552	16	
	1	42799636	C:A	0.192	9.23E-05	-	0.145	42799636	42856304	56	
	2*	5180480	A:G	0.434	2.05E-05	3.90E-05	0.129	5054863	5189396	134	
	5	10646015	C:T	0.153	7.69E-05	-	0.161	10584713	10646015	61	
	6	6996556	T:G	0.091	8.14E-05	-	-0.194	6951049	7001492	50	
	6	7006358	C:G	0.091	8.14E-05	-	-0.210	7001506	7106699	105	
	3#	6374082	T:C	0.219	-	4.25E-05	-0.045	6217543	6439952	222	
	10#	11555942	A:G	0.117	-	9.72E-05	-0.181	11390755	11575800	185	
	RL2530	11*	24267277	A:T	0.066	3.69E-05	7.30E-08	0.294	24267277	24279832	12
		2	503016	A:G	0.124	5.23E-05	-	0.213	503016	536341	11
10#		18971155	C:T	0.234	2.42E-05	-	-0.244	18898657	19018639	119	
6#		7045303	C:T	0.088	3.24E-05	-	-0.281	7001506	7106699	105	
MRL	12*	17607622	G:T	0.131	1.15E-05	3.28E-06	-0.042	17563026	17617181	54	
	12	17780100	C:T	0.135	4.82E-05	-	-0.039	17779917	17952275	172	

Supplementary Table S4. (Continued)

	12	17977281	G:A	0.117	2.46E-05	-	-0.043	17973553	18060777	87
	2*	2783451	C:T	0.206	1.35E-05	1.02E-05	0.035	2749982	2802120	52
RV	11	7124411	T:C	0.091	5.68E-05		0.135	7095402	7124411	29
	9*	14829621	G:A	0.142	7.31E-05	3.84E-07	-0.109	14813317	14833005	19
	1*	23044334	T:C	0.113	7.93E-05	1.94E-06	-0.119	22992632	23095676	103
	12#	26195748	A:G	0.08	-	2.24E-06	0.220	26124690	26202838	78
	11#	22973837	A:G	0.153	-	5.41E-05	-0.168	22703332	22976412	273
SA	1#	23044334	T:C	0.113	-	3.23E-06	-0.157	22992632	23095676	103
	9#	14829621	G:A	0.142	-	1.26E-05	-0.190	14813317	14833005	19
	2#	8835096	G:T	0.149	-	5.91E-05	0.114	8769237	8874697	105
	3#	35654626	A:C	0.106	-	6.12E-06	-0.095	35605462	35654703	49
	5#	14825506	G:A	0.066	-	7.12E-05	0.271	14818383	14881083	62
ART	11*	6245556	C:T	0.255	5.85E-05	4.23E-06	-0.024	6232379	6350995	118
	9	20970824	T:C	0.088	0.0001		-0.029	20953059	21030489	77
SRL	1*	23218344	T:C	0.058	4.31E-06	6.56E-05	0.148	23095746	23298172	202
	1	23095621	A:G	0.062	3.73E-05	-	0.125	22992632	23095676	103
	2	33496059	G:A	0.051	9.36E-06	-	0.143	33487245	33529812	42
	2	24006148	G:C	0.073	1.53E-05	-	0.138	23898412	24059505	161
	2	24122043	C:G	0.084	2.39E-05	-	0.121	24108015	24136056	28
	5*	15673557	G:T	0.073	3.00E-05	7.05E-08	0.121	15469660	15756954	287
	6*	27819933	T:C	0.062	4.96E-05	1.85E-06	0.121	27819933	27872692	52
	8#	51541	T:C	0.102	-	1.05E-04	-0.168	51541	148519	96
RLLA	6*	5760641	T:C	0.087	1.31E-05	9.80E-07	0.116	5758331	5783531	25
	2*	25154659	T:C	0.113	5.54E-05	1.17E-07	0.093	25125170	25212962	87
	8#	27563586	T:C	0.456	-	7.05E-06	0.086	27563572	27583372	19
	3#	27177614	C:A	0.223	-	3.47E-05	0.145	27144252	27252032	107
(D) Root anatomical traits										
SD	9*	13788883	C:A	0.068	7.75E-05	1.63E-07	-0.045	13665706	13788883	123
	5#	3057869	A:G	0.450	-	5.92E-06	0.069	3048995	3074221	25
	2#	17151144	C:T	0.165	-	3.08E-05	-0.086	17075796	17222194	146
	3#	31345248	A:G	0.322	-	4.92E-05	-0.040	31311835	31345248	33
LMXN	11*	25552124	C:A	0.053	2.47E-06	1.84E-07	0.091	25542935	25854764	311
	7*	1316016	A:T	0.319	8.15E-05	1.36E-06	-0.039	1316016	1523942	207
	3#	34487907	G:T	0.161	-	5.30E-05	-0.073	34418455	34496574	78
LMXD	9#	13788883	C:A	0.066	-	2.25E-08	-0.080	13665706	13788883	123
	2#	6749649	A:G	0.405	-	1.77E-08	0.064	6706866	6752341	45
	3#	31305902	A:G	0.478	-	2.47E-05	-0.017	31305888	31311496	5
	5#	10668631	C:T	0.197	-	4.52E-06	-0.036	10641707	10668631	26
	5#	3057869	A:G	0.451	-	3.38E-09	0.063	3048995	3074221	25
	6#	471179	G:A	0.070	-	6.16E-07	0.075	467003	531468	64
	11#	28871551	G:A	0.095	-	2.48E-05	0.101	28864998	28907095	42
SD:RD	11*	25175343	T:C	0.058	2.82E-05	2.99E-06	0.038	25160136	25181615	21
	11	25182643	C:T	0.064	5.67E-05	-	0.036	25182643	25288987	106
	1*	1676898	C:G	0.237	5.74E-05	1.90E-06	0.023	1676850	1833926	157
(E) Dry matter traits										
LW	1	15402532	T:C	0.164	6.23E-05	-	-0.075	15393938	15402532	8
	1*	15402601	C:T	0.164	6.23E-05	6.69E-06	-0.075	15402553	15441315	38
SW	12*	17786153	G:T	0.355	3.67E-05	2.11E-05	0.067	17779917	17952275	172
	3*	11713631	T:C	0.197	4.12E-05	1.05E-05	0.081	11693492	11725360	31
RW	4*	29111186	T:C	0.083	3.44E-06	1.47E-06	0.177	28701604	29126558	424
	6	6579613	T:A	0.120	7.07E-05	-	0.122	6579551	6598292	18
	3	34943958	T:C	0.339	8.21E-05	-	0.097	34927423	34977879	50
	1	23079331	A:G	0.113	9.51E-05	-	-0.122	22992632	23095676	103
RS	4*	29111186	T:C	0.083	9.31E-08	2.75E-11	0.222	28701604	29126558	424
	4	29184866	G:A	0.113	4.37E-06	-	0.111	29126713	29377299	250
	4	29450620	A:G	0.094	7.06E-05	-	0.111	29398010	29526672	128
	1#	1562911	A:C	0.365	1.54E-05	-	-0.133	1532281	1562911	30
LWR	2*	23246559	C:A	0.113	2.26E-05	1.94E-06	0.030	23184521	23514586	330
	2*	20169674	A:G	0.427	8.53E-05	2.16E-05	-0.016	20169653	20202576	32

Supplementary Table S4. (Continued)

	9*	14829621	G:A	0.142	3.49E-05	7.63E-06	-0.027	14813317	14833005	19
	11#	4823624	T:C	0.109	5.67E-06	-	0.041	4583780	4823732	239
SWR	9*	14829621	G:A	0.142	1.81E-07	3.01E-07	0.040	14813317	14833005	19
	9	14847601	A:T	0.131	1.34E-06	-	0.038	14833007	14847696	14
	7	20874845	C:G	0.166	3.41E-05	-	0.030	20774955	20901272	126
	1#	40813452	T:C	0.168	-	4.06E-05	0.051	40813452	40832763	19

Chr: chromosome, MAF: minor allele frequency, RAE: relative allelic effect calculated as a ratio of minor allele effect trait value to population average trait value, LD: linkage disequilibrium.

Supplementary Table S5. Summary of identified genome-wide significant association loci for plasticity of phenotypic traits using compressed mixed linear model (CMLM) and multi-locus mixed model (MLMM) approaches. The loci commonly detected through both the approaches were marked by asterisk sign (*) and those detected through only MLMM were marked by a hashtag sign (#). All the other unmarked loci were detected only through the CMLM approach. Trait acronyms are given in the Table 1.

Traits	Chr	Pos	Allele	MAF	P value _{CMLM}	P value _{MLMM}	AE	LD block		Size (kb)
								From	To	
(A) Shoot morphological traits										
rPHT	2*	24405418	T:C	0.058	4.68E-06	8.53E-07	-0.030	24405418	24432576	27
	6#	19606050	C:T	0.464	-	4.64E-05	0.021	19496375	19730704	234
rTN	12*	25006932	C:T	0.091	4.63E-05	4.40E-05	-0.080	24762153	25006932	244
rTLA	7#	15930391	A:G	0.285	-	1.52E-05	0.026	15930391	16109354	178
	7#	9463744	A:G	0.080	-	1.27E-05	-0.088	9317314	10004086	186
	3#	1706123	T:A	0.066	-	5.22E-05	-0.068	1705565	1730221	24
rSLA	11*	19245430	C:T	0.124	6.18E-05	2.56E-05	-0.030	19197921	19245506	47
	3	34125791	T:G	0.270	9.80E-05	-	-0.023	34069089	34183243	114
(B) Physiological traits										
rCWT	7*	9463744	G:A	0.080	1.29E-05	1.77E-05	-0.052	9317314	10004086	186
	1	33277486	T:C	0.467	2.62E-05	-	-0.030	32994632	33284067	289
	1	33293954	G:A	0.471	5.65E-05	-	-0.030	33293954	33727514	433
	1	33755921	T:G	0.493	4.48E-05	-	-0.028	33755921	34165612	409
	1	34280616	G:A	0.453	7.83E-05	-	0.028	34184887	34357192	172
	1*	42575227	A:G	0.069	3.81E-05	8.09E-05	-0.050	42467072	42587728	120
(C) Root morphological traits										
rTRL	12*	25006932	C:T	0.093	6.73E-05	3.66E-09	-0.094	24762153	25006932	244
	7#	9463744	G:A	0.080	-	3.81E-06	-0.150	9317314	10004086	186
	1#	26826635	T:C	0.120	-	2.91E-05	-0.123	26709644	26847391	137
	4#	30764890	A:G	0.354	-	2.20E-05	-0.107	30690751	30790417	99
	2#	4943157	C:T	0.343	-	5.81E-05	-0.050	4868972	4950264	95
rRL005	12	25006932	C:T	0.093	8.33E-05	-	-0.098	24762153	25006932	244
rRL1015	3#	35780154	A:G	0.343	-	3.23E-07	0.054	35765758	35793182	27
	12#	6154896	A:G	0.120	-	1.67E-05	0.109	6141695	6218230	76
	3#	26828159	A:G	0.073	-	9.66E-05	-0.131	26756997	26978105	221
rRL2025	4#	16463674	A:G	0.423	-	4.35E-05	-0.170	16397482	16542176	144
rRL2530	3	2553785	A:G	0.055	1.70E-05	-	-0.370	2497861	2572474	74
	3	2714299	C:A	0.062	5.95E-05	-	-0.320	2630128	2714299	84
	3*	34392848	C:T	0.080	5.64E-05	3.71E-05	-0.280	34389921	34415828	25
	rSA	12*	25006932	C:T	0.093	4.46E-05	6.33E-05	-0.079	24762153	25006932
rRV	7#	9463899	T:C	0.091	-	1.47E-05	-0.128	9317314	10004086	186
rRV	12*	25006932	C:T	0.093	5.43E-05	2.07E-05	-0.068	24762153	25006932	244
	1#	42575227	A:G	0.069	-	2.07E-05	-0.137	42467072	42587728	120
rMRL	12	17977281	G:A	0.117	2.31E-05	-	0.052	17973553	18060777	87
	12	17607622	G:T	0.131	0.0001	-	0.050	17563026	17617181	54
	2*	26794003	A:T	0.084	3.88E-05	2.58E-06	-0.060	26585953	26796794	210
	6#	25183518	C:T	0.142	-	3.33E-06	0.077	25177943	25227042	49
rSRL	8*	26362631	T:A	0.051	1.77E-05	1.66E-08	-0.150	26333486	26384762	51
	3#	34024418	C:T	0.080	-	2.08E-06	0.180	34004938	34069043	64
	1#	20574500	C:T	0.307	-	2.97E-07	-0.147	20478562	20579687	101
	5#	2184238	A:C	0.324	-	1.56E-05	-0.100	2102183	2197641	95
rART	1	29981149	T:G	0.055	9.06E-05	-	-0.056	29935443	30019818	84
	1	30060278	G:A	0.055	9.06E-05	-	-0.056	30027570	30084144	56
	1*	34378789	G:C	0.254	6.43E-05	1.43E-07	0.029	34378789	34396661	17
	5#	28880707	A:G	0.165	8.13E-06	-	-0.063	28862506	28957228	94
	5#	2184238	A:C	0.324	5.93E-05	-	0.027	2102183	2197641	95
rTRWD	1*	25703110	G:T	0.095	2.07E-05	6.51E-06	-0.090	25666408	26101392	434
	1#	20571077	A:C	0.270	-	7.82E-05	0.090	20478562	20579687	101
rRLLA	5	213976	C:A	0.151	6.44E-05	2.63E-05	-0.100	192969	219803	26

Supplementary Table S5. (Continued)

(D) Root anatomical traits										
rRD	1*	11038867	T:G	0.307	3.17E-06	2.09E-07	-0.036	10947296	11220396	273
	1	11596350	A:G	0.276	8.12E-06	-	-0.034	11502214	11611147	108
	5*	15841709	G:A	0.279	4.77E-05	2.51E-06	-0.032	15709743	15874456	164
	11#	25434106	G:C	0.338	1.86E-05	-	0.040	25434106	25522849	88
rCD	1*	11038867	T:G	0.306	1.65E-06	3.79E-09	-0.073	10947296	11220396	273
	1	11596350	A:G	0.275	7.48E-05	-	-0.990	11502214	11611147	108
	5*	15841709	G:A	0.279	7.87E-05	6.64E-07	0.042	15709743	15874456	164
	3#	27843993	C:T	0.237	-	3.74E-06	0.027	27703252	27847143	143
4#	33647561	G:A	0.179	-	7.35E-05	0.061	33647561	33661659	14	
rSD	1*	11038867	T:G	0.307	1.00E-05	1.49E-06	-0.029	10947296	11220396	273
	1	11596350	A:G	0.276	2.39E-05	-	-0.028	11502214	11611147	108
	7	27122192	G:T	0.215	7.09E-05	-	0.028	27021782	27141446	119
	11	25434106	G:C	0.338	-	5.23E-05	0.032	25434106	25522849	88
rLMD	7*	27141434	C:T	0.219	4.06E-05	3.41E-05	0.028	27021782	27141446	119
	4#	32411349	T:C	0.410	-	8.11E-05	0.042	32404768	32451098	46
(E) Dry matter traits										
rLW	7#	15930391	A:G	0.285	-	3.69E-05	0.023	15930391	16109354	178
rSW	6#	7840678	A:G	0.296	-	4.90E-05	-0.114	7785975	7909286	123
rRW	4#	29184866	A:G	0.113	-	1.21E-05	-0.108	29126713	29377299	250
rRS	2*	651557	A:C	0.292	1.78E-05	5.11E-06	-0.061	636695	672438	35
	3*	26825291	G:C	0.102	2.00E-05	1.70E-06	-0.096	26756997	26978105	221
	8#	17221046	C:T	0.055	-	5.37E-05	0.084	17176998	17243358	66
	12	19648498	G:A	0.073	2.91E-05	-	-0.100	19628587	19662212	33
rLWR	9#	1450424	C:T	0.237	-	4.36E-07	-0.031	1317383	1826588	509
	9#	14127114	C:T	0.193	-	1.88E-06	-0.038	14053172	14127114	73
	2#	25453820	T:G	0.252	-	1.36E-05	0.021	25442913	25550826	107
	5#	925555	C:T	0.394	-	9.62E-06	0.019	925555	966011	40
rSWR	2#	35635147	G:T	0.102	-	5.65E-06	-0.053	35378463	35635147	256
	2#	24133875	C:G	0.143	-	2.72E-07	-0.065	24108015	24136056	28
	2#	25596944	A:G	0.172	-	7.99E-05	-0.046	25568600	25609348	40

Chr: chromosome, MAF: minor allele frequency, RAE: relative allelic effect calculated as a ratio of minor allele effect trait value to population average trait value, LD: linkage disequilibrium.

Supplementary Table S6: Genetic loci associated with more than one phenotypic traits in control (22 loci), water-deficit stress (10 loci) and for phenotypic plasticity (9 loci).

Chr	Control		Water-deficit		Phenotypic plasticity	
	Position	Traits	Position	Traits	Position	Traits
1	29132939	CWT and SW	23044334	RL1015, RV and SA	11038867	rRD, rCD, and rSD
	29441428	CWT, SW and TW	23079331	RL0510 and RW	11596350	rRD, rCD, and rSD
	29575437	CWT and SW	23207640/23218344	CWT/SRL	42575227	rCWT and rRV
	29600620	CWT and SW				
	29620240	CWT and SW				
3	29981149	CWT and SW				
	30060278	CWT and SW				
2	14788199	LWR and SWR				
	1099857/1111294	ART/RD				
	24961280	RL1015 and RV	8835096	TRL, RL005 and SA		
	25265958	RL1520 and RL2025				
3	34358656	TRL and RL005				
	23497636	TRL and RL005				
4			29111186	TRL, RL005, RW and RS		
5	7131196	CWT, RL1015, RL1520, RV, SW, LW, RW and TW	3057869	SD and LMXD	2184238	rSRL and rART
	16517488	RL1015 and RV			15841709	rRD and rCD
6	366330	RL0510 and LW				
7	6865357	RL1015 and RV			9463744/9463899	rTLA, rCWT, rTRL
	21266079	RD, CD, SD, RD and LWR			15930391	rTLA and rLW
8	3265446	LWR and SWR				
	17150092	TRL and RL005				
9	14127114	LWR and SWR	13788883	SD and LMXD		
			14829621	RL0510, RV, SA, LWR and SWR		
11	7124411	CWT and LW	7124411	TRL, RL005 and SA	25434106	rRD and rSD
12			26195748	RL0510 and RV	25006932	rTLN, rTRL, rRL005 and rRV

Supplementary Table S7. Genetic loci for total root length (TRL) and root length of different root thickness classes (as a component trait of TRL) in control (C), water-deficit (WD), and for their phenotypic plasticity (PP). Genetic loci (L) for TRL and its component traits are numbered from L1 to L14 (C), L15 to L35 (WD) and L36-L44 (PP). In the table, numbers are significant SNPs position and superscript numbers in brackets are chromosome number. SNPs number with number in bracket are assigned to unique loci and common loci are indicated only by genetic loci mentioned in brackets. †=novel loci identified for TRL component traits only.

Treatment	TRL	Root length of different root thickness classes								Novel loci†
		RL005	RL0510	RL1015	RL1520	RL2025	RL2530			
C (L1 to L14)	17150092 (L1 ⁸)	(L1 ⁸)	9082010 (L5 ⁸)	7131196 (L7 ²)	(L7 ²)	(L11 ²)	(L11 ²)	-	-	10
	23497636 (L2 ³)	(L2 ³)	366330 (L6 ⁶)	16517488 (L8 ⁵)	25265958 (L11 ²)	17321714 (L12 ⁸)	-	-		
	34358656 (L3 ²)	(L3 ²)	-	6865357 (L9 ⁷)	-	28515026 (L13 ⁴)	-	-		
	416782 (L4 ⁶)	-	-	24961280 (L10 ²)	-	24210664 (L14 ²)	-	-		
WD (L15 to L35)	8835096 (L15 ²)	(L15 ²)	24625645 (L18 ¹¹)	23044334 (L23 ⁴)	-	4421833 (L24 ⁴)	24267277 (L32 ¹¹)	-	-	18
	2911186 (L16 ⁴)	(L16 ⁴)	25317141 (L19 ¹¹)	-	-	42799636 (L25 ⁴)	503016 (L33 ²)	-	-	
	7124411 (L17 ¹¹)	(L17 ¹¹)	23079331 (L20 ⁴)	-	-	5180480 (L26 ³)	18971155 (L34 ¹⁰)	-	-	
	-	-	26195748 (L21 ¹²)	-	-	10646015 (L27 ⁵)	7045303 (L35 ⁶)	-	-	
	-	-	14829621 (L22 ⁹)	-	-	6996556 (L28 ⁶)	-	-	-	
	-	-	-	-	-	7006358 (L29 ⁶)	-	-	-	
PP (L36 to L44)	25006932 (L36 ¹²)	(L36 ¹²)	-	-	-	6374082 (L30 ³)	-	-	-	4
	9463744 (L37 ⁷)	-	-	-	-	11555942 (L31 ¹⁰)	-	-	-	
	26826635 (L38 ¹)	-	-	-	-	16463674 (L41 ⁴)	2553785 (L42 ²)	2714299 (L43 ⁵)	-	
	30764890 (L39 ⁴)	-	-	-	-	-	-	34392848 (L44 ³)	-	
4943157 (L40 ²)	-	-	-	-	-	-	-	-	-	

Supplementary Table S8: The *a priori* candidate genes underlying different loci/locus of shoot morphological, physiological, dry matter traits in control (C; 32 genes), water-deficit stress conditions (WD; 21 genes) and for its phenotypic plasticity (PP;17 genes) as a relative measure. *A priori* candidate gene annotations in bold were responsive to abiotic stress stimulus (Gene Ontology:0009628) according to Rice genome browser database. Trait acronyms are given in the Table 1. †=Distance of gene from peak SNP.

Traits	Trt	Chr	SNP	Gene ID	Distance (kb)†	Acr	Gene annotation	General description	Ref
PHT	C	1*	38286772	LOC_Os01g66100.1	95	GA20OX	Gibberellin 20 oxidase 2	The mutant semi dwarf (<i>sd1</i> - "green revolution rice") phenotype in rice is the result of a deficiency of active GA in the elongating stem arising from a defective 20-oxidase GA biosynthetic enzyme.	(Spielmeyer et al., 2002)
		5	2173057	LOC_Os05g04610.1	4	ABC	ABC transporter, ATP-binding protein	Basipetal and acropetal auxin transport and previous study predicted this candidate gene in one of the QTLs on chromosome 1 for plant height in rice.	(Ishimaru et al., 2004)
TN	C	2*	31650233	LOC_Os02g51670.1	Within	ERF1	Ethylene-responsive transcription factor	Involved in the cross talk between ethylene and GA; down regulates ethylene-induced enhancement of GA synthase. Rice ERF (<i>Ose1TB</i>) regulates tillering.	(Qi et al., 2011)
		5*	16091302	LOC_Os09g26590.1	34	SAUR	OsSAUR37 - Auxin-responsive SAUR	Early auxin responsive gene, multicellular organism development, rice mutant showed dwarfism, sterility and lower tillering.	(Jain et al., 2006)
				LOC_Os09g26610.1	53	SAUR	OsSAUR38 - Auxin-responsive SAUR		
		12*	22528624	LOC_Os12g36770.2	2	LipIII	Lipase class 3 family protein	Regulates tillering, plant height and spikelet fertility in rice. Possibly involved in phytohormone signalling of strigolactone and auxin.	(Liu et al., 2013)
CWT and TW	C	1	29132939	LOC_Os01g50720.1	Within	MYB	MYB family transcription factor	Phytohormone signalling, response to water-deficit and salt stress, regulates root development and lateral root by modulating auxin inducible genes.	(Ambawat et al., 2013)
		1*	29441428	LOC_Os01g51154.1	35	MYB	Single myb histone	Phytohormone signalling, response to water-deficit and salt stress, regulates root development and lateral root by modulating auxin inducible genes.	(Ambawat et al., 2013)
CWT and SW	C			LOC_Os01g51260.1	28	MYB	MYB family transcription factor	Phytohormone signalling, response to water-deficit and salt stress, regulates root development and lateral root by modulating auxin inducible genes.	(Ambawat et al., 2013)
		1	29575437	LOC_Os01g51300.1	74	Gβ	WD domain, G-beta repeat domain containing protein	Subunit of large heterotrimeric G protein (<i>gβr</i>) negatively regulates auxin induced signalling. Loss of function mutant in G-protein have altered auxin mediated cell division during formation of lateral and adventitious root primordia.	(Ullah et al., 2003)
				LOC_Os01g51420.1	7	CALB	Calcineurin B	Plays critical role in diverse Ca ²⁺ -dependent processes in plants. Interacts with protein kinase CIPK23 and regulates leaf transpiration and root potassium uptake in <i>Arabidopsis</i> .	(Cheong et al., 2007)
		1	29620240	LOC_Os01g51780.1	158	AEC	Auxin efflux carrier component	Polar auxin transport and homeostasis, auxin activated signalling and mutant shows defects in root development. Regulates leaf formation and phyllotaxis.	(Griencisen et al., 2007), (Reinhardt et al., 2003)
CWT, LW, SW and TW	C	5	7131196	LOC_Os05g12180.1	96	PIP1	CAPI1	The <i>Arabidopsis</i> orthologue encodes regulatory elements (PYL8 or RCAR3) of ABA receptor. Positive regulation of abscisic acid-activated signalling pathway. Promotes lateral root development by enhancing MYB77-dependent transcription of auxin-responsive genes.	(Zhao et al., 2014)
				LOC_Os05g12400.1	4	BURP	BURP domain containing protein	ABA responsive and loss of function increased moisture stress resistance	(Harshavardhan et al., 2014)
				LOC_Os05g12410.1	6	BURP	BURP domain containing protein	ABA responsive and loss of function increased moisture stress resistance	(Harshavardhan et al., 2014)
CWT	C	11*	7124411	LOC_Os11g12620.1	20	CLV1	Receptor protein kinase CLAVATA1	Regulates root meristems, regulation of root plasticity in response to nitrogen.	(Stahl et al., 2013), (Araya et al., 2014)
WUE	C	4	3707267	LOC_Os04g07150.1	84	AGAP	AGAP002737-PA	The <i>Arabidopsis</i> orthologue of unknown protein response to ABA.	NA
		7*	20000202	LOC_Os07g33440.1	14	CYP450	Cytochrome P450	The <i>Arabidopsis</i> orthologue catalyses essential oxidative step in the biosynthesis of brassinosteroid (BR). BR in interaction with auxin promotes lateral root developments and regulates stomatal development.	(Bao et al., 2004), (Kim et al., 2012)
LW	C	12*	22169193	LOC_Os12g36194.1	14	NDPK	Nucleoside diphosphate kinase	Regulates expression of antioxidant enzymes and multiple environmental stress tolerance.	(Tang et al., 2008)
		6	366330	LOC_Os06g01620.1	Within	SCR	Scarecrow	Transcription factor (TF) from GRAS family contributes to the specification and determination of root quiescent centre (QC). Together with SHORTROOT (another GRAS TF) controls the division of endoderm/cortex cells. Regulates radial patterning mechanism of root and shoot.	(Mai et al., 2014), (Wysocka-Diller et al., 2000)
		11*	7124411	LOC_Os11g12620.1	20	CLV1	Receptor protein kinase CLAVATA1	Regulates root and shoot apical meristems, regulation of root plasticity in response to nitrogen.	(Stahl et al., 2013), (Araya et al., 2014), (Kalve et al., 2014)
TW	C	1	39058787	LOC_Os01g67410.1	86	AP2/ERF	AP2/EREBP transcription factor BABY BOOM	Regulates adventitious root growth, improves water-deficit and other abiotic stress tolerance, involved in auxin and other phytohormone activated signalling pathway.	(Kitomi et al., 2011), (Quan et al., 2010)

Supplementary Table S8. (Continued)

		8 [*] and 8	3265446	LOC_Os08g06060.1	42	CLKC	CGMC-includes CDA, MAPK, GSK3, and CLKC kinases	CGMC kinase group includes MAP kinase (MAPK), regulates biotic and abiotic stress response.	(Rohila and Yang, 2007), (Wang et al., 2004)
LWR and SWR	C	9	14127114	LOC_Os09g23650.1	67	FAM10	FAM10 family protein	Also, known as HSC70 interacting protein belonging from HSP70 family protein. Regulates cellular redox homeostasis, heat acclimation and protein folding.	(Lippold et al., 2012)
		1 and 1 [*]	14788199	LOC_Os01g26039.1	24	EP	Expressed protein	The Arabidopsis orthologue encodes PHYTYL ESTER SYNTHASE 1 involved in the deposition of free phytol and free fatty acids in the form of phytol esters in chloroplasts that maintain the integrity of the photosynthetic membrane during abiotic stress and senescence.	(Lippold et al., 2012)
				LOC_Os03g57290.1	78	CUL	Cullin	Cullin proteins are molecular scaffolds that have crucial roles in the post-translational modification of cellular proteins involving ubiquitin (protein ubiquitination). Combines with RING proteins to form Cullin-RING ubiquitin ligases (CRLs) and plays a role in cellular processes under abiotic stress pathway.	(Guo et al., 2013)
LWR	C	3	32750373	LOC_Os03g57340.1	42	DnaJ	Chaperone protein dnaJ	Components of macromolecular chaperone complexes (DnaJ-HSP70). DnaJ-like protein (ARG1) involved in gravity signal transduction in root. Maintains cellular protein homeostasis in normal and stress conditions.	(Rosen et al., 1999)
		3	32750373	LOC_Os03g57560.1	63	PIWI	Piwi domain containing protein	Conserved domain protein of ARGONAUTE protein regulates leaf and multicellular organisms development.	(Bohmer et al., 1998)
SWR	C	9	14829621	LOC_Os09g24840.1	13	GASA	GASR10 - Gibberellin-regulated GASA/GAST/Snakin family protein	Phytohormone cross-talk and redox homeostasis, regulates root, stem and other organ growth and development.	(Nahiriak et al., 2012)
		11 [†]	18947620	LOC_Os11g32110.1	6	ARF	Auxin response factor	Auxin activated signalling, mutant showed defects in plant growth and development.	(Guilfoyle and Hagen, 2007)
		1		LOC_Os01g66100.1 38286772	95	GA20OX	Gibberellin 20 oxidase 2	The mutant semi dwarf (<i>sd1</i> -"green revolution rice") phenotype in rice is the result of a deficiency of active GA in the elongating stem arising from a defective 20-oxidase GA biosynthetic enzyme.	(Spielmeyer et al., 2002)
PHT	WD	3 [*]	30407838	LOC_Os03g53020.1	Within	BHLH	Helix-loop-helix DNA-binding domain containing protein	Arabidopsis orthologue regulating stress-related transcriptional signalling and drought tolerance.	NA
				LOC_Os03g53150.1	73	AUX/IAA	OsIAA13 - Auxin-responsive Aux/IAA gene family member	Auxin activated signalling, agravitopic root and shoot, defect in root hairs.	(Reed, 2001)
		5 [*]	2173057	LOC_Os05g04610.1	4	ABC	ABC transporter	Basipetal and acropetal auxin transport and previous study predicted this candidate gene in one of the QTLs on chromosome 1 for plant height in rice.	(Ishimaru et al., 2004)
TN	WD	3 [*]	9995472	LOC_Os03g18050.1	62	SAUR13	OsSAUR13 - Auxin-responsive SAUR gene family member	Early auxin responsive gene, multicellular organism development, rice mutant showed dwarfism, sterility and lower tillering.	(Jain et al., 2006)
TLA	WD	8 [*]	25121944	LOC_Os08g39840.1	102	LOXs	Lipoxygenase, chloroplast precursor	Increased activity in leaves and root and associated with lipid peroxidation mechanism under water-deficit stress.	(Sofa et al., 2004)
TLA and SW		3 [†] and 3 [*]	11725360	LOC_Os03g20700.2	13	MgC	Magnesium-chelatase	Arabidopsis orthologue regulate chlorophyll biosynthesis and photosynthesis	NA
		1 [†]	23207640	LOC_Os01g41050.1	43	SULT	Sulfate transporter	Sulfate uptake, strongly regulated in roots under water-deficit and salinity stress, response to ABA.	(Gallardo et al., 2014)
CWT	WD	4 [†]	34640918	LOC_Os04g58130.1	18	KAT	Katanin p80 WD40 repeat-containing subunit B1 homolog 1	A microtubule severing enzyme. Overexpression of OsKTN80a caused the retarded root growth of rice seedlings.	(Wan et al., 2014)
		6 [†]	13412649	LOC_Os06g22960.1	4	AQP	Aquaporin protein	Cellular water homeostasis and transport, response to ABA, lateral root emergence and elongation, maintains root hydraulic conductivity.	(Reinhardt et al., 2016)
		9 [†]	15426362	LOC_Os09g25850.1	66	WAX	WAX2	Involved in cuticle membrane development and wax production. Arabidopsis mutant (<i>wax2</i>) showed altered cuticle membrane. Higher epicuticular wax improves water use efficiency (WUE).	(Chen et al., 2003)
WUE	WD	11 [†]	27574096	LOC_Os11g45560.1	3	MBTB	MBTB68 - Bric-a-Brac, Tramtrack, Broad Complex BTB domain	Response to salt, water-deficit stress and osmotic stress, protein ubiquitination, interact with CULLIN3 to regulate root growth.	(Thomann et al., 2009)
		6 [†]	23297154	LOC_Os06g39240.1	4	EDR	Endothelial differentiation-related factor 1	Also known as MULTIPROTEIN BRIDGING FACTOR 1C, enhances the tolerances to heat and osmotic stress by partially activating, or perturbing, the ethylene-response signal transduction pathway.	(Suzuki et al., 2005)
SW	WD	12 [*]	17786153	LOC_Os12g29980.1	129	GRF	Growth regulating factor protein	Cell expansion and proliferation, root development, coordination of growth in water-deficit stress condition.	(Omidbakhshfar et al., 2015)
LW	WD	1 [*]	15402601	LOC_Os01g27630.1	8	GST	Glutathione S-transferase	Over-expression of GST in soybean showed longer root length and less growth retardation in drought and salinity stress.	(Ji et al., 2010)

Supplementary Table S8. (Continued)

LWR	WD	2 [#]	2016974	LOC_Os02g33860.1	13	Gβ	WD domain, G-beta repeat domain containing protein	Subunit of large heterotrimeric G protein (<i>αβγ</i>) negatively regulates auxin induced signalling. Loss of function mutants in G-protein have altered auxin mediated cell division during formation of lateral and adventitious root primordia.	(Ullah et al., 2003)
		2 [#]	23246559	LOC_Os02g38440.1	5	OXR	Oxidoreductase, short chain dehydrogenase/reductase family	The Arabidopsis orthologue encodes BETA-KETOACYL REDUCTASE 1 protein regulating cuticular waxes production.	(Hooker et al., 2002)
				LOC_Os02g38480.1	18	EP	Expressed protein	Arabidopsis orthologue regulating salt stress response	NA
LWR and SWR	WD and 9 [#]	9	14829621	LOC_Os09g24840.1	Within	GASA	GASR10-Gibberellin-regulated GASA/GAST/Snakin family protein	Phytohormone cross-talk and redox homeostasis, regulates root, stem and other organ growth and development.	(Nahiriak et al., 2012)
SWR	WD	7	20874845	LOC_Os07g34670.1	92	POX	Peroxidase precursor	Involved in the scavenging of reactive oxygen species (ROS) in water-deficit and other abiotic stresses.	(Chakrabarty et al., 2016)
		1 [#]	40813452	LOC_Os01g70490.1	12	KT	Potassium transporter	Overexpression improved rice osmotic and drought stress tolerance by increasing tissue levels of K ⁺ in the root.	(Ahmad et al., 2016)
rPHT	PP	2 [#]	24405418	LOC_Os02g40320.1	Within	PNH	PINHEAD	Required for reliable formation of primary and axillary shoot apical meristems.	(Lynn et al., 1999)
				LOC_Os06g33480.1	102	PNH	PINHEAD	Required for reliable formation of primary and axillary shoot apical meristems.	(Lynn et al., 1999)
		6 [#]		LOC_Os06g33690.1	Within	PIP1	CAPP1	The Arabidopsis orthologue encodes regulatory elements (PYL8 or RCAR3) of ABA receptor. Positive regulation of abscisic acid-activated signalling pathway. Promotes lateral root development by enhancing MYB77-dependent transcription of auxin-responsive genes.	(Zhao et al., 2014)
rTN	PP	12 [#]	25006932	LOC_Os12g40190.1	134	Gα	G-protein alpha subunit	Regulates root morphogenesis, mutant shows reduced root growth in rice (<i>dl</i>) maize (<i>ct2</i>) and Arabidopsis (<i>gpa1</i>). Arabidopsis orthologue involved in ABA signalling and root morphogenesis.	(Ullah et al., 2001), (Uranio et al., 2016),
rTLA and rCWT	PP	7 [#]	9463744	LOC_Os07g16224.1	Within	PIWI	Piwi domain containing protein	Conserved domain protein of ARGOUNATE protein regulates leaf and multicellular organisms development.	(Bohmer et al., 1998)
rSLA	PP	11 [#]	19245430	LOC_Os11g32610.1	9	CHS	Chalcone and stilbene synthases	Flavonoid biosynthesis, regulates polar auxin transport, mutant <i>tt4</i> (2Y6) shows delayed root gravity response.	(Buer et al., 2006)
rCWT	PP	1	33277486	LOC_Os01g57210.1	226	KAT	Katanin p80 WD40 repeat-containing subunit B1 homolog 1	A microtubule severing enzyme. Overexpression of OskTN80a caused the retarded root growth of rice seedlings. Involved in the	(Wan et al., 2014),
		1	33293954	LOC_Os01g57730.1	88	POD	Peroxidase precursor	scavenging of reactive oxygen species (ROS) in water-deficit and other abiotic stresses.	(Chakrabarty et al., 2016)
				LOC_Os01g58420.1	110	AP2/ERF	AP2 (ERF/AP2) domain containing protein	Regulates adventitious root growth, improves water-deficit and other abiotic stress tolerance, involved in auxin and other phytohormone activated signalling pathways.	(Kitomi et al., 2011), (Quan et al., 2010)
		1	33755921	LOC_Os01g58860.1	80	AEC	Auxin efflux carrier component, putative, expressed	Polar auxin transport and homeostasis, auxin activated signalling and mutant shows defects in root development. Regulates leaf formation and phyllotaxis.	(Grieneisen et al., 2007), (Reinhardt et al., 2003)
rLWR	PP	1	34280616	LOC_Os01g59360.1	45	CAMK	CAMK-calcium/calmodulin dependent protein kinases	ABA activated signalling pathway and stomatal closure.	(Grabov and Blatt, 1998)
		1 [#]	42575227	LOC_Os01g73310.1	91	ACT	Actin	Actins function is essential for cytoplasmic streaming, organelle orientation, cell elongation and root tip growth. Actin filament regulates stomatal movement.	(Gilliland et al., 2003), (Kim et al., 1995)
rSWR	PP	9 [#]	14127114	LOC_Os09g23650.1	76	FAM	FAM10 family protein	Also known as HSC70 interacting protein belonging from HSP70 family protein. Regulates cellular redox homeostasis, heat acclimation and protein folding.	(Wang et al., 2004)
		2 [#]	35635147	LOC_Os02g58020.1	117	ABC	ABC transporter, ATP-binding protein	Basipetal and acropetal auxin transport and previous study predicted this candidate gene in one of the QTLs on chromosome 1 for plant height in rice.	(Ishimaru et al., 2004)
rSWR	PP	2 [#]	24133875	LOC_Os02g39910.1	Within	BTB	B4-BTB1 - Bric-a-Brac, Tramtrack, Broad Complex BTB domain	Response to salt, water-deficit stress and osmotic stress, protein ubiquitination, interacts with CULLIN3 to regulate root growth.	(Thomann et al., 2009)
		2 [#]		LOC_Os02g42585.1	Within	AP2/ERF	AP2 domain containing protein	Regulates adventitious root growth, improves water-deficit stress tolerance, involved in auxin and other phytohormone activated signalling.	(Kitomi et al., 2011), (Quan et al., 2010)

Trt: treatment, Chr: chromosome, Acr: gene acronym, Ref: reference.

Supplementary Table S9: The predicted *a priori* candidate genes (total 40 unique *a priori* genes excluding loci associated with more than one trait) underlying different loci/locus of root traits in control (C) condition and demonstrating to play a role in root growth and development. *A priori* candidate gene annotations in bold are responsive to abiotic stress stimulus (Gene Ontology:0009628) according to Rice genome browser database. Trait acronyms are given in the Table 1. †=Distance of gene from peak SNP.

Traits	Chr	SNP	Gene	Distance (kbp)†	Acr	Gene annotation	General description	Ref
(A) Root morphological traits								
TRL	6 [#]	416782	LOC_Os06g01670.1	13	MYB	MYB family transcription factor	Phytohormone signalling, response to water-deficit and salt stress, regulates root development and lateral root by modulating auxin inducible genes.	(Ambawat et al., 2013)
			LOC_Os06g01780.1	7	AP2/ERF	Ethylene-responsive element-binding protein	Regulates adventitious root growth, improves water-deficit stress tolerance, auxin and other phytohormone activated signalling pathways.	(Kitomi et al., 2011),(Quan et al., 2010)
TRL and RL005	2 [#]	34358656	LOC_Os02g56120.2	10	Aux/IAA	OsIAA9 - Auxin-responsive Aux/IAA	Auxin activated signalling, agravitropic root and shoot, defect in root hairs.	(Reed, 2001)
RL0510	6 [#]	366330	LOC_Os06g01620.1	Within	SCR	Scarecrow	Transcription factor (TF) from GRAS family contributes to the specification and determination of root quiescent centre (QC). Together with SHORTRoot (another GRAS TF) controls the division of endoderm/cortex cells. Regulates radial patterning mechanism of root and shoot.	(Mai et al., 2014),(Wysocka-Diller et al., 2000)
RL1015, RL1520, RV and RW	5 [#]	7131196	LOC_Os05g12180.1	96	PIP1	CAPIPI	The Arabidopsis orthologue encodes regulatory elements (PYL8 or RCAR3) of ABA receptor. Positive regulation of abscisic acid-activated signalling pathway. Promotes lateral root development by enhancing MYB77-dependent transcription of auxin-responsive genes.	(Zhao et al., 2014)
LOC_Os05g12400.1			4	BURP	BURP domain containing protein	ABA responsive and loss of function increased moisture stress resistance	(Harshavardhan et al., 2014)	
LOC_Os05g12410.1			6					
RL1015 and RV	5 [#]	16517488	LOC_Os05g27930.1	217	AP2/ERF	AP2 domain containing protein	Regulates adventitious root growth, improves water-deficit stress tolerance, auxin and other phytohormone activated signalling pathways.	(Kitomi et al., 2011),(Quan et al., 2010)
RL1015	7 [#]	6865357	LOC_Os07g12130.1	84	MYB	MYB family transcription factor	Phytohormone signalling, response to water-deficit and salt stress, regulates root development and lateral root by modulating auxin inducible genes.	(Ambawat et al., 2013)
RL1520 and RL2025	2 and 2 [#]	25265958	LOC_Os02g41860.1	103	AQP	Aquaporin protein	Cellular water homeostasis and transport, response to ABA, lateral root emergence and elongation, maintains root hydraulic conductivity.	(Reinhardt et al., 2016)
			LOC_Os02g41800.1	132	ARF	Auxin response factor	Regulates auxin responsive genes, root cap development and mutant showed reduced adventitious and lateral roots.	(Guilfoyle and Hagen, 2007)
RL2025	1 [#]	28515026	LOC_Os01g49710.1	52	GST	Glutathione S-transferase	Over-expression of GST in soybean showed longer root length and less growth retardation in drought and salinity stress.	(Ji et al., 2010)
MRL	6 [#]	27819933	LOC_Os06g45940.2	Within	KT	Potassium transporter	Regulate root tip growth in Arabidopsis	(Rigas et al., 2001)
			LOC_Os06g45950.1	11	SAUR	OsSAUR25 and OsSAUR26 - Small auxin UP-RNA	Early auxin responsive gene, multicellular organism development, regulation of growth by root cell elongation, regulates root meristematic activity.	(Markakis et al., 2013)
			LOC_Os06g45970.1	42				
RV	1 [#]	40526762	LOC_Os01g70050.1	Within	SAUR	OsSAUR3 - Auxin-responsive SAUR	Early auxin responsive gene, multicellular organism development, regulation of growth by root cell elongation, regulates root meristematic activity.	(Markakis et al., 2013)
ART	1	10998576	LOC_Os11g47760.1	Within	DnaK	DnaK family protein, putative	Molecular chaperone protein response to heat and drought, in interaction with brassinosteroid signalling, regulates root development, regulates root gravity response.	(Bekh-Ochir et al., 2013),(Sedbrook et al., 1999)
			LOC_Os01g19380.1	33	PPR	Pentatricopeptide	Response to salt stress, regulates size of root apical meristem and mutant (<i>slg1</i>) shows reduced root growth.	(Hsieh et al., 2015)
			LOC_Os01g19750.1	209	GLH	Glycosyl hydrolase	Cell wall remodelling (loosening, degradation and reorganization) and mutant (<i>glh</i>) showed reduced root growth.	(Swarup et al., 2008)
			LOC_Os01g59440.1	307bp	BR11	BRASSINOSTEROID INSENSITIVE 1	Overexpression line of this gene shows impaired root growth compared to wild type but under heat and cold stress roots are more elongated in overexpressed line than in wild type.	(Singh et al., 2016)

Supplementary Table S9. (Continued)

SRL	1	25773127	LOC_Os01g45550.1	90	AEC	Auxin efflux carrier component	Polar auxin transport and homeostasis, auxin activated signalling and mutant showed defects in root growth and development.	(Grieneisen et al., 2007)
			LOC_Os01g74450.1	9	AQP	Aquaporin protein	Cellular water homeostasis and transport, response to ABA, lateral root emergence and elongation, maintains root hydraulic conductivity.	(Reinhardt et al., 2016)
	1 [#]	43108024	LOC_Os01g74470.1	26	ABC	ABC transporter, ATP-binding protein	Basipetal and acropetal auxin transport and involved in auxin mediated lateral and root hair development. Mutant (<i>mdr1</i>) showed defect in lateral root growth.	(Santelia et al., 2005)(Wu et al., 2007)
			LOC_Os01g74410.1	12	MYB	MYB family transcription factor	Phytohormone signalling, response to water-deficit and salt stress, regulates root development and lateral root by modulating auxin inducible genes.	(Ambawat et al., 2013)
		LOC_Os01g74590.1	87					
(C) Root anatomical traits								
RD	1 [*]	11112944	LOC_Os01g19380.1	33	PPR	Pentatricopeptide	Response to salt stress, regulates size of root apical meristem and mutant (<i>slg1</i>) shows reduced root growth.	(Hsieh et al., 2015)
			LOC_Os01g19750.1	20	9	GLH	Glycosyl hydrolase	Cell wall remodelling (loosening, degradation and reorganization) and mutant (<i>ghh</i>) showed reduced root growth.
RD, CD and SD-RD	7 [*]	21266079	LOC_Os07g35560.1	17	GLUB3	Glucan endo-1,3-beta-glucosidase precursor	Belongs to cell wall remodelling (loosening, degradation and reorganisation) enzyme glycosyl hydrolase family protein and degrade beta-glucan—component of hemicelluloses which builds cell walls. Some studies showed that the increase in the synthesis of beta-glucosidase is associated with a higher plant tolerance to osmotic stress while another study showed decreased expression in response to osmotic stress in roots.	(Budak et al., 2013)(Grębo sz et al., 2014)
RD	3 [#]	4913579	LOC_Os03g09930.1	37	SULT	Sulfate transporter	Sulfate uptake, strongly regulated in roots under water-deficit and salinity stress, response to ABA.	(Gallardo et al., 2014)
			LOC_Os03g51710.1	54	HP	Homeobox protein knotted-1	Multicellular organismal development and cell differentiation, Arabidopsis orthologue regulate xylem development	NA
	3 [#]	29686521	LOC_Os03g51740.1	24	ACC	Aminotransferase similar ACC Synthase	Ethylene biosynthesis and regulates rice root growth in deep water, induced by water-deficit stress in rice.	(Lorbiecke and Sauter, 1999)(Wang et al., 2011)
	5 [#]	28880728	LOC_Os05g50460.1	43	PPR	Pentatricopeptide	Response to salt stress, regulates size of root apical meristem and mutant (<i>slg1</i>) shows reduced root growth	(Hsieh et al., 2015)
LMXD			LOC_Os04g49450.1	53	MYB	MYB family transcription factor	Phytohormone signalling, response to water-deficit and salt stress, regulates root development and lateral root by modulating auxin inducible genes.	(Ambawat et al., 2013)
	4 [*]	29450620	LOC_Os04g49410.1	35	EXP	Expansin precursor	Cell wall loosening and maintains root cell elongation, supports acid growth theory.	(Wu et al., 1996; Cosgrove, 1998)
	4	29606053	LOC_Os04g49570.2	36	GLR	Glutamate receptor	Calcium ion transport and homeostasis and transduction of gravitropism signal in root.	(Miller et al., 2010)
	12 [#]	22371182	LOC_Os12g36620.1	56	PPR	Pentatricopeptide	Response to salt stress, regulates size of root apical meristem and mutant (<i>slg1</i>) shows reduced root growth.	(Hsieh et al., 2015)
LMXD			LOC_Os01g34850.1	64	HKT	OsHKT2;3 - Na⁺ transporter	HKT-type transporters play key roles in Na ⁺ accumulation and salt sensitivity in plants. Arabidopsis HKT1,1 has been proposed to influx Na ⁺ into roots, recirculates Na ⁺ in the phloem and controls root: shoot allocation of Na ⁺ .	(Davenport et al., 2007)
	1 [#]	19177575	LOC_Os01g34880.1	83	CAS	Callose synthase	Necessary for normal phloem development and cell signalling. The roots of <i>cal3-d</i> gain-of-function mutants were shown to accumulate more callose at the plasmodesmata and defects in root development, callose regulates symplastic trafficking during root development.	(Vatén et al., 2011)
LMXN	11	2838776	LOC_Os11g06010.1	7	bHLH	Helix-loop-helix DNA-binding protein	Arabidopsis orthologue LONESOME HIGHWAY with sequence similarity to bHLH-domain proteins. It promotes the production of stele cells in root meristems and maintain the normal vascular cell number in coordination with auxin in primary and lateral roots.	(Ohashi-Ito et al., 2014), (Ohashi-Ito et al., 2013)
(E) Dry matter trait								
RS	1 [*]	39255482	LOC_Os01g67650.1	63	DEL	Gibberellin response modulator protein	Cell proliferation and expansion, root growth in interaction with auxin.	(Fu and Harberd, 2003)
			LOC_Os01g67670.1	70	DEL			

Trt: treatment, Chr: chromosome, Acr: gene acronym, Ref: reference.

Supplementary Table S10: The predicted *a priori* candidate genes (total 57 unique *a priori* genes excluding loci associated with more than one trait) underlying different loci/locus of root traits in water-deficit stress (WD) conditions and demonstrating to have a role in root growth and development. Candidate *a priori* gene annotations in bold are responsive to abiotic stress stimulus (Gene Ontology:0009628) according to Rice genome browser database. Trait acronyms are given in the Table 1. †=Distance of gene from peak SNP.

Traits	Chr	SNP	Gene	Distance (kbp)†	Ac	Gene annotation	Description	Ref
(A) Root morphological traits								
TRL, RL005 and SA	2 [#]	8835096	LOC_Os02g15620.1	53	PIP1	CAPIP1	The Arabidopsis orthologue encodes a regulatory element (PYL8 or RCAR3) of ABA receptor. Positive regulation of abscisic acid-activated signalling pathway. Promotes lateral root development by enhancing MYB77-dependent transcription of auxin-responsive genes.	(Zhao et al., 2014)
TRL and RL005	4 [#]	29111186	LOC_Os04g48510.1	189	GRF	Growth regulating factor protein	Cell expansion and proliferation, root development, coordination of growth in water-deficit stress condition.	(Omidbakhsh fard et al., 2015)
TRL and RL005	11 [#]	7124411	LOC_Os11g12620.1	20	CLV1	Receptor protein kinase CLAVATA1 precursor	Regulates root and shoot meristems, regulation of root plasticity in response to nitrogen.	(Stahl et al., 2013),(Araya et al., 2014), (Kalve et al., 2014)
RL0510 and RV	12 [#]	26195748	LOC_Os12g42150.1	65	Gβ	WD domain, G-beta repeat domain containing protein	Subunit of large heterotrimeric G protein ($\alpha\beta\gamma$) negatively regulates auxin induced signalling. Loss of function mutants in G-protein have altered auxin mediated cell division - formation of lateral and adventitious root primordia.	(Ullah et al., 2003)
RL0510 and SA	9 [#]	14829621	LOC_Os09g24840.1	Within	GASA	GASR10 - Gibberellin-regulated GASA/GAST/Snakin family protein	Phytohormone cross-talk and redox homeostasis, regulates root, stem and other organ growth and development.	(Nahiriak et al., 2012)
RL0510	11 [#]	25317141	LOC_Os11g42200.1	106	LAC	Laccase precursor protein	Lignin synthesis, role in roots development during acclimation to salinity stress.	(Liang et al., 2006)
RL0510, RL1015 and RV	1 [*]	23079331	LOC_Os01g40680.1	87	PPR	Pentatricopeptide	Response to salt stress, regulates size of root apical meristem and mutant (<i>slg1</i>) showed reduced root growth.	(Hsieh et al., 2015)
	2 [*]	5180480	LOC_Os02g09910.1 LOC_Os02g09920.1	49 35	PHD	PHD-finger domain containing protein	Multicellular organismal development, anatomical development and response to abiotic stimulus in rice.	NA
	6	6996556	LOC_Os06g12790.1	6	RAS	Ras-related protein	Small GTPase mediated signal transduction, root hair initiation and root tip growth.	(Molendijk et al., 2001), (Jones et al., 2002)
RL2025			LOC_Os03g12236.1	48	DnaJ	Heat shock protein DnaJ	Components of macromolecular chaperone complexes (DnaJ-HSP70). DnaJ-like protein (ARG1) involved in gravity signal transduction in root. Maintains cellular protein homeostasis in normal and stress condition.	(Rosen et al., 1999)
	3 [#]	6374082	LOC_Os03g11910.1	127	DnaK	DnaK family protein	Molecular chaperone protein response to heat and drought, in interaction with brassinosteroid signalling, regulates root development, regulates root gravity response.	(Bekh-Ochir et al., 2013),(Sedbrook et al., 1999)
	10 [#]	11555942	LOC_Os10g22310.1	18	GST	Glutathione S-transferase GST 26	Over-expression of GST in soybean showed longer root length and less growth retardation in drought and salinity stress.	(Ji et al., 2010)
	11 [*]	24267277	LOC_Os11g40680.1	11	MBTB	MBTB64 - Bric-a-Brac, Tramtrack, Broad Complex BTB domain	Response to salt, water-deficit stress and osmotic stress, protein ubiquitination, interacts with CULLIN3 to regulate root growth.	(Thomann et al., 2009)
RL2530			LOC_Os10g35560.1	54	EP	Expressed protein	The Arabidopsis orthologue encodes a nuclear targeted protein (ATSR6) that plays a role in the CBF pathway -downstream of CBF translation. NAC transcription factor promotes lateral root growth through activation of DREB-CBF-COR pathway.	(Hao et al., 2011)
	10 [#]	18971155	LOC_Os10g35460.1	5	COBRA	COBRA	Cellular component organization and response to abiotic stress stimulus. Arabidopsis orthologue regulates multidimensional cell growth and response to salt stress.	NA

Supplementary Table S10. (Continued)

MRL	12*	17607622	LOC_Os12g29520.1	36	ARF	Auxin response factor	Auxin activated signalling, root cap development and mutant showed reduced adventitious and lateral roots.	(Guilfoyle and Hagen, 2007)
	12	17780100	LOC_Os12g29980.1	139	GRF	Growth regulating factor protein	Cell expansion and proliferation, root development, coordination of growth in water-deficit stress condition.	(Omidbakhshfard et al., 2015)
	2*	2783451	LOC_Os02g05640.1	26	HD-Zip	Homeobox associated leucine zipper	Root development, ABA signalling, response to water-deficit, anatomical morphogenesis.	(Elhiti and Stasolla, 2009)
RV	11	7124411	LOC_Os11g12620.1	20	CLV1	Receptor protein kinase CLAVATA1	Regulates root and shoot meristems, regulation of root plasticity in response to nitrogen.	(Stahl et al., 2013),(Araya et al., 2014), (Kalve et al., 2014)
	9*	14829621	LOC_Os09g24840.1	Within	GASA	GASR10 - Gibberellin-regulated GASA/GAST/Snakin family protein	Phytohormone cross-talk and redox homeostasis, regulates root, stem and other organ growth and development.	(Nahirniak et al., 2012)
SA	1*	23044334	LOC_Os01g40680.1	52	PPR	Pentatricopeptide	Response to salt stress, regulates size of root apical meristem and mutant (<i>sgl1</i>) shows reduced root growth.	(Hsieh et al., 2015)
	5*	14825506	LOC_Os05g25560.1	29	GLH	Glycosyl hydrolase family 10 protein	Cell wall remodelling (loosening, degradation and reorganization) and mutant (<i>glh</i>) showed reduced root growth.	(Swarup et al., 2008)
	5*	14825506	LOC_Os05g25490.1	4	ACC	Aminotransferase similar to 1-Aminocyclopropane-1-carboxylate synthase (ACC Synthase)	Ethylene biosynthesis and regulates rice root growth in deep water, induced by water-deficit stress in rice.	(Lorbiecke and Sauter, 1999), (Wang et al., 2011)
RW	6* and 6	6579613	LOC_Os06g12250.1	12	SUR2	Sphingolipid C4-hydroxylase SUR2	Fatty acid biosynthesis and mutant (<i>shh1/shh2-1</i>) showed reduced root length due to defect in both cell elongation and division.	(Chen et al., 2008)
RW and SRL	1	23079331	LOC_Os01g40680.1	87	PPR	Pentatricopeptide	Response to salt stress, regulates size of root apical meristem and mutant (<i>sgl1</i>) showed reduced root growth.	(Hsieh et al., 2015)
ART	11*	6245556	LOC_Os11g11410.1	90	AUX/IAA	OsIAA27 and OsIAA28 - Auxin-responsive Aux/IAA gene family member	Auxin activated signalling, agravitropic root and shoot, defect in root hairs.	(Reed, 2001)
			LOC_Os11g11420.1	103				
	9	20970824	LOC_Os09g36420.1		HSP90	Hsp90 protein	Regulates plasticity of root elongation and response to gravity.	(Sangster and Quetsch, 2005)
1* and 8#	23218344	LOC_Os01g41050.1	32	SULT	Sulfate transporter	Sulfate uptake, strongly regulated in roots under water-deficit and salinity stress, response to ABA.	(Gallardo et al., 2014)	
	51541	LOC_Os08g01120.1	35					
2	33496059	LOC_Os02g54720.1	6	EP	Expressed protein	Arabidopsis orthologue of this gene (SMAX2) responds to strigolactone, mutant (<i>smx16,7,8</i>) showed reduced polar auxin transport and lateral root growth.	(Soundappan et al., 2015)	
2	24006148	LOC_Os02g39750.1	Within	IPT	Inorganic phosphate transporter	Response to phosphate starvation, altering root system architecture in response to phosphate starvation, response to heat.	(Sato and Miura, 2011),(Pacak et al., 2016)	
2	24122043	LOC_Os02g39910.1	11	B4BTB	B4-BTB1 - Bric-a-Brac, Tramtrack, Broad Complex BTB	Response to salt, water-deficit stress and osmotic stress, protein ubiquitination, interacts with CULLIN3 to regulate root growth.	(Thomann et al., 2009)	
5*	15673557	LOC_Os05g26890.1	64	Ga	G-protein alpha subunit	Regulates root morphogenesis, mutant shows reduced root growth in rice (<i>d1</i>) maize (<i>ct2</i>) and arabidopsis (<i>gpa1</i>). Arabidopsis orthologue involved in ABA signalling and root morphogenesis.	(Ullah et al., 2001),(Urano et al., 2016)	
6*		LOC_Os06g45950.1	10	SAUR	OsSAUR25 and OsSAUR26 - Small auxin UP-RNA	Early auxin responsive gene, multicellular organism development, regulation of growth by root cell elongation, regulates root meristematic activity.	(Markakis et al., 2013)	
	27819933	LOC_Os06g45970.1	42					
		LOC_Os06g45940.2	Within	KT	Potassium transporter	Regulate root tip growth in Arabidopsis	(Rigas et al., 2001)	
RLLA	2*	25154659	LOC_Os02g41860.1	7	AQP	Aquaporin protein	Cellular water homeostasis and transport, response to ABA, lateral root emergence and elongation, maintains root hydraulic conductivity.	(Reinhardt et al., 2016)
			LOC_Os02g41800.1	19	ARF	Auxin response factor	Regulates auxin responsive genes, root cap development and mutant showed reduced adventitious and lateral roots.	(Guilfoyle and Hagen, 2007)
	3*	27177614	LOC_Os03g47830.1	Within	ARG	Argonaute	Arabidopsis mutant showed defects in root vascular tissue.	(Lynn et al., 1999)

Supplementary Table S10. (Continued)

(D) Root anatomical traits									
SD and LMXD	9 ^a and 9 ^b	13788883	LOC_Os09g23200.1	24	KAN1	KANAD11	Lateral root development, vascular tissue development in root.	(Hawker and Bowman, 2004),(Zhao et al., 2005)	
			LOC_Os09g23220.1	8	GLH16	Glycosyl hydrolases family 16	Cell wall remodelling (loosening, degradation and reorganization) and mutant (<i>g/h</i>) showed reduced root growth.	(Swarup et al., 2008)	
SD and LMXD	5 ^a	3057869	LOC_Os05g06110.1	843bp	VIL	Villin	Actin binding protein involved in root hair growth through actin organisation.	(Zhang et al., 2011)	
SD:RD	1 [*]	1676898	LOC_Os01g03950.1	21	GLH31	Glycosyl hydrolase, family 31	Cell wall remodelling (loosening, degradation and reorganization) and mutant (<i>g/h</i>) showed reduced root growth.	(Swarup et al., 2008)	
			LOC_Os01g04020.2	69	AP2/ERF	AP2 domain containing protein	Regulates adventitious root growth, improves water-deficit stress tolerance, auxin and other phytohormone activated signalling pathways.	(Kitomi et al., 2011),(Quan et al., 2010)	
LMXN	7 [*]	1316016	LOC_Os07g03270.1	Within	DnaJ	Heat shock protein DnaJ	Components of macromolecular chaperone complexes (DnaJ-HSP70). DnaJ-like protein (ARG1) involved in gravity signal transduction in root. Maintains cellular protein homeostasis in normal and stress conditions.	(Rosen et al., 1999)	
			LOC_Os03g60550.1	75	THIF	ThIF family domain containing protein	Associated with production of ubiquitin-activating enzyme E1. Controls root and shoot architecture, Arabidopsis orthologue plays a role in auxin activated signalling.	(Prince et al., 2015)	
			LOC_Os03g60580.1	57	ADF	Actin-depolymerizing factor	Capable of rapid and reversible disruption of actin cytoskeleton. Disturbs root elongation and root hair formation.	(Baluška et al., 2000),(Baluška et al., 2001)	
			LOC_Os03g60620.1	37	DnaK	DnaK family protein	Molecular chaperone protein responds to heat and drought, in interaction with brassinosteroid signalling, regulates root development, regulates root gravity response.	(Bekh-Ochir et al., 2013), (Sedbrook et al., 1999)	
LMXD	6 ^a	471179	LOC_Os06g01890.1	23	MADS	MADS-box transcription factor	Plays diverse roles in plant development and one of the Arabidopsis MADS (ANR1) is a key regulator of root developmental plasticity in response to nitrate.	(Zhang and Forde, 1998)	
			LOC_Os05g06110.1	843bp	VIL	Villin	Actin binding protein involved in root hair growth through actin organisation.	(Zhang and Forde, 1998)	
			LOC_Os06g01920.1	41	EXP	Expansin precursor	Cell wall loosening and maintain root cell elongation, supports acid growth theory.	(Wu et al., 1996),(Cosgrove, 1998)	
LMXD	11 ^a	28871551	LOC_Os11g47870.1	Within			Auxin responsive transcription factor (TF) from GRAS family contributes to the specification and determination of root quiescent centre (QC). Together with SHORTROOT (another GRAS TF) controls the division of endoderm/cortex cells.	(Gao et al., 2004; Mai et al., 2014),(Wysocka-Diller et al., 2000)	
			LOC_Os11g47900.1	19					
			LOC_Os11g47910.1	24	SCR	SCARECROW	Regulates radial patterning mechanism of root and shoot.		
(E) Dry matter traits									
RS	4	29184866	LOC_Os04g48850.1	53	ACC	Aminotransferase similar to 1-Aminocyclopropane-1-carboxylate Synthase (ACC Synthase)	Ethylene biosynthesis and regulates rice root growth in deep water, induced by water-deficit stress in rice.	(Lorbiecke and Sauter, 1999), (Wang et al., 2011)	
			LOC_Os04g49130.1	104	SUMO	Ubiquitin-conjugating enzyme	The Arabidopsis orthologue encodes SUMO E3 ligase and one of the SUMO E ligase AtMMS21controls root cell proliferation via cell cycle regulation and Cytokinin signalling.	(Huang et al., 2009)	
4	29450620		LOC_Os04g49450.1	50	MYB	MYB family transcription factor	Phytohormone signalling, response to water-deficit and salt stress, regulates root development and lateral root by modulating auxin inducible genes.	(Ambawat et al., 2013)	
			LOC_Os04g49410.1	34	EXP	Expansin precursor	Cell wall loosening and maintains root cell elongation, supports an acid growth theory.	(Wu et al., 1996),(Cosgrove, 1998)	
1 ^a	1562911		LOC_Os01g03720.1	12	MYB	MYB family transcription factor	Phytohormone signalling, response to water-deficit and salt stress, regulates root development and lateral root by modulating auxin inducible genes.	(Ambawat et al., 2013)	
			LOC_Os04g48510.1	189	GRF	Growth regulating factor protein	Cell expansion and proliferation, root development, coordination of growth in water-deficit stress condition.	(Omidbakhshfar et al., 2015)	
RW	3	34943958	LOC_Os03g61670.1	8	CRT	Calreticulin precursor	Enhances root regeneration and response to oxidative and salt stress.	(Jin et al., 2005)	

Chr: chromosome, Acr: gene acronym, Ref: reference.

Supplementary Table S11: The *a priori* candidate genes (41 *a priori* genes) underlying different loci/locus for plasticity of root traits as the relative value of the water-deficit stress treatment over the control treatment and demonstrating to have a role in root growth and development. Candidate *a priori* gene annotations in bold are responsive to abiotic stress stimulus (Gene Ontology:0009628) according to the rice genome browser database. Trait acronyms are given in the Table 1. †=Distance of gene from peak SNP.

Traits	Chr	SNP	Gene	Distance (kbp)†	Acr	Gene annotation	General description	Ref
(A) Root morphological								
rTRL and rSA	7 [#]	9463744	LOC_Os07g16224.1	Within	PIWI	Piwi domain containing protein	Conserved domain protein of ARGONATE protein regulates leaf and multicellular organisms development.	(Bohmert et al., 1998)
rTRL, rRV, rSA and rRL005	12'	25006932	LOC_Os12g40190.1	134	Ga	G-protein alpha subunit	Regulates root morphogenesis, mutant shows reduced root growth in rice (<i>d1</i>) maize (<i>z12</i>) and Arabidopsis (<i>gpa1</i>). Arabidopsis orthologue involved in ABA signalling and root morphogenesis.	(Ullah et al., 2001),(Urano et al., 2016)
			LOC_Os01g46860.1	101	IPT	Inorganic phosphate transporter	Response to phosphate starvation, altering root system architecture in response to phosphate starvation, response to heat.	(Sato and Miura, 2011),(Pacak et al., 2016)
	1 [#]	26826635	LOC_Os01g46870.1	93	AP2/ERF	AP2 domain containing protein	Regulates adventitious root growth, improves water-deficit stress tolerance, auxin and other phytohormone activated signalling pathways.	(Kitomi et al., 2011),(Quan et al., 2010)
			LOC_Os01g46940.1	36	SUR2	Spingolipid C4-hydroxylase SUR2	Fatty acid biosynthesis and mutant (<i>sbh1-1 sbh2-1</i>) showed reduced root length due to defect in both cell elongation and division.	(Chen et al., 2008)
rTRL			LOC_Os04g51890.1	19	SAUR	OsSAUR20 - Auxin-responsive SAUR	Early auxin responsive gene, multicellular organism development, regulation of growth by root cell elongation, regulates root meristematic activity.	(Markakis et al., 2013)
	4 [#]	30764890	LOC_Os04g51800.1	54	MYB	MYB protein, putative	Phytohormone signalling, response to water-deficit and salt stress, regulates root development and lateral root by modulating auxin inducible genes.	(Ambawat et al., 2013)
			LOC_Os04g51820.2	41	HKT	OsHKT1;1 - Na⁺ transporter	HKT-type transporters play key roles in Na ⁺ accumulation and salt sensitivity in plants. Arabidopsis HKT1;1 has been proposed to influx Na ⁺ into roots, recirculate Na ⁺ in the phloem and control root: shoot allocation of Na ⁺ .	(Davenport et al., 2007)
	2 [#]	4943157	LOC_Os02g09480.1	75	MYB	MYB-like DNA-binding domain containing protein	Phytohormone signalling, response to water-deficit and salt stress, regulates root development and lateral root by modulating auxin inducible genes.	(Ambawat et al., 2013)
rRL2025	4 [#]	16463674	LOC_Os04g27980.1	56	GLH	Glycosyl hydrolase	Cell wall remodelling (loosening, degradation and reorganization) and mutant (<i>glh</i>) showed reduced root growth.	(Swarup et al., 2008)
	3	2553785	LOC_Os03g05290.1	10	AQP	Aquaporin protein	Cellular water homeostasis and transport, response to ABA, lateral root emergence and elongation, maintains root hydraulic conductivity.	(Reinhardt et al., 2016)
	3 and 3'	2553785	LOC_Os03g05280.1	10			Small GTPase mediated signal transduction, root hair initiation and root tip growth.	(Molendijk et al., 2001), (Jones et al., 2002)
rRL2530	3'	34392848	LOC_Os03g60530.1	14	RAS	Ras-related protein	Associated with the production of ubiquitin-activating enzyme E1 and controls root and shoot architecture, Arabidopsis orthologue plays role in auxin activated signalling.	(Prince et al., 2015)
rRV	1 [#]	42575227	LOC_Os01g73310.1	91	ACT	Actin	Actin function is essential for cytoplasmic streaming, organelle orientation, cell elongation and root tip growth.	(Gilliland et al., 2003)
	12	17607622	LOC_Os12g29520.1	36	ARF	Auxin response factor	Auxin activated signalling, root cap development and mutant showed reduced adventitious and lateral roots.	(Guilfoyle and Hagen, 2007)
rMRL			LOC_Os02g44108.1	185	EXP	Expansin precursor	Cell wall loosening and maintaining root cell elongation, supports acid growth theory.	(Wu et al., 1996),(Cosgrove, 1998)
	2 [#]	26794003	LOC_Os02g44080.1	143	AQP	Aquaporin protein	Cellular water homeostasis and transport, response to ABA, lateral root emergence and elongation, maintains root hydraulic conductivity.	(Chaumont et al., 2001)

Supplementary Table S11. (Continued)

			LOC_Os01g52130.1	13	SULT	Sulfate transporter	Sulfate uptake, strongly regulated in roots under water-deficit stress, response to ABA.	(Gallardo et al., 2014)	
rART	1	29981149	LOC_Os01g52070.1	37	AKT1	Potassium channel AKT1	Root potassium uptake and potassium homeostasis and facilitates growth in potassium limitation condition. Growth retardation in Arabidopsis akt1-1 and akt1-1 mutants under K starvation.	(Geiger et al., 2009)	
			LOC_Os01g59440.1	307bp	BRI1	BRASSINOSTEROID INSENSITIVE 1-associated receptor kinase 1 precursor	Overexpression line of this gene shows impaired root growth compared to wild type but under heat and cold stress roots are more elongated in overexpressed line than in wild type.	(Singh et al., 2016)	
rSRL and rART	5*	2184238	LOC_Os05g04610.1	15	ABC	ABC transporter, ATP-binding protein	Basipetal and acropetal auxin transport and involved in auxin mediated lateral and root hair development. Mutant (<i>mdr1</i>) showed defect in lateral root growth.	(Santelia et al., 2005),(Wu et al., 2007)	
			LOC_Os05g04600.1	19					
rSRL	8*	26362631	LOC_Os08g41720.1	30	AEC	Auxin efflux carrier component	Polar auxin transport and homeostasis, auxin activated signalling and mutant shows defects in root development.	(Grieneisen et al., 2007)	
rTRWD	1*	25703110	LOC_Os01g45550.1	160					
rSRL	3*	34024418	LOC_Os03g59730.1	21	NAM	No apical meristem	NAC domain containing protein regulates multicellular	(He et al., 2005)	
			LOC_Os01g36830.1	86	PG	Polygalacturonase	Involved in cell elongation and expansion and expressed during root and other organ development.	(Xiao et al., 2014)	
(D) Root anatomical									
rRD, rCD and rSD	1*	11038867	LOC_Os01g19380.1	74	PPR	Pentatricopeptide	Response to salt stress, regulates size of root apical meristem and mutant (<i>slg1</i>) shows reduced root growth.	(Hsieh et al., 2015)	
			LOC_Os01g19750.1	169	GLH	Glycosyl hydrolase	Cell wall remodelling (loosening, degradation and reorganization) and mutant (<i>glh</i>) showed reduced root growth.	(Swarup et al., 2008)	
rRD	11*	27205864	LOC_Os11g44930.1	5	PPR	Pentatricopeptide	Response to salt stress, regulates size of root apical meristem and mutant (<i>slg1</i>) shows reduced root growth.	(Hsieh et al., 2015)	
			LOC_Os11g44950.2	2	GLH	Glycosyl hydrolase 3	Cell wall remodelling (loosening, degradation and reorganization) and mutant (<i>glh</i>) showed reduced root growth.	(Swarup et al., 2008)	
rSD and rLMXD	7 and 7*	27141434	LOC_Os07g45290.1	122	CYP450	Cytochrome P450 72A1	The Arabidopsis orthologue catalyses essential oxidative step in the biosynthesis of Brassinosteroids (BR). BR in interaction with auxin promote lateral root development.	(Bao et al., 2004)	
			LOC_Os07g45400.1	71	EP	Expressed protein	Arabidopsis orthologue regulate radial pattern formation.	NA	
rRD and rSD	11*	25434106	LOC_Os11g42220.1	Within	LAC	Laccase precursor protein	Lignin synthesis, role in roots development during acclimation to salinity stress.	(Liang et al., 2006)	
rCD	4*	33647561	LOC_Os04g56460.1	10	MBTB	MBTB9 - Bric-a-Brac, Trantrack, Broad Complex BTB	Response to salt, water-deficit stress and osmotic stress, protein ubiquitination, interacts with CULLIN3 to regulate root growth.	(Thomann et al., 2009)	
(E) Dry matter traits									
rRW	4*	29184866	LOC_Os04g49130.1	104	SUMO	Ubiquitin-conjugating enzyme	The Arabidopsis orthologue encodes SUMO E3 ligase and one of the SUMO E ligase AtMMS21 controls root cell proliferation via cell cycle regulation and cytokinin signalling.	(Huang et al., 2009)	
			LOC_Os04g48850.1	53	ACS	Aminotransferase similar to 1-Aminocyclopropane-1-carboxylate synthase (ACC Synthase)	Ethylene biosynthesis and regulates rice root growth in deep water, induced by water-deficit stress in rice.	(Lorbieck and Sauter, 1999), (Wang et al., 2011)	
rRS	2*	651557	LOC_Os02g02190.1	15	TR	Transporter, major facilitator family	The Arabidopsis orthologue encodes high affinity nitrate transporter, plays a role in nitrate assimilation and regulates lateral root development.	(Little et al., 2005)	
			LOC_Os02g02140.1	14	CLV1	Receptor protein kinase CLAVATA1	Regulates root and shoot meristems, regulates root plasticity in response to nitrogen.	(Stahl et al., 2013), (Araya et al., 2014), (Kalve et al., 2014)	
	3*	26825291	LOC_Os03g47530.1	50	GLT	Glycosyl transferase 8 domain protein	Cell wall thickening, xylem pattern formation and differentiation, mutant showed swollen root and reduced growth.	(Schuetz et al., 2012),(Scheible and Pauly, 2004)	
	8*	17221046	LOC_Os08g28190.1	16	ACT	Actin	Actin function is essential for cytoplasmic streaming, organelle orientation, cell elongation and root tip growth.	(Gilliland et al., 2003)	

Chr: chromosome, Acr: gene acronym, Ref: reference.

Supplementary Data Sets 1 to 4 are available online in Supplementary data of Plant Physiology:
<http://www.plantphysiol.org/content/174/4/2302>

CHAPTER 4

Genome wide association reveals genetic basis of rice grain yield and its component traits under water-deficit stress during the reproductive stage

Niteen N. Kadam^{1,2}, Paul C. Struik², Xinyou Yin², Krishna S.V. Jagadish^{1,3}

¹International Rice Research Institute (IRRI), DAPO, Box 7777, Metro Manila, Philippines

²Centre for Crop Systems Analysis, Department of Plant Sciences, Wageningen University & Research, PO Box 430, 6700 AK Wageningen, The Netherlands

³Department of Agronomy, Kansas State University, Manhattan, USA

Abstract

A diversity panel comprising of 296 indica rice genotypes was phenotyped under non-stress and reproductive stage water-deficit stress conditions during 2013 and 2014 dry seasons at IRRI, Philippines. We investigated the genotypic variability for grain yield as well as yield components and related traits, and conducted the single-locus and multi-locus genome-wide association studies (GWAS) using high-density 45K single nucleotide polymorphisms. One hundred two loci were detected in non-stress conditions (38 loci in 2013 and 64 loci in 2014) and 124 loci (69 loci in 2013 and 55 in 2014) in water-deficit stress. Desynchronised flowering time strongly confounded the grain yield and its components in 2013 water-deficit. However, statistically corrected grain yield and yield component values using days to flowering allowed to minimise the confounding effect, and helped to detect 31 additional genetic loci for grain yield, its components and harvest index in 2013. These genetic analyses also provided important insights into genetic architecture of grain yield and its potential link with seed set and assimilate partitioning. Interestingly key *a priori* candidate genes were identified within the linkage disequilibrium block of grain yield loci regulating physiological, reproductive and abiotic stress tolerant biological processes.

Keywords: *Oryza sativa*, synchronized phenology, linkage disequilibrium, *a priori* candidate genes, multi-locus GWAS analysis, reproductive stage drought stress.

Introduction

Rice (*Oryza sativa* L.) is a staple food crop for more than half of the world population, and its high yield potential with good yield stability is imperative for future food security. However, global climate change, with frequent episodes of abiotic stresses (water-deficit and heat stress), reduces the productivity of rice (Kadam et al., 2014; Reynolds et al., 2016), as rice is more sensitive to water-deficit than other cereals (Kadam et al., 2015). Nearly 20% rice production is affected by water-deficit around the world (Bouman et al., 2005). Water-deficit can occur at any time of the growing season, but stress occurring during reproductive phase (i.e. from meiosis to flowering) causes the greatest grain yield losses (Liu et al., 2006). The physiological effects of water-deficit during the reproductive phase have been discussed (Saini and Lalonde, 1997; Saini et al., 1999; Barnabás et al., 2008).

Increasing tolerance to water-deficit has been considered as a breeding target, although knowledge on phenotypic traits linked with stress tolerance is limited. Increasing grain yield has been considered as the primary goal in breeding programmes. Recent evidence in rice has demonstrated that progress can be made through direct selection of grain yield under reproductive stage water-deficit (Venuprasad et al., 2007; Kumar et al., 2014). Physiologically, grain yield is a very complex trait determined by different component traits (Slafer, 2003). Hence, exploring ideotype breeding based on selection for component traits is proposed as a complementary route for further yield improvement (Donald, 1968).

Revealing the genetic basis of grain yield and its component traits is essential for providing the breeders the tools for efficient development of stress resilient crop cultivars. The genetic control of grain yield under reproductive stage water-deficit has been investigated extensively using linkage analysis of biparental crosses in rice. This approach is proven to be powerful in detecting quantitative trait loci (QTLs) for grain yield and its components under stress (Lanceras et al., 2004; Bernier et al., 2007; Vikram et al., 2011; Dixit et al., 2014; Kumar et al., 2014). Few of these QTLs regulating grain yield, for instance *qDTY1.1*, were introgressed into elite cultivars to improve stress tolerance (Vikram et al., 2011). However, most of these QTLs identified with the above approach are only based on a small fraction of the genetic variation present in the rice germplasm. Identifying the allelic variation assembled in a genetic pool that is large due to divergent selection pressure, has great potential in grain yield improvement under water-deficit stress. This approach using natural allelic variation is studied in rice under non-stress conditions for grain yield and its component traits through genome-wide association studies (GWAS; Agrama et al., 2007; Borba et al., 2010; Huang et al., 2010;

Zhao et al., 2011; Huang et al., 2012; Begum et al., 2015; Spindel et al., 2015; Rebolledo et al., 2016; Yano et al., 2016). Yet, very few studies are published for reproductive stage water-deficit conditions (Ma et al., 2016; Pantalião et al., 2016; Swamy et al., 2017). This was partly due to difficulty in implementing the stress at this stage under field conditions for a large GWAS panel that usually consists of genotypes having diverse phenological characteristics. Only the study of Ma et al. (2016) followed a staggered sowing to account for variation in flowering phenology under stress.

This study is aimed at (1) exploring the natural variation in grain yield as well as components and related traits in non-stress and reproductive stage water-deficit conditions; (2) linking the variation of these phenotypic traits with single nucleotide polymorphisms (SNPs) through GWAS; and (3) identify the most likely underlying candidate genes near to the significant SNP markers.

Materials and Methods

Association mapping population

We used a diverse set of 296 indica rice genotypes consisting of improved and traditional genotypes with (sub)tropical adaptation. This panel was assembled at International Rice Research Institute (IRRI) for the Phenomics of Rice Adaptation and Yield potential (PRAY) project in the context of Global Rice Phenotyping Network (<http://ricephenonetwork.irri.org>). Recent studies have reported a GWAS analysis using this population for grain quality traits (Qiu et al., 2016), salinity tolerance (Al-Tamimi et al., 2016), panicle architecture (Rebolledo et al., 2016), planting density (Kikuchi et al., 2017), and root morphological and anatomical plasticity in Chapter 3 (Kadam et al., 2017).

Strategy to cope with variation in flowering phenology

The PRAY panel was screened in non-stress and reproductive stage water-deficit conditions under field experiments conducted at the upland farm of IRRI, Philippines (14°11'N, 121°15'E; elevation 21 m above sea level) in 2013 and 2014 dry seasons (DS). Seeds were sown from December of the preceding year to late January or early February of each year (Fig. 1). As expected, a strong genotypic variation in flowering phenology was observed that confounds the true water-deficit response (Fukai et al., 1999) and inevitably induces bias with interpretation of genetic mapping outcomes (Pinto et al., 2010; Kumar et al., 2014). We followed staggered sowing in seedbeds and transplanting in main plots to synchronise flowering and thus minimize

phenological differences under stress imposition (Fig. 1). Briefly, in the 2013 DS experiment, we divided 296 genotypes into six groups with a 10-day interval based on days to flowering data collected in a pre-experiment in the 2012 wet season (WS), our only source of flowering dates for this population grown at IRRI. While the expected date of flowering was 29 March to 08 April 2013 (Fig. 1A), we observed deviation in days to flowering in the 2013 DS experiment, where the staggered sowing was based on the 2012 WS data. Therefore, in the 2014 DS experiment, we regrouped the 296 genotypes into eight groups with a 7-day interval using 2013 DS flowering data to improve synchrony within the whole population. The expected date of flowering was 28 March to 05 April 2014 for these genotypes (Fig. 1B). In each year, the sowing date chosen for the stress treatment was the same for the non-stress treatment of the same genotype.

Crop management

The soil type of the upland farm is Maahas clay loam, isohyperthermic mixed Typic Tropudalf. The experiments were laid out in a group block design with three replications for each genotype in both treatments (Supplementary Figure S1). Seeds were first exposed to 50 °C for 3 days to break the dormancy and then hand sown in a seedbed nursery. Twenty-one-day-old seedlings were transplanted (two seedlings per hill) for each genotype in four rows per replication. In both years, row distance was 0.2 m and row length was 2.4 m. The seeds of one genotype in 2013 and 8 genotypes in 2014 germinated poorly and hence were excluded. In addition, four genotypes completed flowering and maturity before stress imposition in 2013 and were excluded. This resulted in the final sets of 291 genotypes in 2013 and 288 genotypes in 2014; and with 3 replications and 2 treatments, these gave 1746 and 1728 plots for 2013 and 2014, respectively. One day before transplanting, 30 kg P ha⁻¹ (as single superphosphate), 40 kg K ha⁻¹ (as KCl), and 5 kg Zn ha⁻¹ (as zinc sulfate heptahydrate) fertilizers were manually applied. Nitrogen fertilizer as urea was applied in three splits: 45 kg ha⁻¹ before transplanting, 30 kg ha⁻¹ at mid-tillering, and 45 kg ha⁻¹ at panicle initiation. The IRRI standard management practices were followed to control weeds, insects and diseases. In both years, all plots were maintained like irrigated lowlands with ~5 cm standing water until maturity except for the water-deficit plots during the stress period (see below).

Reproductive stage water-deficit stress imposition

There was variation in synchronizing days to flowering among rice genotypes in 2013, resulting

in deviation from our expected flowering window (29 March to 08 April). In rice, the reproductive stage initiation ranges between from 19 and 25 days, starting at panicle initiation and ending with flowering (Moldenhauer and Slaton, 2001). Therefore, before imposing stress, we manually dissected the main tillers of the middle two plants of border rows from water-deficit plot for all the genotypes, primarily to check the reproductive stage development. When majority of genotypes reached the panicle initiation stage, we imposed stress on 23 March 2013 by draining water out from the field. The stress continued for 14 days until 5 April 2013. In the 2014 experiment, the synchronisation was more precise with expected dates of flowering occurring between 28 March and April 5, as predicted. The same dissection approach as in 2013 was followed and stress was imposed on 26 March 2014 and continued for 14 days until 8 April.

To quantify the stress intensity, 26 tensiometers were installed randomly across the entire stress field at 30 cm depth in each season. A polythene sheet was inserted at 2-meter depth by digging a deep and narrow trench in between stress and non-stress fields to prevent water seepage during the stress period from the adjacent non-stress field. The intensity of stress was higher in 2014 than in 2013 (Supplementary Figure S2A). There was no rainfall during the peak stress period in both seasons, except rainfall during the first day of stress period in 2013 (Supplementary Figure S2B). Higher stress intensity in 2014 compared to 2013 could be due to higher maximum temperature and higher vapour-pressure deficit (Supplementary Figure S3B and D), leading to quicker loss of soil moisture in 2014. A weather station was placed between the non-stress and water-deficit plots (see Supplementary Figure S1). Detailed weather data are given in Supplementary Figure S3.

Observations

At maturity, plants of 16 hills from the middle two rows i.e. 0.64 m² plot area (excluding the border rows) were harvested to assess grain yield (14% moisture), its components and related traits in both experiments, following Shi et al. (2016). Days to flowering was assessed as the interval between the date of sowing and the date when panicles of 50% plants per plot were fully exerted. Days to maturity was assessed as the interval between the flowering date and date when panicles on most plants in a plot turned yellow and ready for harvest. Plant height was measured from the base of the root-shoot junction to the tip of the flag leaf. Non-grain dry weight was assessed as the sum of leaf, stem and rachis dry weight. The total aboveground dry weight was the sum of non-grain dry weight and grain dry weight. Harvest index was the ratio of grain dry weight to total aboveground dry weight.

Statistical analysis of phenotypic data

Analysis of variance (ANOVA)

A combined linear mixed model based ANOVA was performed to test the effect of genotype (G), treatment (T) and year (Y) with their interactions using the following model in Genstat V17.1.

$$Y_{ijkl} = \mu + G_i + T_j + Y_k + R_l[(T_j(Y_k))] + (G \times T \times Y)_{ijk} + E_{ijkl}$$

where Y_{ijkl} is the phenotypic trait value recorded in a plot, μ is the overall mean, G_i is the effect of the i^{th} genotype, T_j is the effect of the j^{th} treatment, Y_k is the effect of the k^{th} year, $R_l[(T_j(Y_k))]$ is the effect of the l^{th} replication within the j^{th} treatment of the k^{th} year, $(G \times T \times Y)_{ijk}$ is the effect of three-way interaction between the i^{th} genotype, the j^{th} treatment and the k^{th} year, and E_{ijkl} is the error. Apart from three-way interaction, we also consider two-way interactions of main factors in all possible combinations.

Linear mixed model to estimate best linear unbiased estimators

We estimated the best linear unbiased estimators (BLUEs) of phenotypic traits for individual genotype across years and treatments, separately. The following linear mixed model was used in Genstat release V17.1 to estimate the BLUEs separately in non-stress and stress conditions across years, using genotypes as a fixed effect and replications as a random effect.

$$Y_{ij} = \mu + G_i + R_j + E_{ij}$$

where Y_{ij} is the phenotypic trait value recorded in a plot, μ is the overall mean, G_i is the effect of the i^{th} genotype, R_j is the effect of the j^{th} replication, and E_{ij} is the error.

Days to flowering had a strong confounding effect on grain yield and its components under stress, particularly in 2013 (Fig. 1C). Therefore, we performed the linear mixed model based ANOVA analysis using the above equation with days to flowering as covariate. If the effect of days to flowering was significant, corrected BLUEs of grain yield and its components and related traits were estimated in stress treatments.

Principal component analysis, trait correlation and multiple regression analysis

A multivariate principal component analysis (PCA) was performed in XLSTAT across years and treatments. The chart. Correlation() function within the R package “*Performance*

Analytics” was used to generate the correlation scatter plot. The `lm()` function within the R statistical framework was used for multiple linear regression analysis of grain yield with its component and related traits.

Heritability estimates

Broad-sense heritability (H^2), capturing the proportion of phenotypic variance explained by genetic factors that is due to dominance, epistatic and additive effects, was calculated using the below equation across years and treatments separately:

$$H^2 = \frac{\sigma_G^2}{\sigma_G^2 + \frac{\sigma_E^2}{r}}$$

where σ_G^2 and σ_E^2 are the genotypic and residual variances respectively and r is the number of replications. The restricted maximum likelihood estimate was used to calculate the variance components in Genstat release 17.1. The narrow-sense heritability (h^2), capturing the proportion of total phenotypic variance explained by the additive genetic variance, was estimated using the equation in Genomic Association and Prediction Integrated Tool (GAPIT) function:

$$h^2 = \frac{\sigma_a^2}{\sigma_a^2 + \sigma_e^2}$$

where σ_a^2 is the additive genetic variance and σ_e^2 is the residual variance.

Genetic analysis of marker-trait associations

The 291 genotypes in 2013, and 288 genotypes in 2014 experiments had complete phenotypic data. However, 20 genotypes were missing in the data of 45,699 (46K) SNPs, meaning only 271 genotypes in 2013 and 268 in 2014 were used for our GWAS analysis. The detailed genotype-by-sequencing protocol of SNPs genotyping, population structure and linkage disequilibrium (LD) for this population are explained in Chapter 3 (Kadam et al., 2017). The GWAS was performed on a set of 271 (2013) and 268 (2014) genotypes separately, with the 267 genotypes being common across both years. Two GWAS methods were used to test the marker-trait associations: the single-locus and the multi-locus analysis.

Single-locus GWAS analysis

Single-locus analysis is a one-dimensional scan, typically identifying associations between single marker and traits in the population. We performed this analysis using a compressed mixed-linear model (CMLM; Zhang et al., 2010) in the GAPIT (Lipka et al., 2012). In the

mixed model, we included population structure and family kinship (family relatedness), that were calculated by the GAPIT function using SNPs with ≥ 0.05 minor allele frequency (MAF).

$$Y = X\alpha + P\beta + K\mu + e$$

where Y represents the vector of phenotype, X represents the vector of SNPs, P is the PCA matrix and K is the relative kinship matrix. $X\alpha$ and $P\beta$ are the fixed effect, and $K\mu$ is the random effects and e represents the random error. The P and K matrices help to reduce the spurious false positive associations. Correction for population structure (P) substantially reduces the false positives but it sometimes eliminates true positive associations due to overcorrection. Therefore, the optimal number of principal components was estimated for each trait before incorporating them for CMLM tests, based on the forward model selection method using the Bayesian information criterion (BIC). This method helps to control both false-positive and false-negative associations more effectively although it cannot eliminate both completely. We used a lower suggestive threshold probability P value $1.0E-04$ and upper Bonferroni corrected threshold (at $\alpha=0.05$) to detect significant associations.

Multi-locus GWAS analysis

The single-locus analysis corrects the confounding effects of population structure and family kinship but does not consider the confounding effect of causal genetic loci. The multi-locus GWAS is a method that corrects not only the confounding effects of population structure and family kinship but also the confounding and/or interaction effects of causal loci present in the genome due to LD (Segura et al., 2012). We performed the multi-locus GWAS using a modified version of the multi-locus mixed linear model (MLMM) in R studio (R script for `mlmm.cof.r` available at <https://cynin.gmi.oeaw.ac.at/home/resources/mlmm>). We ran the complete model as recommended with stepwise forward inclusion of the strongest significant markers (lower P value) and stepwise backward elimination of the last forward model (that is least significant markers). Significant markers were selected based on the criteria explained in Chapter 3 (Kadam et al., 2017). Briefly, in the first step (like single-locus GWAS without any marker as a cofactor), we manually checked the P value of SNPs before including them as a cofactor in model. Then we continued adding markers to the model as cofactor based on cut-off threshold p -value $\leq 1.00E-04$. Once there are no significant loci appeared above the threshold P value, the model was stopped. All the significant cofactor identified were considered as significant genetic loci.

Selecting *a priori* candidate genes underlying the genetic loci

The detailed protocol to select *a priori* candidate genes near to significant SNPs was followed as explained in Chapter 3 (Kadam et al., 2017).

Results

The flowering time was sensitive to seasonal climate variations

The flowering time synchronisation approach was followed to reduce the confounding effect of flowering time differences of rice genotypes on grain yield and its components and related traits under stress (Fig. 1A-B). However, we witnessed deviation of our observed days to flowering from expected days ($R^2=0.53$ in non-stress and $R^2=0.46$ in stress; Fig. 1C) in 2013. As rice flowering time is regulated by internal genetic cues and external stimuli such as photoperiod and temperature (Yin et al., 1997), such deviations were anticipated, since the synchronisation in 2013 was based on 2012 WS pre-experiment data due to lack of DS data. Many genotypes exhibited photothermal sensitivity across wet and dry seasons. Therefore, some genotypes experienced stress during the flowering period (31%), whereas others experienced stress either before (60%) or immediately after flowering (8%). In 2014, we restructured the synchronisation based on 2013 DS data. This resulted in better synchronisation with only small deviation observed from expected days to flowering ($R^2=0.91$ in non-stress and $R^2=0.85$ in stress; Fig. 1D). Further, to test the effect of days to flowering, we performed the analysis with days to flowering as a covariate in the mixed model ANOVA. The moderate to strong significant effect of days to flowering on grain yield, its components and harvest index were detected in 2013 stress, most likely due to desynchronised flowering time. Conversely, the improved flowering synchronization caused no significant effect in 2014 stress. The marginal ($P < 0.05$) to moderate ($P < 0.01$) effect of days to flowering on grain yield, seed set and harvest index was detected in both years under non-stress conditions (Fig. 1C-D). This could be due to the pleiotropic effect of flowering genes on panicle development (Crowell et al., 2016), a key determinant of rice grain yield.

Genotype effects and genotype-by-environment interactions accounted for variations in grain yield and other traits

A combined mixed model ANOVA across years was carried out to divide the variation in genotype, treatment and year components and their interactions (Table 1). The variation in grain yield, its components and related traits differed significantly between genotype (G ; $P < 0.001$),

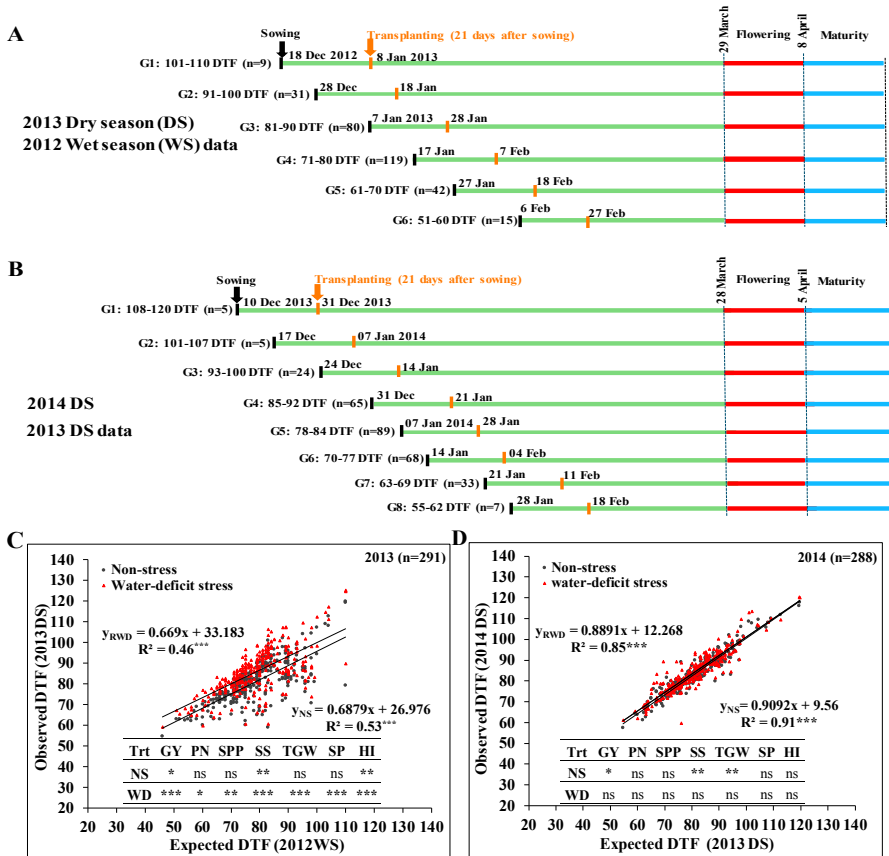


Figure 1: Schematic representation of staggered sowing and transplanting approach followed for screening of indica rice diversity panel under reproductive stage water-deficit stress in dry season (DS) of 2013 (**Panel A**) and 2014 (**Panel B**). Days to flowering interval was 10 days between groups (G) in 2013 and 7 days in 2014 DS experiments. The expected and observed days to flowering (DTF) in non-stress (NS) and water-deficit stress (WD) in 2013 (**Panel C**) and 2014 dry season (**Panel D**) experiments. The ANOVA results with the effect of DTF (as a covariate in mixed linear model) on grain yield and its key component traits are given in panel. n = number of genotypes; Trt = treatments; GY=grain yield; PN=panicles per m²; SPP=spikelets per panicle; SS= seed set; TGW=thousand grain weight; SP=spikelets per m²; HI=harvest index. Significance levels: **P*<0.05, ***P*<0.01, ****P*<0.001.

treatment (T; *P*<0.001) and year (Y; *P*<0.01 to *P*<0.001). Further, the grain yield, its components and related traits of each genotype responded differently to treatment (G×T; *P*<0.001) and year (G×Y; *P*<0.001). The detailed descriptive statistics of these traits are given in Supplementary Table S1. The traits showed different distributions in non-stress and stress conditions (Fig. 2). Grain yield ranged from 106.3 to 727.0 g m⁻² in non-stress,

and from 16.7 to 622.6 g m⁻² under stress in 2013, and from 102.8 to 839.7 g m⁻² in non-stress, and from 78.1 to 761.1 g m⁻² under stress conditions in 2014. Across all observations, H² and *h*² estimates ranged from 0.73 to 0.99 and from 0.27 to 0.94, respectively, in 2013; and from 0.62 to 0.99 and from 0.69 to 0.93, respectively, in 2014 (Supplementary Table S1). The higher reduction of grain yield, seed set and harvest index under stress in 2014 was due to higher stress intensity during 2014 (-64 kPa) compared to 2013 (-46 kPa), because of higher vapour-pressure deficit (Supplementary Figures S2A and S3D). However, a higher reduction of spikelets per panicle and spikelets per m² despite lower stress intensity was observed during 2013 than during 2014 (Fig. 2C-E). This could be due to variation in flowering time synchronisation with more genotypes experiencing stress before flowering in 2013 than in 2014. These results clearly illustrate that stress affects the number of spikelets per m² when imposed before flowering, but spikelet fertility when imposed during flowering (Lanceras et al., 2004) as seen in Fig. 2C-E. The days to flowering differed significantly ($P = 0.002$) between non-stress and stress in 2013, but not ($P > 0.05$) in 2014 (Fig. 2I). The first two principal components cumulatively explained >55% (non-stress: 55.61%; stress: 59.59%) in 2013 and >61% (non-stress: 61.26%; stress: 63.66%) in 2014 of the total phenotypic variation (Fig. 3). The genotypic variation in the first PC was mostly explained by grain yield, harvest index and spikelets per m² in non-stress (2013: PC1=29.09%; 2014: PC1=34.69%) and grain yield, harvest index, spikelets per m² and total dry weight in stress (2013: PC1=35.51%; 2014: PC1=37.54%). The genotypic variation in second PC was explained by non-grain dry weight, days to flowering and total dry weight in non-stress (2013: PC2= 26.52%; 2013: PC2=26.56%) and plant height, non-grain dry weight and days to flowering in stress (2013: PC2=24.08%; 2014: PC2=26.12%). In addition, the phenotypic traits with their magnitude (the length of the vector) and orientation were elucidating that the principal component variations differed in response to treatment and year (Fig. 3). This confirms our ANOVA results. For instance, variation in traits were higher in 2014 than in 2013, indicating a G×Y interaction. The trait variation was higher in stress (2013=59.59%; 2014=63.66%) compared to non-stress (2013=55.61%; 2014=61.26%) conditions, indicating that stress increased genotypic variability (G×T interaction).

Phenotypic trait correlations and contribution of component traits to grain yield

Grain yield was significantly ($P < 0.05$) correlated with most of its components and related traits across treatments and years (Supplementary Figures S4-S7). However, non-significant ($P > 0.05$) correlations of grain yield were found with thousand grain weight and non-grain dry

Table 1: Analysis of variance (ANOVA) of grain yield and its components and related traits in 2013 and 2014 dry season experiments.

Class	Trait	Unit	G	T	Y	G×T	G×Y	T×Y	G×T×Y
A	Grain yield	g m ⁻²	***	***	***	***	***	***	**
B	Grain yield component traits								
	Panicles per m ²	m ⁻²	***	***	***	***	***	ns	***
	Spikelets per panicle	-	***	***	***	***	***	ns	
	Seed set	%	***	***	***	***	***	***	***
	Thousand grain weight	g	***	***	**	***	***	ns	***
	Spikelets per m ² (×10 ³)	m ⁻²	***	***	***	***	***	***	
C	Grain yield related traits								
	Harvest index	-	***	***	***	***	***	***	***
	Total dry weight	kg m ⁻²	***	***	***	***	***	ns	ns
	Non-grain dry weight	kg m ⁻²	***	***	***	***	***	***	***
	Plant height	cm	***	***	***	***	***	*	ns
	Days to flowering	-	***	***	***	***	***	***	***
	Days to maturity	-	-	-	-	-	-	-	-

G = genotype, T = treatment, Y = year, ns= non-significant. Spikelets per m² is not an independent yield component and it is the product of panicles per m² and spikelets per panicle. Significance level: **P*<0.05, ***P*<0.01, ****P*<0.001.

weight in non-stress, and with panicle number in 2013 stress. Grain yield was not significantly (*P*>0.05) correlated with non-grain dry weight across treatments in 2014. The correlation of grain yield with spikelets per panicle was higher in stress (2013: *r*=0.73; 2014: *r*=0.46) than in non-stress conditions (2013: *r* = 0.40; 2014: *r* = 0.36) in both years, and increase was more in 2013. Similarly, the correlation between grain yield and seed set increased from 0.62 in non-stress to 0.75 in stress conditions in 2014. The increased correlation of grain yield with spikelets per panicle in 2013 and with seed set in 2014 in stress reflects the effect of variation in days to flowering synchronisation. Further, correlations of grain with days to flowering was increased weakly under stress in 2013 (non-stress: *r* = 0.16; stress *r* = 0.29), but remained unchanged across treatments in 2014 (non-stress and stress: *r*=0.30). The correlation between grain yield and harvest index was marginally increased in water-deficit (2013: *r* = 0.85, 2014: *r* = 0.86) compared with non-stress (2013: *r* = 0.83, 2014: *r* = 0.81). We also tested the relative contribution of each component and related trait to grain yield through multiple linear regression. All components and related traits significantly contributed to grain yield except for plant height and days to flowering in non-stress and only days to flowering in stress during 2013 and 2014, respectively (Supplementary Table S2). The cumulative variation of grain yield explained by its components and related traits was marginally higher in 2014 (*R*²: 0.94 in non-stress and *R*²=0.93 in stress) than in 2013 (*R*²: 0.89 in non-stress and *R*²=0.88 in stress).

Treatment and year specific genetic loci for grain yield and other traits

Grain yield and its components and related traits followed a normal distribution (Supplementary Figures S4-S7), indicating the quantitative pattern suitable for genetic analysis. To identify marker-trait association, we used a lower suggestive threshold P value $1.0E-04$ ($-\text{Log}_{10} P=4$) and superior Bonferroni corrected threshold as an upper limit (2013: $-\text{Log}_{10} (0.05/45,437) =6$; 2014: $-\text{Log}_{10} (0.05/45,414) =6$). A summary of GWAS results is given in Table 2, while the detailed results are in Supplementary Tables S3-S6. In total, we identified 38 significant loci in non-stress, and 69 loci in stress during 2013, and 64 significant loci in non-stress, and 55 in stress during 2014. Most loci were specific across treatments within years and within treatments across the years. Nevertheless, we also detected 14 common loci (9 in 2013 and 5 in 2014) across treatments and 8 common loci within treatments (6 in non-stress and 2 in stress conditions) across years only for the same components and related traits (Supplementary Table S7).

Genetic analysis after correcting for days to flowering under stress in 2013

Flowering time synchronisation was strongly confounding the grain yield and its component traits in 2013 stress (Fig. 1C-D). We corrected grain yield and its components and related (only harvest index in this class) traits using days to flowering as a covariate in the mixed model. The single-locus and multi-locus analysis of corrected trait values evidenced 31 additional loci using similar threshold P -values as mentioned earlier (Table 2; Supplementary Table S8). Most genetic loci detected for non-corrected traits disappeared when corrected trait values were subject to GWAS analysis. This suggested that the trait variation associated with these loci were mostly explained by variation in days to flowering. Only five genetic loci (one on chromosome 4 for grain yield [Q9]; one on chromosome 12 for spikelets per m^2 [1, 41,599] and 3 loci on chromosome 11 for harvest index [10,627,944; 10,131,062; 10,329,677] were common to corrected and non-corrected trait values. The common loci detected for grain yield (Q9; Table 3 and Figure 4) and harvest index (Supplementary Figure S8; Supplementary Tables S4 and S8) recorded lower P -value (improved statistical power) for corrected value through single-locus analysis. Despite correction, the novel locus Q10 on chromosome 3 for corrected grain yield, seed set and harvest index overlapped with days to flowering (Table 3). In conclusion, statistical correction helped to explain the confounding effect of days to flowering and could eliminate its effect on grain yield under water-deficit. Unless otherwise mentioned, all results discussed in the following sections were for the corrected trait loci in 2013 stress.

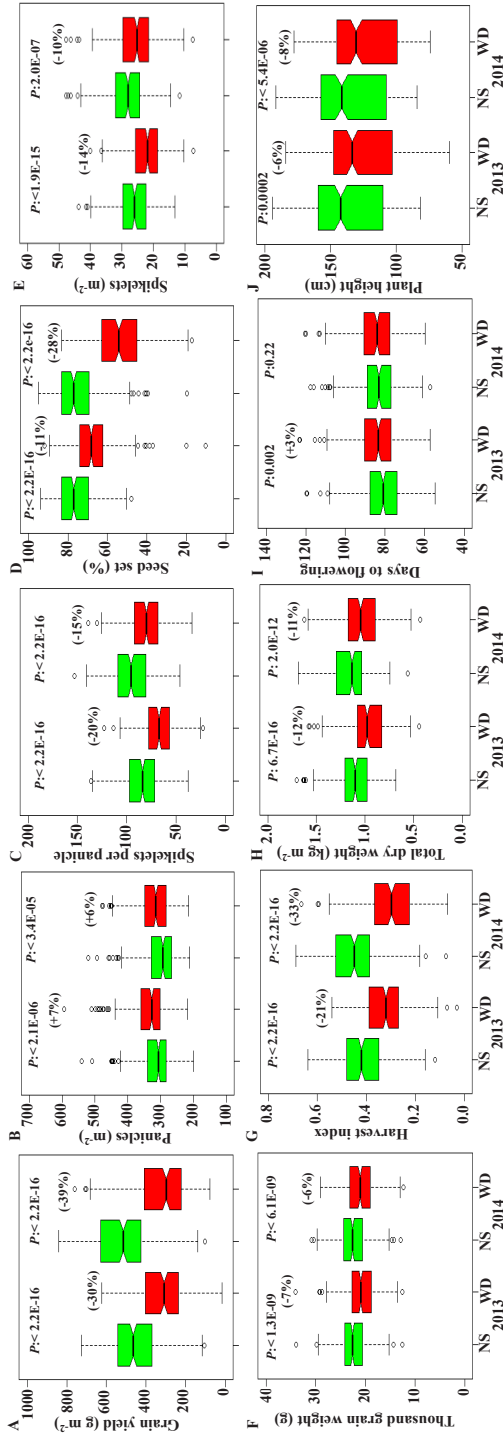


Figure 2: Box-plot showing phenotypic distribution of grain yield and its components and related traits in non-stress (NS) and water-deficit stress (WD) during 2013 (n=271) and 2014 (n=268). Two sample t-test *P* value showing the significant difference between grain yield (Panel A), its components (Panels B-F) and related traits (Panels G-J) in NS and WD conditions. n=number of genotypes. Inside boxplot, the bold line represents the median, box edges represent upper and lower quartiles, and whiskers are 1.5 times the quartile of the data. Outliers are shown as open dots. Values in parentheses represent the significant percentage change (increase [+]) or decrease [-] in WD over NS conditions. Days to maturity across treatments in 2013 and data for non-grain tissue dry weight across treatments and years are given in **Supplementary Table 1**. The value of grain yield and its component and related traits under water-deficit in 2013 are not adjusted for variation in flowering synchronisation.

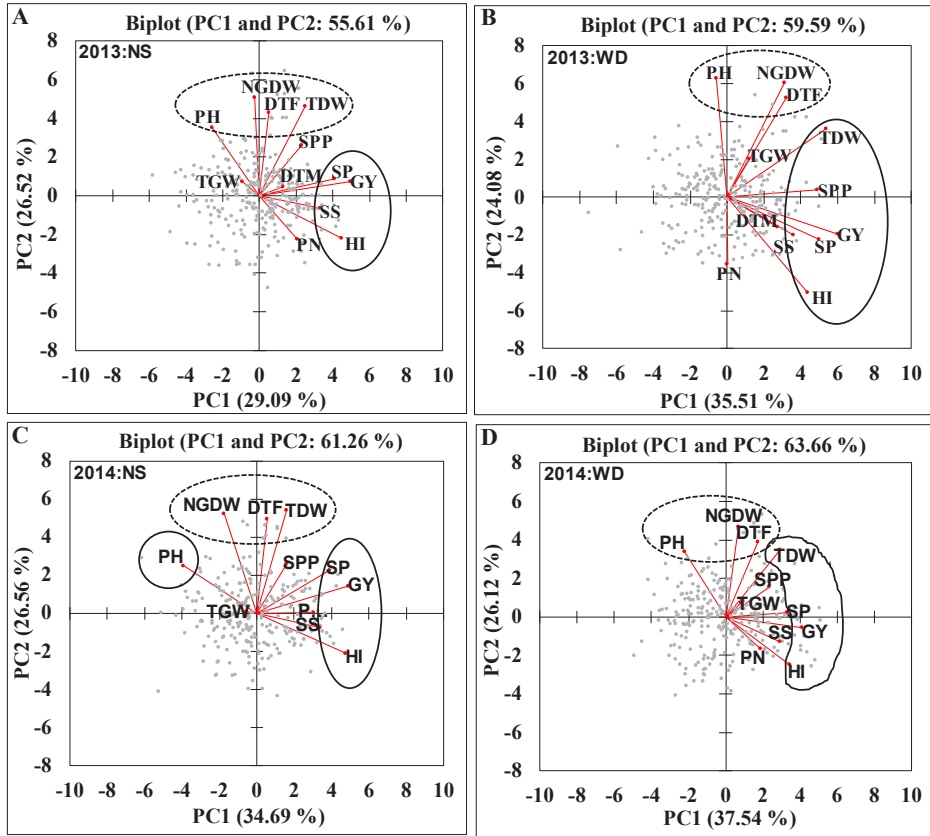


Figure 3: The principal component analysis of grain yield, its component and related traits with first two principal components (PC1 and PC2) in non-stress (NS) and water-deficit stress (WD) during 2013 (NS=Panel A; WD=Panel B) and 2014 DS (NS=Panel C; WD=Panel D). The traits marked inside the solid circle/ellipses contributed more to the variation explained by PC1 and marked inside the dashed circle/ellipses to PC2. GY=grain yield; PN=panicles per m^2 ; SPP=spikelets per panicle; SS= seed set; TGW= thousand grain weight; SP=spikelets per m^2 ; HI=harvest index; TDW= total dry weight; NGDW= non-grain dry weight; PH= plant height; DTF=days to flowering; DTM=days to maturity.

Eight grain-yield loci revealed small to medium allelic effect in non-stress conditions

We identified two (Q1 and Q2) and six (Q3-Q8) loci for grain yield in 2013 and 2014, respectively (Table 3). There were no common loci across years, most likely due to significant variations in minimum and maximum temperature and vapour-pressure deficit (VPD; Supplementary Figure S3). These loci had a positive or negative effect (small to medium) on grain yield regarding its minor allele (allele refers to the 0.05 frequency in studied population). In 2013, the minor allele of Q1 (30.13 $g m^{-2}$) had a positive effect on grain yield. Conversely, the minor allele of Q2 (-175.9 $g m^{-2}$) locus had a negative effect on grain yield. In 2014, Q3

Table 2: Summary of genetic loci detected for grain yield; its components and related traits in 2013 and 2014 under non-stress (NS) and water-deficit stress (WD) conditions.

Class	Traits	2013			2014	
		NS	WD	WD [†]	NS	WD
A	Grain yield	2	4	2	6	5
B	Grain yield component traits					
	Panicles per m ²	6	12	7	9	3
	Spikelets per panicle	5	9	6	2	na
	Seed set	3	7	7	8	11
	Thousand grain weight	3	4	na	6	8
	Spikelets per m ²	1	4	1	4	3
	Subtotal B	18	36	21	29	25
C	Grain yield related traits					
	Harvest index	6	7	8	4	2
	Total dry weight	3	2	-	4	11
	Non-grain dry weight	3	3	-	5	2
	Plant height	2	6	-	6	4
	Days to flowering	3	11	-	10	6
	Days to maturity	1	na	-	-	-
	Subtotal C	18	29	8	29	25
	Total (A+B+C)	38	69	31	64	55

na = no marker-trait association; † = marker-trait associations detected for corrected trait values in water-deficit stress.

(30.40 g m⁻²), Q5 (13.98 g m⁻²) and Q6 (74.08 g m⁻²) all had a positive effect, while Q4 (-46.18 g m⁻²), Q7 (-186.24 g m⁻²) and Q8 (-97.80 g m⁻²) all had a negative effect on grain yield regarding the minor allele. Eighteen and sixty-eight *a priori* (known or characterized) candidate genes were harboured within the expected LD block by Q1 and Q2 in 2013, and Q3-Q8 in 2014, respectively. Interestingly eight *a priori* candidate genes were identified. Some are presented below while others are given in Supplementary Table S9. Q1 was close to *OsPTR2* (6 and 31 kb; two copies in LD block). The rice homologue of this gene *short panicle 1* (*OsPTR2*) regulates panicle and grain size and nitrate transport in rice (Li et al., 2009). The homologue of *OsPTR2* was recently detected at *q-28* locus (*OsPTR9*) for spikelet number per panicle (a key determinant of grain yield) in the same rice association panel as we used in this study (Rebolledo et al., 2016). Likewise, Q4 was close (34 kb from peak SNP) to serine-threonine kinase (*OsSTE*). The Arabidopsis orthologue of *OsSTE* (*AtSTE*) is the major regulator of stomatal opening (Supplementary Table S9).

Seven grain-yield loci revealed small to medium allelic effect in response to reproductive stage water-deficit

We identified two loci (Q9 and Q10) for grain yield under stress in 2013. The minor allele of both loci had a negative effect (Q9: -81.29 g m^{-2} and Q10: -40.61 g m^{-2}) on grain yield. Five significant loci Q11-Q15 were detected for grain yield under stress in 2014, (Figure 5). The minor allele of Q11 (31.47 g m^{-2}), Q12 (6.10 g m^{-2}) and Q15 (33.65 g m^{-2}) had a positive effect on grain yield. While the minor allele of two loci, Q13 (-49.86 g m^{-2}) and Q14 (-23.54 g m^{-2}), had a negative effect on grain yield. The Q9, Q10, and Q11-Q15 harboured 18 and 16 *a priori* candidate genes within the expected LD block region, respectively (Table 3). Seven *a priori* candidate genes, mostly near significant SNPs, are given in Supplementary Table S9. The Q9 locus was close (13 kb) to the Phosphomannomutase gene regulating L-Ascorbic acid (Asc) biosynthesis and response to abiotic stress stimulus (Gene Ontology [GO]: 0009628). Asc acts as a redox buffer to detoxify reactive oxygen species (ROS; Arrigoni and De Tullio, 2002). Q11 was close to Squalene monooxygenase or epoxidase (16 and 23 kb; two copies in LD block) and response to abiotic stress stimulus (GO: 0009628). This gene is known to regulate ROS, stomatal responses and water-deficit stress tolerance in Arabidopsis (Posé et al., 2009).

Only three loci for grain yield acted *via* change in seed set percentage

Although rice grain yield is co-determined by panicle number, spikelets per panicle, seed set percentage and grain weight, very few loci of these component traits were coinciding with loci for grain yield *per se*. The seed set percentage is one of the most important yield components as indicated by its strong correlation with grain yield (Supplementary Figures S4-S7). Three loci were regulating grain yield through changes in seed set percentage, i.e., two loci designated as Q2 (2013) and Q7 (2014) in non-stress, and Q10 (2013) in stress. The major (allele refers to the 0.95 frequency in studied population) allele of these loci had a positive effect on grain yield, seed set and harvest index, respectively (Fig. 6). In addition, the Q10 was also detected for days to flowering. No loci were common for grain yield and seed set in 2014 stress, but one of the loci on chromosome 1 (29,223,354) was commonly detected for seed set and harvest index (Supplementary Figure S9). Similarly, the major alleles had a positive effect on seed set, harvest index, and grain yield (irrespective of genetic significance), respectively (Fig. 7). Hence, these above loci were regulating grain yield through the effect of seed set on harvest index. Four *a priori* candidate genes were predicted within the expected LD block of these loci. The Q2 was close (55 kb from peak SNP) to Plastocyanin gene that regulates flower development (GO:

0009908) and pollination (GO: 0009856) in rice (Supplementary Table S9). The Arabidopsis orthologue of this gene regulates the seed set and pollen tube growth (Dong et al., 2005). Q7 was within the novel expressed protein, which provides an entry point for future study. Sugar transport or uptake is essential for normal pollen development (Reinders, 2016), while the lack of starch synthesis arrests the pollen development in water-deficit thereby regulating seed set (Sheoran and Saini, 1996). Our Q10 locus was within the sugar transporter gene that plays an important role in sugar distribution. The rice grain yield *MQTL_{2.1}* (meta-analysis QTL) detected in water-deficit was also containing sugar transporter gene (Swamy et al., 2011). Similarly, the locus on chromosome 1 for seed set and harvest index in 2014 stress was near (34 kb from peak SNP) to the nitrate transporter gene that plays a role in rice grain yield increment (Fan et al., 2016).

Discussion

The main aim of this study was linking the phenotypic variation with genetic markers, thereby gaining insights about promising candidate genes and the genetic architecture controlling yield traits. To the best of our knowledge, this is the first study conducted on rice PRAY association mapping panel under reproductive stage water-deficit stress. The key findings from our study are discussed below.

Statistical trait adjustment can reduce confounding effect of desynchronised flowering on genetic analysis under water-deficit stress

The desynchronised flowering time may result in the identification of QTLs, often coinciding with QTLs for phenology and grain yield in reproductive stage stress (Pinto et al., 2010). Our genetic analysis of statistically corrected trait values was effective in minimizing the effect of desynchronised flowering time, as it led to detection of several novel loci that were not detected for non-corrected trait values. Despite of statistical adjustment for flowering time, our novel Q10 for grain yield was co-localised with flowering time (different SNP but falls within the same gene and LD block). In addition, it was also co-localised with seed set and harvest index. Previous studies in rice have identified several grain yield QTLs using linkage mapping under reproductive water-deficit stress conditions (Bernier et al., 2007; Venuprasad et al., 2009; Vikram et al., 2011; Swamy et al., 2013; Mishra et al., 2013), of which some were co-localised with plant height (qDTY_{6.2}), days to flowering (qDTY_{3.2}) or both (qDTY_{1.1}). Interestingly, the major effect of qDTY_{1.1} was consistent even after statistical correction of grain yield using

flowering time and plant height as covariates (Vikram et al., 2011), and the recent detailed characterisation confirmed the tight linkage and not the pleiotropy of this QTL with plant phenology (Vikram et al., 2015). Our novel Q10 provided higher confidence of causative SNP placed directly within the sugar transporter gene. However, this SNP was just 5 kb away from the COP9 signalosome complex subunit 4 gene within the same LD block (Supplementary Table S9). The COP9 signalosome complex gene is known to regulate flower development in *Arabidopsis* (Wang et al., 2003), although no study so far reported the role of this gene in rice flowering. Therefore, a future characterisation of Q10 would be interesting to decipher the relationship with flowering time and stress tolerance to test linkage versus pleiotropy. Nevertheless, the effect of our consistent Q9 for grain yield (detected using either corrected or non-corrected values) was independent of flowering time stress conditions. More precise flowering time synchronisation in 2014, which allowed identifying the genetic loci without having any co-localisation with flowering time in stress conditions added value to the findings. To the best of our knowledge, this is the first report demonstrating the better synchronisation of flowering time phenology on a large GWAS panel under stress conditions at field level.

Genetic control of grain yield, its components and related traits was mostly independent and environment specific

Grain yield is a complex trait determined by many interactive physiological processes changing temporally during the growing period. These processes often match the development of the key yield components in cereals that are genetically less complex than yield *per se* (Yin et al., 2002). In rice, grain yield is the product of the panicle number/productive tiller (determined during the vegetative phase), spikelets per panicle (determined during panicle initiation), seed set percentage (determined during panicle initiation and anthesis) and individual grain weight (determined during grain filling). The genetic selection for each of these traits during rice domestication has given rise to rich genetic diversity (Doebley et al., 2006; Sweeney and McCouch, 2007). To date, molecular genetic studies have detected QTLs underlying these genetic changes in rice yield components (<http://www.gramene.org/>). From these QTLs some of the candidate genes were successfully identified, notably displaying the improvement in grain yield (Ashikari et al., 2005; Fan et al., 2006 ; Song et al., 2007; Shomura et al., 2008; Huang et al., 2009; Miura et al., 2010). For instance, the SPIKE gene/allele regulating the spikelet numbers indicated 13-36 % yield increment in rice (Fujita et al., 2013). In the present study, genetic dissection of these yield components enabled us to detect more loci than yield

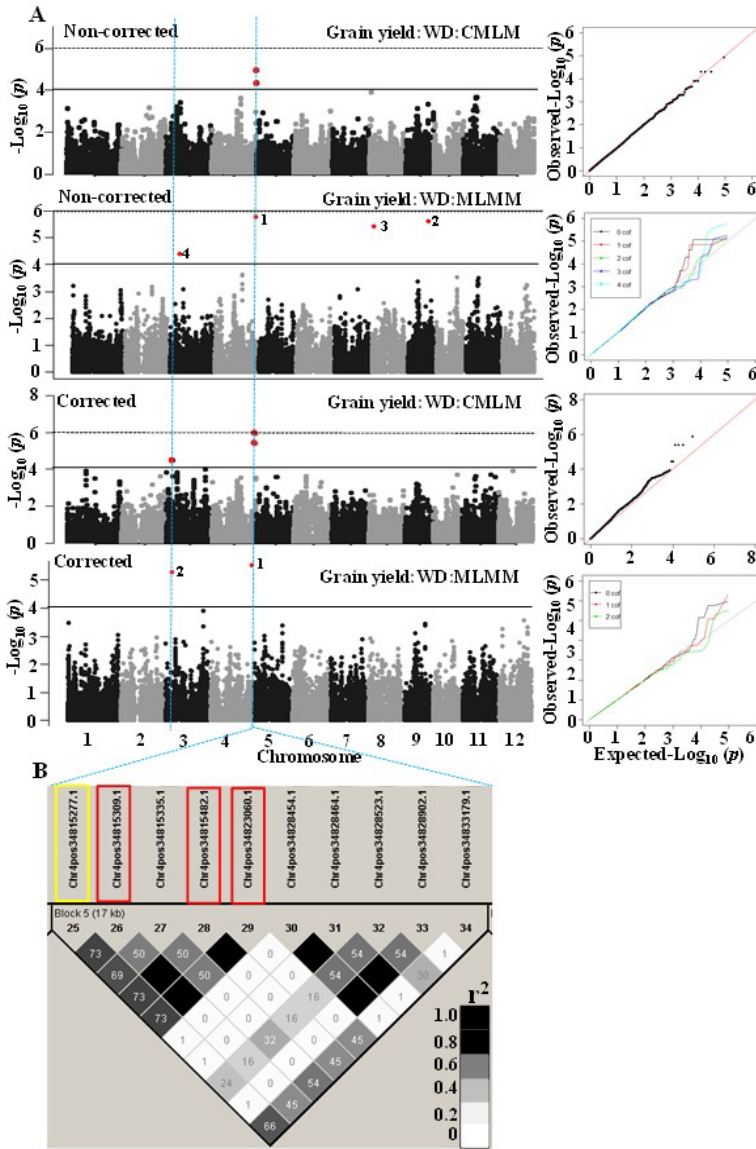


Figure 4: GWAS results (Manhattan and Quantile-Quantile plot) detected through single-locus compressed mixed linear model (CMLM) and multi-locus mixed model (MLMM) for non-corrected and corrected (using days to flowering as covariate) grain yield in 2013 water-deficit stress (WD) conditions (**Panel A**). Significant SNPs in the Manhattan plot of MLMM are numbered according to the order in which they were included as a cofactor in regression model. Identified LD block (17 kb) based on r^2 value between SNPs on chromosome 4 and the colour intensity of the box on the LD plot corresponds with r^2 (multiplied by 100) according to legend (**Panel B**). Significant SNP/SNPs marked in yellow rectangle was detected by CMLM and MLMM and in red rectangle only by CMLM approach.

Table 3: GWAS results for final set of genetic loci detected for grain yield in non-stress and water-deficit stress conditions during 2013 and 2014. Detailed GWAS results for yield components and related traits across treatments and years are given in Supplementary Tables S3-S6 and Supplementary Table S8.

Trt ^a	Year	Locus	SNP pos ^b	Chr ^c	Allele	MAF ^d	P-CMLM ^e	P-MLMM ^f	AE ^g	LD block ^h	Start	End	Size (kb)	Genes ⁱ
Non-stress	2013	Q1	10101900	11	C:G	0.336	2.72E-05	-	30.13	10101900	10173685	71	2	
		Q2	30523925	2	G:A	0.070	-	5.78E-08	-175.90	30397910	30541202	143	16	
		Q3	13199901	12	C:T	0.468	6.84E-05	-	30.04	12917853	13298195	380	8	
	2014	Q4	26796595	3 [*]	C:T	0.097	9.91E-05	2.20E-06	-46.18	26756997	26978105	221	9	
		Q5	29142398	2 [#]	C:A	0.179	-	4.19E-05	13.98	29122557	29261158	138	9	
		Q6	19367031	10 [#]	T:G	0.466	-	1.75E-06	74.08	19280939	19474522	193	21	
		Q7	5105627	12 [#]	A:C	0.078	-	3.03E-05	-186.24	5101105	5390949	289	12	
		Q8	42643337	1 [#]	A:G	0.347	-	6.58E-05	-97.80	42587683	42643699	56	9	
Water-deficit	2013	Q9 [†]	34815277	4	C:T	0.074	1.17E-05	1.77E-06	-81.29	34815277	34833179	17	5	
		-	-	-	-	-	-	-	-	-	-	-	-	
		Q10 [‡]	5113428	3 [*]	T:C	0.424	3.55E-05	5.17E-06	-40.61	5021158	5167439.00	146	13	
	2014	Q11	6934188	3 [*]	A:G	0.397	8.26E-05	8.73E-06	31.47	6908684	7020707	112	7	
		Q12	42144827	1 [#]	T:C	0.366	-	1.86E-07	6.10	42123552	42144993	21	2	
		Q13	16038003	10 [#]	T:C	0.358	-	5.46E-06	-49.86	16024382	16110372	85	6	
		Q14	23005301	11 [#]	G:A	0.276	-	1.12E-05	-23.54	22976390	23005386	28	0	
		Q15	27115652	11 [#]	G:A	0.075	-	4.92E-05	33.65	27115609	27123090	7	1	

a = Treatment; **b** = Single nucleotide polymorphism (SNP) position; **c** = Chromosome; **d** = minor allele frequency (MAF); **e** = *P*-value of single-locus compressed mixed linear model (CMLM); **f** = *P* value of multi-locus mixed model (MLMM); **g** = Allelic effect with respect to minor allele=(average traits value of genotypes carrying minor allele-average traits value of genotypes carrying major allele); **h** = linkage disequilibrium block; **i** = total number of known characterised genes in LD block. † = genetic locus detected for non-corrected and corrected grain yield value; ‡ = genetic locus detected for corrected grain yield value and coincided with days to flowering; * = genetic locus detected through CMLM and MLMM methods; # = genetic locus detected through MLMM only. All the unmarked loci are detected through CMLM method. The bold italic *P* value for corrected grain yield value.

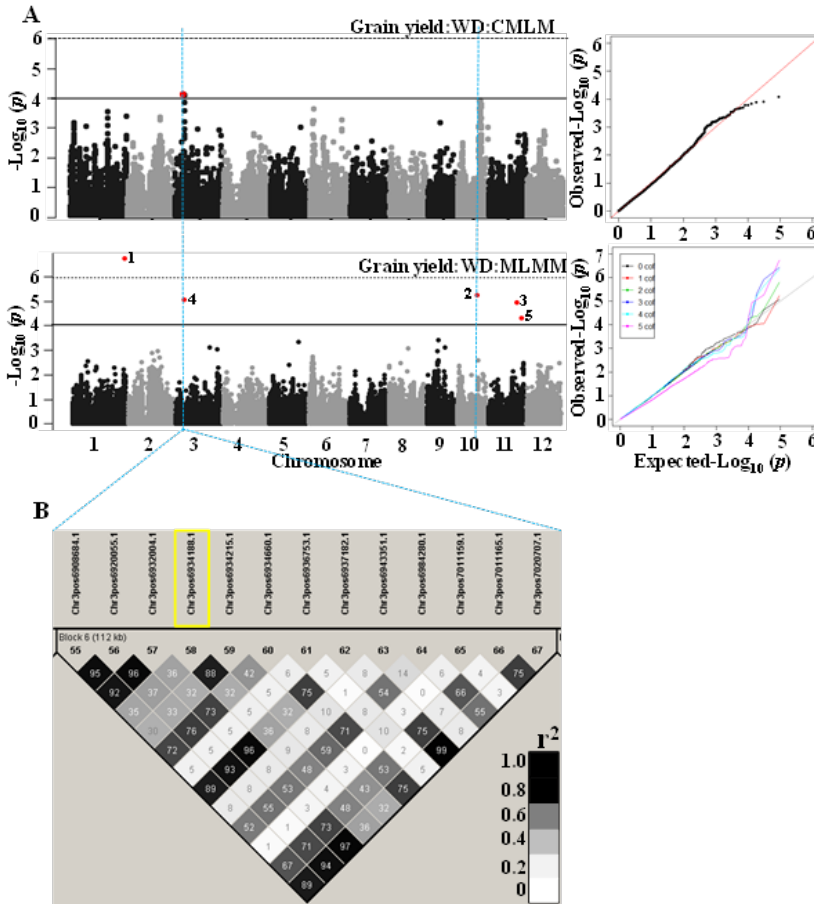


Figure 5: GWAS results (Manhattan and Quantile-Quantile plot) detected through single-locus compressed mixed linear model (CMLM) and multi-locus mixed model (MLMM) for grain yield in 2014 water-deficit stress (WD) conditions (**Panel A**). Significant SNPs on the Manhattan plot of MLMM are numbered according to the order in which they included as a cofactor in regression model. Identified LD block (112 kb) based on r^2 value between SNPs on chromosome 3 and the colour intensity of the box on the LD plot corresponds with r^2 (multiplied by 100) according to the legend (**Panel B**). Significant SNP marked in yellow rectangle was detected by CMLM and MLMM.

per se, which were directly or indirectly contributing to rice grain yield. The colocalization of grain yield loci with yield components was limited in this study compared to other studies in rice (Lanceras et al., 2004). This could be due to compensation among the yield components. In addition, these results emphasize the need for genetic analysis of yield components to identify additional genetic determinants having indirect effect on grain yield, providing alternative routes to enhance yield under water-deficit.

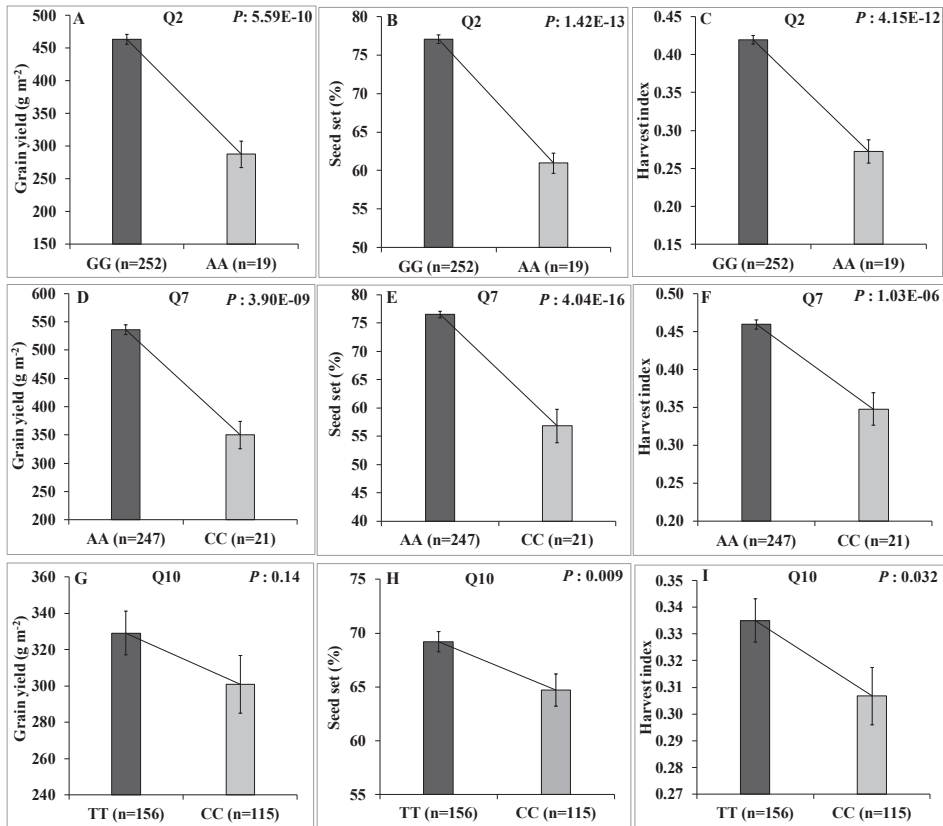


Figure 6: Allelic effect of Q2 (**Panels A-C**; 2013), Q7 (**Panels D-F**; 2014) in non-stress and Q10 (**Panels G-I**; 2013) in water-deficit stress conditions on grain yield, seed set and harvest index. Allelic effect of Q7 on harvest index was significant regardless of GWAS significance. Two sample t-test P value showing significant allelic effect difference regarding major and minor allele.

Except for one locus on chromosome 12 for spikelets per m^2 in 2014, majority of the loci for grain yield and its component traits were specific to non-stress or stress conditions in both years. These results are in agreement with previous studies in rice (Lanceras et al., 2004; Vikram et al., 2011; Kumar et al., 2014) and other crop species (Yin et al., 2002; Millet et al., 2016). Hence, the greater dependence on environments appeared to be a common characteristic of QTLs, although this does not negate their importance in marker-assisted selection (MAS). Despite the strong variation in weather, we also detected four consistent loci: one each for panicles per m^2 and spikelets per panicle on chromosome 10 (19,903,199) and 4 (23,423,399) respectively, and two loci on chromosome 2 (30,699,332) and 5 (53,664,89) for thousand grain weight across years in non-stress conditions (Supplementary Table S7). These consistent

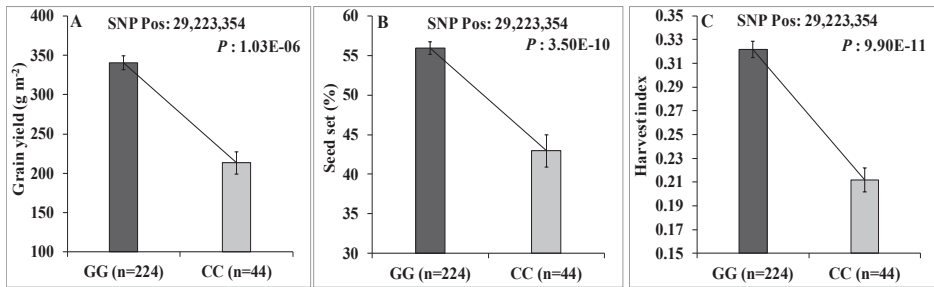


Figure 7: Allelic effect of chromosome 1 locus (29,223,354) on grain yield (**Panel A**), seed set (**Panel B**), and harvest index (**Panel C**) in 2014 water-deficit stress conditions. Allelic effect on grain yield was significant regardless of GWAS significance. Two sample t-test *P* value showing significant allelic effect difference regarding major and minor allele.

regions with favourable alleles could be used for improving yield.

The PRAY population have been previously used in GWAS for a range of phenotypic traits (Qiu et al., 2016; Al-Tamimi et al., 2016; Rebolledo et al., 2016; Kikuchi et al., 2017; Kadam et al., 2017). When comparing our results with those of these previous studies, we could not find any overlap between significant markers, except for plant height for which we detected a SNP marker (position: 38286772) that was also detected in our previous study (Kadam et al. 2017). The most likely reasons for such variation in results are the difference in target phenotypic traits, type and timing of stress treatments, population size, and genotypic marker data used by previous studies. Further, there was also no overlap of significant marker for grain yield and its components when comparing to other studies conducted under reproductive stage water-deficit for similar traits using different mapping panels (Ma et al., 2016; Pantalião et al., 2016; Swamy et al., 2017). The major reasons for this may be different rice accessions, population size and inherent environmental and field variation for stress treatment. Another possible reason could be use of indica subspecies genotypes in this study while previous studies either used japonica subspecies (Pantalião et al., 2016) or small population size (75 genotypes) with SSR markers for mapping (Swamy et al., 2017). In addition, it can be expected that the genomic regions/genes determining the trait difference across subspecies/genotypes could be difficult to identify.

Seed set regulates the assimilate partitioning and grain yield

Better optimisation of assimilate partitioning to reproductive organs with minimal competition among reproductive organs is essential to achieve stable and higher grain yield. So far, the physiological and genetic basis of above processes has been poorly understood in rice and other

cereal crops. Our study showed that the co-localisation of grain yield loci with its components was rare. However, four genetic loci namely Q2, Q7 in non-stress, Q10 and 29,223,354 (SNP position) in stress conditions were regulating the grain yield and harvest index through changes in the seed set (Figs. 6-7). This indicates that the seed set is a critical determinant of assimilate partitioning (harvest index), thereby regulating the final expression of grain yield. A recent GWAS analysis confirmed these interactions in wheat (Guo et al., 2017). Hence, these identified loci could be pyramided into an “ideotype” at genomic level through MAS to enhance rice grain yield in non-stress and stress conditions. In addition, such loci could also be interesting in identifying the physiological and molecular basis of assimilates partitioning to reproductive organs.

Promising *a priori* candidate genes for grain yield and water-deficit stress resilience

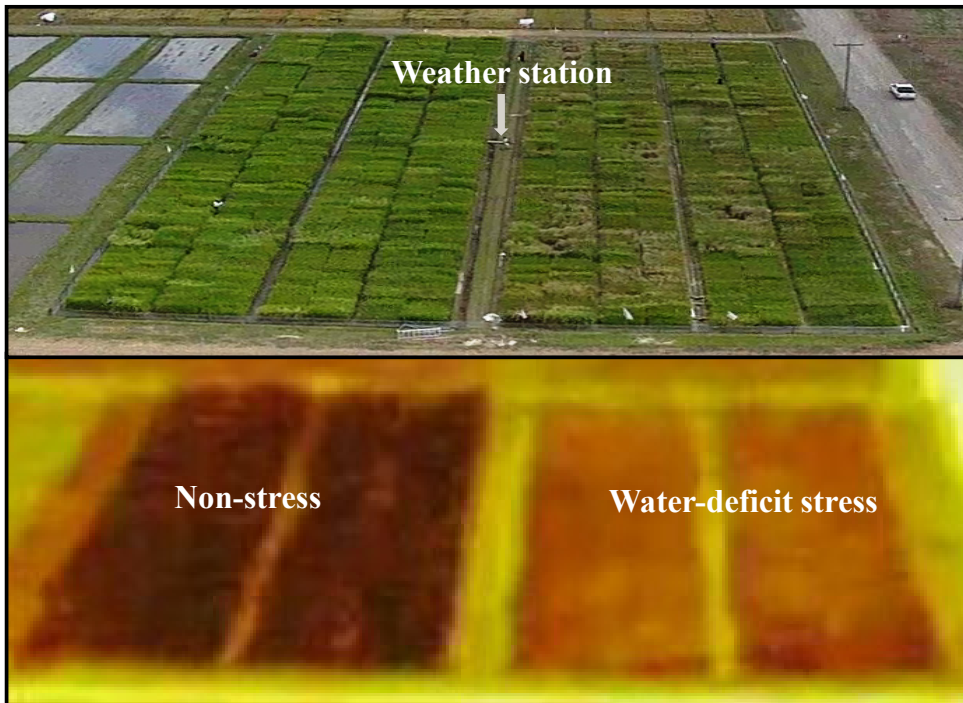
We detected *a priori* candidate genes near of peak SNP/SNPs within the LD block for grain yield loci (Supplementary Table S9). *A priori* candidate genes of grain yield loci can indicate possible roles of underlying physiological (SET kinase, sugar and nitrate transporter genes) and reproductive developmental (Plastocyanin gene) processes in regulating the grain yield. Likewise, the abiotic stress tolerance candidate genes were detected near to grain yield loci in water-deficit, of which genes regulating the detoxification of ROS (Phosphomannomutase and Squalene epoxidase genes) seem to be critical in rice stress tolerance (Pyngrope et al., 2013; Selote and Chopra, 2004). In addition, these candidate genes need to be considered to detect the most likely causal genes. However, detailed large-scale molecular validations need to be conducted using the available approaches of RNAi, knockout mutants and transgenic overexpression. Similarly, the loci for components and related traits that were not co-localised with grain yield *per se*, could also be an interesting candidate for further identification of novel genes.

Concluding remarks

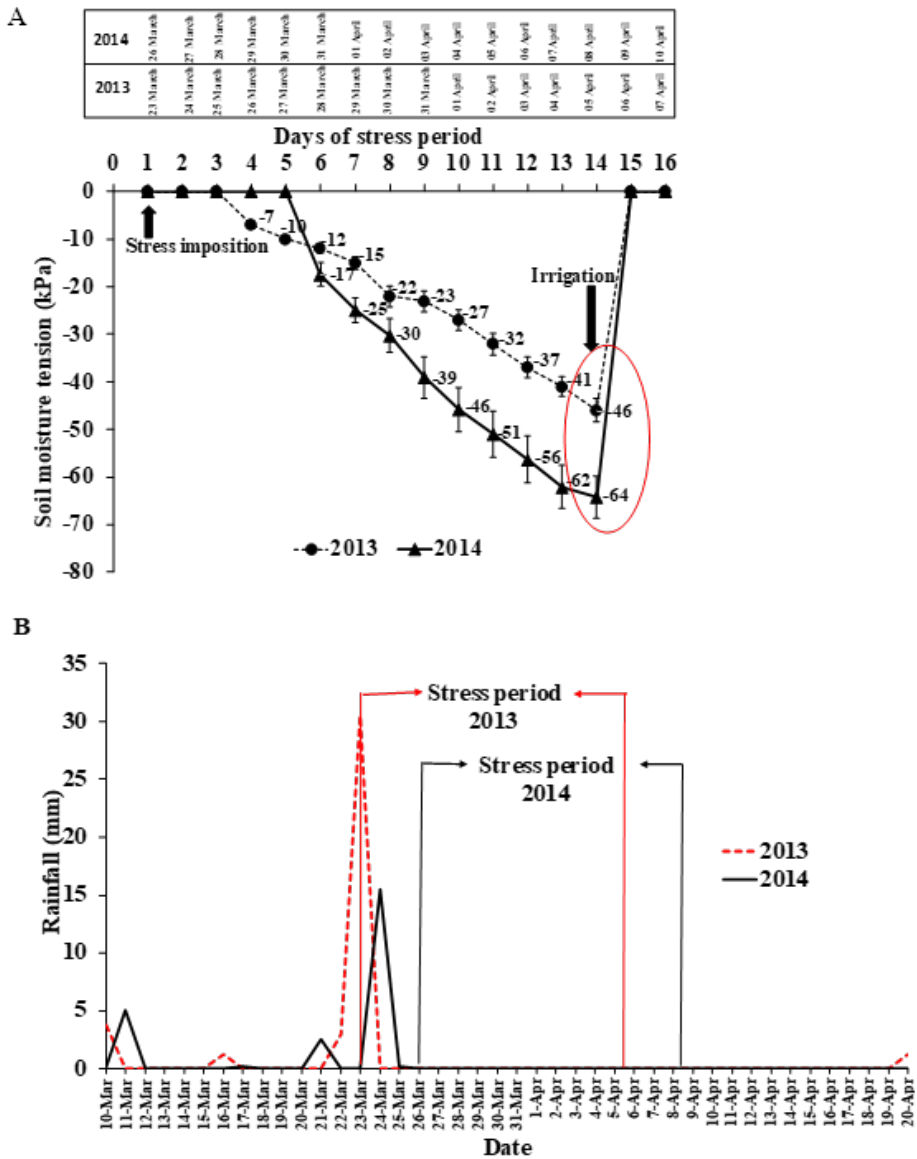
This study provides the genetic basis of grain yield of rice, its components and related traits in non-stress and stress conditions in field phenotyping experiments. We detected several favourable alleles regulating these traits that, upon validation, can be effectively used in improving grain yield. Additional genetic loci with limited overlap of yield component traits to grain yield *per se* clearly indicate the independent genetic architectures of these traits. Thus, many loci for component traits had an indirect effect on yield, which cannot be detected while

mapping yield directly. This indicates the complexity of yield as a trait despite moderate to high h^2 which is most often used as a selection criterion to improve yield potential and stress tolerance. Hence, future studies should also explore the genetic basis of individual component traits that are genetically less complex—an approach expected to give additional useful information to further enhance yield. Present study suggest that maintenance of higher seed set is a vital component for enhancing yield potential and water-deficit tolerance.

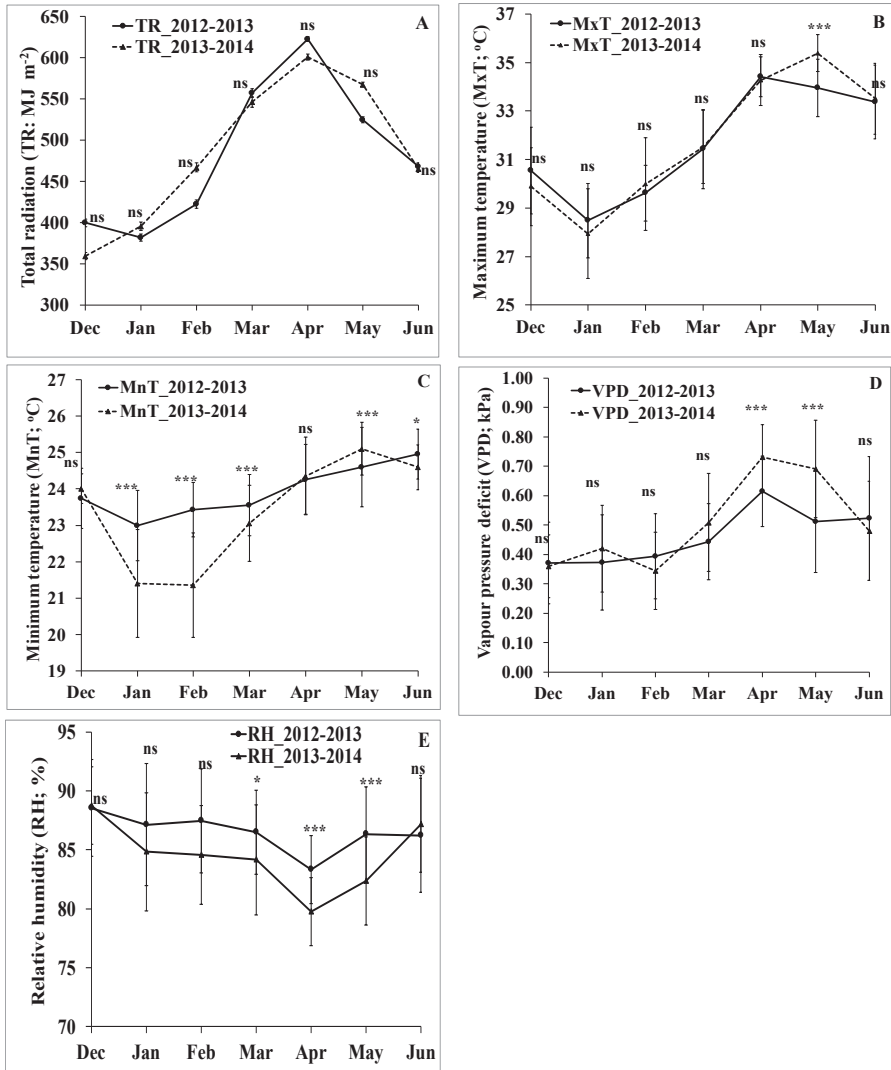
Supplementary information in Chapter 4



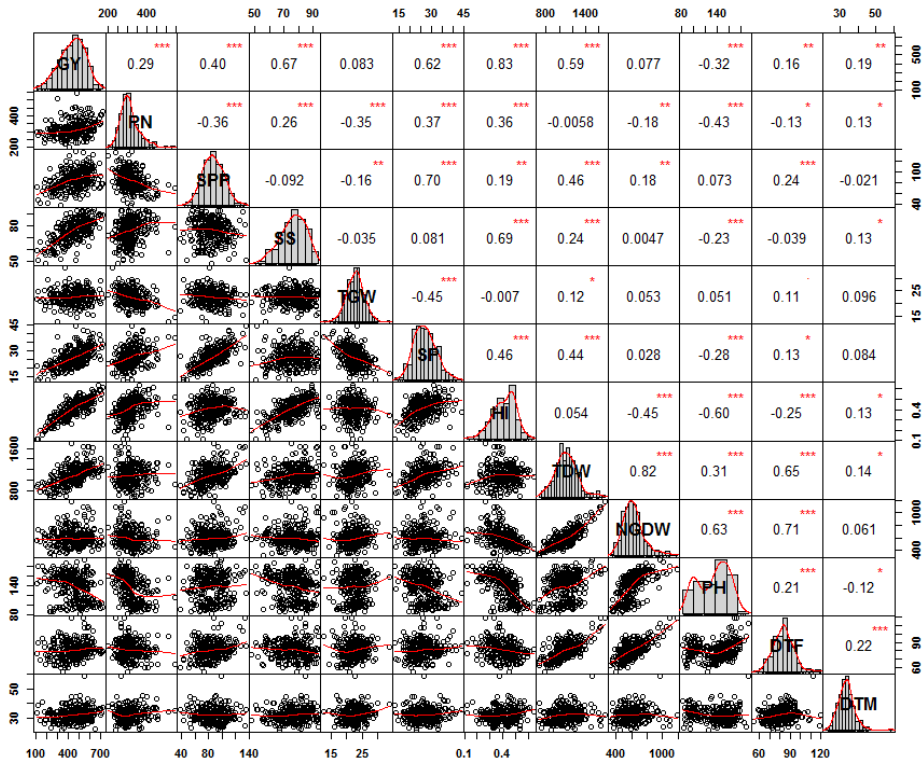
Supplementary Figure S1: Field set-up of 296 genotypes screened under non-stress and reproductive stage water-deficit stress in 2013 and 2014 experiments. Aerial picture of experiment plot taken in 2014 and lower panel was the thermal image taken during stress period showing canopy temperature difference in non-stress and water-deficit stress conditions.



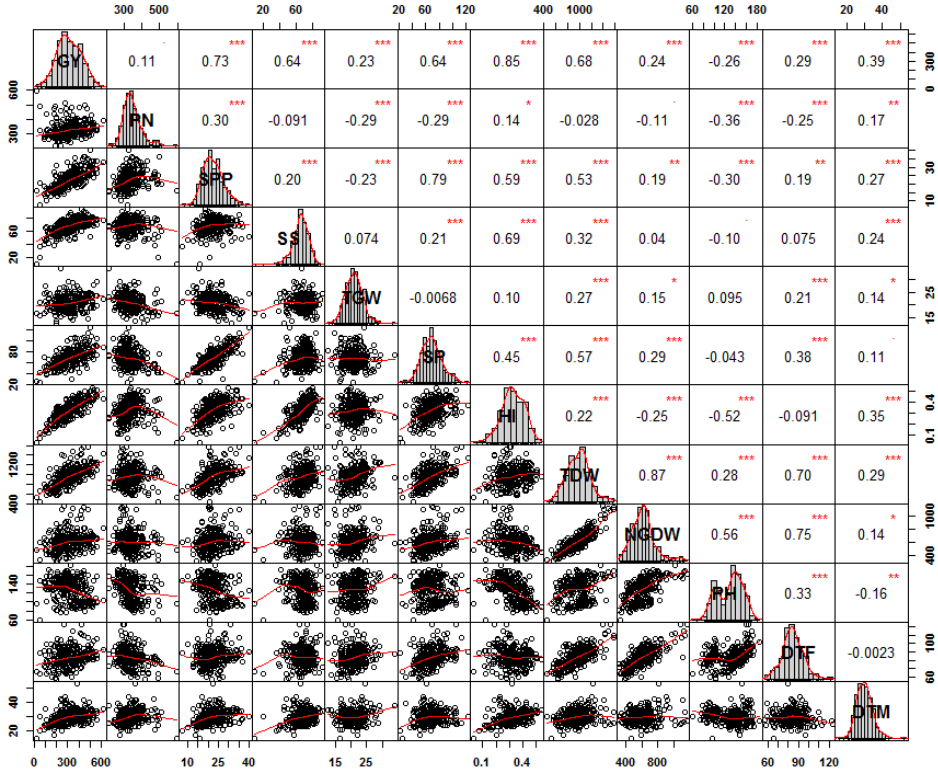
Supplementary Figure S2: Soil moisture tension measured using tensiometers in water-deficit stress field during 2013 and 2014 (**Panel A**), and rainfall pattern measured during stress period in 2013 and 2014 (**Panel B**). Soil moisture was measured using the 26 tensiometers randomly placed in the stress field at 30 cm depth and numbers above the symbols in Fig. 2A are the average soil moisture tension from 26 tensiometers.



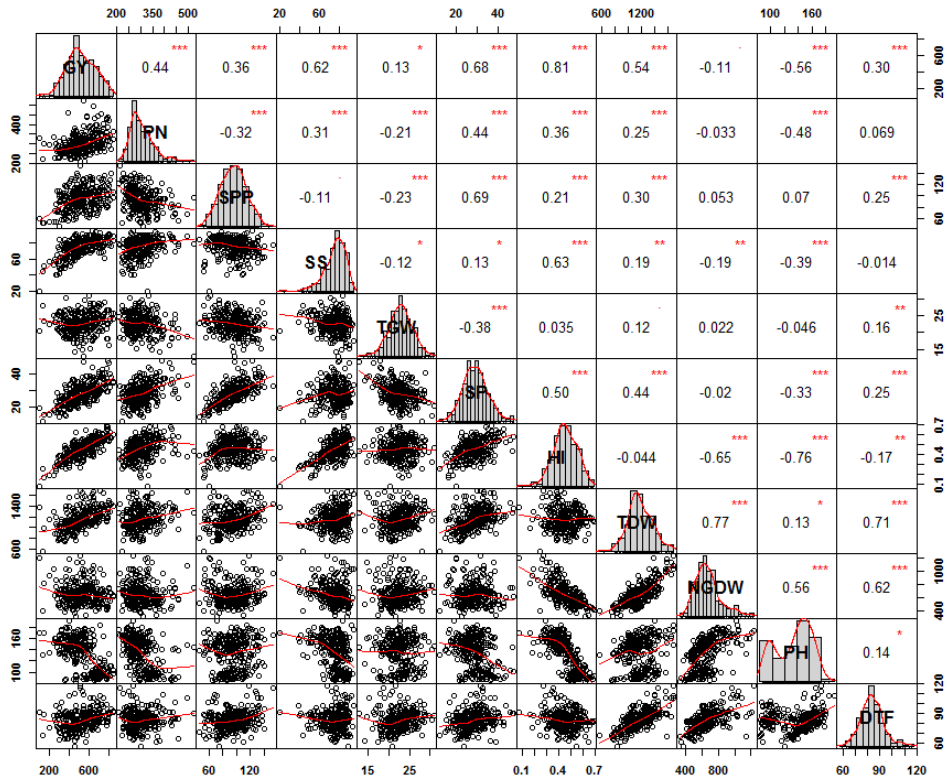
Supplementary Figure S3: Climate parameters observed during the growing period: Total radiation (**Panel A**), maximum temperature (**Panel B**), minimum temperature (**Panel C**), vapour pressure deficit (**Panel D**) and relative humidity (**Panel E**). Bar represent standard deviation. Paired t-test *P* value is used to compare the monthly climate difference across years with significance level of **P*<0.05, ***P*<0.01, ****P*<0.001, and ns = non-significant.



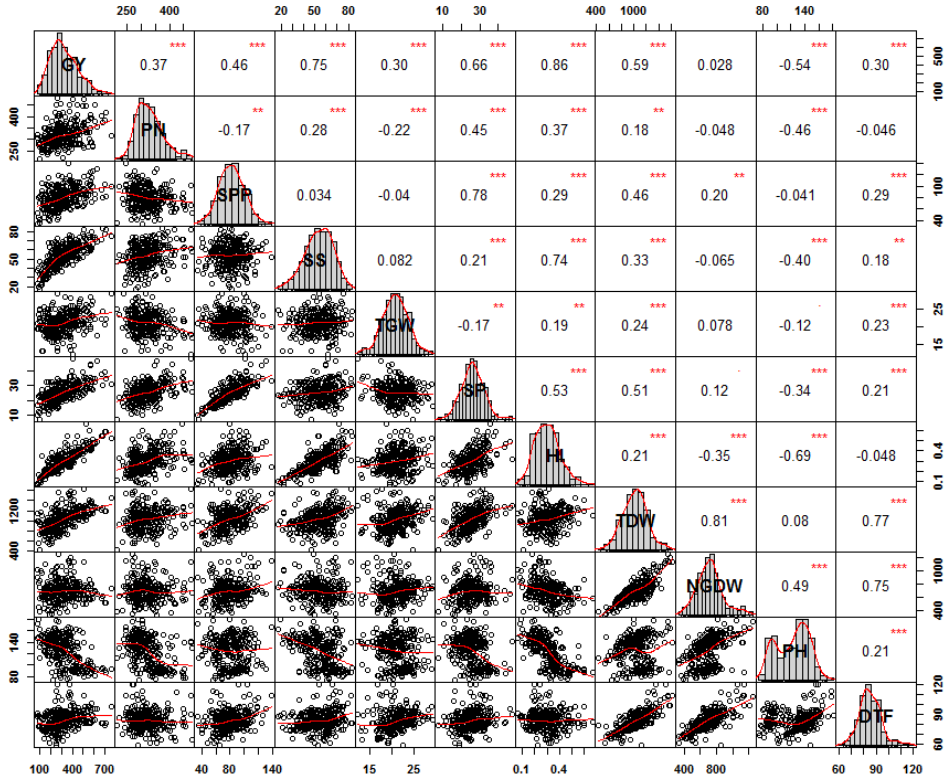
Supplementary Figure S4: Pearson correlation coefficient between grain yield and its components and related traits in 2013 non-stress conditions. Phenotypic traits with their histograms are given in the diagonal panel. Lower diagonal panel represents the scatter plot with red line depicting the best fit. The upper panel represents the Pearson correlation coefficient value and size of the correlation coefficient is proportional to the strength of the correlation. The correlation coefficient significance level: * $P < 0.05$, ** $P < 0.01$, *** $P < 0.001$. GY=grain yield; PN=panicles per m^2 ; SPP=spikelets per panicle; SS=seed set; TGW=thousand grain weight; SP=spikelets per m^2 ; HI=harvest index; TDW=total dry weight; NGDW=non-grain dry weight; PH=plant height; DTF= days to flowering; DTM=days to maturity.



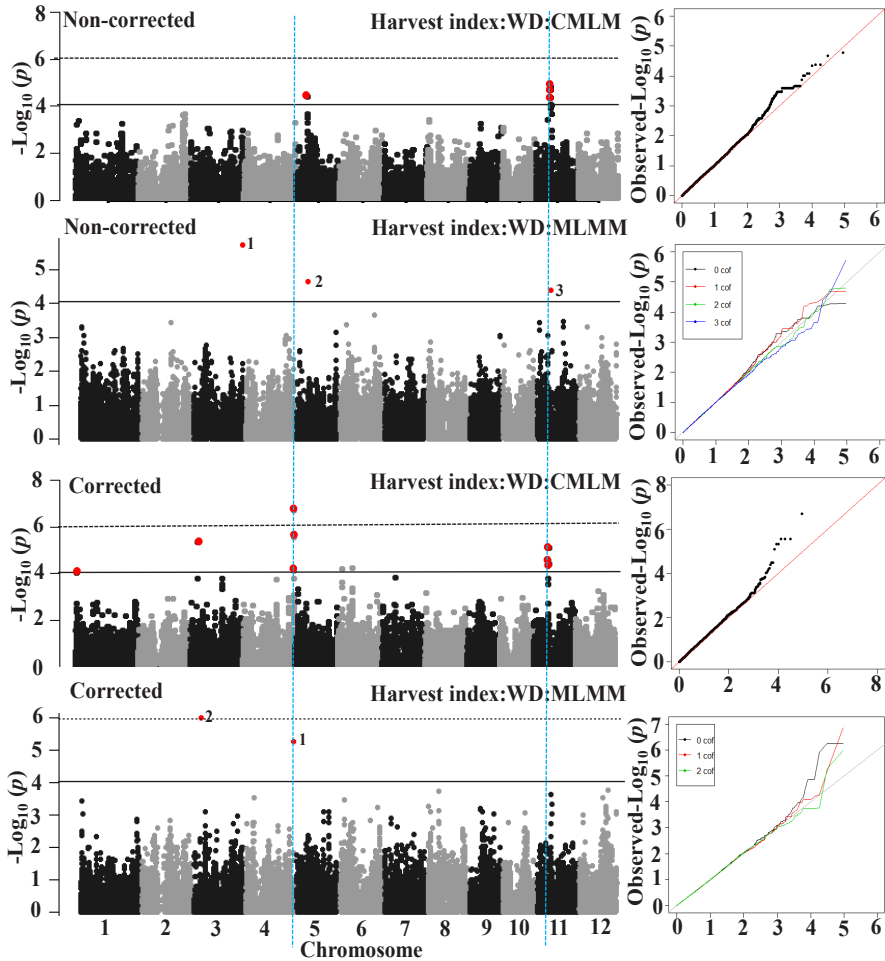
Supplementary Figure S5: Pearson correlation coefficient between grain yield and its components and related traits in 2013 water-deficit stress conditions. Phenotypic traits with their histograms are given in the diagonal panel. Lower diagonal panel represents the scatter plot with red line depicting the best fit. The upper panel represents the Pearson correlation coefficient value and size of the correlation coefficient is proportional to the strength of the correlation. The correlation coefficient significance level: * $P < 0.05$, ** $P < 0.01$, *** $P < 0.001$. GY=grain yield; PN=panicles per m²; SPP=spikelets per panicle; SS=seed set; TGW=thousand grain weight; SP=spikelets per m²; HI=harvest index; TDW=total dry weight; NGDW=non-grain dry weight; PH=plant height; DTF= days to flowering; DTM=days to maturity.



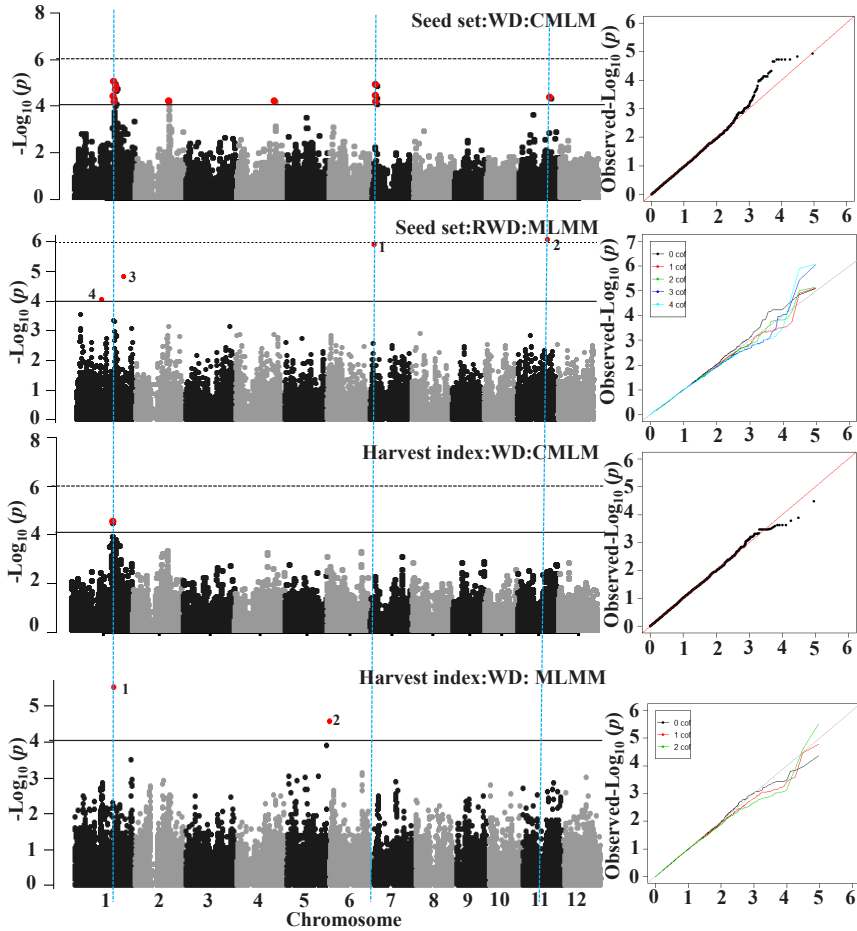
Supplementary Figure S6: Pearson correlation coefficient between grain yield and its components and related traits in 2014 non-stress conditions. Phenotypic traits with their histograms are given in the diagonal panel. Lower diagonal panel represents the scatter plot with the red line depicting the best fit. The upper panel represents the Pearson correlation coefficient value and size of the correlation coefficient is proportional to the strength of the correlation. The correlation coefficient significance level: * $P < 0.05$, ** $P < 0.01$, *** $P < 0.001$. GY=grain yield; PN=panicles per m²; SPP=spikelets per panicle; SS=seed set; TGW=thousand grain weight; SP=spikelets per m²; HI=harvest index; TDW=total dry weight; NGDW=non-grain dry weight; PH=plant height; DTF= days to flowering.



Supplementary Figure S7: Pearson correlation coefficient between grain yield and its components and related traits in 2014 water-deficit stress conditions. Phenotypic traits with their histograms are given in the diagonal panel. Lower diagonal panel represents the scatter plot with the red line depicting the best fit. The upper panel represents the Pearson correlation coefficient value and size of the correlation coefficient is proportional to the strength of the correlation. The correlation coefficient significance level: * $P < 0.05$, ** $P < 0.01$, *** $P < 0.001$. GY=grain yield; PN=panicles per m²; SPP=spikelets per panicle; SS=seed set; TGW=thousand grain weight; SP=spikelets per m²; HI=harvest index; TDW=total dry weight; NGDW=non-grain dry weight; PH=plant height; DTF= days to flowering.



Supplementary Figure S8: GWAS results (Manhattan and Quantile-Quantile plot) detected through single-locus compressed mixed linear model (CMLM) and multi-locus mixed model (MLMM) for non-corrected and corrected harvest index (using days to flowering as a covariate) in 2013 water-deficit stress (WD) conditions. Significant SNPs in Manhattan plot of MLMM were numbered according to order in which they were included as a cofactor in regression model.



Supplementary Figure S9: GWAS results (Manhattan and Quantile-Quantile plot) detected through single-locus compressed mixed linear model (CMLM) and multi-locus mixed model (MLMM) for seed-set and harvest index in 2014 water-deficit stress (WD) conditions. Significant SNPs in Manhattan plot of MLMM were numbered according to order in which they were included as a cofactor in regression model.

Supplementary Table S1: Summary statistics of grain yield and its components and related traits in 2013 and 2014 non-stress (NS) and water-deficit stress (WD) conditions.

Trait	Trt	2013					2014				
		M±SD	Min	Max	H ²	h ²	M±SD	Min	Max	H ²	h ²
GY	NS	451.1±123.2	106.3	727.0	0.92	0.27	521.9±143.3	102.8	839.7	0.93	0.75
	WD	317.3±112.9	16.7	622.6	0.84	0.64	319.5±134.3	78.1	761.1	0.73	0.73
Grain yield component traits											
PN	NS	316.8±56.7	200.8	540.8	0.82	0.88	302.7±51.7	212.0	520.3	0.89	0.92
	WD	340.4±69.5	219.2	593.6	0.87	0.87	321.0±50.0	215.1	479.2	0.80	0.90
SPP	NS	84.9±17.6	37.8	136.3	0.79	0.92	95.1±20.0	46.4	153.2	0.89	0.90
	WD	68.3±16.0	22.8	122.9	0.77	0.77	80.4±18.3	34.0	139.3	0.70	0.92
SS	NS	76.0±9.6	47.7	93.7	0.85	0.65	75.0±11.3	19.7	94.9	0.89	0.75
	WD	67.3±10.5	10.4	91.8	0.73	0.83	53.8±13.0	17.2	83.3	0.62	0.72
TGW	NS	22.5±2.9	12.5	34.0	0.99	0.86	22.6±3.0	12.9	30.9	0.99	0.88
	WD	20.9±3.0	12.6	34.1	0.97	0.85	21.1±3.4	12.3	29.1	0.77	0.90
SP	NS	26.3±5.4	13.1	43.8	0.88	0.88	28.4±6.2	11.7	47.8	0.91	0.92
	WD	22.5±5.3	7.3	40.1	0.85	0.84	25.5±6.3	7.6	47.7	0.83	0.93
Grain yield related traits											
HI	NS	0.4±0.09	0.1	0.6	0.93	0.44	0.4±0.1	0.08	0.7	0.95	0.90
	WD	0.3±0.09	0.03	0.5	0.83	0.63	0.3±0.1	0.07	0.7	0.66	0.69
TDW	NS	1.1±0.1	0.7	1.7	0.87	0.80	1.1±0.2	0.5	1.7	0.89	0.80
	WD	0.9±0.2	0.4	1.5	0.90	0.87	1.0±0.2	0.4	1.6	0.86	0.83
NGDW	NS	0.6±0.1	0.3	1.1	0.93	0.94	0.6±0.1	0.3	1.2	0.92	0.90
	WD	0.6±0.1	0.3	1.1	0.92	0.90	0.7±0.1	0.3	1.2	0.89	0.89
PH	NS	136.6±27.6	81.8	193.9	0.98	0.88	135.2±27.8	84.3	191.4	0.98	0.86
	WD	128.1±25.6	59.7	184.1	0.97	0.90	125.0±27.0	74.0	280.1	0.90	0.86
DTF	NS	81.0±10.4	54.7	119.7	0.98	0.88	83.3±9.8	57.3	117.7	0.99	0.91
	WD	83.8±10.8	57.3	123.3	0.99	0.88	84.4±9.9	59.7	120.3	0.96	0.90
DTM	NS	32.3±4.7	21.7	59.0	0.84	0.31	-	-	-	-	-
	WD	29.7±4.7	14.8	53.0	0.86	0.47	-	-	-	-	-

Trt= treatment; M±SD= mean and standard deviation; Min= minimum; Max= maximum; H²= broad-sense heritability; h²= narrow-sense heritability. GY=grain yield; PN=panicles per m²; SPP=spikelets per panicle; SS=seed set; TGW=thousand grain weight; SP=spikelets per m²; HI=harvest index; TDW=total dry weight; NGDW=non-grain dry weight; PH=plant height; DTF= days to flowering; DTM=days to maturity. Data for days to maturity was not available for 2014 experiment.

Supplementary Table S2: Multiple linear regression of grain yield with its components and related traits in non-stress and water-deficit stress conditions during 2013 and 2014. Note that spikelets per m², harvest index and total dry weight were not included in the regression because spikelets per m² is the product of panicles and spikelets per panicles, and not an independent component. Similarly harvest index is the ratio of grain yield to total dry weight. Total dry weight is the sum of non-grain dry weight and grain dry weight.

Year	Treatment	Traits	P-value	R²
2013	Non-stress	Panicles	<0.001	0.89
		Spikelets per panicle	<0.001	
		Seed set	<0.001	
		Thousand grain weight	<0.001	
		Plant height	0.069	
		Days to flowering	0.055	
	Water-deficit	Panicles	<0.001	0.88
		Spikelets per panicle	<0.001	
		Seed set	<0.001	
		Thousand grain weight	<0.001	
		Plant height	<0.001	
		Days to flowering	<0.001	
2014	Non-stress	Panicles	<0.001	0.94
		Spikelets	<0.001	
		Seed set	<0.001	
		Thousand grain weight	<0.001	
		Plant height	<0.001	
		Days to flowering	<0.01	
	Water-deficit	Panicles	<0.001	0.93
		Spikelets per panicle	<0.001	
		Seed set	<0.001	
		Thousand grain weight	<0.001	
		Plant height	<0.001	
		Days to flowering	0.404	

Supplementary Table S3. The details of genetic loci detected for grain yield components and related traits in 2013 non-stress conditions using compressed mixed linear-model (CMLM) and multi-locus mixed model (MLMM) methods. The chromosome loci detected through both the methods were marked by asterisk sign (*); those detected through only by MLMM were marked by hashtag (#) sign. The remaining all unmarked chromosome loci were detected only through CMLM method. Trait acronyms are given in Table 1.

Traits	Chr	Pos	Allele	MAF	P value _{CMLM}	P value _{MLMM}	AE	LD block		Size(kb)	Known genes
								Start	End		
Grain yield component											
PN	4	2481502	T:A	0.100	4.11E-05	-	28.53	2463707	2502477	38	2
	12	1691509	C:G	0.066	4.69E-05	-	27.81	1594015	1691770	97	12
	6	9369614	C:A	0.059	7.89E-05	-	32.90	9329842	9371867	42	4
	12	1691771	C:T	0.068	8.33E-05	-	26.60	1691771	1734838	43	7
	4	23514625	A:C	0.118	9.81E-05	-	24.72	23514625	23597658	83	3
	10 [#]	19903199	T:A	0.148	-	8.47E-19	51.58	19882559	19916740	34	3
SPP	4 [*]	23423399	A:G	0.288	4.70E-06	1.23E-07	-7.15	23423240	23512064	88	11
	11 [*]	19641458	C:T	0.391	5.47E-05	1.20E-05	-5.13	19609894	19645174	35	4
	4	23417928	C:G	0.256	6.95E-05	-	-6.31	23357356	23417928	60	5
	3 [#]	15094434	G:A	0.236	5.31E-06	-	9.21	14873722	15132484	258	17
	2 [#]	24278919	G:C	0.332	2.13E-05	-	9.09	24265692	24283607	17	4
SS	2 [*]	30523925	G:A	0.072	3.85E-05	5.56E-07	-7.55	30397910	30541202	143	16
	10 [#]	18906753	G:C	0.303	-	1.76E-05	6.50	18898657	19018639	119	14
	2 [#]	17591863	T:C	0.491	-	7.03E-05	-5.18	17591863	17806312	214	3
TGW	2	308723	A:T	0.458	5.35E-05	-	-0.73	221193	338309	117	8
	5 [*]	5366489	G:A	0.387	5.45E-05	1.79E-05	0.82	5365520	5448285	82	6
	2 [*]	30699332	T:C	0.295	7.75E-05	1.94E-05	0.81	30684655	30784063	99	9
SP	7 [*]	22699138	T:C	0.185	3.18E-05	2.06E-05	2.04	22653977	22805994	152	12
Grain yield related traits											
HI	8	20255596	G:T	0.063	5.45E-06	-	-0.06	20221039	20450490	229	12
	2 [*]	30523925	G:A	0.072	7.68E-06	3.29E-10	-0.07	30397910	30541202	143	16
	8	20221030	G:A	0.068	1.12E-05	-	-0.05	20165675	20221035	55	5
	8	20160760	A:T	0.066	1.23E-05	-	-0.06	20144631	20165644	21	1
	10	2163454	C:T	0.493	7.00E-05	-	-0.02	2151405	2181552	30	1
	7 [#]	17712506	T:C	0.240	2.79E-05	-	-0.05	17539335	17785193	245	7
	TDW	4	21345052	G:C	0.063	1.84E-05	-	90.75	21337500	21360699	23
5		26477176	A:G	0.063	9.24E-05	-	83.90	26473392	26847502	374	41
4 [#]		34815309	G:A	0.055	3.11E-05	-	-209.0	34815277	34833179	17	5
NGDW	2 [*]	945729	A:T	0.225	1.14E-05	5.10E-07	43.23	944109	972602	28	4
	10	19874918	C:T	0.232	9.57E-05	-	36.54	19874875	19874918	44bp	0
	12 [#]	24162384	G:C	0.306	2.18E-08	-	83.60	24070904	24389670	318	17
PH	1 [*]	38286772	G:A	0.292	2.75E-07	9.46E-08	-12.37	38178239	38437530	259	29
	1	34203951	T:A	0.454	9.80E-05	-	5.99	34184887	34357192	172	6
DTF	3	21686259	T:C	0.185	5.26E-05	-	2.92	21660582	21686259	25	4
	3	21686358	T:C	0.185	5.26E-05	-	2.92	21686358	21944343	257	11
	3 [#]	5113428	T:C	0.424	2.15E-05	-	-2.61	5021158	5167439	146	13
DTM	2 [*]	19163866	T:G	0.093	5.91E-05	2.92E-05	2.08	19151240	19163870	12	1

Chr=chromosome; Pos= physical position of SNP; MAF=minor allele frequency; AE=allelic effect regarding the minor allele (average traits value of genotypes carrying minor allele – average traits value of genotypes carrying major allele). LD= linkage disequilibrium. Known genes= total known genes observed within the LD block.

Supplementary Table S4. The details of genetic loci detected for uncorrected grain yield, its components and related traits in 2013 water-deficit stress conditions using compressed mixed linear-model (CMLM) and multi-locus mixed model (MLMM) methods. The chromosome loci detected through both the methods were marked by asterisk sign (*); those detected through only by MLMM were marked by hashtag (#) sign. The remaining all unmarked chromosome loci were detected only through CMLM method. Trait acronyms are given in Table 1. For legends see the Supplementary Table S3.

Traits	Chr	Pos	Allele	MAF	P value _{CMLM}	P value _{MLMM}	AE	LD block		Size (kb)	known genes
								Start	End		
GY	4*	34815277	C:T	0.074	1.17E-05	1.77E-06	-51.28	34815277	34833179	17	5
	9#	17886901	G:C	0.063	-	2.55E-06	89.60	17886901	18067376	180	15
	8#	1541432	C:T	0.133	-	3.88E-06	-107.75	1541432	15816677	40	5
	3#	8548868	A:G	0.439	-	4.06E-05	16.61	8532555	8673763	141	14
Grain yield component traits											
PN	12*	19257052	G:A	0.052	1.28E-06	1.84E-24	42.98	19188352	19339344	150	3
	4	31801144	C:G	0.066	3.57E-06	-	34.70	31784370	31819723	35	6
	6	27932410	A:G	0.055	3.87E-06	-	42.40	27930905	27935874	4	0
	6	27946105	T:C	0.057	1.48E-05	-	42.73	27939637	27954294	14	0
	2	29554958	G:A	0.114	1.90E-05	-	27.96	29550199	29554298	4	1
	6	29086891	C:T	0.055	2.71E-05	-	35.05	28969471	29138444	169	15
	6	880574	C:T	0.054	5.33E-05	-	38.32	818175	887142	68	9
	12	1691770	A:G	0.092	5.35E-05	-	27.49	1594015	1691770	97	12
	6	27918615	G:C	0.061	7.59E-05	-	38.18	27888568	27924404	35	1
	8	8333808	G:A	0.148	7.94E-05	-	24.50	8259055	8390193	131	7
	2	4668201	A:G	0.472	9.55E-05	-	-16.76	4668201	4711157	47	6
	12#	19121161	A:G	0.052	-	5.19E-18	8.52	19115304	19156989	41	5
SPP	7	22858259	C:T	0.203	6.74E-06	-	5.53	22815780	22877074	61	7
	7	22699138	T:C	0.185	1.35E-05	-	5.59	22653977	22805994	152	12
	4*	23423399	A:G	0.288	1.48E-05	1.66E-06	-5.68	23423240	23512064	88	11
	4	20084244	T:G	0.369	2.24E-05	-	4.17	20042539	20145355	102	8
	7	19654477	T:G	0.055	2.28E-05	-	8.01	19615905	19654863	38	2
	7	22815780	A:G	0.159	3.52E-05	-	5.50	22805994	22827392	21	2
	7	23086735	C:A	0.170	3.94E-05	-	5.11	22927040	23237152	310	26
	1	39831573	C:T	0.135	6.33E-05	-	5.82	39781249	39868654	87	13
	7*	21708194	T:C	0.125	8.61E-05	3.65E-05	5.30	21673763	21761328	87	9
	SS	11	10232787	C:T	0.074	2.34E-05	-	-5.61	10204901	10235132	30
11*		10131031	A:G	0.052	3.51E-05	4.64E-06	-6.15	9838715	10131062	292	3
12*		27244607	G:A	0.055	4.04E-05	3.55E-08	-5.72	27093600	27244607	151	14
11		10329677	C:A	0.055	5.65E-05	-	-6.24	10265286	10341103	75	2
2		31546589	C:G	0.081	6.34E-05	-	-5.03	31397497	31602859	205	23
11#		3111523	G:C	0.328	-	7.33E-06	1.50	2942864	3111772	168	7
3#		35539634	C:T	0.151	-	1.90E-05	-3.00	35509880	35593310	83	8
TGW		2*	10359249	G:C	0.129	4.59E-05	2.03E-05	1.09	10205033	10369901	164
	3#	16725803	G:A	0.439	-	5.12E-05	1.57	16665467	16804385	138	6
Grain yield related traits											
HI	11	10232787	C:T	0.074	1.65E-05	-	-0.04	10204901	10235132	30	2
	5*	7978268	C:T	0.125	4.23E-05	2.32E-05	-0.04	7951244	8096795	145	8
	11	10131062	T:C	0.055	8.42E-05	-	-0.05	9838715	10131062	292	3
	11	10329677	C:A	0.055	8.42E-05	-	-0.05	10265286	10341103	75	2
	11	10627944	A:C	0.074	9.75E-05	-	-0.04	10627944	10863355	235	9
	11*	10392338	C:T	0.074	9.96E-05	4.00E-05	-0.04	10353380	10416332	62	1
	3#	35539634	C:T	0.151	-	1.93E-06	-0.03	35509880	35593310	83	8
TDW	4*	34815277	C:T	0.074	5.84E-05	2.15E-06	-89.16	34815277	34833179	17	5
	11#	16582568	C:T	0.203	-	5.54E-05	34.25	16511087	16623466	112	1
NGDW	1*	18626303	C:G	0.343	9.85E-05	6.28E-05	39.34	18626303	18888393	262	5
	2#	1006437	T:C	0.406	-	1.66E-06	58.94	1006427	1103758	97	15
	12#	24162384	G:C	0.306	-	3.61E-05	97.16	24070904	24389670	318	17
PH	1*	38286772	G:A	0.292	1.24E-07	3.15E-10	-11.76	38178239	38437530	259	29
	1	35548077	C:T	0.197	1.37E-05	-	-8.47	35504716	35595543	90	9
	1	35062897	C:T	0.205	5.86E-05	-	-7.57	35031550	35099986	68	6
	5	1910382	C:T	0.177	9.27E-05	-	5.62	1864314	2107292	242	22
	7#	58252	T:A	0.125	-	2.35E-06	-7.16	19107	134004	114	10
	4#	5806676	C:T	0.210	-	4.71E-05	3.99	5683343	5816801	133	7
DTF	12	1881367	T:A	0.109	5.58E-06	-	-4.63	1753092	1886677	133	18
	3	21670338	T:C	0.280	6.75E-06	-	3.55	21660582	21686259	25	4
	3	21944343	A:G	0.277	1.59E-05	-	3.39	21686358	21944343	257	11
	3	22056925	A:G	0.196	4.83E-05	-	2.99	22056925	22107644	50	2
	3	22164972	A:G	0.255	9.27E-05	-	3.15	22120547	22205824	85	4
	12	1691771	C:T	0.068	7.64E-06	-	-4.90	1691771	1734838	43	7
	12	1691509	C:G	0.066	7.80E-06	-	-4.86	1594015	1691770	97	12
	3*	5113535	G:C	0.310	2.05E-05	9.53E-06	-3.23	5021158	5167439	146	13
	11	23178024	C:T	0.085	2.77E-05	-	4.27	23178024	23183705	5	1
	3	21659472	A:G	0.251	2.99E-05	-	3.40	21315611	21660079	344	20
	1	15153868	C:A	0.175	9.03E-05	-	-3.30	15027451	15169454	142	7

Supplementary Table S5. The details of genetic loci detected for grain yield components and related traits in 2014 non-stress conditions using compressed mixed linear-model (CMLM) and multi-locus mixed model (MLMM) methods. The chromosome loci detected through both the methods were marked by asterisk sign (*); those detected through only by MLMM were marked by hashtag (#) sign. The remaining all unmarked chromosome loci were detected only through CMLM method. Trait acronyms are given in Table 1. For legends see the Supplementary Table S3.

Traits	Chr	Pos	Allele	MAF	P value _{CMLM}	P value _{MLMM}	AE	LD block		Size (kb)	Known genes
								Start	End		
Grain yield component traits											
PN	10	19650831	A:C	0.149	2.05E-06	-	19.35	19474964	19665687	190	14
	10*	19903199	T:A	0.146	2.41E-06	1.16E-06	19.55	19882559	19916740	34	3
	10	19713719	T:G	0.157	6.46E-06	-	17.98	19665880	19778630	112	11
	10	19463253	T:C	0.153	2.08E-05	-	16.79	19280939	19474522	193	21
	10	19107872	A:T	0.175	2.32E-05	-	17.78	19049329	19219240	169	21
	10	19788019	A:G	0.157	4.75E-05	-	16.93	19787326	19827002	39	1
	4*	28829512	G:A	0.101	6.10E-05	8.74E-05	21.71	28701604	29126558	424	31
	8	27367304	C:T	0.175	7.25E-05	-	15.97	27364583	27381695	17	5
3#	30407838	C:G	0.295	-	1.18E-06	14.84	30407838	30499464	91	10	
SPP	4*	23423399	A:G	0.287	2.44E-05	2.41E-05	-7.40	23423240	23512064	88	11
	11*	22233662	G:T	0.104	8.24E-05	5.36E-05	-8.48	22203908	22242728	38	2
SS	6*	1174802	T:C	0.084	8.61E-05	2.64E-08	-4.54	1117344	1208291	90	2
	10	22428992	A:T	0.052	8.77E-05	-	-5.57	22419446	22436125	16	3
	1#	19327482	T:C	0.183	-	1.09E-06	-14.32	19247447	19360189	112	6
	8#	10059172	G:A	0.056	-	1.72E-06	-4.12	9997926	10079318	81	4
	11#	19108095	A:G	0.224	-	1.77E-06	6.09	19075632	19130323	54	4
	12#	5105627	A:C	0.078	-	1.42E-05	-19.68	5101105	5390949	289	12
	2#	4862726	G:A	0.239	-	1.60E-05	-7.84	4774730	4869814	95	15
	4#	21381516	C:A	0.063	-	7.34E-05	2.37	21360906	21381516	20	5
TGW	2	30699332	T:C	0.291	4.21E-05	-	0.90	30684655	30784063	99	9
	2#	10359249	G:C	0.131	-	8.66E-08	2.42	10205033	10369901	164	8
	7#	22413176	C:G	0.396	-	3.01E-14	-1.04	22404388	22606330	201	14
	5#	5366489	G:A	0.388	-	1.32E-06	1.19	5365520	5448285	82	6
	3#	16736753	C:T	0.455	-	4.58E-06	-1.47	16665467	16804385	138	6
	3#	12760491	A:C	0.075	-	1.39E-05	2.38	12717890	12764642	46	5
SP	11*	18102156	A:C	0.295	6.13E-05	1.81E-06	-1.75	18095189	18129687	34	2
	12#	10443628	C:A	0.478	-	1.38E-06	2.26	10320934	10622432	301	10
	4#	4550145	C:T	0.313	-	1.41E-05	-0.47	4521317	4558051	36	1
	11#	22065446	T:C	0.134	-	2.08E-05	-5.65	22065446	22150769	85	3
Grain yield related traits											
HI	10	22419446	A:G	0.056	1.71E-05	-	-0.05	22419446	22436125	16	3
	8	16617975	T:C	0.259	7.73E-05	-	-0.02	16611066	16619402	8	3
	1*	42643328	G:A	0.272	9.78E-05	3.36E-06	-0.02	42627969	42643337	15	3
	8#	16324317	A:T	0.097	-	2.04E-06	-0.10	16308107	16398979	90	5
TDW	2*	945729	A:T	0.224	4.92E-05	1.29E-06	63.09	944109	972602	28	4
	4#	30764890	A:G	0.354	-	2.59E-08	-3.62	30690751	30790417	99	7
	1#	143282	G:A	0.116	-	2.40E-05	20.85	19837	197790	177	16
	3#	33546549	C:A	0.291	-	4.08E-05	-40.90	33518876	33569432	50	5
NGDW	5*	21385305	C:T	0.090	1.37E-05	9.65E-05	76.41	21312370	21385305	72	4
	1*	42363099	C:T	0.101	1.37E-05	2.92E-05	73.35	42326848	42367533	40	3
	11	10867613	C:T	0.153	6.24E-05	-	58.86	10834263	10928827	94	3
	3	34032565	A:G	0.246	6.71E-05	-	-48.68	34004938	34069043	64	5
	7#	21850303	C:T	0.437	-	2.59E-05	100.45	21814261	21908474	94	13
PH	1*	38286772	G:A	0.291	6.03E-09	2.57E-14	-13.34	38178239	38437530	259	29
	1	34280616	G:A	0.455	9.54E-06	-	6.22	34184887	34357192	172	6
	1	35548077	C:T	0.196	2.51E-05	-	-8.04	35504716	35595543	90	9
	1	35062897	C:T	0.203	2.93E-05	-	-7.80	35031550	35099986	68	6
	1	33059505	T:A	0.332	4.31E-05	-	-5.36	32994632	33284067	289	30
	9#	20537268	C:T	0.078	-	3.52E-06	4.87	20428722	20537316	108	6
	3#	5113428	T:C	0.425	-	5.53E-09	-2.03	5021158	5167439	146	13
	3#	72105	C:T	0.086	-	1.36E-10	7.98	6480	197654	191	22
DTF	3#	28533036	C:A	0.056	-	2.57E-09	13.33	28529762	28761862	232	28
	7#	21266079	C:T	0.029	-	2.12E-05	-4.68	21245869	21290877	45	3
	4#	30764890	A:G	0.354	-	1.01E-07	-0.05	30690751	30790417	99	7
	9#	21199373	C:T	0.164	-	8.11E-07	4.08	11299269	11315063	15	1
	12#	24162384	G:C	0.310	-	1.44E-07	6.04	24070904	24389670	318	17
	11#	18168801	G:T	0.052	-	8.16E-06	-7.33	18134653	18242389	107	1
	6#	10389819	G:T	0.071	-	2.17E-05	-4.58	10279684	10410579	130	8

Supplementary Table S6. The details of genetic loci detected for grain yield components and related traits in 2014 water-deficit stress conditions using compressed mixed linear-model (CMLM) and multi-locus mixed model (MLMM) methods. The chromosome loci detected through both the methods were marked by asterisk sign (*); those detected through only by MLMM were marked by hashtag (#) sign. The remaining all unmarked chromosome loci were detected only through CMLM method. Trait acronyms are given in Table 1. For legends see the Supplementary Table S3.

Traits	Chr	Pos	Allele	MAF	P value _{CMLM}	P value _{MLMM}	AE	LD block		Size (kb)	Known genes	
								Start	End			
Grain yield component traits												
PN	11*	2170439	C:A	0.073	2.67E-05	3.21E-06	29.60	1940541	2291962	351	39	
	1#	39886933	G:C	0.254	-	3.60E-05	-37.99	39886933	40061573	174	15	
	3#	32507536	T:G	0.489	-	4.56E-05	-14.37	32507536	32594052	86	9	
SS	1	29223354	G:C	0.164	1.17E-05	-	-5.16	29135405	29300574	165	13	
	7*	3293128	G:T	0.172	1.46E-05	1.27E-06	5.18	3293128	3297350	4	2	
	1	30657333	G:A	0.198	1.86E-05	-	-4.63	30583128	30819501	236	25	
	1	29483935	T:A	0.104	2.22E-05	-	-5.94	29394012	29600705	206	19	
	11*	23110189	G:A	0.063	4.73E-05	8.69E-07	-6.95	23066834	23133274	66	6	
	1	28427790	C:T	0.097	5.69E-05	-	-5.47	28406849	28444503	37	1	
	4	27444465	G:T	0.175	7.38E-05	-	-4.90	27316695	27568586	251	27	
	2	23767444	G:T	0.067	7.47E-05	-	-6.78	23754037	23767444	13	3	
	2	24234634	T:G	0.093	9.39E-05	-	-6.55	24228897	24236361	7	1	
	1#	35548077	C:T	0.194	-	1.47E-05	11.27	35504716	35595543	90	9	
	1#	19262986	G:A	0.138	-	8.75E-05	-2.72	19248831	19360189	111	6	
	TGW	1*	3398710	A:G	0.338	1.76E-05	9.80E-08	-1.14	3398710	3538828	140	16
		3	16725803	G:A	0.435	2.23E-05	-	1.23	16665467	16804385	138	6
4		16574303	C:T	0.104	7.98E-05	-	1.58	16574289	16642369	68	5	
5#		7021512	C:T	0.063	-	2.94E-07	3.00	7021378	7039434	18	1	
1#		21362367	G:A	0.086	-	1.77E-08	-1.24	21348660	21627407	278	8	
3#		22959891	C:T	0.075	-	2.62E-06	2.16	22817514	22959891	142	7	
9#		17852034	A:G	0.06	-	1.10E-05	2.85	17844173	17979314	135	13	
3#		7043553	T:C	0.44	-	1.98E-05	-0.93	7030587	7070877	40	6	
SP		12*	10611754	C:A	0.496	4.26E-05	1.01E-08	1.83	10320934	10622432	301	10
	12#	16565406	G:A	0.407	-	7.30E-05	2.77	16565406	16584455	19	1	
	11#	3518037	G:A	0.101	-	6.62E-05	2.61	3368572	3562283	198	18	
Grain yield related traits												
HI	1*	29223354	G:C	0.164	3.31E-05	3.03E-06	-0.03	29135405	29300574	165	13	
	6#	217858	C:T	0.119	-	2.59E-05	-0.001	132127	366436	234	25	
TDW	3*	15532341	T:C	0.481	5.81E-05	3.76E-05	58.79	15532341	15564883	32	2	
	12	23011365	A:C	0.067	7.82E-05	-	-102.57	23004415	23141150	136	13	
	12	2589690	C:T	0.146	9.78E-05	-	-67.86	2567973	2594603	26	4	
	6*	9774102	C:T	0.144	9.93E-05	1.01E-09	-75.66	9655595	9774102	118	2	
	7#	27620959	C:T	0.09	-	4.12E-10	71.75	27479689	27620959	141	8	
	1#	42643699	C:T	0.104	-	4.22E-06	-88.94	42627969	42691537	63	5	
	7#	26457561	G:A	0.06	-	5.90E-06	248.12	26450722	26548855	98	12	
	9#	6323526	G:A	0.299	-	6.60E-07	136.50	6195580	6323526	127	7	
	10#	17454693	A:G	0.078	-	2.00E-06	134.78	17378773	17548721	169	9	
	6#	2721526	A:T	0.231	-	1.94E-06	-39.32	2662180	2726347	64	10	
6#	7135140	A:G	0.306	-	1.90E-05	12.67	7110053	7136325	26	4		
NGDW	11*	10867613	C:T	0.153	4.42E-05	2.44E-05	61.13	10834263	10928827	94	3	
	7	3488686	C:G	0.312	5.84E-05	-	-55.51	3454851	3619076	164	15	
PH	1*	38286772	G:A	0.291	1.39E-07	3.49E-08	-13.23	38178239	38437530	259	29	
	2	23720396	C:G	0.295	4.62E-05	-	5.87	23720396	23720592	197bp	1	
	11	586603	C:T	0.093	9.70E-05	-	-10.55	566590	642837	76	16	
	5	16676691	C:T	0.070	2.86E-05	-	8.89	16588982	16785352	196	9	
DTF	3*	72105	C:T	0.086	6.61E-08	3.74E-08	1.82	6480	197654	191	22	
	4#	23430194	T:C	0.257	-	6.09E-07	-3.18	23424327	23483270	58	6	
	1#	855970	G:C	0.172	-	8.52E-07	1.94	769982	931087	161	19	
	4#	34314696	G:T	0.052	-	2.23E-05	-2.33	34284403	34314696	30	3	
	12#	24162384	G:C	0.31	-	8.53E-06	5.83	24070904	24389670	318	17	
	11#	10867613	C:T	0.153	-	2.26E-05	3.48	10834263	10928827	94	3	

Supplementary Table S7. Common genetic loci detected across treatments (non-stress [NS] vs. water-deficit stress [WD]) in 2013 or 2014 (A). Similarly, common genetic loci detected across years (2013 vs. 2014) in NS or WD conditions (B). Trait acronyms are given in Table 1.

(A) Common genetic loci detected across treatments in either 2013 or 2014						
2013			2014			
Chromosome	Position	NS	WD	Chromosome	Position	NS
7	22699138	SP	SP and SPP	1	38286772	PH
4	23423399	SPP	SPP	3	72105	DTF
5	5366489	TGW	TGW	12	24162384	DTF
1	38286772	PH	PH	11	10867613	NGDW
3	21686259/ 21670338	DTF	DTF	12	10443628/ 10611754	SP
3	21686358/ 21944343	DTF	DTF			
3	5113428/ 5113535	DTF	DTF			
12	24162384	NGDW	NGDW			
4	34815309/ 34815277	TDW	TDW			

(B) Common genetic loci detected across years in NS or WD conditions						
		2013	2014			
Chromosome	Position	NS	NS	Chromosome	Position	2013
10	19903199	PN	PN	3	16725803	TGW
4	23423399	SPP	SPP	1	38286772	PH
2	30699332	TGW	TGW			
5	5366489	TGW	TGW			
1	38286772	PH	PH			
3	5113428	DTF	DTF			

Bold SNPs are detected in WD conditions and falling within the same linkage disequilibrium (LD) block. PN=panicles per m², SP=spikelets per m², SPP=spikelets per panicle; TGW=thousand grain weight; PH=plant height; DTF=days to flowering; NGDW=non grain dry weight; TDW=total dry weight.

Supplementary Table S8: The details of genetic loci detected for corrected grain yield components and related traits (only on harvest index excluding the other traits in this class) in 2013 water-deficit stress conditions using compressed mixed linear-model (CMLM) and multi-locus mixed model (MLMM) methods. The chromosome loci detected through both the methods were marked by asterisk sign (*); those detected through only by MLMM were marked by hashtag (#) sign. The remaining all unmarked chromosome loci were detected only through CMLM method. Trait acronyms are given in Table 1.

Traits	Chr	Pos	Allele	MAF	P value _{CMLM}	P value _{MLMM}	AE	LD block		Size (kb)	Known genes
								Start	End		
Grain yield component traits											
PN	8*	20408464	G:T	0.052	1.39E-06	1.77E-06	44.65	20199466	20450490	251	14
	6*	9774102	C:T	0.151	7.57E-06	5.05E-11	28.01	9774102	9992897	218	10
	2	4668201	A:G	0.476	9.44E-05	-	-15.91	4668201	4711157	42	6
	7#	15365358	T:C	0.351	-	1.57E-06	-16.42	15293375	15388056	94	5
	4#	22006507	C:T	0.264	-	1.85E-05	15.47	21989957	22015135	25	3
	8#	27943348	G:A	0.052	-	1.25E-05	24.89	27905391	27943348	37	8
	4#	15853443	C:G	0.374	-	4.76E-05	14.6	15637881	15853443	215	2
SPP	4*	23471311	C:G	0.365	7.00E-06	3.09E-08	-8.96	23428565	23483270	54	5
	4	20027177	A:G	0.052	4.32E-05	-	14.81	20014494	20066427	51	4
	6*	9871701	A:G	0.144	6.33E-05	8.99E-06	-9.89	9774102	9992897	218	10
	3#	29663197	C:T	0.257	-	4.69E-06	-6.79	29614230	29742101	127	7
	1#	855970	G:C	0.167	-	1.85E-05	5.76	769982	931087	161	19
	11#	23178024	C:T	0.086	-	3.18E-05	8.37	23178024	23183705	5	1
SS	6*	9871701	A:G	0.144	1.37E-05	5.46E-09	-5.93	9774102	9992897	218	10
	11	17886595	C:T	0.297	7.11E-05	-	-3.64	17874496	18026910	152	2
	3*	5113428	T:C	0.424	8.63E-05	4.12E-08	-3.76	5021158	5167439	146	13
	6	10086748	C:G	0.188	9.81E-05	-	-4.26	10086745	10132707	45	4
	7#	21266079	C:T	0.096	-	6.95E-06	-3.49	21245869	21290877	45	3
	5#	29213653	C:A	0.140	-	2.96E-05	3.38	29213653	29238030	24	4
	12#	27244607	G:A	0.055	-	7.01E-05	-5.56	27093600	27244607	151	14
SP	12*	141599	G:A	0.122	2.66E-05	2.52E-05	-2.29	141599	148272	6	1
Grain yield related traits											
HI	4*	34815277	C:T	0.074	1.98E-07	5.40E-06	-0.06	34815277	34833179	17	5
	3*	5113428	T:C	0.424	4.62E-06	1.03E-06	-0.03	5021158	5167439	146	13
	11	10627944	A:C	0.074	8.20E-06	-	-0.05	10627944	10863355	235	9
	11	10131062	T:C	0.055	3.20E-05	-	-0.06	9838715	10131062	292	3
	11	10329677	C:A	0.055	3.20E-05	-	-0.06	10265286	10341103	75	2
	6	10086748	C:G	0.188	5.88E-05	-	-0.03	10036641	10086748	50	1
	6	2950054	G:T	0.092	6.57E-05	-	-0.04	2888879	2981224	92	12
	1	604746	A:G	0.452	9.43E-05	-	-0.03	557715	717021	159	12

Chr=chromosome; Pos= physical position of SNP; MAF=minor allele frequency; AE=allelic effect regarding the minor allele (average traits value of genotypes carrying minor allele - average traits value of genotypes carrying major allele). Known genes=total known genes observed within the LD block.

Supplementary Table S9: The list of *a priori* candidate genes within the linkage disequilibrium block of GWAS bold annotation was responsive to abiotic stress stimulus (Gene Ontology [GO]:0009628). Trt: Treatment, NS: non-stress, WD: water-deficit. *At*: *Arabidopsis thaliana*.

Trt	Year	Locus Name	Distance to peak SNP	Gene ID	Gene annotation	Putative function	Reference
2013		Q1	6	LOC_Os11g17970.1	Pot family protein also called as PTR2 peptide transport	ABA and nitrate transport; Rice homologue <i>short panicle 1 (PTR2)</i> regulate panicle and grain size.	(Li et al., 2009)
		Q2	55	LOC_Os02g49850.1	Plastocyanin	Flower development (GO:0009908) and pollination (GO:0009856) in rice; <i>At</i> orthologue regulate another development, seed set and pollen tube growth.	(Dong et al., 2005)
		Q3	Within	LOC_Os12g23310.1	Expressed protein	-	-
NS		Q4	34	LOC_Os03g47470.1	STE kinases include homologs to sterile 7, 11 and 20	<i>At</i> orthologue (<i>AtSTE</i>) of this gene (AT4G14480.1) is a major stomatal regulator to enhance CO ₂ assimilation.	-
		Q5	48	LOC_Os02g47744.1	MYB family transcription factor	Cell growth and differentiation; response to biotic and abiotic stress	(Ambawat et al., 2013)
		Q6	3	LOC_Os10g36229.1	Mov34/MPN/PAD-1 family protein	Multicellular organismal development; <i>AT</i> (AT5G56280.1) regulate COP9 signalosome assembly and photomorphogenesis.	-
2014		Q7	Within	LOC_Os12g09670.1	Expressed protein	-	-
		Q8	13	LOC_Os01g73580.1	Glycosyl hydrolases	Carbohydrate metabolic process; role in rice grain filling.	(Liu et al., 2010)
		Q9	13	LOC_Os04g58580.1	Phosphomannomutase	Carbohydrate metabolic process; L-ascorbic acid biosynthesis that act as a redox buffer to detoxify reactive oxygen species.	(Arrigoni and De Tullio, 2002)
2013		Q10	Within	LOC_Os03g10100.1	Sugar transporter	Allocation of sugar between sinks; regulate water-deficit stress tolerance.	(Jarzyniak and Jasinski, 2014)
		Q11	5	LOC_Os03g10120.1	COP9 signalosome complex subunit 4	Arabidopsis flower development.	(Wang et al., 2003)
		Q12	6	LOC_Os01g72630.1	Expressed protein	Regulates reactive oxygen species, stomatal responses and water-deficit stress tolerance.	(Posé et al., 2009)
WD		Q13	3	LOC_Os10g30790.2	Inorganic phosphate transporter	Response to phosphate starvation, altering root system architecture in response to phosphate starvation, response to heat.	(Miura et al., 2011), (Pacak et al., 2016)
		Q15	712bp	LOC_Os11g44810.1	Auxin-repressed protein	Induced under water-deficit stress.	(Govind et al., 2009)

**Linking eco-physiological modelling with genome wide association
mapping to design crop ideotypes: A case study on rice under
water-deficit conditions**

Niteen N. Kadam^{1,2}, Krishna S.V. Jagadish^{1,3}, Paul C. Struik², C.G. van der Linden⁴, and
Xinyou Yin²

¹International Rice Research Institute, DAPO, Box 7777, Metro Manila, Philippines

²Centre for Crop Systems Analysis, Department of Plant Sciences, Wageningen University &
Research, PO Box 430, 6700 AK Wageningen, The Netherlands

³Department of Agronomy, Kansas State University, Manhattan, Kansas 66506, USA

⁴Plant Breeding, Department of Plant Sciences, Wageningen University & Research, P.O.
Box 386, 6700 AJ Wageningen, The Netherlands

Abstract

Genetic markers can be used in combination with eco-physiological models to predict the performance of genotypes in various environments. We explore the use of crop models to identify markers and design ideotypes of rice (*Oryza sativa* L.) yield under control and water-deficit conditions. Using GECROS, crop yield was dissected into eight parameters, which were estimated from the control treatment in one season for an *indica* rice panel consisting of 267 genotypes. Some parameters had more significant effect on yield than other parameters. The model accounted for 58% of yield variation of 267 genotypes in control and 40% under water-deficit conditions. For each parameter, associated single nucleotide polymorphism (SNP) loci were identified via GWAS in randomly selected 213 genotypes as the training dataset and remaining 54 genotypes were used as testing dataset. The SNP-based parameter values were calculated from estimated effects of the loci, and were fed into the model. The SNP-based model accounted for 37% and 29% of yield variation under control and water-deficit, respectively in training set. However, SNP-based model accounted for 10% of yield variation in control and 15% under water-deficit stress in testing set. In addition, performance was also lower, using either original or SNP-based parameter values, when the model was used to simulate yields in an independent season. Overall, the correlation between simulated yields using original and SNP-based parameter values was above 0.70. The rank of the SNP loci for their relative importance in explaining yield variation in the genotypes, as determined by model-based sensitivity analysis, differed greatly between control and water-deficit environments. The GECROS-based dissection approach detected more SNP loci than the analysis using yield *per se*. Virtual ideotypes based on SNPs identified by modelling had higher yield than those based on SNPs for yield *per se*. Eco-physiological modelling can potentially guide the design of crops for improving grain yields under contrasting conditions, but the resolution of the model in distinguishing the genotypic variation has to be improved.

Keywords: genotype–phenotype relationships, GWAS panel, model-based ideotyping, SNP. *Oryza sativa* L., rice.

Introduction

In the past, genomic information has proven to provide opportunities for detecting genes and quantitative trait loci (QTLs) associated with various morphological and physiological traits. Rice breeding currently exploits these genes and QTLs to improve grain yield potential and yield stability of rice cultivars when exposed to major abiotic stresses (water-deficit, high temperature, salinity and submergence; Zhang et al., 2009; Singh et al., 2009; Vikram et al., 2011; Ali et al., 2013). The recent advent of high-throughput and cost-effective genome sequencing technologies has made it possible to conduct in-depth genome analyses of thousands of individual genotypes and breeding material in many crops. For example, complete genome sequencing was carried out on 3000 diverse genotypes of rice (*Oryza sativa* L.), and this allowed to detect many mutations (Li et al., 2014) and to explain the diversity at genome level in the form of single nucleotide polymorphisms (SNPs). Despite recent advances in knowledge and technological tools in crop genetics, several scientific and technical challenges need to be overcome to exploit this information to further improve grain yield. Grain yield is a complex trait showing a low heritability and strong response to environment (genotype \times environment interaction). To further improve grain yield, a deeper understanding of the complex morphological and physiological traits contributing to grain yield, and how genes or QTLs regulating these traits interact with the environment (gene / QTL \times environment interaction) is required.

Genotype \times environment interaction (G \times E) is a complex phenomenon relevant to both genetics and crop physiology. Its quantification involves the build-up of a model based on the information generated by phenotyping many genotypes in several characterised environments. Then the model application can be illustrated in a step-wise approach using observed information to predict the phenotypic performance of: (1) genotypes phenotyped in new environments, (2) new genotypes in characterised environments, and (3) new genotypes in new environments (Bustos-Korts et al., 2016). While this step-wise approach was proposed largely from the viewpoint of statistical modelling of G \times E, it can also be applied to the eco physiological modelling of G \times E using crop models.

Process-based eco-physiological modelling of crop growth has been widely used to resolve the complexity of grain yield formation under different environments (Soltani et al., 1999; Mo et al., 2005; Tang et al., 2009; Yin and Struik, 2010; Martre et al., 2011). A model can dissect the complex traits such as grain yield into its component traits at lower hierarchical levels. Most traits in the model are believed to be controlled genetically; yet, these traits are

commonly estimated from phenotyping experiments and their genetic basis is largely unknown (Kromdijk et al., 2014). To overcome this limitation several studies have tried to link crop modelling with genetics (Yin and Struik, 2015). Using such an approach grain yield was first predicted in barley (Yin et al., 2000), later followed by grain yield in rice under control and water-deficit conditions (Gu et al., 2014). In addition, such QTL-based crop modelling helps to design virtual ideotypes (hypothetical crop plants combining ideal characteristics known to enhance grain yield), and support marker-assisted selection (MAS) to accelerate traditional crop breeding (Gu et al., 2014; Yin et al., 2016; Xu and Buck-Sorlin, 2016; Hammer et al., 2016).

However, most studies linking crop growth modelling with genetics were conducted on biparental mapping populations representing only a small part of the available genetic diversity. Recently, genome wide association studies (GWAS) have become increasingly popular to dissect the genetic architecture of complex traits, using wider genetic diversity in crops. Only recently, it was recommended to extend the biparental QTL-based eco-physiological modelling to a wider genetic diversity using the GWAS approach (Yin et al., 2016).

To the best of our knowledge only few (and very recent) studies were conducted on linking GWAS with crop growth modelling (Mangin et al., 2017; Dingkuhn et al., 2017a; Dingkuhn et al., 2017b). Mangin et al. (2017) showed that crop models can be used to develop “stress indicators” that explain yield variation across multiple environments, facilitating GWAS application to identify relevant QTLs for yield in response to environmental stresses. Similarly, Dingkuhn et al. (2017a) and Dingkuhn et al. (2017b) have shown that the crop model RIDEV can dissect phenology and spikelet sterility, respectively, into their components, thereby heuristically strengthening the phenotyping and GWAS analysis of these two traits. These studies demonstrated benefit of crop modelling in GWAS analysis. However, whether the genetic approach for GWAS can facilitate the application of crop modelling in plant breeding, e.g. in designing crop ideotypes, has yet to be demonstrated.

Our current study is the first attempt to explore the QTL-based eco-physiological modelling approach on a genome wide association panel of rice following the principles explained for traditional linkage analysis (Yin et al., 2000; Gu et al., 2014). This approach allows dissecting the $G \times E$ and integrating the effects of multiple component traits regulating the complex grain yield trait. To that end, we applied the GECROS (Genotype-by-Environment interaction on CROp growth Simulator; Yin and Van Laar, 2005) model to a rice association mapping panel as a case in point. The model was first parameterised from the control condition in the experiment of one growing season, and evaluated by simulating and estimating the grain

yield across control and water-deficit treatments in the same and other growing seasons. Then GWAS analysis was performed on model input parameters to identify significant SNP markers, and a model-based sensitivity analysis was used to rank the identified SNP markers based on their relative importance in determining the grain yield variation. Based on these analyses, grain yield ideotypes were designed for control and water-deficit conditions.

Material and Methods

We modified the methodology that was explained by (Gu et al., 2014) for model application to a biparental population (Supplementary Figure 1). Each step in this modification sequence is briefly explained in the following sections.

Association mapping panel and field phenotyping

An association mapping panel of *indica* genotypes of rice was developed and assembled at the International Rice Research Institute (IRRI), Philippines, in the context of the Global Rice Phenotyping Network project (<http://ricephenonetwork.irri.org>). Recently, this population was extensively used to study the genetic architecture of a wide range of phenotypic traits (Al-Tamimi et al., 2016; Rebolledo et al., 2016; Kikuchi et al., 2017; Kadam et al., 2017). We phenotyped this population to quantify the variation in grain yield and its component traits under well-watered (control) conditions throughout the crop cycle and under water-deficit conditions during the reproductive stage (focussing on flowering stage). Two field experiments were executed at the upland farm of IRRI, Philippines (14°11'N, 121°15'E; elevation 21 m above sea level) during the dry seasons (DS) of 2013 and 2014. A systematic and well designed staggered sowing and transplanting scheme was followed to synchronise flowering, and thereby the timing of the water-deficit stress with respect to plant developmental stage, for the entire panel. Data on the environmental conditions such as daily radiation, maximum and minimum temperature, vapour pressure, rainfall and wind speed were collected from an on-site weather station. The detailed experimental setup, stress imposition and other relevant details on agronomic management practices are described in Chapter 4.

The GECROS model and its modification

The GECROS model was first described by Yin and Van Laar (2005) and recently updated by Yin and Struik (2017). GECROS simulates crop growth on a daily basis, but with subroutines for photosynthesis, transpiration, and phenology implemented on a shorter time step. The model

simulates yield by considering the effects of interactions and feedback mechanism of physiological processes during crop growth and development. These physiological processes include photosynthesis-transpiration coupled via stomatal conductance, carbon-nitrogen interaction, functional balance between shoot and root activities, and interplay between source supply and sink demand.

Gu et al. (2014) showed poorer performance of GECROS in simulating yield of rice genotypes under drought than under control, due to the model's inability to correctly simulate spikelet number under drought. The number of spikelets per m^2 in the model is assumed to be co-determined by the amounts of carbon and nitrogen accumulated in the plant during the reproductive phase around flowering. However, the percentage of filled spikelets, or grain set, depends on panicle temperature during flowering hours, especially when stress occurs during this phase (Jagadish et al., 2007; Julia and Dingkuhn, 2013). Therefore, we modified the GECROS model to account for the direct effect of panicle temperature on sink size. The simulation of panicle temperature was done using the same algorithms in GECROS (Yin and Struik, 2017) for simulating leaf-surface energy balance, based on a coupled conductance photosynthesis-transpiration routine, whereby panicles were treated as a photosynthesizing organ and its conductance was calculated using a semi-empirical leaf stomatal conductance model. Because the panicle temperature is most crucial in determining the spikelet sterility only during flowering hours of a day (Julia and Dingkuhn, 2013), upscaling instantaneous photosynthesis and transpiration to daily total was changed from the five-point Gaussian integration in GECROS to hourly computation. A factor for reduction induced by any high panicle temperature at flowering hours under stress, relative to the control, was introduced to simulate the actual spikelet fertility under water-deficit stress, based on the linear relationship between sterility and panicle temperature reported by Julia & Dingkuhn (2013). The grain set in control was herein called "the baseline grain set".

Measurement of model input parameters, model calibration and testing

The model requires a certain set of genotype-specific input parameters to simulate grain yield. These input parameters were classified into (1) phenological; (2) morphological; and (3) physiological categories (Table 1). Phenological parameters included pre-flowering duration (m_V), post-flowering duration (m_R), and photoperiod sensitivity (δ). Morphological parameters included maximum plant height (H_{max}) and single-seed weight (S_w). Similarly, physiological parameters included grain set (g_{set}), grain nitrogen concentration (n_{so}), and total crop nitrogen

uptake capacity (N_{\max}). A complete set of model input parameters for the association mapping panel of rice was determined from control condition data of the 2013 DS experiment (Chapter 4). The exception was photoperiod sensitivity parameter δ that was estimated using pre-flowering phenology data collected from the 2013 DS as well as an additional 2012 wet-season phenology experiment, because δ requires at least two photoperiods to estimate. A bell-shaped nonlinear function of the phenological response to temperature in the GECROS model was used to calculate the parameters m_V and δ using the measured flowering time, and m_R calculated using the harvest time, of the association mapping panel. These parameters were estimated, based on daily photoperiod and hourly temperature generated from weather data, using daily maximum and minimum temperatures (Yin et al., 2005). Values of H_{\max} , S_w , and g_{set} were determined directly from the experimental measurements (described in Chapter 4). The value of n_{so} was measured using the micro-Kjeldahl method. N_{\max} is not an input parameter in the default GECROS model, and is used here as a genotype-specific parameter to avoid the confounding effect of the inherent model inaccuracy in simulating crop nitrogen uptake from soil. The value of N_{\max} was assessed based on dry weight and nitrogen concentration in the various plant organs. While calculating N_{\max} , nitrogen concentration was assumed to be 0.463% in the straw (Singh et al., 1998) and 5.0% in the roots (Yin and Van Laar, 2005). Other parameters for which genotype-specific values were lacking were kept at default synthesized from previous studies for the whole panel in the crop model (Yin and Van Laar, 2005).

The GECROS model, calibrated as described above using the model input parameters from the control conditions in the 2013 experiment, was then used to simulate values of grain yield of the genotypes in the water-deficit condition of 2013, as well as in 2014 environments under both control and water-deficit conditions. Relative root mean square error (rRMSE) was used to inspect the quality of model simulation (Brun et al., 2006), and the R^2 coefficient of the linear regression of simulated versus observed values of grain yield was used to show the percentage of phenotypic variation accounted for by the model.

Multiple linear regression to identify the contribution of model input parameters to grain yield

We also performed a multiple linear regression (MLR) analysis to test the contribution of each individual model input parameter (Table 1) to grain yield. The `lm()` function in R was used to perform this analysis.

Identifying SNP markers for model input parameters and grain yield, and estimating SNP-based values of these traits

In this study, we have followed a strategy that was explained by (Gu et al., 2014) for a biparental population, but with some modifications (see Supplementary Figure 1). Firstly, the rice association mapping population of 267 genotypes was randomly divided into a training (213 genotypes; 80% of the population) and a testing (54 genotypes; 20% of the population) set. Then we followed the two-step approach to identify the SNP markers and to calculate the marker-based estimates for the model input parameters and grain yield using the training set. In the first step, we used both the single-locus and the multi-locus GWAS analysis to identify the significant SNP markers for the model input parameters and grain yield. In the second step, these significant SNP markers were fed into a multiple-linear regression framework to estimate the additive effects of the markers, which were subsequently used to estimate the “GECROS” model input parameters and grain yield. A description of each step is explained in more detail below.

Step 1: Single-locus and multi-locus GWAS analysis to identify the significant markers

The single-locus GWAS analysis was performed on model input parameters and grain yield using a 45K SNP dataset by a compressed mixed linear model (CMLM) in the Genomic Association and Prediction Integrated Tool (GAPIT). The detailed protocol was explained in Chapter 4. Using this protocol, we selected the top ten significant markers with lowest P value after excluding the redundant markers within the linkage disequilibrium (LD) of ~55 to 65 kb reported for this population (Kadam et al., 2017). Similarly, we conducted a multi-locus GWAS analysis that in addition to correcting the confounding effect of population structure (PC) and family relatedness (K), corrected for the confounding effect of background loci present due to LD in the genome. We ran the complete model with stepwise forward inclusion of the lowest P value marker as a cofactor until the heritability reached a value close to zero, followed by backward elimination of the least significant markers from the model (Segura et al., 2012). With this protocol, we selected all significant SNP markers associated to traits were incorporated as a cofactor in the model. In fact, multi-locus analysis also corrects the confounding effect of genome LD (Segura et al., 2012). Thus, significant SNP markers associated with traits identified through multi-locus analysis were not within LD region of ~55 to 65 kb reported for this population (Kadam et al., 2017).

Step 2: Multiple-linear regression to estimate the model input parameters and grain yield

All significant SNPs identified in Step 1 were fed into a multiple linear regression (MLR) using the `lm()` function in R with equation 1.

$$Y_k = \mu + \sum_{n=1}^N a_n M_{k,n} \quad (1)$$

where μ = intercept, a_n = additive effect of the n^{th} marker, $M_{k,n}$ = genetic score of the n^{th} of the individual genotypes k that takes either the value -1 (major allele with 0.95 frequency in studied population) or 1 (minor allele with 0.05 frequency in studied population). This analysis with all the SNP markers identified the non-significant markers due to collinearity of markers, which were removed in the next round of the MLR analysis. In addition, we also performed one more round of MLR analysis to remove the markers with cut-off threshold P value <0.01 . Finally, we estimated the SNP markers-based model input parameters using equation 1 in the GECROS model with estimated additive effects of the individual markers, and marker allelic data for each genotype in the whole panel.

Sensitivity analysis to rank the relative importance of individual SNP markers

Sensitivity analysis was performed using the GECROS model to test the effect of individual SNP markers on grain yield simulation following the principle explained by (Yin et al., 2000). First, we conducted the baseline simulation with genotype-specific allelic values of markers as model input to test the percentage of variation in grain yield explained by all markers. In the second step, to identify the important markers, we fixed one marker at a time to zero (i.e. excluding the effect of this marker in the analysis) to examine the variation in grain yield accounted for by the model. We performed such an analysis on all significant SNP markers, and assessed by what percentage the explained variation in grain yield dropped in comparison with the explained percentage of the baseline simulation. Using this protocol, we ranked the relative importance of the markers in determining grain yield variation.

Virtual designing of an ideotype

We followed two approaches to virtually design the ideotype for grain yield using GECROS by pyramiding the positive alleles of significant SNPs detected for model input parameters or of SNPs detected for grain yield. In the first approach, we regressed model input parameters against all the significant SNPs from the GWAS, detected for each model parameter, using equation 1. Similarly, we also regressed model input parameters against the SNPs detected for

grain yield. The top four SNPs for model input parameters were selected based on relative importance in R package *relaimpo* (). Then, we regressed model input parameters against these top four SNP markers (eq. 1) to estimate the additive effect, and to calculate the marker-based value of the model input parameter. We used these marker-based model input parameters to design Ideotype I (using SNPs for model input parameters) and Ideotype II (using SNPs for grain yield). In the second approach, instead of using the top four SNPs, we selected all significant SNPs with P values of <0.01 using equation 1 to estimate the additive effect, and to calculate the marker-based value of model input parameters. This was done for SNPs detected for each model input parameter, and for SNPs detected for grain yield. We used these marker-based model input parameters to design Ideotype III (using significant SNPs for model input parameters) and Ideotype IV (using significant SNPs for grain yield).

Results

Genotypic variation in model input parameters and their relative contribution to yield

We used the control conditions of the 2013 experiment to parameterise or calibrate GECROS. Measured or estimated model input parameters (Table 1) showed a strong genotypic variation (Fig. 1). We used regression analysis to test the relative contribution of each of these model input parameters to grain yield variation. The model input parameter of total crop nitrogen uptake (N_{\max}) accounted for the highest percentage of the grain yield variation in the association mapping panel (72.43%; Table 2). Therefore, multiple linear regression analysis was performed with N_{\max} as a cofactor in the model. Grain yield was significantly correlated with four other input parameters (post-flowering period [m_R], maximum plant height [H_{\max}], grain set [g_{set}], and grain nitrogen concentration [n_{so}]), but not with pre-flowering period (m_V), photoperiod sensitivity [δ] or single-grain weight (S_w).

Model performance in control and water-deficit conditions in the 2013 experiment

We ran the model using the model input parameters of control conditions in the 2013 experiment. Simulating the grain yield under control conditions accounted for 58% of the total variation in grain yield with an rRMSE value of 0.19 in the association mapping panel (Fig. 2A). Using the same input parameter values calibrated with the data from the control conditions to simulate the situation under water-deficit stress of the same year 2013, the model accounted for 40% of the variation in grain yield with an rRMSE value of 0.28 (Fig. 2B).

Table 1: Details of genotype-specific GECROS model input parameters classified in three categories.

Trait	Description	Unit
(A) Phenological		
m_V	Pre-flowering period	thermal day
m_R	Post-flowering period	thermal day
δ	Photoperiod sensitivity	hr ⁻¹
(B) Morphological		
H_{\max}	Maximum plant height	m
S_w	Single-grain weight	g
(C) Physiological		
g_{set}	Grain set	%
n_{so}	Grain nitrogen concentration	g N g ⁻¹ DM
N_{\max}	Total crop nitrogen uptake at maturity	g N m ⁻²

Thermal day is calculated using the bell-shaped temperature response equation as used in GECROS, based on hourly temperatures generated from weather data on daily maximum and minimum temperatures; a thermal day is equivalent to an actual day only if temperature at each hour of the day equals to the optimum temperature for phenological development. So, m_V or m_R in thermal days are lower than their values in actual days for expressing the length of the growth duration. DM = dry matter; N = nitrogen.

Model performance in the 2014 experiment

To simulate grain yield in the control and water-deficit conditions of the 2014 experiment, GECROS was used again with input parameters values from 2013 control conditions. In the 2014 experiment, the simulation was less accurate in both treatments, only accounting for 20% and 13% of the variation in grain yield under control and water-deficit conditions with rRMSE values of 0.31 and 0.40, respectively (Fig. 2C-D). The model tended to underestimate the grain yield in control conditions for most genotypes in the association panel (Fig. 2C). The model overestimated the grain yield at the lower tail of observed grain yield values, and underestimated grain yield at the upper end of the observed grain yield in water-deficit conditions (Fig. 2D).

Identifying SNP markers for model input parameters and for grain yield

To identify the SNP markers for model input parameters and grain yield, a single-locus and a multi-locus GWAS analysis (for more details see Materials and Methods) were performed on the 213 genotypes of the training set from 2013 control conditions. The remaining 54 genotypes were treated as the testing set. In total, we identified 104 SNP markers associated with model input parameters, and 12 SNP markers with grain yield in control conditions (Table 3). In the next step, we selected the final set of 90 out of 104 SNP markers for model input parameters with cut-off threshold P values <0.01 using the MLR equation 1 (Supplementary Table 1). The

Table 2: Linear regression of grain yield (Y in g m^{-2}) with total crop nitrogen uptake (N_{max} in g N m^{-2}) and other individual model input parameters (Table 1) in 2013 control conditions.

Equation	μ	a_1	a_2	R^2 (%)
$Y = \mu + a_1 N_{\text{max}}$	-207.29	81.28***		72.43
$Y = \mu + a_1 N_{\text{max}} + a_2 m_V$	-202.74	81.38***	-0.08 ^{ns}	72.43
$Y = \mu + a_1 N_{\text{max}} + a_2 m_R$	-301.61	79.93***	3.11**	73.39
$Y = \mu + a_1 N_{\text{max}} + a_2 \delta$	-211.24	82.28***	-102.65 ^{ns}	72.79
$Y = \mu + a_1 N_{\text{max}} + a_2 H_{\text{max}}$	-9.60	83.23***	-156.79***	85.05
$Y = \mu + a_1 N_{\text{max}} + a_2 S_w$	-266.67	81.14***	2688.87 ^{ns}	72.85
$Y = \mu + a_1 N_{\text{max}} + a_2 g_{\text{set}}$	-355.65	66.87***	349.30***	77.92
$Y = \mu + a_1 N_{\text{max}} + a_2 n_{\text{so}}$	134.63	76.88***	-22861.21***	82.00

phenotypic variation explained by the final set of SNPs detected for individual model input parameters ranged from 42.2% (g_{set}) to 77.0% (H_{max} ; Supplementary Table 1). In comparison, 12 SNP markers detected when grain yield of the same experiment was subjected to the GWAS analysis, together explaining 44.4% of the total variation in grain yield. No common SNP markers were found among model input parameters. Two markers on chromosome 8 (2341829) and 5 (658940) for N_{max} however were also associated with grain yield.

Performance of SNP-based GECROS simulations on 2013 and 2014 experiments

In the next step, a SNP-based GECROS model was created by linking the additive effect of each SNP for model input parameters estimated from the MLR analysis (eq. 1), and allelic data of each SNP (-1 for major allele and 1 for minor allele) for the whole association mapping panel (including training and testing sets). SNP-based model input parameter values calculated using equation 1 were fed to GECROS to simulate grain yield. The performance of such a model was assessed individually for training and testing sets. In training set, the SNP-based model accounted for 37% and 29% of variation in grain yield under control and water-deficit conditions with rRMSE values of 0.23 and 0.30, respectively, during the 2013 experiment (Fig. 3A). However, model simulation was less robust on testing set, accounting only for 10% of yield variation under control conditions (rRMSE=0.26), and accounting for 15% of yield variation under water-deficit conditions (rRMSE=0.33; Fig. 3B) in 2013.

We also tested the marker-based GECROS model on data from the 2014 experiment. In training set, the model accounted for only 23% and 17% of variation in grain yield under control and water-deficit conditions, respectively (Fig. 3C). For the testing set, the model accounted for only 1% of the variation in grain yield in control and 9% of the variation in grain yield in water-deficit conditions (Fig. 3D). Across both years and both treatments, the model

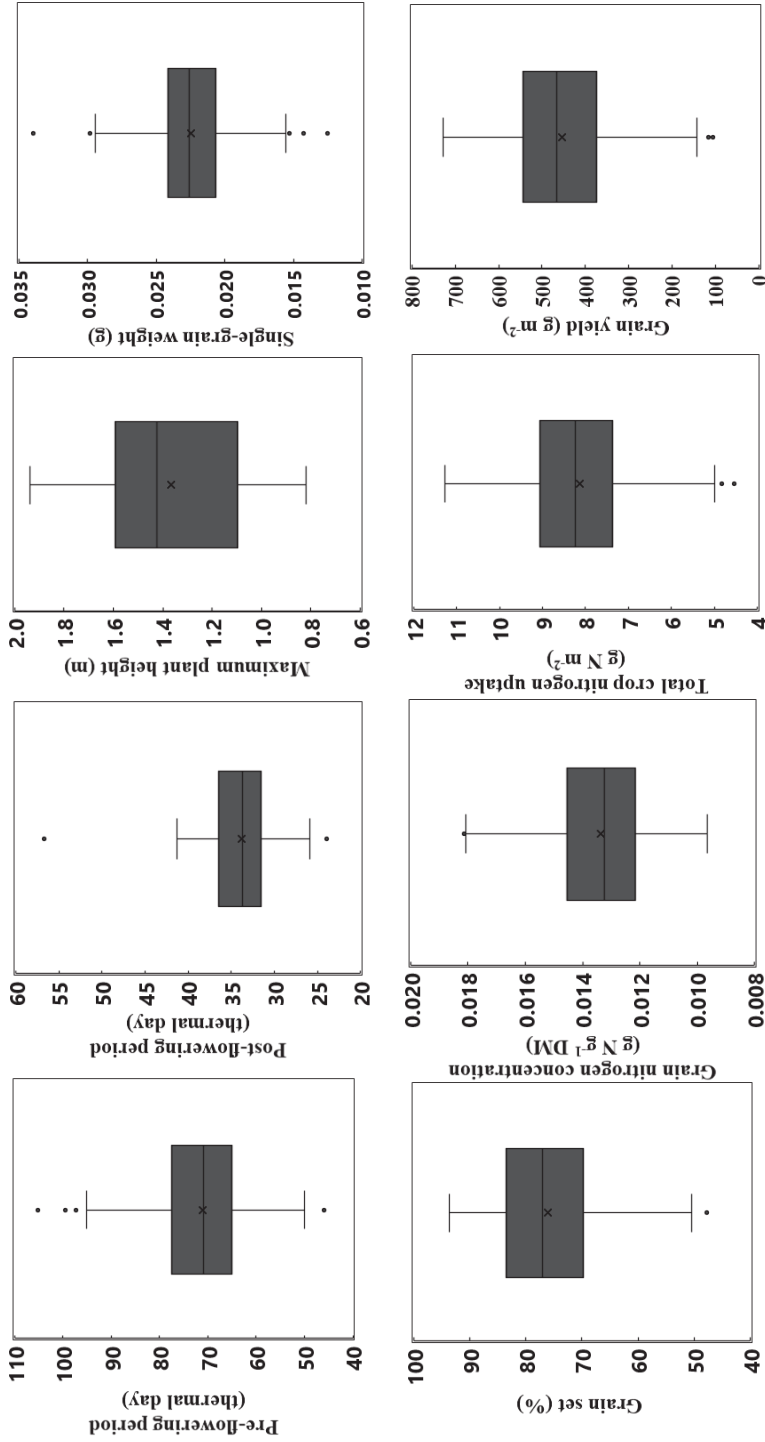


Figure 1: Phenotypic distribution of model input traits and grain yield in 267 genotypes of a rice genome-wide association mapping panel under control conditions of the 2013 dry season.

overestimated the grain yield for genotypes having lower observed grain yield (lower end), and underestimated the grain yield for genotypes having higher observed grain yield (upper end) value (Fig. 3). We also correlated the original parameter-based simulations with SNP-based simulations, for the whole association mapping panel. The SNP-based simulations were well correlated with original parameter-based simulations under control conditions (2013: $r=0.72$ and 2014: $r=0.70$) and water-deficit conditions (2013: $r=0.77$ and 2014: $r=0.74$) in both years (Fig. 4).

Sensitivity analysis to rank the relative importance of SNP markers in determining yield

As stated in an earlier section, we detected 90 significant SNP markers for model input parameters. So, the sensitivity analysis by fixing these markers one at a time involved a total of 180 (90 in control and 90 in water-deficit) simulations to determine their relative importance in determining grain yield under control as well as water-stress conditions of the 2013 experiment. The top four SNP markers on chromosome 6 (1360962; rank 1), 7 (23760855; rank 2), 12 (6720935; rank 3), and 1 (1360962; rank 4) for N_{\max} contributed to variation in grain yield under control conditions. For the top ranked SNP on chromosome 6 (1360962; rank 1), the phenotypic variation accounted for by GECROS decreased from 31.6% to 25.9% in control conditions for N_{\max} (Supplementary Table 2). These results are supported by the linear regression of N_{\max} that explained most of the variation in grain yield (Table 2). Similarly, the top 3 SNP markers on chromosome 4 (19591930; rank 1), 1 (9243669; rank 2), and 2 (4390533; rank 3) for m_v contributed most to grain yield under water-deficit conditions (Supplementary Table 2). The phenotypic variation accounted for by the model for the top ranked SNP on chromosome 4 (19591930; rank 1) decreased from 26.1% to 14.9% in water-deficit. Likewise, the fourth ranked SNP marker on chromosome 7 (58252) contributing to variation in grain yield was detected for H_{\max} under water-deficit. These results clearly indicate that phenology plays a major role in influencing grain yield under stress comparable to that of N_{\max} in control conditions. Nevertheless, the SNP marker on chromosome 6 (1360962; rank 6) influencing N_{\max} and the marker on chromosome 3 (16529108; rank 7) influencing n_{SO} had significant effects on grain yield even under water-deficit (Supplementary Table 2). In addition, we also noticed that excluding the effect of some markers did not affect or change the variation in grain yield explained by the model, while in another situation it increased the explained grain yield variation. For instance, excluding one of the SNPs on chromosome 9 linked with m_R in control increased the explained variation in grain yield from 31.6% (baseline simulations) to 33.5%

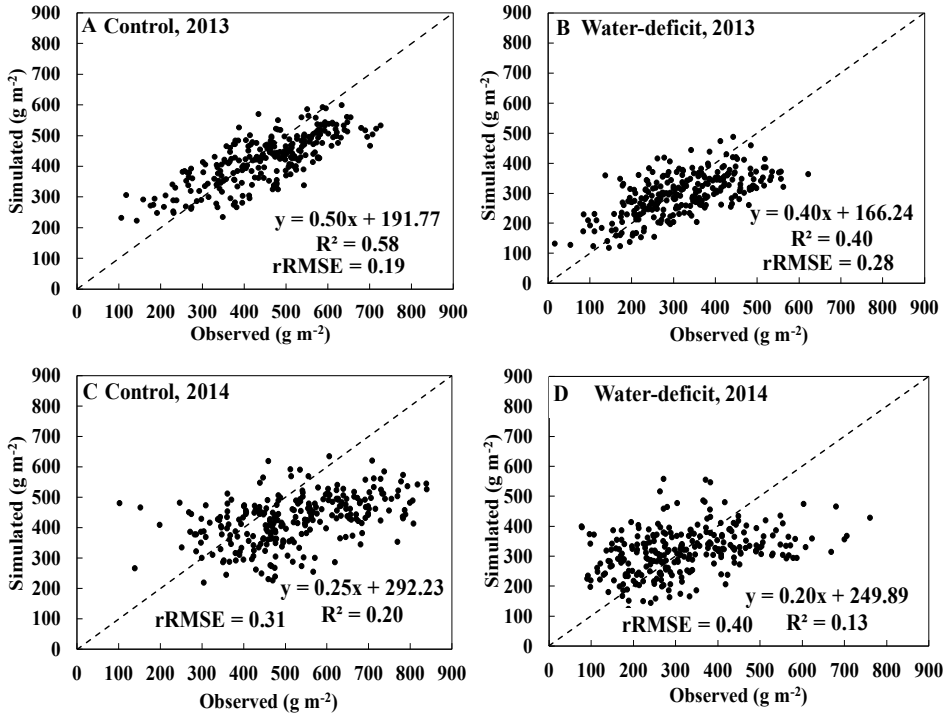


Figure 2: Relationship between simulated and observed values of grain yield in 267 genotypes of rice genome-wide association mapping population under control and water-deficit conditions in the 2013 (**Panels A-B**), and 2014 (**Panels C-D**) dry season experiments.

(Supplementary Table 2).

Designing virtual ideotypes using SNP alleles detected for model input parameters and for grain yield *per se*

Ideotype I showed only 3% simulated grain yield advantage compared with Ideotype II in both treatments (Fig. 5). However, Ideotype III showed 89% and 75% simulated grain yield advantage compared to that of Ideotype IV under control and water-deficit stress, respectively (Fig. 5).

Discussion

In this study, we tried to link the process-based crop growth model GECROS with SNP markers identified through GWAS to simulate variation in grain yield among different rice genotypes in an association mapping panel. Key findings from our analysis are discussed below in detail.

Table 3: Total number of significant SNPs detected through multiple linear regression (MLR) for eight GECROS model input parameters and grain yield of the rice training population (n=213) under control conditions in the 2013 experiment. Percentage of phenotypic variations (R^2) explained by significant SNPs of model parameters and yield are derived from MLR (equation 1). The number mentioned in brackets refers to the number of significant SNP markers originally detected through the genome-wide association mapping study before putting them into the MLR analysis (for more details see Materials and Methods). Coefficients of equation 1 and additive effect of each significant SNP for model input parameters and grain yield are given in the Supplementary Table 1.

Trait	Significant SNPs	R^2 (%)
(A) Phenological		
m_V	16 (20)	74.2
m_R	9 (9)	51.6
δ	9 (9)	65.1
(B) Morphological		
H_{max}	13 (17)	77.0
S_w	8 (9)	47.3
(C) Physiological		
g_{set}	6 (6)	42.2
n_{SO}	16 (19)	70.0
N_{max}	13 (15)	66.8
Total SNPs	90 (104)	
Grain yield	12	44.3

Model-based grain yield simulation in a new environment was less accurate than in the tested environment

It is often difficult to simulate the performance of given genotypes under contrasting environments or simulate the phenotypes of a set of genotypes under a given environment. GECROS works based on the principle of carbon-nitrogen interaction to simulate crop growth and development (Yin and Van Laar, 2005; Yin and Struik, 2010; Yin, 2013). This model was used to simulate grain yield and biomass differences in a biparental segregating population of rice (Gu et al., 2014). For our study, the model was calibrated using eight model input parameters (Table 1) under control conditions from the 2013 experiment. This calibrated model satisfactorily simulated the observed differences in grain yield among the rice association mapping population in tested environments (2013 experiment, Fig. 2A). However, the variation accounted for was lower than in a previous study with a biparental population of introgression lines (Gu et al., 2014). This was mostly because the association mapping panel used in our study contained more much diversified or unrelated genotypes while population derived from biparental crosses are related with each other. The calibrated model showed poor simulation accuracy of

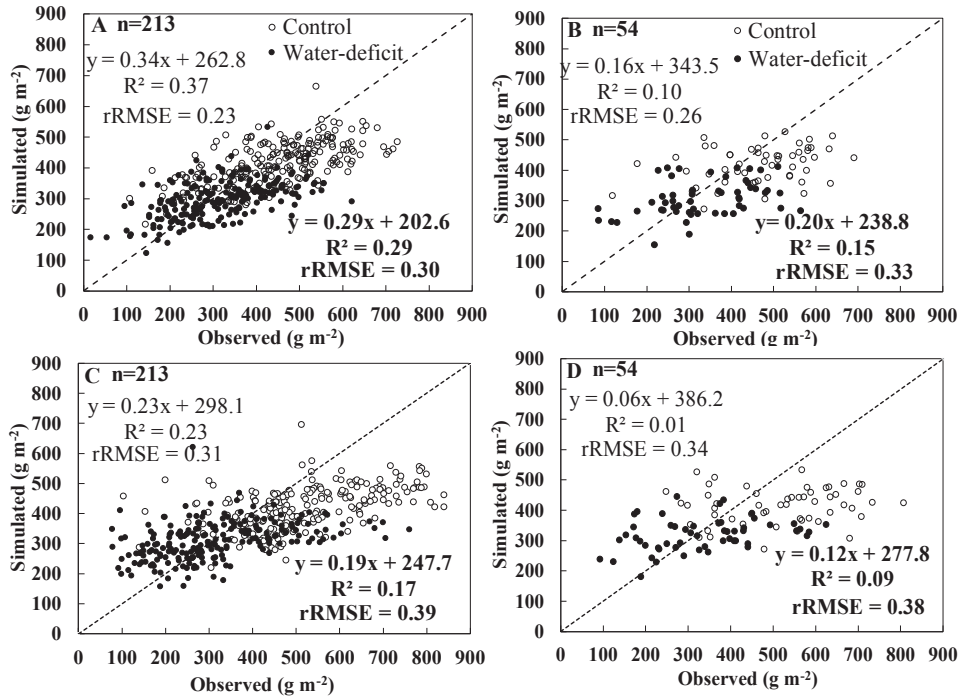


Figure 3: Relationship between SNP-based simulated and observed values of grain yield for training (n=213) and testing (n=54) populations of rice under control (open circle, statistical indicators in non-bold) and water-deficit (closed circle, statistical indicators in bold) conditions during 2013 (**Panels A and B**) and 2014 (**Panels C and D**) dry season experiments.

variation in grain yield in new environments, the 2013 water-deficit condition (Fig. 2B) and both control and water-deficit conditions in the 2014 experiment (Fig. 2C-D), due to strong genotype-by-environment ($G \times E$) interaction. These results also suggest that variations for morpho-physiological traits in our GWAS panel (see Kadam et al., 2017) important for yield determination are not completely accounted for by using the eight GECROS model input parameters chosen in the present study.

Water-deficit reduces transpiration cooling and increases tissue and organ temperature leading to higher spikelets sterility in rice (Jagadish et al., 2007). Potential seed number was determined by carbon and nitrogen accumulation during the vegetative phase in an earlier version of GECROS (Yin and Van Laar, 2005). Hence, the model originally did not have the capacity to account for the effect of organ temperature on spikelet sterility under stress conditions. In the present study, an upgraded version of the model was used to account for organ temperature effects on spikelet fertility while determining variation in grain yield under stress conditions. This indeed allowed to simulate 40% and 13% of the grain yield variation in the

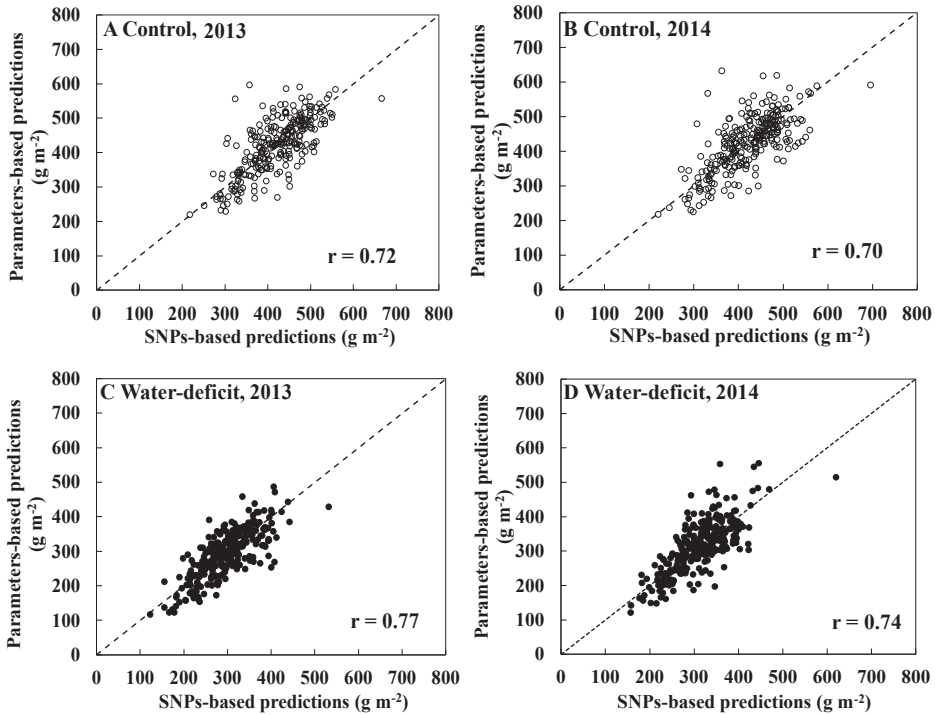


Figure 4: Correlations between GECROS input parameters based prediction of grain yield values and those predicted based on SNP-based model parameters for 267 rice genotypes under control (open circles; **Panels A-B**) and water-deficit (filled circles; **Panels C-D**) conditions during 2013 and 2014 dry season experiments.

association mapping panel under stress conditions during the 2013 (Fig. 2B) and 2014 experiments, respectively (Fig. 2D). The decreased simulated yield for the stress condition was due to an increased spikelet sterility because of simulated warmer panicle temperature by ca 2°C. Such an extent of panicle warming was in line with measurements of canopy temperature in the same experiment (Melandri, personal communication). Individual genotypes may respond differently both in their panicle temperature to water deficit and in their sensitivity of spikelet fertility to warmer panicle temperature. However, we did not have sufficient data on these possible differences; so, a uniform sensitivity parameter was applied to all genotypes, based on the recent report of Julia and Dingkuhn (2013). This may cause the poorer performance of the model in explaining yield differences among genotypes under stress environments, compared to the control conditions (Fig. 2).

The SNP-based model was created by estimating the genetic effect of model input parameters. To evaluate the predictive quality of the SNP-based model, special cross-validation

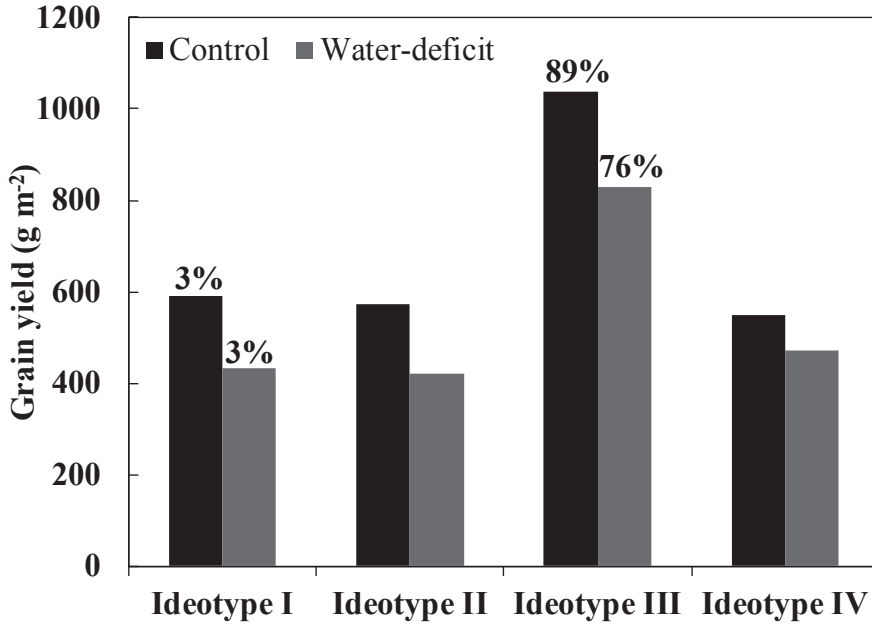


Figure 5: Simulated grain yields using the marker-based GECROS model for four ideotypes in control and water-deficit conditions. Ideotype I is the hypothetical genotype designed by pyramiding the positive alleles of the top 4 SNP markers selected based on relative importance in a multiple linear regression analysis for each model input parameter. Ideotype II is the hypothetical genotype designed by pyramiding the positive alleles of the top 4 SNP markers selected based on relative importance in a multiple linear regression analysis (regardless of significance of the *P* value) for grain yield *per se*. Ideotype III is the hypothetical genotype designed by pyramiding the positive alleles of only significant SNP markers (*P* <0.01) identified by multiple linear regression analysis for each model input parameter. Ideotype IV is the hypothetical genotype designed by pyramiding the positive alleles of only significant SNP markers (*P* <0.01) identified by multiple linear regression analysis for grain yield *per se*. Percentage value indicates the relative advantage of Ideotype I over Ideotype II, and of Ideotype III over Ideotype IV.

schemes were used. In these schemes, the genotypes were randomly subdivided into a training and a testing set. The SNP-based model showed good potential to quantify the grain yield variation in the training set under 2013 control and new environments (Fig. 3A-C). However, the model showed poor simulation in a testing set (Fig. 3B-D). The population size is important for reliable GWAS analysis. Further, the phenotypic variance is strongly determined by how the two allelic variants differ in their phenotypic effect and their allelic frequency in the population sample. Hence, the lower simulation accuracy for the testing set suggests that excluding the testing set of genotypes in the GWAS analysis changed the allelic frequency of a given SNP in the population that had a strong influence on the phenotypic variance and on

detecting the significant marker. Therefore, testing set was not representing the similar genetic diversity or population structure as training set and SNPs alleles may not be similarly represented in both the set. Such distant genetic relationship between training and testing sets might have lower down the prediction accuracy (Isidro et al., 2015). Therefore, it is very important to optimize the population structure using marker data while designing the training and testing sets to maximize the prediction accuracy.

Crop modelling helps to elucidate the genetic control of grain yield by identifying SNPs for yield-determining model input parameters

Complex traits such as grain yield are determined by many interactive physiological processes at the organ, plant and crop canopy level changing over time during the growing period. A deeper understanding of the way these processes contribute to grain yield is a prerequisite for designing the future new plant type for improved grain yield under changing climatic conditions (Peng et al., 2008). Crop growth models have been widely used as a tool to dissect complex traits (e.g., grain yield) as a function of its meaningful physiological components (Yin et al., 2004; Chenu et al., 2008; Hammer et al., 2010). This is the basis of using crop modelling to enhance phenotyping, i.e. what Dingkuhn et al. (2017a,b) called “the heuristic phenotyping” of complex crop traits. We used the model to dissect grain yield into eight simple model input parameters to quantify genetic variation in a rice association mapping panel (Table 1). The multiple linear regression analysis confirmed that N_{\max} had the strongest effect on grain yield among the model input parameters in agreement with a previous study (Gu et al., 2014). The genetic analysis also confirmed this by demonstrating that the two SNP markers for N_{\max} colocalised with grain yield. This indicates that dissecting complex traits into their physiological components helps to pinpoint the exact genetic control and fundamental insights of complex traits such as grain yield (Yin et al., 2002). In addition, the number of QTLs identified for a single trait is always inadequate; however, model-based dissection allows detecting more markers than grain yield *per se* (Table 3). This clearly indicates that model-based dissecting of the complex trait into individual components helps to detect more markers than for the complex trait such as grain yield alone (Gu et al., 2014; Amelong et al., 2015). Similar results have been recently reported for flowering time as a complex trait (Dingkuhn et al. 2017a). Despite this advantage of model-based dissection analysis over complex traits like grain yield *per se*, the latter approach cannot be replaced completely. Grain yield analysis identified SNP markers that were not detected by the model-based dissection, except two SNP

markers for N_{\max} colocalised with grain yield. This could be due to the fact that markers detected for the aggregated trait (such as grain yield) might have less impact on component traits (Yin et al., 2002). Another possibility could be that some of the yield-determining physiological mechanisms are not incorporated in the current GECROS model.

Further, we could not find any common SNP markers between model input parameters. This result is in line with that of Dingkuhn et al. (2017a,b) for a rice association panel, but in contrast to a previous report on a biparental population of introgression lines (Gu et al., 2014). Such contrasting results could also be due to the fact that in a biparental population of introgression lines one or two major segregating genes/QTLs might have a strong influence on multiple phenotypic traits (Yin et al., 2016). However, QTLs detected through GWAS analysis were having smaller effects on the main traits. In addition, their effect on other traits might also be too small, which cannot be detectable by current GWAS threshold P value.

SNP-based GECROS modelling helps to evaluate the benefits of single markers at a time to improve the efficiency of marker assisted selection

In this study, we have demonstrated that GECROS is a useful tool to enhance the efficiency of selection for grain yield. The SNP-based modelling approach was used to rank the relative importance of markers identified for various grain yield determining model input parameters. This enabled to identify the most important yield determining markers that breeders can prioritize to improve the efficiency of MAS for specific environments. In addition, the relative performance of detected markers was different for control and water-deficit conditions of 2013 experiment (Supplementary Table 2). This indicates that the contribution of different physiological and morphological traits to grain yield varies under different environments.

Plant phenology such as flowering time is not only an essential part of reproductive processes but also a critical stage sensitive to various abiotic stresses (e.g. drought and heat) causing highest grain yield losses (Barnabás et al., 2008). In addition, it is evident that altering the flowering time is an avoidance strategy adopted by crops to maximise the fitness under reproductive stage stresses (Kazan and Lyons, 2016). Our SNP-based modelling analysis identified SNP markers linked with flowering time that strongly influenced variation in grain yield under water-deficit conditions in the rice association mapping panel (Supplementary Table 2). However, these SNP markers did not have a strong effect under control conditions, in which markers for N_{\max} were more important (Supplementary Table 2). Hence, the marker based modelling analysis can help to understand how environmental variables affect the relative

importance of phenotypic components and genotypic markers for complex traits. Further, this can greatly improve the selection efficiency for future genetic manipulation of crops to improve the productivity under changing climatic conditions.

Virtual designing new plant types by pyramiding yield-determining positive alleles

Grain yield results from many actions and interacting biochemical, morphological, and physiological processes taking place at different temporal and spatial scales in a crop. There are several lines of evidence for a shift in phenotypic characteristics while breeding the rice for improved grain yield. For instance, 15-20% grain yield increment was obtained by heterosis combined with phenotypic characteristics of new plant type (new plant type concept developed at IRRI was inspired by ideotype breeding) to develop a super hybrid rice (Peng et al., 2008; Yuan et al., 2003). Further, conventional crop models have become effective tools in identifying the best suitable combination of parameters, which helps in designing ideotypes for different environmental conditions (Aggarwal et al., 1997; Dingkuhn et al., 2007), thereby assisting crop breeding. However, such an approach lacks the connection of model input parameters to genetic information while designing the model based ideotype (Hammer et al., 2006; Martre et al., 2015). Recently, attempts were made to connect model input parameters to quantitative genetics and design the ideotype with yield advantage by pyramiding the marker alleles detected for model input parameters rather than grain yield *per se* (Letort et al., 2008; Gu et al., 2014).

Our simulation using a SNP-based model showed that the ideotype designed by pyramiding the positive alleles of only significant markers for model input parameters had higher grain yield potential than the ideotype designed based on markers of grain yield *per se* across control and water-deficit conditions (Fig. 5). The results clearly indicate the great potential of model-based dissection of a complex trait such as grain yield into its meaningful physiological component traits at different levels of biological organisation, and virtual pyramiding of their marker alleles to improve grain yield under different environments. Nevertheless, often ideotypes designed by crop growth modelling are contradictory and we are still far away from developing these virtual genotypes through molecular breeding and testing them under real field conditions. This could be due to the gap existing between model input parameters and genes or physiological function in response to changing environments (G×E/QTL×E interactions). Therefore, to progress in this work, there is a need to narrow down the gap between genetic control relating to model input parameters and physiological processes in the model (Génard et al., 2016).

Challenges in linking the eco-physiological model with genome-wide association mapping

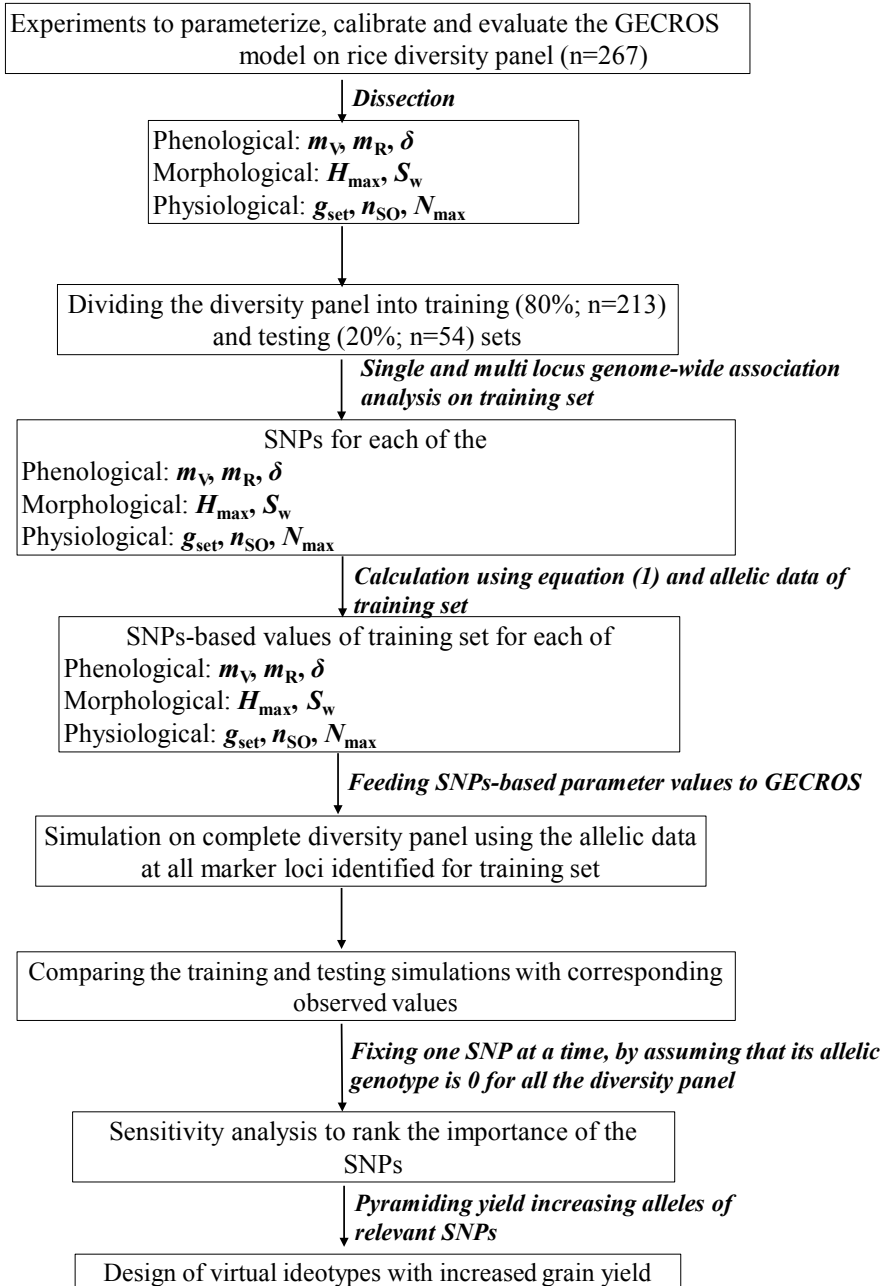
Despite promising results, there are several intrinsic problems when combining eco-physiological modelling with GWAS. First, the calibrated model was only moderately accounting for the genotypic variation in grain yield across treatments in tested environments, and poorly performed under a new environment. Eight simple genotype-specific model input parameters (component traits), which could be estimated from the phenotyping data available in the present study, were not enough to realize a reasonably good yield prediction in diverse rice genotypes under different environmental conditions. Some of the eight parameters even did not contribute much to yield (Table 2). Hence, the current GECROS model needs to be further upgraded in terms of both model structure and model-input parameters, to capture more genotype-specific physiological and morphological processes measured using modern high-throughput phenotyping platforms for better simulation accuracy. Second, in contrast to a biparental QTL analysis, identification and estimation of QTL effects in a GWAS analysis indeed need to account for the population structure and genetic relatedness. We have accounted for both population structure and genetic relatedness while identifying the QTL for model input parameters using GWAS. Yet, later while using equation 1 to deriving model input parameter values from the identified QTL, population structure and genetic relatedness were ignored. To what extent the estimates of additive effect of QTLs on model input parameters using equation 1 without population structure and genetic relatedness could affect the simulation accuracy of grain yield by the crop model would need a further analysis. For that, there is a need for statistical algorithms that can better account for population structure and genetic relatedness inside the model while linking the modelling with the GWAS approach.

Conclusion

In this study, we reported on a genotype-to-phenotype modelling exercise, and how whole crop eco-physiological modelling provides an effective link with quantitative genetics to enhance the efficiency of molecular breeding for crop improvement. Unlike statistical genotype-to-phenotype approaches that require many experiments (although on a single trait) to create a prediction model, eco-physiological genotype-to-phenotype modelling can, in principle, rely on few experiments for model parameterisation because the prediction is made largely based on eco-physiological principles as captured in the models. Our preliminary results when applying marker based modelling to identify key input parameters, were promising accounting for a large portion of the variation in grain yield under different environments, although largely

based on only one treatment in the 2013 experiment for model parameterisation. This approach not only provided more SNP markers for model input parameters than grain yield *per se*, but also ranked the relative importance of these markers for molecular breeding for improved grain yield. This complemented the analysis of grain yield *per se*, and went beyond the existing reports of Mangin et al. (2017) and Dingkuhn et al. (2017a, b), who only illustrated the use of crop modelling to enhance the phenotyping for GWAS. Nevertheless, we also identified several pitfalls of such a modelling approach, which need to be addressed in future studies.

Supplementary information in Chapter 5



Supplementary Figure 1: Flow chart explaining the stepwise methodology adapted to combine the genome-wide association study (GWAS) with an eco-physiological crop modelling (GECROS). This flow chart was modified from Gu et al. (2014).

Supplementary Table 1: Multiple linear regression (MLR) analysis of significant SNPs detected through the genome-wide association analysis against the model input parameters and grain yield. R^2 value represents the percentage of phenotypic variation explained by all the SNP markers for a given trait.

Parameter	Chromosome	Position	u	Additive effects (a_n)	P value	R^2 (%)
(A) Phenological						
m_V	1	28262688	64.19	2.5371	0.001111	74.2
	1	9243669		3.7197	5.24E-08	
	1	7344741		-1.5835	0.000138	
	2	4390533		3.6114	3.17E-12	
	2	23538671		-2.58	1.76E-11	
	3	10106310		-2.3681	0.000467	
	4	19591930		4.8726	5.21E-11	
	4	1258958		-2.6171	0.000878	
	6	26238067		-2.467	1.54E-05	
	7	99783		-4.3277	1.48E-13	
	9	18375567		-1.2878	0.000274	
	10	4760551		-1.3883	0.00039	
	12	1691770		-4.0529	4.73E-09	
	12	18314444		2.5202	9.73E-12	
12	3640868	-2.1222	6.73E-05			
12	7323204	-2.7144	1.81E-07			
m_R	4	33336957	32.95	0.6348	0.003947	51.6
	4	3661992		-2.5713	1.60E-09	
	4	20195438		3.362	2.53E-11	
	4	20014494		-1.7035	7.79E-06	
	5	16151637		0.8617	3.29E-05	
	9	22561421		-13.2386	4.75E-16	
	9	22561709		11.0251	1.79E-12	
	9	16415255		0.6762	0.002308	
11	19245430	1.1817	0.000162			
δ	1	27113695	0.13	-0.022173	0.001154	65.1
	2	5508005		0.024534	0.000143	
	2	30150945		0.039265	3.27E-08	
	4	4499266		0.03125	4.75E-08	
	5	5619386		0.017076	0.000126	
	10	2718469		-0.028512	5.49E-07	
	11	22826451		0.019679	0.000269	
	11	6520591		0.026071	2.78E-05	
	12	15123621		0.043865	< 2e-16	
(B) Morphological						
H_{max}	1	39255482	1.29	-0.06984	0.000147	77.0
	1	38286772		-0.1849	< 2e-16	
	1	21100541		0.10041	1.64E-06	
	1	852462		0.04606	0.000382	
	1	37707297		0.06128	1.44E-05	
	1	6077035		-0.03864	0.000458	
	2	24267632		-0.047	0.000128	
	2	774705		0.05459	1.56E-05	
	4	16556278		0.03247	0.001486	
	7	58252		-0.11813	1.34E-13	
	8	7880762		-0.10699	7.32E-12	
8	19677137	0.08531	0.000217			
10	2506985	-0.06651	0.002954			

Supplementary Table 1. (Continued)

	2	554478		0.0008908	3.21E-08	
	2	30699332		0.0008471	3.22E-06	
	2	17222218		-0.0015312	2.41E-06	
S_w	2	11071729	0.022	0.0005774	0.000404	47.3
	3	16725807		0.0009015	1.12E-07	
	3	12717890		-0.0007547	7.25E-06	
	7	23227646		-0.0008358	3.21E-07	
	12	7731908		0.0011273	1.92E-10	
(C) Physiological						
	2	29373768		-0.05334	2.54E-07	
	6	6585943		0.031565	2.00E-07	
g_{set}	10	14926494	0.732	0.02464	1.97E-05	42.2
	10	18906753		0.023826	9.76E-05	
	12	20014218		-0.032433	3.48E-06	
	12	21173768		0.016498	0.00755	
	1	42643627		4.52E-04	9.10E-05	
	1	6765299		2.66E-04	0.001454	
	1	22900197		-2.82E-04	0.000543	
	2	34358656		6.35E-04	7.67E-10	
	3	25074645		-5.29E-04	5.34E-06	
	3	16529108		5.79E-04	1.92E-12	
	4	1982000		-3.23E-04	0.000173	
n_{SO}	4	31449324	1.13E-02	-3.09E-04	0.000703	70.0
	5	14030811		-3.43E-04	1.59E-05	
	7	467419		-7.43E-04	1.95E-15	
	7	4568023		-4.87E-04	5.93E-10	
	7	9524268		-6.50E-04	1.34E-05	
	9	7207743		-4.18E-04	0.000483	
	11	25041651		-7.32E-04	4.89E-07	
	12	20907521		8.55E-04	< 2e-16	
	12	17569836		-5.84E-04	1.54E-07	
	1	22221764		-0.43691	3.05E-06	
	1	18893159		0.37043	7.18E-05	
	1	41741982		-0.40857	0.000239	
	4	34815309		-0.77981	1.62E-10	
	5	658940		-0.2115	0.000765	
	6	1360962		0.34729	3.56E-05	
N_{max}	7	23760855	5.84	-0.75225	3.80E-08	66.8
	8	2341829		0.28059	0.000122	
	8	20492803		-0.32529	8.02E-08	
	11	10143495		0.27417	7.34E-06	
	11	965990		-0.3564	0.001213	
	12	6720935		-0.45876	5.80E-09	
	12	19666909		-0.46896	1.32E-06	
	1	37302008		-10.331	0.27545	
	1	537855		1.933	0.78126	
	2	26263170		15.201	0.16315	
	2	26654759		19.416	0.05706	
	4	10502119		31.805	0.02564	
	5	658940		-43.576	3.53E-09	
Grain yield	6	10086748	406.63	-20.301	0.01844	44.3
	8	2756338		1.809	0.83464	
	8	2341829		24.607	0.02028	
	11	7789963		-48.323	0.0011	
	11	10101900		-20.479	0.00836	
	12	22741407		-46.749	8.56E-07	

Supplementary Table 2: The SNPs-based GECROS model accounting for the phenotypic variance of grain yield in a rice association mapping panel (n=267) by different sets of simulations by stepwise fixing one marker at a time.

Parameter	Chr	Position	Control		Water-deficit	
			R ² (%)	Rank	R ² (%)	Rank
(A) Phenological						
<i>m_v</i>	1	28262688	30.5	29	20.5	5
	1	9243669	29.4	12	16.0	2
	1	7344741	31.5	49	29.4	86
	2	4390533	29.1	10	18.0	3
	2	23538671	29.6	14	24.0	14
	3	10106310	33.1	87	29.4	85
	4	19591930	28.6	8	14.9	1
	4	1258958	31.8	65	29.1	84
	6	26238067	31.5	47	28.7	80
	7	99783	29.9	19	30.0	88
	9	18375567	31.6	60	26.6	62
	10	4760551	30.9	34	26.9	66
	12	1691770	31.9	69	31.0	89
	12	18314444	31.7	64	23.6	9
	12	3640868	32.1	75	29.0	83
	12	7323204	32.7	82	29.5	87
	<i>m_R</i>	4	33336957	32.0	70	25.8
4		3661992	29.9	20	25.9	44
4		20195438	32.6	81	25.9	45
4		20014494	30.7	31	25.6	37
5		16151637	32.0	71	26.2	57
9		22561421	29.8	18	26.0	49
9		22561709	33.5	90	25.0	33
9		16415255	31.6	50	25.4	35
11	19245430	31.7	61	25.8	41	
<i>δ</i>	1	27113695	31.6	53	26.1	50
	2	5508005	30.6	30	24.5	24
	2	30150945	30.7	32	23.9	12
	4	4499266	30.2	24	24.2	19
	5	5619386	30.5	27	24.9	30
	10	2718469	31.9	66	26.8	63
	11	22826451	30.3	25	24.9	31
	11	6520591	30.1	21	24.5	25
12	15123621	30.1	22	24.1	18	

Supplementary Table 2. (Continued)

(B) Morphological						
H_{\max}	1	39255482	32.3	78	28.9	82
	1	38286772	32.0	73	31.7	90
	1	21100541	32.3	79	28.4	79
	1	852462	31.5	46	27.4	72
	1	37707297	30.5	28	27.3	71
	1	6077035	31.2	39	25.7	39
	2	24267632	31.4	42	24.8	28
	2	774705	31.6	57	28.2	76
	4	16556278	31.1	35	26.3	59
	7	58252	28.8	9	20.5	4
	8	7880762	31.4	41	25.8	42
	8	19677137	32.0	74	28.2	77
	10	2506985	30.4	26	23.6	8
	S_w	2	554478	31.5	43	26.2
2		30699332	31.7	62	26.0	47
2		17222218	31.4	40	26.1	55
2		11071729	31.5	45	26.1	54
3		16725807	31.6	54	26.1	51
3		12717890	31.6	55	26.1	53
7		23227646	32.0	72	26.1	56
12		7731908	31.5	44	26.1	52
(C) Physiological						
g_{set}	2	29373768	31.5	48	24.6	26
	6	6585943	31.6	58	26.5	60
	10	14926494	31.6	51	24.4	21
	10	18906753	29.6	17	24.0	15
	12	20014218	31.6	59	24.0	17
	12	21173768	31.6	52	25.3	34
n_{so}	1	42643627	31.2	37	26.0	48
	1	6765299	31.7	63	27.0	68
	1	22900197	31.2	38	25.0	32
	2	34358656	29.6	15	24.0	16
	3	25074645	32.9	85	26.9	65
	3	16529108	27.7	5	22.4	7
	4	1982000	33.1	86	27.8	74
	4	31449324	31.9	68	27.1	70
	5	14030811	32.6	80	27.0	69
	7	467419	31.9	67	23.7	10
	7	4568023	33.4	89	27.7	73
	7	9524268	33.2	88	26.8	64
	9	7207743	32.9	84	27.9	75
	11	25041651	31.6	56	26.0	46
12	20907521	32.9	83	24.7	27	
12	17569836	31.2	36	26.9	67	

Supplementary Table 2. (Continued)

	1	22221764	27.5	4	24.4	22
	1	18893159	29.2	11	24.5	23
	1	41741982	30.2	23	25.8	43
	4	34815309	32.2	77	25.7	38
	5	658940	29.4	13	25.5	36
	6	1360962	25.9	1	21.5	6
N_{\max}	7	23760855	26.0	2	24.8	29
	8	2341829	28.1	7	24.0	13
	8	20492803	32.2	76	28.7	81
	11	10143495	30.8	33	28.3	78
	11	965990	29.6	16	26.5	61
	12	6720935	27.2	3	24.3	20
	12	19666909	27.9	6	23.8	11
Baseline simulation			31.6		26.1	

CHAPTER 6

General discussion

The current global climate change is well characterized with more frequent occurrence of the major abiotic stresses such as water-deficit and high temperature severely affecting crop productivity. Among the cereals, rice (*Oryza sativa* L.) is likely to become more affected by water-deficit stress than other cereals due to its adaptation to semi-aquatic conditions. Although water-deficit stress during the reproductive stage is most common and devastating, stress during the vegetative stage is also evidenced and can have significant carry-over effects on integrative traits like yield in rice (see Chapter 1). Therefore, it is imperative to develop rice genotypes with improved tolerance to water-deficit stress at any time during the growing period to ensure current and future food security.

During evolution, plants have developed several morphological, physiological and biochemical defence strategies to deal with water-deficit stress, and in most cases these strategies operate in synergy. Because of the multifaceted network of interactions among these strategies, tolerance to water-deficit stress is a complex, quantitative trait. Traditional breeding efforts to improve tolerance to water-deficit stress are indeed hampered by this complexity and by the quantitative nature of the trait (Xiong et al., 2006). Therefore, a better understanding of the above-mentioned defence strategies with their underlying physiological, genetic and molecular determinants is required to improve this stress tolerance.

Progress in developing high-throughput genome sequencing has been rapid over the last decade (Metzker, 2010). This rapid development has made it possible to sequence the whole genome of thousands of crop genotypes. Consequently science is now able to dissect the natural genetic variation resulting in a better scientific understanding of the genotype-to-phenotype relationship through mapping quantitative trait loci (QTLs), and thus provides a new strategic tool to breeders for rapid improvement of stress tolerance (Tuberosa and Salvi, 2006).

Most of the previous ecophysiological crop growth models were developed to predict crop yield, most likely of a few genotypes, in response to environmental variations. However, present generation ecophysiological crop growth models have been developed in a way that they can better handle the genetic difference of quantitative traits (under conditions with and without stress) among many genotypes, notably using genetically mapped QTL information as model input (see review of Yin & Struik, 2016). This further helped to narrow down the gap between genotype and phenotype based on the impact of changing environmental conditions on complex traits (Gu et al., 2014). Such QTL-based crop growth modelling can dissect complex traits (e.g. grain yield) into biologically meaningful, physiological component traits that are genetically less complex. Once such models are properly validated they can assist

marker-assisted selection and can support the design of virtual crop ideotypes (Gu et al., 2014), thereby accelerating traditional crop breeding. The simultaneous development of a new generation of crop models, state-of-the-art genotyping tools and enhanced insight in the crop physiology of stress tolerance opened new opportunities to advance breeding for stress tolerance in rice. Hence, in this dissertation, I have followed a multidisciplinary approach including the physiology, genetics and crop modelling, to better understand the adaptation of rice to water-deficit stress.

In this general discussion, I will provide a comprehensive analysis of my research findings and will cover the following major aspects.

- Physiological, morphological and root anatomical plasticity of rice to water stress during the vegetative stage, in comparison with the plasticity of wheat;
- Genetic control of root morphological and anatomical plasticity to water-deficit stress during the vegetative stage of rice;
- Challenges in phenotyping root traits for a genetic mapping study;
- Genetic control of grain yield and its components under water-deficit stress during the reproductive stage of rice;
- Linking ecophysiological modelling with genome wide association mapping to design a rice ideotype for grain yield.

I strongly believe that the knowledge generated in this study is an invaluable source for future scientific studies, and provides useful fundamental biological insights that help to understand the tolerance to water-deficit stress. Further, these findings can also help to improve the selection efficiency of rice breeding to improve stress adaptation. Finally, further research needs will be discussed.

Rice displays weaker phenotypic plasticity in response to water-deficit stress during the vegetative stage than wheat

Plants display many responses to water-deficit stress including changes in gene expression, metabolite production, gas exchange physiology, and morphology (Chaves and Oliveira, 2004). These responses can be measured as phenotypic plasticity, i.e. the ability of a given genotype to produce multiple phenotypes in response to changing environments (Sultan, 2000). Because

of the primary role in water and nutrient uptake, plasticity in traits related to root morphology and anatomy are of great importance to improve rice stress adaptation and productivity. During its evolution, rice has developed a phenotypic plasticity to adapt to a wide range of moisture regimes, i.e. from traditional lowland (paddy rice) to upland/aerobic (moderately stress conditions) or severe water-deficit stress conditions (Khush, 1997). Indeed, several previous studies on rice have reported the role of root morphological plasticity in water-deficit adaptation. Plasticity in root length density (Kano-Nakata et al., 2011; Tran et al., 2015) and in lateral root length and/or branching (Suralta et al., 2010; Kano et al., 2011; Kano-Nakata et al., 2013) has been known to improve the water uptake and photosynthesis and thereby shoot biomass in rice under water-deficit conditions. Despite these research findings, rice is still considered to be relatively weakly adapted to water-deficit, certainly in comparison to other dryland cereal crops, such as wheat, maize and sorghum. In addition, there is inadequate knowledge on how rice differs from dryland cereals, and on which phenotypic traits related to water-deficit stress adaptation matter most (Praba et al., 2009). To fill this knowledge gap, I have evaluated the physiological, morphological and anatomical response of rice genotypes well adapted to different moisture regimes (lowland, aerobic and water-deficit conditions) with wheat genotypes that are drought tolerant under water-deficit stress during the vegetative stage. In this experiment, a comprehensive analysis between these two divergent species allowed to demonstrate the functional role of organ/tissue plasticity to independently validate known strategies and to identify novel complementary mechanistic means for adapting to water-deficit stress. In general, rice genotypes demonstrated a weaker morphological and anatomical plasticity in the shoot and in the root than wheat under water-deficit stress (Chapter 2).

Passioura (1997) suggested that wheat subjected to water-deficit during the vegetative stage tends to save soil water for sensitive stages in yield formation; the same tendency was suggested for pearl millet (Kholová et al., 2010). Both wheat genotypes studied in my experiment developed thicker leaves, thicker roots and showed moderate tillering under water-deficit stress during the vegetative stage. These responses help to conserve soil moisture for use during later stages of development. The plant ideotype of rice proposed during the 1980s for water-deficit adaption includes most of the traits identified and mentioned above (for details see Henry, 2013). In contrast, two rice genotypes used in the experiment developed thinner roots in response to water-deficit stress, suggesting they were primed towards rapid water consumption, since having thinner roots is associated with an increase in overall root hydraulics enabling rapid uptake of water (Reich et al., 1998; Eissenstat and Achor, 1999; Solari et al.,

2006; Hernández et al., 2010). Such a rapid depletion of soil water reserves by thinner roots can result in higher susceptibility to water-deficit stress (Ryser, 2006).

The effects of water-deficit stress on radial root anatomy is often less studied than the effects on root morphology, but differences in root anatomical characteristics strongly influence water transport. Water transport in the root is proportional to the fourth power of the radius of the xylem conduit (Tyree and Ewers, 1991). The xylem conduit appears to be four times larger in deep roots than in a shallow root system (Jackson et al., 2000). In my study, the xylem diameter was smaller in rice with its shallow root system than in wheat, which has a deep root system. Increasing the water uptake by increasing the xylem size has been suggested in rice (Nguyen et al., 1997). Moreover, the plasticity of xylem diameter and number of xylem vessels in response to water-deficit in wheat was a novel finding, which provided additional mechanistic understanding of the plasticity of wheat roots towards water-deficit stress (Chapter 2). Further, (Parent et al., 2010) suggested that rice could be a species with acceptable water-deficit tolerance after potential genetic improvements of root characteristics. Recently, the relationship between root architectural plasticity and yield stability was established under water-deficit in the field in a rice population derived from crossing traditional and improved genotypes (Sandhu et al., 2016). Therefore, growing rice like wheat is possible, provided additional efforts are made to identify traits that are related to a stress tolerant phenotype or to plasticity towards water-deficit stress, and to integrate such traits in breeding programs with a major emphasis on root morphological and anatomical plasticity.

Genetic control of plasticity in root morphology and anatomy in response to water-deficit stress during the vegetative stage of rice

The comparison of rice with wheat water-deficit tolerant genotypes made it possible to identify the functional relevance of root morphological and anatomical plasticity in water-deficit tolerance (Chapter 2). In addition, previous studies have proven that phenotypic plasticity is heritable (Nicotra and Davidson, 2010), and is controlled by key regulatory genes that regulate the growth and development in response to changing environments (Juenger, 2013). For instance, quantitative genotypic variation has been assessed and relevant QTL regions have been identified for plasticity of root hair length (Zhu et al., 2005a) and lateral root number (Zhu et al., 2005b) in maize under low phosphorus conditions. Similarly, it was demonstrated that genomic regions regulating the plasticity of increased root biomass in response to water-deficit stress were located on chromosome 1BS in wheat (Ehdaie et al., 2012). In addition to root

morphological plasticity, plasticity in root anatomy, water-use efficiency (WUE) and phenology were associated with improved plant performance across changing environments in several species (Sadras et al., 2009; Niones et al., 2012; Niones et al., 2013; Kenney et al., 2014). In the past, hundreds of root traits/water-deficit tolerant QTLs were identified in rice, but genomic regions regulating the phenotypic plasticity of roots traits were rarely addressed. To the best of my knowledge, only QTLs regulating the plasticity of aerenchyma development (Niones et al., 2013), root length density (Kano-Nakata et al., 2011; Tran et al., 2015), lateral root growth (Suralta et al., 2010; Kano-Nakata et al., 2011) and root architectural plasticity (Sandhu et al., 2016) in response to water-deficit were identified in rice. Understanding the genetic and molecular mechanisms controlling the phenotypic plasticity of root morphology and anatomy will be essential for effective selection and breeding to improve rice water-deficit tolerance.

Diverse rice genotypes are a pool of naturally occurring mutations that can give fundamental insights into plant function as well as a vital resource of novel beneficial alleles for crop plant improvement (McCouch et al., 2013). In the experiment described in Chapter 3, diverse indica rice genotypes were used to investigate the genetic architecture of root traits (root morphology and anatomy) across two moisture regimes (control and water-deficit) and of their calculated plasticity through a genome-wide association study (GWAS). Compared to those of many dicot species, the root traits of rice and other cereals are complex due to the fibrous root system consisting of many hierarchical orders of seminal, nodal, and lateral roots and root hairs. These different types of roots are highly plastic in response to water-deficit and nutrient stress and are strongly regulated by a complex network of many small-effect QTLs/genes. Our GWAS analysis identified that the genetic basis of root morphology and anatomy was different for the control and water-deficit conditions. We detected a strong QTL \times environment interaction, in agreement with another recent study in rice (Li et al., 2017). This was further strengthened by the novel loci for plasticity of root traits detected in my study (Chapter 3), which indicated that plasticity of root traits is heritable and under genetic control.

The genetic loci associated with root traits and their plasticity were in proximity to phytohormone genes regulating biosynthesis, transport or signalling. Among the phytohormones, predominately auxin plays a major role in root growth and development (Jung and McCouch, 2013; Wu and Cheng, 2014; Mai et al., 2014). Several of the loci that were significantly associated with root traits across both water-regimes or with the plasticity of these traits was placed near to the auxin transport (e.g. AUXIN EFFLUX CARRIER [PIN]) and

signalling (e.g. auxin response factor [ARF], SMALL AUXIN UP-RNAs [SAUR]) genes. The PIN protein regulates the polar auxin transport and creates a differential auxin level within root system to regulate overall root architecture and growth with mutant alleles (*pin1* & *2*) altering root growth (Grieneisen et al., 2007). Genes regulating the cell division and differentiation (e.g. SCARECROW, EXPANSIN), redox homeostasis, hormone cross-talk (e.g. GASA10) and water transport (e.g. AQUAPORIN) were also detected near the root traits loci. Hence, genetic loci identified in my study (Chapter 3) provide an important basis for revealing the molecular mechanism of plastic root development, to improve the water-deficit tolerance of rice in future.

Phenotyping root systems under greenhouse and field conditions:

Challenges in genetic research on root characteristics

There has been a rapid development in high-throughput genomic technologies enabling to accurately sequence thousands of crop species genotypes. However, exploiting this genomic information in genetic mapping analysis is still challenging because of the lack of a reliable high-throughput phenotyping platform. The GWAS analysis as described in Chapter 3 also highlights the importance of phenotyping in genetic research on root traits of rice, which merits additional discussion here as presented in this section.

Root phenotyping under real field conditions is extremely challenging, and is rapidly becoming the major bottleneck for genetic studies on water-deficit stress tolerance. In the past, several QTLs for root traits in rice were identified by experimenting in polyvinyl chloride (PVC) tubes containing a soil from the field and /or by growing plants under hydroponic conditions in a glasshouse (<http://tropgenedb.cirad.fr/tropgene/JSP/interface.jsp?Module=RICE>). Nevertheless, very few of these QTLs have been validated under field conditions, in terms of their effects on root traits as well as on grain yield or yield components. This is mainly because phenotyping root traits on a large set of genotypes under field conditions is labour intensive, time consuming and costly. It is well known that conditions in pot experiments in the greenhouse strongly differ from field conditions, in terms of soil temperature (especially when the colour of the pot is black), compaction, water content and soil aeration (Poorter et al., 2012). For these reasons, QTLs identified under greenhouse conditions, in most cases, were not reproducible under field conditions.

Although phenotyping the root traits under field conditions is a more reliable and exciting approach, yet it is extremely complicated to retain complete root systems from the field soil. For this reason, PVC pots or hydroponic methods under greenhouse conditions were the

preferred choice in most of the previous studies and in the present study as well. Presently many image analysis tools are available for capturing the root system and extracting quantitative data on root architecture from captured images. For more details please see the online resource (www.plant-image-analysis.org) and few of them have been systematically discussed by Lobet and Draye (2013). In our study, we used the WinRHIZO root image analysis tool (Chapters 2-3), which provided quantitative data on different components of the root system such as root thickness, total root length, root surface area, root volume, root thickness, root length classified for various classes of root thickness and root topology. Such analysis allowed investigating the entire root system and expanding our analysis beyond what could be traditionally measured by hand such as maximum root length. In addition, our genetic analysis identified the core regions of the rice genomes (SNPs or sometime termed QTLs) that had most significant impact on root development and their plasticity in response to water-deficit stress. Further, our gene content analysis also identified the most likely underlying *a priori* candidate genes, although the detailed future molecular characterization of these genes is essential to validate their roles in root development. Most of the root image analysis tools, including the one I have used in this study, are requiring destructive root sampling, which do not allow understanding the dynamics of root growth over time and space. Therefore, in the future, there is a need of non-invasive root phenotyping tools to measure the dynamic nature of root growth during different phases of plant development under target field conditions. Availability of such root phenotyping tools will be expected to provide tremendous information on the network of QTLs or genes regulating the root growth and development during the entire growing period of the plant or crop.

Harnessing the QTL alleles for tolerance to water-deficit stress during the reproductive stage to improve rice yield

High yielding semi-dwarf rice varieties that have been developed during the Green Revolution by the introduction of the dwarfing *sd1* allele are better suited to optimal conditions, but typically sensitive to water-deficit stress (Vikram et al., 2015). Rice is affected by water-deficit stress throughout its life cycle, with the greatest grain yield losses reported for water-deficit stress during the reproductive stage (Venuprasad et al., 2007). To date, breeders have improved the tolerance to water-deficit stress during the reproductive stage by QTL alleles for grain yield and its components, detected in bi-parental mapping populations of rice (Venuprasad et al., 2009; Bernier et al., 2009; Vikram et al., 2011). This strategy has made promising progress in tolerance to water-deficit stress in rice, but still many of the QTLs/genes/alleles remain hidden

in the genetic diversity that rice possesses and cannot be explored through traditional linkage analysis. In the experiments described in Chapter 4, I have explored the *indica* rice diversity panel to identify those hidden QTLs/genes for grain yield and its components through a GWAS under well-watered conditions and under water-deficit stress during the reproductive stage for two years. To date very few studies have considered the water-deficit stress during the reproductive stage using a GWAS approach (Ma et al., 2016; Pantalhão et al., 2016; Swamy et al., 2017). The reason for this is that it is difficult to manage the plant phenology, especially the flowering time, in such a way that all genotypes are synchronized in terms of the timing of the stress treatment. In my study, I have followed staggered sowing of rice genotypes to synchronize their phenology and thus the phenological timing of exposure to water-deficit stress. Significant numbers of QTLs (SNPs) were detected for grain yield and its component traits, but most of these QTLs were specific to treatment and years, which means that there was a high QTL \times environment interaction (QEI).

Crop plants have developed a remarkable ability to respond to changing environments, and understanding the proximate and final mechanism behind these responses remains challenging. It is important to note that genotype \times environment interactions are common for both QTL and gene expression, which are primarily determined by differential sensitivity of alleles (Marais et al., 2013). In our study, most of the QTLs for yield and its components were showing QEI. Sometimes these QEI can also be termed a QTL-effect plasticity. Grain yield is a complex trait with low heritability and strong environment interaction, mostly controlled by small-effect loci, and seldom by large-effect loci. To date, breeders have often used large- and consistent-effect grain yield QTLs under varying environments, to improve tolerance to water-deficit stress during the reproductive stage in rice (Bernier et al., 2009; Vikram et al., 2011). QTLs identified through the GWAS of this study for grain yield and its component traits were small-effect loci with a strong QEI.

The QEI plays an important role in adaptation to changing environments, and is regulated by key environmental sensing genes (Marais et al., 2013). To understand the molecular basis of QEI for yield and its components, it is necessary to identify the underlying genes. The grain yield QTL loci Q9 (2013) and Q11 (2014) detected under water-deficit stress (Chapter 4) were placed near Phosphomannose mutase and Squalene epoxidase genes. Both genes were strongly responsive to abiotic stress and have a role in reactive oxygen species detoxification. Therefore, cloning and characterizing the genes from QTLs displaying QEI in

water-deficit will provide much needed molecular causes of genotype \times environment interactions, to improve stress tolerance of rice.

Under water-deficit stress, the selection for secondary traits such as canopy temperature could be used effectively to screen many genotypes. Low canopy temperature contributing to stress resistance through efficient water uptake by the roots helps to maintain cooler canopy (Richards et al., 2010). In my experiment, canopy temperature showed a negative correlation with grain yield under water-deficit ($r = -0.48$; data from measurements in the same experiment conducted by another PhD candidate), and therefore identifying the QTLs for desirable secondary traits, in addition to grain yield, could be an effective approach to improve stress tolerance of rice. Moreover, I could not find any root trait QTLs (Chapter 3) that were co-localized with QTLs identified for grain yield and its components under water-deficit stress (Chapter 4), despite using the same rice accessions in both chapters. This was mainly because QTLs for root traits were identified in PVC pots with water deficit stress during the vegetative stage under natural greenhouse conditions, while QTLs identified for grain yield and its components were identified under field water-deficit stress during the reproductive stage. Such results are obvious because the plant responses to water-deficit stress during the vegetative stage differ from those to water-deficit stress during the reproductive stage. In addition, growth conditions and stress level in pot experiments in the greenhouse (Chapter 3) strongly differ from those in real field experiments (Chapter 4), which might have also reduced the reproducibility of our root QTLs under field conditions. Thus, a tolerance mechanism observed for one type of water-deficit stress may not be effective in another type of stress under different growth and management conditions, which will eventually cause additional complexity in the breeding programme for tolerance to water-deficit stress.

Merging eco-physiological modelling with genome-wide association mapping genetics

The use of crop growth models is rapidly increasing to understand complex traits such as grain yield under water-deficit stress. Crop models dissect the complex grain yield and its response to environment into simple, biologically meaningful, physiological components. In addition, Yin et al. (2002) proposed the integration of QTL information into a process-based mechanistic crop growth model to design the grain yield ideotype and to support marker assisted selection under target environments. Further, linking the QTL information into an ecophysiological model can create a model that predicts the final phenotype (e.g. grain yield) from the

combination of alleles by analysis of QTLs for model input traits. For example, grain yield was predicted under water-deficit, and was broken down into seven component physiological traits in rice (Gu et al., 2014). Similarly, the response of leaf growth to high temperature and water-deficit stress was broken down to three components in maize (Reymond et al., 2003). In Chapter 5, the same principal was also followed, and I tried to link the QTL information detected through a GWAS analysis to the processed-based ecophysiological GECROS model. The QTL-based model moderately simulated the grain yield variation of rice diversity panel in tested environments (2013 experiment) but poorly in completely new environments (2014 experiment). The grain yield variation in the well-watered treatment was mainly explained by the input trait total crop nitrogen uptake (N_{\max}) and in the treatment with water-deficit stress during the reproductive stage by pre-flowering time (m_v). Hence, crop phenology is a critical component of yield physiology strongly influenced by prevalent environmental conditions (Boonjung and Fukai, 1996). The QTLs identified for most of the model input trait did not coincide with the regions of the genome for grain yield *per se* except for N_{\max} in control conditions, suggesting that mapping the input traits identified additional QTLs affecting grain yield. In addition, my analysis not only identified more markers for model input traits but also assessed their relative importance in explaining the grain yield variation, which can enhance the efficacy of marker-assisted selection. Moreover, my ideotype designing analysis clearly indicated that pyramiding the markers of model input traits had higher grain yield advantage than pyramiding the markers for grain yield *per se*. Therefore, the approach of linking crop modelling with GWAS has added values to studies on mapping grain yield *per se*. Most existing modelling studies have shown that crop models can assist to improve the phenotyping of GWAS (Mangin et al., 2017; Dingkuhn et al., 2017b; Dingkuhn et al., 2017a). Chapter 5 demonstrates that crop modelling not only assists the phenotyping, but also can integrate with GWAS into a promising strategy of crop ideotype design. In conclusion, the use of models provides an efficient platform to integrate the genetics and crop physiology to narrow down the genotype-phenotype gap.

Final remarks and future research

The data generated in my study is very rich and powerful. However, the information collected requires further analysis and suggests the need to carry out additional trials, especially to validate candidate genes and to supplement our understanding of the diverse mechanisms of tolerance to water-deficit stress. The combination of genetics and crop growth modelling offers

great potential to rapidly assess the importance of model input traits and their impact on final grain yield in response to changing environments. Nevertheless, combining the crop modelling with GWAS to predict grain yield identified several challenges (see Chapter 5).

Current advanced crop models may miss important traits that determine yield differences among genotypes. For example, many morphological traits were identified relevant for genotypic differences in response to water-deficit stress (Chapters 3 and 4), but they are not yet captured in generic crop models like GECROS that was used in my study, for expressing differences among rice genotypes.

- Population structure and genetic relatedness strongly influencing the QTL genetic effect on trait was accounted for while identifying the markers for model input traits in GWAS analysis. However, while feeding the effect of identified QTLs for model input traits to the ecophysiological crop growth model, the population structure and genetic relatedness was ignored due to lack of statistical algorithms.
- Recently, genomic selection has been revolutionizing the marker-assisted breeding mainly because it includes all marker information in the prediction model, avoiding the biased estimation of QTL effect -a major disadvantage retained by GWAS (Meuwissen et al., 2001), thereby capturing the large part of phenotypic variation explained by small effect QTLs. Therefore, future studies should consider integrating crop growth models and genomic selection, with better optimisation of population structure in training and testing sets.

There is no doubt that generic crop models like GECROS need refining and further calibration, when applied to specific crops for analysing genotype-to-phenotype relationships. Another route is to seek advanced statistical approaches to enhance the resolution of the genetic prediction. One way of improvement is to integrate crop growth modelling with genomic selection or prediction. I expect that a new class of refined ecophysiological crop growth models, when integrated with advanced genomic and genetic prediction tools, will further narrow down genotype-phenotype gaps, thereby improving the efficiency of applied genetics and traditional breeding for tolerance to water-deficit stress.

In addition, studies for unravelling the mechanism related to abiotic stress in cereals, including this study for water-deficit stress, have been mostly independent, not considering multiple stress (drought, high temperature and flooding) imposition. However, under actual field conditions often these abiotic stresses occur simultaneously and interact with each other (Jagadish et al., 2012). Among the abiotic stresses, combined occurrence of water-deficit stress

and high-temperature stress is identified to be the most commonly occurring companion stress (Mittler, 2006). In this context, I have systematically reviewed some progress on individual and combined effects of water-deficit stress and high-temperature stress in interaction with elevated CO₂ on agronomic and physiological responses (Kadam et al., 2014). However, it is essential to dissect the tolerance of complex abiotic stresses in interaction through an integrative multidisciplinary approach of crop physiology, genetics and crop modelling, to create the next generation rice that can cope with climate change.

References

- Abdurakhmonov, I.Y., and Abdugarimov, A.** (2008) Application of association mapping to understanding the genetic diversity of plant germplasm resources. *International Journal of Plant Genomics* 2008: 18.
- Abramoff, M.D., Magalhaes, P.J., Ram, S.J.** (2004) Image processing with ImageJ. *Biophotonics International* 11: 36-42.
- Acevedo, E.H., Silva, P.C., Silva, H.R., Solar, B.R.** (1999) Wheat production in Mediterranean environments. In: Satorre, E.H., Slafer, G.A. (Eds.), *Wheat: ecology and physiology of yield determination*. Food Products Press, Binghamton, NY, pp. 295–331.
- Adachi, S., Tsuru, Y., Kondo, M., Yamamoto, T., Arai-Sanoh, Y., Ando, T., Ookawa, T., Yano, M., and Hirasawa, T.** (2010) Characterization of a rice variety with high hydraulic conductance and identification of the chromosome region responsible using chromosome segment substitution lines. *Annals of Botany* 106: 803-811.
- Aggarwal, P.K., Kropff, M.J., Cassman, K.G., and ten Berge, H.F.M.** (1997) Simulating genotypic strategies for increasing rice yield potential in irrigated, tropical environments. *Field Crops Research* 51: 5-17.
- Agrama, H.A., Eizenga, G.C., Yan, W.** (2007) Association mapping of yield and its components in rice cultivars. *Molecular Breeding* 19: 341-356.
- Aguilar, E.A.** (1998) Responses of banana roots to oxygen deficiency and its implications for *Fusarium* wilt. PhD Thesis. The University of Western Australia, Australia.
- Ahmad, I., Mian, A., Maathuis, F.J.M.** (2016) Overexpression of the rice *AKT1* potassium channel affects potassium nutrition and rice drought tolerance. *Journal of Experimental Botany* 67: 2689-2698.
- Ali, S., Gautam, R.K., Mahajan, R., Krishnamurthy, S.L., Sharma, S.K., Singh, R.K., and Ismail, A.M.** (2013) Stress indices and selectable traits in *SALTOL* QTL introgressed rice genotypes for reproductive stage tolerance to sodicity and salinity stresses. *Field Crops Research* 154: 65-73.
- Al-Tamimi, N., Brien, C., Oakey, H., Berger, B., Saade, S., Ho, Y.S., Schmöckel, S.M., Tester, M., Negrão, S.** (2016) Salinity tolerance loci revealed in rice using high-throughput non-invasive phenotyping. *Nature Communications* 7: 13342.
- Ambawat, S., Sharma, P., Yadav, N.R., Yadav, R.C.** (2013) MYB transcription factor genes as regulators for plant responses: an overview. *Physiology and Molecular Biology of Plants* 19: 307-321.
- Amelong, A., Gambín, B.L., Severini, A.D., and Borrás, L.** (2015) Predicting maize kernel number using QTL information. *Field Crops Research* 172: 119-131.
- Araus, J.L., Amaro, T., Zuhair, Y., Nachit, M.M.** (1997) Effect of leaf structure and water status on carbon isotope discrimination in field-grown durum wheat. *Plant, Cell & Environment* 20: 1484-1494.
- Araus, J.L., Slafer, G.A., Reynolds, M.P., and Royo, C.** (2002) Plant breeding and drought in C₃ cereals: What should we breed for? *Annals of Botany* 89: 925-940.
- Araya, T., Miyamoto, M., Wibowo, J., Suzuki, A., Kojima, S., Tsuchiya, Y.N., Sawa, S., Fukuda, H., von Wirén N., Takahashi, H.** (2014) *CLE-CLAVATA1* peptide-receptor signaling module regulates the expansion of plant root systems in a nitrogen-dependent manner. *Proceedings of the National Academy of Sciences* 111: 2029-2034.
- Armstrong, W., Beckett, P.M.** (1987) Internal aeration and the development of stellar anoxia in submerged roots. A multishelled mathematical model combining axial diffusion of oxygen in the cortex with radial losses to the stele, the wall layers and the rhizosphere. *New Phytologist* 105: 221-245.

- Armstrong, W., Beckett, P.M., Justin, S.H.F.W., Lythe, S. (1991) Modelling, and other aspects of root aeration by diffusion. In MB Jackson, DD Davies and H Lambers, eds, *Plant Life Under Oxygen Deprivation*, SPB Academic Publishing, The Hague, pp 267-282.
- Arrighoni, O., De Tullio, M.C. (2002) Ascorbic acid: much more than just an antioxidant. *Biochimica et Biophysica Acta* (BBA)-General Subjects 1569: 1-9.
- Ashikari, M., Sakakibara, H., Lin, S., Ymamoto, T., Takashi, T., Nishimura, A., Angeles, E.R., Qian, Q., Kitano, H., Matsuoka, M. (2005) Cytokinin oxidase regulates rice grain production. *Science* 309: 741-745.
- Aslam, M., Zamir, M.S.I., Afzal, I., Yaseen, M., Mubeen, M., Shoai, B.A. (2013) Drought stress, its effect on maize production and development of drought tolerance through potassium application. *Cercetări Agronomice în Moldova* 46: 99-114.
- Baluška, F., Jasik, J., Edelmann, H.G., Salajová, T., Volkmann, D. (2001) Latrunculin B-induced plant dwarfism: Plant cell elongation is F-actin-dependent. *Developmental Biology* 231: 113-124.
- Baluška, F., Salaj, J., Mathur, J., Braun, M., Jasper, F., Šamaj, J., Chua, N.H., Barlow, P.W., Volkmann, D. (2000) Root hair formation: F-actin-dependent tip growth is initiated by local assembly of profilin-supported F-actin meshworks accumulated within expansin-enriched bulges. *Developmental Biology* 227: 618-632.
- Bao, F., Shen, J., Brady, S.R., Muday, G.K., Asami, T., Yang, Z. (2004) Brassinosteroids interact with auxin to promote lateral root development in Arabidopsis. *Plant Physiology* 134: 1624-1631.
- Barnabás, B., Jäger, K., and Fehér, A. (2008) The effect of drought and heat stress on reproductive processes in cereals. *Plant, Cell & Environment* 31: 11-38.
- Barrett, J.C., Fry, B., Maller, J., Daly, M.J. (2005) Haploview: analysis and visualization of LD and haplotype maps. *Bioinformatics* 21: 263-265.
- Begum, H., Spindel, J.E., Lalusin, A., Borromeo, T., Gregorio, G., Hernandez, J., Virk, P., Collard, B., McCouch, S.R. (2015) Genome-wide association mapping for yield and other agronomic traits in an elite breeding population of tropical rice (*Oryza sativa*). *PLoS ONE* 10: e0119873.
- Bekh-Ochir, D., Shimada, S., Yamagami, A., Kanda, S., Ogawa, K., Nakazawa, M., Matsui, M., Sakuta, M., Osada, H., Asami, T., Nakano, T. (2013) A novel mitochondrial DnaJ/Hsp40 family protein *BIL2* promotes plant growth and resistance against environmental stress in brassinosteroid signaling. *Planta* 237: 1509-1525.
- Bernier, J., Serraj, R., Kumar, A., Venuprasad, R., Impa, S., Gowda, R.P.V., Oane, R., Spaner, D., Atlin, G. (2009) The large-effect drought-resistance QTL *qtl12.1* increases water uptake in upland rice. *Field Crops Research* 110: 139-146.
- Bernier, J., Kumar, A., Venuprasad, R., Spaner, D., and Atlin, G. N. (2007) A large-effect QTL for grain yield under reproductive-stage drought stress in upland rice. *Crop Science* 47: 507-516.
- Bernier, J., Kumar, A., Venuprasad, R., Spaner, D., Verulkar, S., Mandal, N. P., Sinha, P. K., Peeraju, P., Dongre, P. R., Mahto, R. N., and Atlin, G. (2009) Characterization of the effect of a QTL for drought resistance in rice, *qtl12.1*, over a range of environments in the Philippines and eastern India. *Euphytica* 166: 207-217.
- Bindi, M., and Olesen, J.E. (2011) The responses of agriculture in Europe to climate change. *Regional Environmental Change* 11: 151-158.
- Bindrabán, P.S., Hengsdijk, H., Cao, W., Shi, Q., Thiyagarajan, T.M., Van der Krogt, W., Wardana, I.P. (2006) Transforming inundated rice cultivation. *International Journal of Water Resources Development* 22: 87-100.

- Biscarini, F., Cozzi, P., Casella, L., Riccardi, P., Vattari, A., Orasen, G., Perrini, R., Tacconi, G., Tondelli, A., Biselli, C., Cattivelli, L., Spindel, J., McCouch, S., Abbruscato, P., Valé, G., Piffanelli, P., Greco, R. (2016) Genome-wide association study for traits related to plant and grain morphology, and root architecture in temperate rice accessions. *PLoS ONE* 11: e0155425.
- Blum, A. (2009) Effective use of water (EUW) and not water-use efficiency (WUE) is the target of crop yield improvement under drought stress. *Field Crops Research* 112: 119-123
- Bohmert, K., Camus, I., Bellini, C., Bouchez, D., Caboche, M., Benning, C. (1998) *AGO1* defines a novel locus of Arabidopsis controlling leaf development. *The EMBO Journal* 17: 170-180.
- Boonjung, H., and Fukai, S. (1996) Effects of soil water deficit at different growth stages on rice growth and yield under upland conditions. 2. Phenology, biomass production and yield. *Field Crops Research* 48: 47-55.
- Borba, T.C.D.O., Brondani, R.P.V., Breseghello, F., Coelho, A.S.G., Mendonça, J.A., Rangel P.H.N., Brondani, C. (2010) Association mapping for yield and grain quality traits in rice (*Oryza sativa* L.). *Genetics and Molecular Biology* 33: 515-524.
- Bouma, T.J., Nielsen, K.L., Koutstaal, B. (2000) Sample preparation and scanning protocol for computerised analysis of root length and diameter. *Plant and Soil* 218: 185-196.
- Bouman, B.A.M., Peng, S., Castañeda, A.R., and Visperas, R.M. (2005) Yield and water use of irrigated tropical aerobic rice systems. *Agricultural Water Management* 74: 87-105.
- Bouman, B.A.M., Yang, X., Wang, H., Wang, Z., Zhao, J., and Chen, B. (2006) Performance of aerobic rice varieties under irrigated conditions in North China. *Field Crops Research* 97: 53-65.
- Bradbury, P.J., Zhang, Z., Kroon, D.E., Casstevens, T.M., Ramdoss, Y., Buckler, E.S. (2007) TASSEL: software for association mapping of complex traits in diverse samples. *Bioinformatics* 23: 2633-2635.
- Bramley, H., Turner, N.C., Turner, D.W., Tyerman, S.D. (2009) Roles of morphology, anatomy, and aquaporins in determining contrasting hydraulic behavior of roots. *Plant Physiology* 150: 348-364.
- Brun, F., Wallach, D., Makowski, D., and Jones, J.W. (2006) "Working with dynamic crop models: evaluation, analysis, parameterization, and applications," Elsevier.
- Budak, H., Akpinar, B.A., Unver, T., Turktas, M. (2013) Proteome changes in wild and modern wheat leaves upon drought stress by two-dimensional electrophoresis and nanoLC-ESI-MS/MS. *Plant Molecular Biology* 83: 89-103.
- Buer, C.S., Sukumar, P., Muday, G.K. (2006) Ethylene modulates flavonoid accumulation and gravitropic responses in roots of Arabidopsis. *Plant Physiology* 140: 1384-1396.
- Bustos-Korts, D., Malosetti, M., Chapman, S., and van Eeuwijk, F. (2016) Modelling of genotype by environment interaction and prediction of complex traits across multiple environments as a synthesis of crop growth modelling, genetics and statistics. In "Crop Systems Biology: Narrowing the gaps between crop modelling and genetics" (X. Yin and P. C. Struik, eds.), pp. 55-82. Springer International Publishing, Cham.
- Chakrabarty, A., Aditya, M., Dey, N., Banik, N., Bhattacharjee, S. (2016) Antioxidant signaling and redox regulation in drought- and salinity-stressed plants. In MA Hossain, SH Wani, S Bhattacharjee, DJ Burritt, L-SP Tran, eds, *Drought Stress Tolerance in Plants, Vol 1: Physiology and Biochemistry*. Springer International Publishing, Cham, pp 465-498.

- Chaumont, F., Barrieu, F., Wojcik, E., Chrispeels, M.J., Jung, R.** (2001) Aquaporins constitute a large and highly divergent protein family in maize. *Plant Physiology* 125: 1206-1215.
- Chaves, M.M., and Oliveira, M.M.** (2004) Mechanisms underlying plant resilience to water deficits: prospects for water-saving agriculture. *Journal of Experimental Botany* 55: 2365-2384.
- Chaves, M.M., Maroco, J.P., and Pereira, J.S.** (2003) Understanding plant responses to drought-from genes to the whole plant. *Functional Plant Biology* 30: 239-264.
- Chen, M., Markham, J.E., Dietrich, C.R., Jaworski, J.G., Cahoon, E.B.** (2008) Sphingolipid long-chain base hydroxylation is important for growth and regulation of sphingolipid content and composition in Arabidopsis. *The Plant Cell* 20: 1862-1878.
- Chen, X., Goodwin, S.M., Boroff, V.L., Liu, X., Jenks, M.A.** (2003) Cloning and characterization of the *WAX2* gene of Arabidopsis involved in cuticle membrane and wax production. *The Plant Cell* 15: 1170-1185.
- Chenu, K., Chapman, S.C., Hammer, G.L., McLean, G., Salah, H.B.H., and Tardieu, F.** (2008) Short-term responses of leaf growth rate to water deficit scale up to whole-plant and crop levels: an integrated modelling approach in maize. *Plant, Cell & Environment* 31: 378-391.
- Cheong, Y.H., Pandey, G.K., Grant, J.J., Batistic, O., Li, L., Kim, B.G., Lee, S.C., Kudla, J., Luan, S.** (2007) Two calcineurin B-like calcium sensors, interacting with protein kinase CIPK23, regulate leaf transpiration and root potassium uptake in Arabidopsis. *The Plant Journal* 52: 223-239.
- Chimungu, J.G., Brown, K.M., Lynch, J.P.** (2014) Reduced root cortical cell file number improves drought tolerance in maize. *Plant Physiology* 166: 1943-1955.
- Ciais, P., Reichstein, M., Viovy, N., Granier, A., Ogee, J., Allard, V., Aubinet, M., Buchmann, N., Bernhofer, C., Carrara, A., Chevallier, F., De Noblet, N., Friend, A. D., Friedlingstein, P., Grunwald, T., Heinesch, B., Keronen, P., Knohl, A., Krinner, G., Loustau, D., Manca, G., Matteucci, G., Miglietta, F., Ourcival, J. M., Papale, D., Pilegaard, K., Rambal, S., Seufert, G., Soussana, J. F., Sanz, M. J., Schulze, E. D., Vesala, T., and Valentini, R.** (2005) Europe-wide reduction in primary productivity caused by the heat and drought in 2003. *Nature* 437: 529-533.
- Condon, A.G., Farquhar, G.D., Richards, R.A.** (1990) Genotypic variation in carbon isotope discrimination and transpiration efficiency in wheat. Leaf gas exchange and whole plant studies. *Functional Plant Biology* 17: 9-22.
- Cooper, M., Rajatasereekul, S., Immark, S., Fukai, S., and Basnayake, J.** (1999a) Rainfed lowland rice breeding strategies for Northeast Thailand.: I. Genotypic variation and genotype \times environment interactions for grain yield. *Field Crops Research* 64: 131-151.
- Cooper, M., Rajatasereekul, S., Somrith, B., Sriwisut, S., Immark, S., Boonwite, C., Suwanwongse, A., Ruangsook, S., Hanviriyapant, P., Romyen, P., Porn-uraisanit, P., Skulku, E., Fukai, S., Basnayake, J., and Podlich, D. W.** (1999b) Rainfed lowland rice breeding strategies for Northeast Thailand II. Comparison of intrastation and interstation selection. *Field Crops Research* 64: 153-176.
- Cosgrove, D.J.** (1998) Cell wall loosening by expansins. *Plant Physiology* 118: 333-339.
- Coudert, Y., Périn, C., Courtois, B., Khong, N.G., Gantet, P.** (2010) Genetic control of root development in rice, the model cereal. *Trends in Plant Science* 15: 219-226.
- Courtois, B., Ahmadi, N., Khowaja, F., Price, A.H., Rami, J.F., Frouin, J., Hamelin, C., Ruiz, M.** (2009) Rice root genetic architecture: Meta-analysis from a drought QTL database. *Rice* 2: 115-128.

- Courtois, B., Audebert, A., Dardou, A., Roques, S., Ghneim-Herrera, T., Droc, G., Frouin, J., Rouan, L., Gozé, E., Kilian, A., Ahmadi, N., Dingkuhn, M. (2013) Genome-wide association mapping of root traits in a japonica rice panel. *PLoS ONE* 8: e78037.
- Craufurd, P.Q., Wheeler, T.R., Ellis, R.H., Summerfield, R.J., Williams, J.H. (1999) Effect of temperature and water deficit on water-use efficiency, carbon isotope discrimination, and specific leaf area in peanut. *Crop Science* 39: 136-142.
- Crowell, S., Korniliev, P., Falcao, A., Ismail, A., Gregorio, G., Mezey, J., McCouch, S. (2016) Genome-wide association and high-resolution phenotyping link *Oryza sativa* panicle traits to numerous trait-specific QTL clusters. *Nature Communications* 7: 10527.
- Davenport, R.J., Muñoz-Mayor, A., Jha, D., Essah, P.A., Rus, A.N.A., Tester, M. (2007) The Na⁺ transporter *AtHKT1;1* controls retrieval of Na⁺ from the xylem in Arabidopsis. *Plant, Cell & Environment* 30: 497-507.
- Davies, W.J., Bacon, M.A. (2003) Adaptation of roots to drought. In H Kroon, EJW Visser, eds, *Root ecology*, Vol 168. Springer, Berlin, pp 173-192.
- De Datta, S.K. (1975) Major research in upland rice. International Rice Research Institute. Los Baños, Philippines.
- Dimkpa, S.O.N., Lahari, Z., Shrestha, R., Douglas, A., Gheysen, G., Price, A.H. (2016) A genome-wide association study of a global rice panel reveals resistance in *Oryza sativa* to root-knot nematodes. *Journal of Experimental Botany* 67: 1191-1200.
- Ding, S., Zhang, B., Qin, F. (2015) Arabidopsis *RZFP34/CHYR1*, a ubiquitin E3 ligase, regulates stomatal movement and drought tolerance via *SnRK2.6*-mediated phosphorylation. *The Plant Cell* 27: 3228-3244.
- Dingkuhn, M., Luquet, D., Clément-Vidal, A., Tambour, L., Kim, H.K., and Song, Y. (2007) Is plant growth driven by sink regulation? Implications for crop models, phenotyping approaches and ideotypes. *Frontis* 21: 155-168.
- Dingkuhn, M., Pasco, R., Pasuquin, J.M., Damo, J., Soulié, J.C., Raboin, L.M., Dusserre, J., Sow, A., Manneh, B., Shrestha, S., Balde, A., and Kretschmar, T. (2017a) Crop-model assisted phenomics and genome-wide association study for climate adaptation of indica rice. 1. Phenology. *Journal of Experimental Botany* 68: 4369-4388.
- Dingkuhn, M., Pasco, R., Pasuquin, J.M., Damo, J., Soulié, J.C., Raboin, L.M., Dusserre, J., Sow, A., Manneh, B., Shrestha, S., and Kretschmar, T. (2017b) Crop-model assisted phenomics and genome-wide association study for climate adaptation of indica rice. 2. Thermal stress and spikelet sterility. *Journal of Experimental Botany* 68: 4389-4406.
- Dixit, S., Singh, A., Sta Cruz, M.T., Maturan, P.T., Amante, M., Kumar, A. (2014) Multiple major QTL lead to stable yield performance of rice cultivars across varying drought intensities. *BMC Genetics* 15: 16.
- Doebley, J.F., Gaut, B.S., Smith, B.D. (2006) The molecular genetics of crop domestication. *Cell* 127: 1309-1321.
- Donald, C.M. (1968) The breeding of crop ideotypes. *Euphytica* 17: 385-403.
- Dong, J., Kim, S.T., Lord, E.M. (2005) Plantacyanin plays a role in reproduction in Arabidopsis. *Plant Physiology* 138: 778-789.
- Duitama, J., Quintero, J.C., Cruz, D.F., Quintero, C., Hubmann, G., Foulquié-Moreno, M.R., Verstrepen, K.J., Thevelein, J.M., Tohme, J. (2014) An integrated framework for discovery and genotyping of genomic variants from high-throughput sequencing experiments. *Nucleic Acids Research* 42: e44-e44.
- Ehdaie, B., Layne, A.P., and Waines, J.G. (2012) Root system plasticity to drought influences grain yield in bread wheat. *Euphytica* 186: 219-232.

- Eissenstat, D.M., Achor, D.S. (1999) Anatomical characteristics of roots of citrus rootstocks that vary in specific root length. *New Phytologist* 141: 309-321.
- Elhiti, M., Stasolla, C. (2009) Structure and function of homodomain-leucine zipper (HD-Zip) proteins. *Plant Signaling & Behavior* 4: 86-88.
- Elshire, R.J., Glaubitz, J.C., Sun, Q., Poland, J.A., Kawamoto, K., Buckler, E.S., Mitchell, S.E. (2011) A robust, simple genotyping-by-sequencing (GBS) approach for high diversity species. *PLoS ONE* 6: e19379.
- Fan, C., Xing, Y., Mao, H., Lu, T., Han, B., Xu, C., Li, X., Zhang, Q. (2006) *GS3*, a major QTL for grain length and weight and minor QTL for grain width and thickness in rice, encodes a putative transmembrane protein. *Theoretical and Applied Genetics* 112: 1164-1171.
- Fan, X., Tang, Z., Tan, Y., Zhang, Y., Luo, B., Yang, M., Lian, X., Shen, Q., Miller, A.J., Xu, G. (2016) Overexpression of a pH-sensitive nitrate transporter in rice increases crop yields. *Proceedings of the National Academy of Sciences* 113: 7118-7123.
- Farquhar, G.D., Ehleringer, J.R., Hubick, K.T. (1989) Carbon isotope discrimination and photosynthesis. *Annual Review of Plant Biology* 40: 503-537.
- Fischer, R.A., and Edmeades, G.O. (2010) Breeding and cereal yield progress. *Crop Science* 50: S-85-S-98.
- Fitter, A. (2002) Characteristics and functions of root systems. In Y Waisel, A Eshel, T Beeckman, U Kafkaf, eds, *Plant Roots: The Hidden Half*, ED 3, NY: Marcel Dekker, Inc., New York, pp 15-32.
- Fleury, D., Jefferies, S., Kuchel, H., and Langridge, P. (2010) Genetic and genomic tools to improve drought tolerance in wheat. *Journal of Experimental Botany* 61: 3211-3222.
- Flexas, J., Ribas-Carbó, M., Hanson, D.T., Bota, J., Otto, B., Cifre, J., McDowell, N., Medrano, H., Kaldenhoff, R. (2006) Tobacco aquaporin *NtAQPI* is involved in mesophyll conductance to CO₂ in vivo. *The Plant Journal* 48: 427-439.
- Foulkes, M.J., Sylvester-Bradley, R., Weightman, R., and Snape, J.W. (2007) Identifying physiological traits associated with improved drought resistance in winter wheat. *Field Crops Research* 103: 11-24.
- Fu, X., Harberd, N.P. (2003) Auxin promotes Arabidopsis root growth by modulating gibberellin response. *Nature* 421: 740-743.
- Fujita, D., Trijatmiko, K.R., Tagle, A.G., Sapasap, M.V., Koide, Y., Sasaki, K., Tsakirpaloglou, N., Gannaban, R.B., Nishimura, T., Yanagihara, S., Fukuta, Y., Koshiba, T., Slamet-Loedin, I.H., Ishimaru, T., Kobayashi, N. (2013) *NAL1* allele from a rice landrace greatly increases yield in modern indica cultivars. *Proceedings of the National Academy of Sciences* 110: 20431-20436.
- Fukai, S., Pantuwan, G., Jongdee, B., Cooper, M. (1999) Screening for drought resistance in rainfed lowland rice. *Field Crops Research* 64: 61-74.
- Gallardo, K., Courty, P.E., Le Signor, C., Wipf, D., Vernoud, V. (2014) Sulfate transporters in the plant's response to drought and salinity: regulation and possible functions. *Frontiers in Plant Science* 5: 580.
- Gao, M.J., Parkin, I., Lydiate, D., Hannoufa, A. (2004) An auxin-responsive *SCARECROW*-like transcriptional activator interacts with histone deacetylase. *Plant Molecular Biology* 55: 417-431.
- Geiger, D., Becker, D., Vosloh, D., Gambale, F., Palme, K., Rehers, M., Anschuetz, U., Dreyer, I., Kudla, J., Hedrich, R. (2009) Heteromeric *AtKCI*-*AKT1* channels in Arabidopsis roots facilitate growth under K⁺ limiting conditions. *Journal of Biological Chemistry* 284: 21288-21295.
- Génard, M., Memmah, M.M., Quilot-Turion, B., Vercambre, G., Baldazzi, V., Le Bot, J., Bertin, N., Gautier, H., Lescouret, F., and Pagès, L. (2016) Process-based

- simulation models are essential tools for virtual profiling and design of ideotypes: example of fruit and root. In "Crop Systems Biology: *Narrowing the gaps between crop modelling and genetics*" (X. Yin and P. C. Struik, eds.), pp. 83-104. Springer International Publishing, Cham.
- Gilliland, L.U., Pawloski, L.C., Kandasamy, M.K., Meagher, R.B.** (2003) Arabidopsis actin gene *ACT7* plays an essential role in germination and root growth. *The Plant Journal* 33: 319-328.
- Govind, G., Vokkaliga Thammegowda, H., Jayaker Kalaiarasi, P., Iyer, D.R., Muthappa, S.K., Nese, S., Makarla, U.K.** (2009) Identification and functional validation of a unique set of drought induced genes preferentially expressed in response to gradual water stress in peanut. *Molecular Genetics and Genomics* 281: 591-605.
- Gowda, V.R.P., Henry, A., Yamauchi, A., Shashidhar, H.E., and Serraj, R.** (2011) Root biology and genetic improvement for drought avoidance in rice. *Field Crops Research* 122: 1-13.
- Grabov, A., Blatt, M.R.** (1998) Membrane voltage initiates Ca^{2+} waves and potentiates Ca^{2+} increases with abscisic acid in stomatal guard cells. *Proceedings of the National Academy of Sciences* 95: 4778-4783.
- Greacen, E.L., Ponsana, P., Barley, K.P.** (1976) Resistance to water flow in the roots of cereals. In OL Lango, L Kappen and ED Schulze, eds, *Water and Plant Life*, Ed 1 Vol 19. Springer, Berlin, pp 86-100.
- Grębosz, J., Badowiec, A., Weidner, S.** (2014) Changes in the root proteome of *Triticosecale* grains germinating under osmotic stress. *Acta Physiologiae Plantarum* 36: 825-835.
- Griencisen, V.A., Xu, J., Marec, A.F.M., Hogeweg, P., Scheres, B.** (2007) Auxin transport is sufficient to generate a maximum and gradient guiding root growth. *Nature* 449: 1008-1013.
- Gu, J., Yin, X., Struik, P.C., Stomph, T.J., and Wang, H.** (2012) Using chromosome introgression lines to map quantitative trait loci for photosynthesis parameters in rice (*Oryza sativa* L.) leaves under drought and well-watered field conditions. *Journal of Experimental Botany* 63: 455-469.
- Gu, J., Yin, X., Zhang, C., Wang, H., and Struik, P.C.** (2014) Linking ecophysiological modelling with quantitative genetics to support marker-assisted crop design for improved yields of rice (*Oryza sativa*) under drought stress. *Annals of Botany* 114: 499-511.
- Guilfoyle, T.J., Hagen, G.** (2007) Auxin response factors. *Current Opinion in Plant Biology* 10: 453-460.
- Guo, L., Nezames, C.D., Sheng, L., Deng, X., Wei, N.** (2013) *Cullin-RING* ubiquitin ligase family in plant abiotic stress pathways. *Journal of Integrative Plant Biology* 55: 21-30.
- Guo, Z., Chen, D., Alqudah, A.M., Röder, M.S., Ganai, M.W., Schnurbusch, T.C.** (2017) Genome-wide association analyses of 54 traits identified multiple loci for the determination of floret fertility in wheat. *New Phytologist* 214: 257-270.
- Hammer, G.L., van Oosterom, E., McLean, G., Chapman, S.C., Broad, I., Harland, P., and Muchow, R. C.** (2010) Adapting APSIM to model the physiology and genetics of complex adaptive traits in field crops. *Journal of Experimental Botany* 61: 2185-2202.
- Hammer, G., Cooper, M., Tardieu, F., Welch, S., Walsh, B., van Eeuwijk, F., Chapman, S., and Podlich, D.** (2006) Models for navigating biological complexity in breeding improved crop plants. *Trends in Plant Science* 11: 587-593.
- Hammer, G., Messina, C., van Oosterom, E., Chapman, S., Singh, V., Borrell, A., Jordan, D., and Cooper, M.** (2016) Molecular breeding for complex adaptive traits: How integrating crop ecophysiology and modelling can enhance efficiency. In "Crop

- Systems Biology: *Narrowing the gaps between crop modelling and genetics*" (X. Yin and P. C. Struik, eds.), pp. 147-162. Springer International Publishing, Cham.
- Hao, Y.J., Wei, W., Song, Q.X., Chen, H.W., Zhang, Y.Q., Wang, F., Zou, H.F., Lei, G., Tian, A.G., Zhang, W.K., Ma, B., Zhang, J.S., Chen, S.Y.** (2011) Soybean NAC transcription factors promote abiotic stress tolerance and lateral root formation in transgenic plants. *The Plant Journal* 68: 302-313.
- Harshavardhan, V.T., Van Son, L., Seiler C., Junker A., Weigelt-Fischer K., Klukas C., Altmann T., Sreenivasulu N., Bäumlein H., Kuhlmann, M.** (2014) *AtRD22* and *AtUSPL1*, members of the plant-specific BURP domain family involved in *Arabidopsis thaliana* drought tolerance. *PLoS ONE* 9: e110065.
- Hawker, N.P., Bowman, J.L.** (2004) Roles for class III *HD-Zip* and *KANADI* genes in Arabidopsis root development. *Plant Physiology* 135: 2261-2270.
- He, X.J., Mu, R.L., Cao, W.H., Zhang, Z.G., Zhang, J.S., Chen, S.Y.** (2005) *AtNAC2*, a transcription factor downstream of ethylene and auxin signaling pathways, is involved in salt stress response and lateral root development. *The Plant Journal* 44: 903-916.
- Henry, A., Gowda, V.R., Torres, R.O., McNally, K.L., Serraj, R.** (2011) Variation in root system architecture and drought response in rice (*Oryza sativa*): phenotyping of the OryzaSNP panel in rainfed lowland fields. *Field Crops Research* 120: 205-214.
- Henry, A.** (2013) IRRI's drought stress research in rice with emphasis on roots: accomplishments over the last 50 years. *Plant Root* 7: 92-106.
- Henry, A., Cal, A.J., Batoto, T.C., Torres, R.O., and Serraj, R.** (2012) Root attributes affecting water uptake of rice (*Oryza sativa*) under drought. *Journal of Experimental Botany* 63: 4751-4763.
- Hernández, E.I., Vilagrosa, A., Pausas, J.G., Bellot, J.** (2010) Morphological traits and water use strategies in seedlings of Mediterranean coexisting species. *Plant Ecology* 207: 233-244.
- Hooker, T.S., Millar, A.A., Kunst, L.** (2002) Significance of the expression of the *CER6* condensing enzyme for cuticular wax production in Arabidopsis. *Plant Physiology* 129: 1568-1580.
- Hsieh, W.Y., Liao, J.C., Hsieh, M.H.** (2015) Dysfunctional mitochondria regulate the size of root apical meristem and leaf development in Arabidopsis. *Plant Signaling & Behavior* 10: e1071002.
- Huang, L., Yang, S., Zhang, S., Liu, M., Lai, J., Qi, Y., Shi, S., Wang, J., Wang, Y., Xie, Q., Yang, C.** (2009) The Arabidopsis *SUMO E3* ligase *AtMMS21*, a homologue of NSE2/MMS21, regulates cell proliferation in the root. *The Plant Journal* 60: 666-678.
- Huang, X., Qian, Q., Liu, Z., Sun, H., He, S., Luo, D., Xia, G., Chu, C., Li, J., Fu, X.** (2009) Natural variation at the *DEPI* locus enhances grain yield in rice. *Nature Genetics* 41: 494-497.
- Huang, X., Wei, X., Sang, T., Zhao, Q., Feng, Q., Zhao, Y., Li, C., Zhu, C., Lu, T., Zhang, Z., Li, M., Fan, D., Guo, Y., Wang, A., Wang, L., Deng, L., Li, W., Lu, Y., Weng, Q., Liu, K., Huang, T., Zhou, T., Jing, Y., Li, W., Lin, Z., Buckler, E.S., Qian, Q., Zhang, Q.F., Li, J., Han, B.** (2010) Genome-wide association studies of 14 agronomic traits in rice landraces. *Nature Genetics* 42: 961-967.
- Huang, X., Zhao, Y., Wei, X., Li, C., Wang, A., Zhao, Q., Li, W., Guo, Y., Deng, L., Zhu, C., Fan, D., Lu, Y., Weng, Q., Liu, K., Zhou, T., Jing, Y., Si, L., Dong, G., Huang, T., Lu, T., Feng, Q., Qian, Q., Li, J., Han, B.** (2012) Genome-wide association study of flowering time and grain yield traits in a worldwide collection of rice germplasm. *Nature Genetics* 44: 32-39.

- Impa, S.M., Nadaradjan, S., Boominathan, P., Shashidhar, G., Bindumadhava, H.Y., Sheshshayee, M.S.** (2005) Carbon isotope discrimination accurately reflects variability in WUE measured at a whole plant level in rice. *Crop Science* 45: 2517-2522
- Ingvarsson, P.K., Street, N.R.** (2011) Association genetics of complex traits in plants. *New Phytologist* 189: 909-922.
- IPCC** (2013). Working group, I contribution to the IPCC fifth assessment report climate change: The physical science basis, summary for policymakers. www.climatechange2013.org/images/uploads/WGIAR5-SPM_Approved27Sep2013.pdf.
- Ishimaru, K., Ono, K., Kashiwagi, T.** (2004) Identification of a new gene controlling plant height in rice using the candidate-gene strategy. *Planta* 218: 388-395.
- Isidro, J., Jannink, J.L., Akdemir, D., Poland, J., Heslot, N., and Sorrells, M.E.** (2015) Training set optimization under population structure in genomic selection. *Theoretical and Applied Genetics* 128: 145-158.
- Jackson, R.B., Sperry, J.S., and Dawson, T.E.** (2000) Root water uptake and transport: using physiological processes in global predictions. *Trends in Plant Science* 5: 482-488.
- Jagadish, S.K., Muthurajan, R., Rang, Z.W., Malo, R., Heuer, S., Bennett, J., Craufurd, P.Q.** (2011) Spikelet proteomic response to combined water deficit and heat stress in rice (*Oryza sativa* cv. N22). *Rice* 4: 1-11.
- Jagadish, S.V.K., Craufurd, P.Q., and Wheeler, T.R.** (2007) High temperature stress and spikelet fertility in rice (*Oryza sativa* L.). *Journal of Experimental Botany* 58: 1627-1635.
- Jagadish, S.V.K., Septiningsih, E.M., Kohli, A., Thomson, M.J., Ye, C., Redoña, E., Kumar, A., Gregorio, G.B., Wassmann, R., Ismail, A.M., and Singh, R.K.** (2012) Genetic advances in adapting rice to a rapidly changing climate. *Journal of Agronomy and Crop Science* 198: 360-373.
- Jain, M., Tyagi, A.K., Khurana, J.P.** (2006) Genome-wide analysis, evolutionary expansion, and expression of early auxin-responsive SAUR gene family in rice (*Oryza sativa*). *Genomics* 88: 360-371.
- Jansen, R.C., Stam, P.** (1994) High resolution of quantitative traits into multiple loci via interval mapping. *Genetics* 136: 1447-1455.
- Jarzyniak, K.M., Jasiński, M.** (2014) Membrane transporters and drought resistance-a complex issue. *Frontiers in Plant Science* 5: 687.
- Jensen, W.A.** (1962) Botanical histochemistry: Principles and practice. W.H. Freeman, San Francisco.
- Ji, W., Zhu, Y., Li, Y., Yang, L., Zhao, X., Cai, H., Bai, X.** (2010) Over-expression of a glutathione S-transferase gene, *GsGST*, from wild soybean (*Glycine soja*) enhances drought and salt tolerance in transgenic tobacco. *Biotechnology Letters* 32: 1173-1179.
- Jin, Z.L., Hong, J.K., Yang, K.A., Koo, J.C., Choi, Y.J., Chung, W.S., Yun, D.J., Lee, S.Y., Cho, M.J., Lim, C.O.** (2005) Over-expression of chinese cabbage calreticulin 1, *BrCRT1*, enhances shoot and root regeneration, but retards plant growth in transgenic tobacco. *Transgenic Research* 14: 619-626.
- Jones, M.A., Shen, J.J., Fu, Y., Li, H., Yang, Z., Grierson, C.S.** (2002) The Arabidopsis *Rop2 GTPase* is a positive regulator of both root hair initiation and tip growth. *The Plant Cell* 14: 763-776.
- Juenger, T.E.** (2013) Natural variation and genetic constraints on drought tolerance. *Current Opinion in Plant Biology* 16: 274-281.
- Julia, C., and Dingkuhn, M.** (2013) Predicting temperature induced sterility of rice spikelets requires simulation of crop-generated microclimate. *European Journal of Agronomy* 49: 50-60.

- Jung, J., and McCouch, S.** (2013) Getting to the roots of it: Genetic and hormonal control of root architecture. *Frontiers in Plant Science* 4: 186.
- Kadam, N., Tamilselvan, A., Lawas, L.M.F., Quinones, C., Bahuguna, R., Thomson, M.J., Dingkuhn, M., Muthurajan, R., Struik, P., Yin, X., Jagadish, S.V.K.** (2017) Genetic control of plasticity in root morphology and anatomy of rice in response to water-deficit. *Plant Physiology* 174: 2302-2315.
- Kadam, N.N., Yin, X., Bindraban, P.S., Struik, P.C., Jagadish, K.S.V.** (2015) Does morphological and anatomical plasticity during the vegetative stage make wheat more tolerant of water deficit stress than rice? *Plant Physiology* 167: 1389-1401.
- Kadam, N.N., Xiao, G., Melgar, R.J., Bahuguna, R.N., Quinones, C., Tamilselvan, A., Prasad, P. V.V., and Jagadish, K.S.V.** (2014) Agronomic and physiological responses to high temperature, drought, and elevated CO₂ interactions in cereals. *Advances in Agronomy* 127: 111-156.
- Kalve, S., De Vos, D., Beemster, G.T.S.** (2014) Leaf development: a cellular perspective. *Frontiers in Plant Science* 5: 362.
- Kamoshita, A., Babu, R.C., Boopathi, N.M., and Fukai, S.** (2008) Phenotypic and genotypic analysis of drought-resistance traits for development of rice cultivars adapted to rainfed environments. *Field Crops Research* 109: 1-23.
- Kang, Y., Khan, S., and Ma, X.** (2009) Climate change impacts on crop yield, crop water productivity and food security-A review. *Progress in Natural Science* 19: 1665-1674.
- Kano M, Inukai Y, Kitano H, Yamauchi, A.** (2011) Root plasticity as the key root trait for adaptation to various intensities of drought stress in rice. *Plant and Soil* 342: 117-128.
- Kano-Nakata, M., Gowda, V.R.P., Henry, A., Serraj, R., Inukai, Y., Fujita, D., Kobayashi, N., Suralta, R.R., and Yamauchi, A.** (2013) Functional roles of the plasticity of root system development in biomass production and water uptake under rainfed lowland conditions. *Field Crops Research* 144: 288-296.
- Kano-Nakata, M., Inukai, Y., Wade, L.J., Siopongco, J. D. L.C., and Yamauchi, A.** (2011) Root development, water uptake, and shoot dry matter production under water deficit conditions in two CSSLs of rice: Functional roles of root plasticity. *Plant Production Science* 14: 307-317.
- Kato, Y., Abe, J., Kamoshita, A., Yamagishi, J.** (2006) Genotypic variation in root growth angle in rice (*Oryza sativa* L.) and its association with deep root development in upland fields with different water regimes. *Plant and Soil* 287: 117-129.
- Kato, Y., Kamoshita, A., Yamagishi, J., Imoto, H., Abe, J.** (2007) Growth of rice (*Oryza sativa* L.) cultivars under upland conditions with different levels of water supply. 3. Root system development, soil moisture change and plant water status. *Plant Production Science* 10: 3-13.
- Kato, Y., Okami, M.** (2011) Root morphology, hydraulic conductivity and plant water relations of high-yielding rice grown under aerobic conditions. *Annals of Botany* 108: 575-583.
- Kato, Y., Okami, M., Tajima, R., Fujita, D., Kobayashi, N.** (2010) Root response to aerobic conditions in rice, estimated by Comair root length scanner and scanner-based image analysis. *Field Crops Research* 118: 194-198.
- Kato, Y., Kamoshita, A., and Yamagishi, J.** (2008) Preflowering abortion reduces spikelet number in upland rice (*Oryza sativa* L.) under water stress. *Crop Science* 48: 2389-2395.
- Kawahara, Y., De la Bastide, M., Hamilton, J.P., Kanamori, H., McCombie, W.R., Ouyang, S., Schwartz, D.C., Tanaka, T., Wu, J., Zhou, S., Childs, K.L., Davidson, R.M., Lin, H., Quesada-Ocampo, L., Vaillancourt, B., Sakai, H., Lee, S.S., Kim J., Numa, H., Itoh, T., Buell, C.R., Matsumoto, T.** (2013) Improvement of the *Oryza*

- sativa* nipponbare reference genome using next generation sequence and optical map data. *Rice* 6: 4.
- Kazan, K., and Lyons, R.** (2016) The link between flowering time and stress tolerance. *Journal of Experimental Botany* 67: 47-60.
- Kenney, A.M., McKay, J.K., Richards, J.H., and Juenger, T.E.** (2014) Direct and indirect selection on flowering time, water-use efficiency (WUE, $\delta^{13}\text{C}$), and WUE plasticity to drought in *Arabidopsis thaliana*. *Ecology and Evolution* 4: 4505-4521.
- Kholová, J., Hash, C.T., Kumar, P.L., Yadav, R.S., Kočová, M., and Vadez, V.** (2010) Terminal drought-tolerant pearl millet [*Pennisetum glaucum* (L.) R. Br.] have high leaf ABA and limit transpiration at high vapour pressure deficit. *Journal of Experimental Botany* 61: 1431-1440.
- Khush, G.S.** (1997) Origin, dispersal, cultivation and variation of rice. In *Oryza: Plant Molecular Biology* 35: 25-34.
- Kikuchi, S., Bheemanahalli, R., Jagadish, K.S.V., Kumagai, E., Masuya, Y., Kuroda, E., Raghavan, C., Dingkuhn, M., Abe, A., Shimono, H.C.P.C.E.R.** (2017) Genome-wide association mapping for phenotypic plasticity in rice. *Plant, Cell & Environment* 40: 1565-1575.
- Kim, M., Hepler, P.K., Eun, S.O., Ha, K.S., Lee, Y.** (1995) Actin filaments in mature guard cells are radially distributed and involved in stomatal movement. *Plant Physiology* 109: 1077-1084.
- Kim, T.W., Michniewicz, M., Bergmann, D.C., Wang, Z.Y.** (2012) Brassinosteroid regulates stomatal development by *GSK3*-mediated inhibition of a *MAPK* pathway. *Nature* 482: 419-422.
- Kitomi, Y., Ito, H., Hobo, T., Aya, K., Kitano, H., Inukai, Y.** (2011) The auxin responsive AP2/ERF transcription factor *CROWN ROOTLESS5* is involved in crown root initiation in rice through the induction of *OsRR1*, a type-A response regulator of cytokinin signaling. *The Plant Journal* 67: 472-484.
- Kobata, T., Tanaka, S., Utumi, M., Hara, S., and Imaki, T.** (1994) Sterility in rice (*Oryza Sativa* L.) subject to drought during the booting stage occurs not because of lack of assimilate or of water deficit in the shoot but because of dehydration of the root zone. *Japanese journal of crop science* 63: 510-517.
- Kromdijk, J., Bertin, N., Heuvelink, E., Molenaar, J., de Visser, P.H.B., Marcelis, L.F. M., and Struik, P.C.** (2014) Crop management impacts the efficiency of quantitative trait loci (QTL) detection and use: case study of fruit load \times QTL interactions. *Journal of Experimental Botany* 65: 11-22.
- Kumar, A., Dixit, S., Ram, T., Yadav, R.B., Mishra, K.K., Mandal, N.P.** (2014) Breeding high-yielding drought-tolerant rice: genetic variations and conventional and molecular approaches. *Journal of Experimental Botany* 65: 6265-6278.
- Kumar, R., Venuprasad, R., and Atlin, G.N.** (2007) Genetic analysis of rainfed lowland rice drought tolerance under naturally-occurring stress in eastern India: heritability and QTL effects. *Field Crops Research* 103: 42-52.
- Lanceras, J.C., Pantuwan, G., Jongdee, B., and Toojinda, T.** (2004) Quantitative trait loci associated with drought tolerance at reproductive stage in rice. *Plant Physiology* 135: 384-399.
- Leakey, A.D.B., Ainsworth, E.A., Bernacchi, C.J., Rogers, A., Long, S.P., and Ort, D.R.** (2009) Elevated CO₂ effects on plant carbon, nitrogen, and water relations: six important lessons from FACE. *Journal of Experimental Botany* 60: 2859-2876.
- Letort, V., Mahe, P., Cournède, P.H., de Reffye, P., and Courtois, B.** (2008) Quantitative genetics and functional–structural plant growth models: Simulation of quantitative trait

- loci detection for model parameters and application to potential yield optimization. *Annals of Botany* 101: 1243-1254.
- Li, S., Qian, Q., Fu, Z., Zeng, D., Meng, X., Kyojuka, J., Maekawa, M., Zhu, X., Zhang, J., Li, J., Wang, Y.** (2009) Short panicle1 encodes a putative *PTR* family transporter and determines rice panicle size. *The Plant Journal* 58: 592-605.
- Li, J.Y., Wang, J., and Zeigler, R.S.** (2014) The 3,000 rice genomes project: new opportunities and challenges for future rice research. *Giga Science* 3: 8.
- Li, X., Guo, Z., Lv, Y., Cen, X., Ding, X., Wu, H., Li, X., Huang, J., and Xiong, L.** (2017) Genetic control of the root system in rice under normal and drought stress conditions by genome-wide association study. *PLoS Genetics* 13: e1006889.
- Liang, M., Haraldsen, V., Cai, X., Wu, Y.** (2006) Expression of a putative laccase gene, *ZmLAC1*, in maize primary roots under stress. *Plant, Cell & Environment* 29: 746-753.
- Lipiec, J., Doussan, C., Nosalewicz, A., and Kondracka, K.** (2013) Effect of drought and heat stresses on plant growth and yield: a review. *International Agrophysics* 27: 463-477.
- Lipka, A.E., Tian, F., Wang, Q., Peiffer, J., Li, M., Bradbury, P.J., Gore, M.A., Buckler, E.S., Zhang, Z.** (2012) GAPIT: genome association and prediction integrated tool. *Bioinformatics* 28: 2397-2399.
- Lippold, F., vom Dorp, K., Abraham, M., Hölzl, G., Wewer, V., Yilmaz, J.L., Lager, I., Montandon, C., Besagni, C., Kessler, F., Stymne, S., Dörmann, P.** (2012) Fatty acid phytyl ester synthesis in chloroplasts of Arabidopsis. *The Plant Cell* 24: 2001-2014.
- Little, D.Y., Rao, H., Oliva, S., Daniel-Vedele, F., Krapp, A., Malamy, J.E.** (2005) The putative high-affinity nitrate transporter *NRT2.1* represses lateral root initiation in response to nutritional cues. *Proceedings of the National Academy of Sciences* 102: 13693-13698.
- Liu, J.X., Liao, D.Q., Oane, R., Estenor, L., Yang, X.E., Li, Z.C., Bennett, J.** (2006) Genetic variation in the sensitivity of anther dehiscence to drought stress in rice. *Field Crops Research* 97: 87-100.
- Liu, W., Zhang, D., Tang, M., Li, D., Zhu, Y., Zhu, L., Chen, C.** (2013) *THIS1* is a putative lipase that regulates tillering, plant height, and spikelet fertility in rice. *Journal of Experimental Botany* 64: 4389-4402.
- Liu, X., Guo, T., Wan, X., Wang, H., Zhu, M., Li, A., Su, N., Shen, Y., Mao, B., Zhai, H., Mao, L., Wan, J.** (2010) Transcriptome analysis of grain-filling caryopses reveals involvement of multiple regulatory pathways in chalky grain formation in rice. *BMC Genomics* 11: 730.
- Lobell, D.B., Schlenker, W., and Costa-Roberts, J.** (2011) Climate trends and global crop production since 1980. *Science* 333: 616-620.
- Lobet, G., and Draye, X.** (2013) Novel scanning procedure enabling the vectorization of entire rhizotron-grown root systems. *Plant Methods* 9: 1-1.
- Lopes, M.S., Reynolds, M.P.** (2010) Partitioning of assimilates to deeper roots is associated with cooler canopies and increased yield under drought in wheat. *Functional Plant Biology* 37: 147-156.
- Lorbiecke, R., Sauter, M.** (1999) Adventitious root growth and cell-cycle induction in deepwater rice. *Plant Physiology* 119: 21-30.
- Ludlow, M.M., and Muchow, R.C.** (1990) A critical evaluation of traits for improving crop yields in water-limited environments. *Advances in Agronomy* 43:107-153.
- Lynn, K., Fernandez, A., Aida, M., Sedbrook, J., Tasaka, M., Masson, P., Barton, M.K.** (1999) The *PINHEAD/ZWILLE* gene acts pleiotropically in Arabidopsis development and has overlapping functions with the *ARGONAUTE1* gene. *Development* 126: 469-481.

- Ma, X., Feng, F., Wei, H., Mei, H., Xu, K., Chen, S., Li, T., Liang, X., Liu, H., Luo, L. (2016) Genome-wide association study for plant height and grain yield in rice under contrasting moisture regimes. *Frontiers in Plant Science* 7: 1801.
- Mackay, I., Powell, W. (2007) Methods for linkage disequilibrium mapping in crops. *Trends in Plant Science* 12: 57-63.
- Mai, C.D., Phung, N.T., To, H.T., Gonin, M., Hoang, G.T., Nguyen, K.L., Do, V.N., Courtois, B., and Gantet, P. (2014) Genes controlling root development in rice. *Rice* 7: 30.
- Mangin, B., Casadebaig, P., Cadic, E., Blanchet, N., Boniface, M.-C., Carrère, S., Gouzy, J., Legrand, L., Mayjonade, B., Pouilly, N., André, T., Coque, M., Piquemal, J., Laporte, M., Vincourt, P., Muños, S., and Langlade, N. B. (2017) Genetic control of plasticity of oil yield for combined abiotic stresses using a joint approach of crop modelling and genome-wide association. *Plant, Cell & Environment* 40: 2276-2291.
- Marais, D.L.D., Hernandez, K.M., and Juenger, T.E. (2013) Genotype-by-Environment interaction and plasticity: Exploring genomic responses of plants to the abiotic environment. *Annual Review of Ecology, Evolution, and Systematics* 44: 5-29.
- Markakis, M.N., Boron, A.K., Van Loock, B., Saini, K., Cirera, S., Verbelen, J.P., Vissenberg, K. (2013) Characterization of a small auxinup RNA (SAUR)-like gene involved in *Arabidopsis thaliana* development. *PLoS ONE* 8: e82596.
- Martre, P., Bertin, N., Salon, C., and Génard, M. (2011) Modelling the size and composition of fruit, grain and seed by process-based simulation models. *New Phytologist* 191: 601-618.
- Martre, P., Quilot-Turion, B., Luquet, D., Memmah, M.-M. O.-S., Chenu, K., and Debacle, P. (2015) Model-assisted phenotyping and ideotype design. *Crop physiology: applications for genetic improvement and agronomy*, 349-373.
- Mather, K.A., Caicedo, A.L., Polato, N.R., Olsen, K.M., McCouch, S., Purugganan, M.D. (2007) The extent of linkage disequilibrium in rice (*Oryza sativa* L.). *Genetics* 177: 2223
- Matsuo, N., Ozawa, K., Mochizuki, T. (2009) Genotypic differences in root hydraulic conductance of rice (*Oryza sativa* L.) in response to water regimes. *Plant and Soil* 316: 25-34.
- McCouch, S., Baute, G.J., Bradeen, J., Bramel, P., Bretting, P.K., Buckler, E., Burke, J.M., Charest, D., Cloutier, S., Cole, G., Dempewolf, H., Dingkuhn, M., Feuillet, C., Gepts, P., Grattapaglia, D., Guarino, L., Jackson, S., Knapp, S., Langridge, P., Lawton-Rauh, A., Lijua, Q., Lusty, C., Michael, T., Myles, S., Naito, K., Nelson, R.L., Pontarollo, R., Richards, C.M., Rieseberg, L., Ross-Ibarra, J., Rounsley, S., Hamilton, R.S., Schurr, U., Stein, N., Tomooka, N., van der Knaap, E., van Tassel, D., Toll, J., Valls, J., Varshney, R.K., Ward, J., Waugh, R., Wenzl, P., Zamir, D. (2013) Agriculture: Feeding the future. *Nature* 499: 23-24.
- McDonald, M.P., Galwey, N.W., Colmer, T.D. (2002) Similarity and diversity in adventitious root anatomy as related to root aeration among a range of wetland and dryland grass species. *Plant, Cell & Environment* 25: 441-451.
- Metzker, M. L. (2010) Sequencing technologies-the next generation. *Nature Reviews Genetics* 11: 31-46.
- Meuwissen, T.H.E., Hayes, B.J., and Goddard, M.E. (2001) Prediction of total genetic value using genome-wide dense marker maps. *Genetics* 157: 1819-1829.
- Miller, N.D., Durham Brooks, T.L., Assadi, A.H., Spalding, E.P. (2010) Detection of a gravitropism phenotype in glutamate receptor-like 3.3 mutants of *Arabidopsis thaliana* using machine vision and computation. *Genetics* 186: 585-593.

- Millet, E., Welcker, C., Kruijjer, W., Negro, S., Nicolas, S., Praud, S., Ranc, N., Presterl, T., Tuberosa, R., Bedo, Z., Draye, X., Usadel, B., Charcosset, A., van Eeuwijk, F., Tardieu, F., Coupel-Ledru, A., Bauland, C. (2016) Genome-wide analysis of yield in Europe: allelic effects as functions of drought and heat scenarios. *Plant Physiology* 172: 749-764.
- Mir, R.R., Zaman-Allah, M., Sreenivasulu, N., Trethowan, R., and Varshney, R.K. (2012) Integrated genomics, physiology and breeding approaches for improving drought tolerance in crops. *Theoretical and Applied Genetics* 125: 625-645.
- Mishra, K.K., Vikram, P., Yadaw, R.B., Swamy, B.M., Dixit, S., Cruz, M.T.S., Maturan, P., Marker, S., Kumar, A. (2013) *qDTY12.1*: a locus with a consistent effect on grain yield under drought in rice. *BMC Genetics* 14: 12.
- Mittler, R. (2006) Abiotic stress, the field environment and stress combination. *Trends in Plant Science* 11: 15-19.
- Miura, K., Ikeda, M., Matsubara, A., Song, X.J., Ito, M., Asano, K., Matsuoka, M., Kitano, H., Ashikari, M. (2010) *OsSPL14* promotes panicle branching and higher grain productivity in rice. *Nature Genetics* 42: 545-549.
- Miura, K., Lee, J., Gong, Q., Ma, S., Jin, J.B., Yoo, C.Y., Miura, T., Sato, A., Bohnert, H.J., Hasegawa, P.M. (2011) *SIZ1* regulation of phosphate starvation-induced root architecture remodeling involves the control of auxin accumulation. *Plant Physiology* 155: 1000-1012.
- Miyamoto, N., Steudle, E., Hirasawa, T., Lafitte, R. (2001) Hydraulic conductivity of rice roots. *Journal of Experimental Botany* 52: 1835-1846.
- Mo, X., Liu, S., Lin, Z., Xu, Y., Xiang, Y., and McVicar, T.R. (2005) Prediction of crop yield, water consumption and water use efficiency with a SVAT-crop growth model using remotely sensed data on the North China Plain. *Ecological Modelling* 183: 301-322.
- Molden, D., Oweis, T., Steduto, P., Bindraban, P., Hanjra, M.A., and Kijne, J. (2010) Improving agricultural water productivity: Between optimism and caution. *Agricultural Water Management* 97: 528-535.
- Moldenhauer, K., Slaton, N. (2001) Rice growth and development. Rice production handbook, 7-14.
- Molendijk, A.J., Bischoff, F., Rajendrakumar, C.S.V., Friml, J., Braun, M., Gilroy, S., Palme, K. (2001) Arabidopsis thaliana *Rop GTPases* are localized to tips of root hairs and control polar growth. *The EMBO Journal* 20: 2779-2788.
- Nahirñak, V., Almasia, N.I., Hopp, H.E., Vazquez-Rovere, C. (2012) Snakin/GASA proteins: Involvement in hormone crosstalk and redox homeostasis. *Plant Signaling & Behavior* 7: 1004-1008.
- Nakagawa, H., Yamagishi, J., Miyamoto, N., Motoyama, M., Yano, M., and Nemoto, K. (2005) Flowering response of rice to photoperiod and temperature: a QTL analysis using a phenological model. *Theoretical and Applied Genetics* 110: 778-786.
- Nautiyal, P.C., Rachaputi, N.R., Joshi, Y.C. (2002) Moisture-deficit-induced changes in leaf-water content, leaf carbon exchange rate and biomass production in groundnut cultivars differing in specific leaf area. *Field Crops Research* 74: 67-79.
- Nguyen, H.T., Babu, R.C., and Blum, A. (1997) Breeding for drought resistance in rice: Physiology and molecular genetics considerations. *Crop Science* 37: 1426-1434.
- Nicotra, A.B., Atkin, O.K., Bonser, S.P., Davidson, A.M., Finnegan, E.J., Mathesius, U., Poot, P., Purugganan, M.D., Richards, C.L., Valladares, F., van Kleunen, M. (2010) Plant phenotypic plasticity in a changing climate. *Trends in Plant Science* 15: 684-692.

- Nicotra, A.B., Davidson, A.** (2010) Adaptive phenotypic plasticity and plant water use. *Functional Plant Biology* 37: 117-127.
- Niklas, K.J.** (1985) The evolution of tracheid diameter in early vascular plants and its implications on the hydraulic conductance of the primary xylem strand. *Evolution* 39: 1110-1122.
- Niones, J.M., Suralta, R.R., Inukai, Y., and Yamauchi, A.** (2012) Field evaluation on functional roles of root plastic responses on dry matter production and grain yield of rice under cycles of transient soil moisture stresses using chromosome segment substitution lines. *Plant and Soil* 359: 107-120.
- Niones, J. M., Suralta, R. R., Inukai, Y., and Yamauchi, A.** (2013) Roles of root aerenchyma development and its associated QTL in dry matter production under transient moisture stress in rice. *Plant Production Science* 16: 205-216.
- Norton, G.J., Douglas, A., Lahner, B., Yakubova, E., Guerinot, M.L., Pinson, S.R.M., Tarpley, L., Eizenga, G.C., McGrath, S.P., Zhao, F.J., Islam, M.R., Islam, S., Duan, G., Zhu, Y., Salt, D.E., Meharg, A.A., Price, A.H.** (2014) Genome wide association mapping of grain arsenic, copper, molybdenum and zinc in rice (*Oryza sativa* L.) grown at four international field sites. *PLoS ONE* 9: e89685.
- Ohashi-Ito, K., Oguchi, M., Kojima, M., Sakakibara, H., Fukuda, H.** (2013) Auxin-associated initiation of vascular cell differentiation by *LONESOME HIGHWAY*. *Development* 140: 765-769.
- Ohashi-Ito, K., Saegusa, M., Iwamoto, K., Oda, Y., Katayama, H., Kojima, M., Sakakibara, H., Fukuda, H.** (2014) A *bHLH* complex activates vascular cell division via cytokinin action in root apical meristem. *Current Biology* 24: 2053-2058.
- Olesen, J. E., Trnka, M., Kersebaum, K. C., Skjelvåg, A.O., Seguin, B., Peltonen-Sainio, P., Rossi, F., Kozyra, J., and Micale, F.** (2011) Impacts and adaptation of European crop production systems to climate change. *European Journal of Agronomy* 34: 96-112.
- Olivares-Villegas J.J., Reynolds, M.P., McDonald, G.K.** (2007) Drought-adaptive attributes in the Seri/Babax hexaploid wheat population. *Functional Plant Biology* 34: 189-203.
- Omidbakhshfard Mohammad, A., Proost, S., Fujikura, U., Mueller-Roeber, B.** (2015) Growth-regulating factors (GRFs): A small transcription factor family with important functions in plant biology. *Molecular Plant* 8: 998-1010.
- Ostonen, I., Puttsepp, U., Biel, C., Alberton, O., Bakker, M.R., Lohmus, K., Brunner, I.** (2007) Specific root length as an indicator of environmental change. *Plant Biosystems* 141: 426-442.
- Pacak, A., Barciszewska-Pacak, M., Swida-Barteczka, A., Kruszka, K., Sega, P., Milanowska, K., Jakobsen, I., Jarmolowski, A., Szweykowska-Kulinska, Z.** (2016) Heat stress affects Pi-related genes expression and inorganic phosphate deposition/accumulation in barley. *Frontiers in Plant Science* 7: 926.
- Pandey, S., Bhandari, H., Hardy, B., eds** (2007) Economic costs of drought and rice farmers coping mechanisms: A cross-country comparative analysis, International Rice Research Institute, Manila, pp 203.
- Pantalião, G.F., Narciso, M., Guimarães, C., Castro, A., Colombari, J.M., Breseghello, F., Rodrigues, L., Vianello, R.P., Borba, T.O., Brondani, C.** (2016) Genome wide association study (GWAS) for grain yield in rice cultivated under water deficit. *Genetica* 144: 651-664.
- Parent, B., Suard, B., Serraj, R., and Tardieu, F.** (2010) Rice leaf growth and water potential are resilient to evaporative demand and soil water deficit once the effects of root system are neutralized. *Plant, Cell & Environment* 33: 1256-1267.
- Passioura, J.B.** (1977) Grain yield harvest index and water use of wheat. *Journal of the Australian Institute of Agricultural Science* 43: 117-120.

- Pearson, P.N., and Palmer, M.R.** (2000) Atmospheric carbon dioxide concentrations over the past 60 million years. *Nature* 406: 695-699.
- Peng, S., Bouman, B., Visperas, R.M., Castañeda, A., Nie, L., and Park, H.K.** (2006) Comparison between aerobic and flooded rice in the tropics: Agronomic performance in an eight-season experiment. *Field Crops Research* 96: 252-259.
- Peng, S., Khush, G.S., Virk, P., Tang, Q., and Zou, Y.** (2008) Progress in ideotype breeding to increase rice yield potential. *Field Crops Research* 108: 32-38.
- Pfeiffer, W.H.** (1988) Drought tolerance in bread wheat – analysis of yield improvement over the years in CIMMYT germplasm. In AR Klatt eds, Wheat production constraints in tropical environments, Proceedings of the international conference, CIMMYT, Mexico City, pp 274-284.
- Phung, N.T.P., Mai, C.D., Hoang, G.T., Truong, H.T.M., Lavarenne, J., Gonin, M., Nguyen, K.L., Ha, T.T., Do, V.N., Gantet, P., Courtois, B.** (2016) Genome-wide association mapping for root traits in a panel of rice accessions from Vietnam. *BMC Plant Biology* 16: 64.
- Poorter, H., Bühler, J., van Dusschoten, D., Climent, J., Postma, J.A.** (2012) Pot size matters: a meta-analysis of the effects of rooting volume on plant growth. *Functional Plant Biology* 39: 839-850.
- Poorter, H., Fiorani, F., Stitt, M., Schurr, U., Finck, A., Gibon, Y., Usadel, B., Munns, R., Atkin, O.K., Tardieu, F., Pons, T.L.** (2012) The art of growing plants for experimental purposes: a practical guide for the plant biologist. *Functional Plant Biology* 39: 821-838.
- Posé, D., Castanedo, I., Borsani, O., Nieto, B., Rosado, A., Taconnat, L., Ferrer, A., Dolan, L., Valpuesta, V., Botella, M.A.** (2009) Identification of the Arabidopsis dry2/sqe1-5 mutant reveals a central role for sterols in drought tolerance and regulation of reactive oxygen species. *The Plant Journal* 59: 63-76.
- Powell, N., Ji, X., Ravash, R., Edlington, J., and Dolferus, R.** (2012) Yield stability for cereals in a changing climate. *Functional Plant Biology* 39: 539-552.
- Praba, M.L., Cairns, J.E., Babu, R.C., and Lafitte, H.R.** (2009) Identification of physiological traits underlying cultivar differences in drought tolerance in rice and wheat. *Journal of Agronomy and Crop Science* 195: 30-46.
- Premachandra, G.S., Hahn, D.T., Axtell, J.D., Joly, R.J.** (1994) Epicuticular wax load and water-use efficiency in bloomless and sparse-bloom mutants of *Sorghum bicolor* L. *Environmental and Experimental Botany* 34: 293-301.
- Prentice, I.C.** (2001) **The carbon cycle and atmospheric carbon dioxide.** In: Houghton, J.T., Ding, Y., Griggs, D.J., Noguer, M., van der Linden, P.J., Dai, X., Maskell, K., Johnson, C.A. (Eds.), *Climate Change 2001: The Scientific Basis*. Cambridge University Press, Cambridge, pp. 183–237.
- Prince, S.J., Song, L., Qiu, D., Maldonado dos Santos, J.V., Chai, C., Joshi, T., Patil, G., Valliyodan, B., Vuong, T.D., Murphy, M., Krampis, K., Tucker, D.M., Biyashev, R., Dorrance, A.E., Maroof, M.S., Xu, D., Shannon, J.G., Nguyen, H.T.** (2015) Genetic variants in root architecture-related genes in a *Glycine soja* accession, a potential resource to improve cultivated soybean. *BMC Genomics* 16: 1-20.
- Pyngrupe, S., Bhoomika, K., Dubey, R.S.** (2013) Reactive oxygen species, ascorbate–glutathione pool, and enzymes of their metabolism in drought-sensitive and tolerant indica rice (*Oryza sativa* L.) seedlings subjected to progressing levels of water deficit. *Protoplasma* 250: 585-600.
- Qi, W., Sun, F., Wang, Q., Chen, M., Huang, Y., Feng, Y.Q., Luo, X., Yang, J.** (2011) Rice ethylene-response AP2/ERF factor *OsEATB* restricts internode elongation by down-regulating a gibberellin biosynthetic gene. *Plant Physiology* 157: 216-228.

- Qin, L.X., Li, Y., Li, D.D., Xu, W.L., Zheng, Y., Li, X.B.** (2014) Arabidopsis drought-induced protein *Di19-3* participates in plant response to drought and high salinity stresses. *Plant Molecular Biology* 86: 609-625.
- Qiu, X., Pang, Y., Yuan, Z., Xing, D., Xu, J., Dingkuhn, M., Li, Z., and Ye, G.** (2016) Genome-wide association study of grain appearance and milling quality in a worldwide collection of indica rice germplasm. *PLoS ONE* 10: e0145577.
- Quan, R., Hu, S., Zhang, Z., Zhang, H., Zhang, Z., Huang, R.** (2010) Overexpression of an ERF transcription factor *TSRF1* improves rice drought tolerance. *Plant Biotechnology Journal* 8: 476-488.
- Rafalski, J.A.** (2010) Association genetics in crop improvement. *Current Opinion in Plant Biology* 13: 174-180.
- Raju, B.R., Narayanaswamy, B.R., Mohankumar, M.V., Sumanth, K.K., Rajanna, M.P., Mohanraju, B., Udaykumar, M., Sheshshayee, M.S.** (2014) Root traits and cellular level tolerance hold the key in maintaining higher spikelet fertility of rice under water limited conditions. *Functional Plant Biology* 41: 930-939.
- Ranathunge, K., Steudle, E., Lafitte, R.** (2003) Control of water uptake by rice (*Oryza sativa* L.): role of the outer part of the root. *Planta* 217: 193-205.
- Rang, Z.W., Jagadish, S.V.K., Zhou, Q.M., Craufurd, P.Q., Heuer, S.** (2011) Effect of high temperature and water stress on pollen germination and spikelet fertility in rice. *Environmental and Experimental Botany* 70: 58-65.
- Rao, R.C., Wright, G.C.** (1994) Stability of the relationship between specific leaf area and carbon isotope discrimination across environments in peanut. *Crop Science* 34: 98-103.
- Ravi, K., Vadez, V., Isobe, S., Mir, R.R., Guo, Y., Nigam, S. N., Gowda, M.V.C., Radhakrishnan, T., Bertoli, D.J., Knapp, S.J., and Varshney, R.K.** (2011) Identification of several small main-effect QTLs and a large number of epistatic QTLs for drought tolerance related traits in groundnut (*Arachis hypogaea* L.). *Theoretical and Applied Genetics* 122: 1119-1132.
- Rebolledo, M.C., Peña, A.L., Duitama, J., Cruz, D.F., Dingkuhn, M., Grenier, C., Tohme, J.** (2016) Combining image analysis, genome wide association studies and different field trials to reveal stable genetic regions related to panicle architecture and the number of spikelets per panicle in rice. *Frontiers in Plant Science* 7: 1384.
- Reed, J.W.** (2001) Roles and activities of *Aux/IAA* proteins in Arabidopsis. *Trends in Plant Science* 6: 420-425.
- Reich, P.B., Walters, M.B., Tjoelker, M.G., Vanderklein, D., and Buschena, C.** (1998) Photosynthesis and respiration rates depend on leaf and root morphology and nitrogen concentration in nine boreal tree species differing in relative growth rate. *Functional Ecology* 12: 395-405.
- Reinders, A.** (2016) Fuel for the road-sugar transport and pollen tube growth. *Journal of Experimental Botany* 67: 2121-2123.
- Reinhardt, D., Pesce, E.R., Stieger, P., Mandel, T., Baltensperger, K., Bennett, M., Traas, J., Friml, J., Kuhlemeier, C.** (2003) Regulation of phyllotaxis by polar auxin transport. *Nature* 426: 255-260.
- Reinhardt, H., Hachez, C., Bienert, M.D., Beebo, A., Swarup, K., Voß, U., Bouhidel, K., Frigerio, L., Schjoerring, J.K., Bennett, M.J., Chaumont, F.** (2016) Tonoplast aquaporins facilitate lateral root emergence. *Plant Physiology* 170: 1640-1654.
- Reymond, M., Muller, B., Leonardi, A., Charcosset, A., and Tardieu, F.** (2003) Combining quantitative trait loci analysis and an ecophysiological model to analyze the genetic variability of the responses of maize leaf growth to temperature and water deficit. *Plant Physiology* 131: 664-675.

- Reynolds, M., Dreccer, F., Trethowan, R. (2007) Drought-adaptive traits derived from wheat wild relatives and landraces. *Journal of Experimental Botany* 58: 177-186.
- Reynolds, M.P., Quilligan, E., Aggarwal, P.K., Bansal, K.C., Cavalieri, A.J., Chapman, S.C., Chapotin, S.M., Datta, S.K., Duveiller, E., Gill, K.S., Jagadish, K.S.V., Joshi, A.K., Koehler, A.K., Kosina, P., Krishnan, S., Lafitte, R., Mahala, R.S., Muthurajan, R., Paterson, A.H., Prasanna, B.M., Rakshit, S., Rosegrant, M.W., Sharma, I., Singh, R.P., Sivasankar, S., Vadez, V., Valluru, R., Vara Prasad, P.V., Yadav, O.P. (2016) An integrated approach to maintaining cereal productivity under climate change. *Global Food Security* 8: 9-18.
- Richards, R.A., Rebetzke, G.J., Watt, M., Condon, A.G., Spielmeyer, W., and Dolferus, R. (2010) Breeding for improved water productivity in temperate cereals: phenotyping, quantitative trait loci, markers and the selection environment. *Functional Plant Biology* 37: 85-97.
- Rieger, M., Litvin, P. (1999) Root system hydraulic conductivity in species with contrasting root anatomy. *Journal of Experimental Botany* 50: 201-209.
- Rigas, S., Debrosses, G., Haralampidis, K., Vicente-Agullo, F., Feldmann, K.A., Grabov, A., Dolan, L., Hatzopoulos, P. (2001) *TRH1* encodes a potassium transporter required for tip growth in Arabidopsis root hairs. *The Plant Cell* 13: 139-151.
- Ristic, Z., and Cass, D.D. (1992) Chloroplast structure after water and high-temperature stress in two lines of maize that differ in endogenous levels of abscisic acid. *International Journal of Plant Sciences* 153: 186-196.
- Rohila, J.S., Yang, Y. (2007) Rice mitogen-activated protein kinase gene family and its role in biotic and abiotic stress response. *Journal of Integrative Plant Biology* 49: 751-759.
- Rosegrant, M.W., Ringler, C., Sulser, T.B., Ewing, M., Palazzo, A., Zhu, T., Nelson, G.C., Koo, J., Robertson, R., Msangi, S., Batka, M. (2009) Agriculture and food security under global change: Prospects for 2025/2050. *Background note for supporting the development of CGIAR Strategy and Results Framework*. International Food Policy Research Institute: Washington, DC.
- Rosen, E., Chen, R., Masson, P.H. (1999) Root gravitropism: a complex response to a simple stimulus? *Trends in Plant Science* 4: 407-412.
- Ryser, P. (2006) The mysterious root length. *Plant Soil* 286: 1-6.
- Sadras, V.O., Reynolds, M.P., de la Vega, A.J., Petrie, P.R., and Robinson, R. (2009) Phenotypic plasticity of yield and phenology in wheat, sunflower and grapevine. *Field Crops Research* 110: 242-250.
- Saini, H.S., Lalonde, S. (1997) Injuries to reproductive development under water stress, and their consequences for crop productivity. *Journal of Crop Production* 1: 223-248.
- Saini, H.S., Westgate, M.E., Donald, L.S. (1999) Reproductive development in grain crops during drought. *Advances in Agronomy* 68: 59-96.
- Samarah, N.H. (2005) Effects of drought stress on growth and yield of barley. *Agronomy for Sustainable Development* 25: 145-149.
- Sambatti, J.B.M., Caylor, K.K. (2007) When is breeding for drought tolerance optimal if drought is random? *New Phytologist* 175: 70-80.
- Sandhu, N., Raman, K.A., Torres, R.O., Audebert A, Dardou A, Kumar A, Henry, A. (2016) Rice root architectural plasticity traits and genetic regions for adaptability to variable cultivation and stress conditions. *Plant Physiology* 171: 2562-2576.
- Sandhu, N., Singh, A., Dixit, S., Sta Cruz, M.T., Maturan, P.C., Jain, R.K., Kumar, A. (2014) Identification and mapping of stable QTL with main and epistasis effect on rice grain yield under upland drought stress. *BMC Genetics* 15: 1-15.

- Sangster, T.A., Queitsch, C. (2005) The HSP90 chaperone complex, an emerging force in plant development and phenotypic plasticity. *Current Opinion in Plant Biology* 8: 86-92.
- Santelia, D., Vincenzetti, V., Azzarello, E., Bovet, L., Fukao, Y., Düchtig, P., Mancuso, S., Martinoia, E., Geisler, M. (2005) MDR-like ABC transporter *AtPGP4* is involved in auxin-mediated lateral root and root hair development. *FEBS Letters* 579: 5399-5406.
- Sato, A., Miura, K. (2011) Root architecture remodeling induced by phosphate starvation. *Plant Signaling & Behavior* 6: 1122-1126.
- Scheet, P., Stephens, M. (2006) A fast and flexible statistical model for large-scale population genotype data: applications to inferring missing genotypes and haplotypic phase. *American Journal of Human Genetics* 78: 629-644.
- Scheible, W.R., Pauly, M. (2004) Glycosyltransferases and cell wall biosynthesis: novel players and insights. *Current Opinion in Plant Biology* 7: 285-295.
- Schneider, C.A., Rasband, W.S., Eliceiri, K.W. (2012) NIH Image to ImageJ: 25 years of image analysis. *Nature Methods* 9: 671-675.
- Schuetz, M., Smith, R., Ellis, B. (2012) Xylem tissue specification, patterning, and differentiation mechanisms. *Journal of Experimental Botany* 64: 11-31.
- Sedbrook, J.C., Chen, R., Masson, P.H. (1999) *ARG1* (Altered Response to Gravity) encodes a DnaJ-like protein that potentially interacts with the cytoskeleton. *Proceedings of the National Academy of Sciences* 96: 1140-1145.
- Segura, V., Vilhjalmsón, B.J., Platt, A., Korte, A., Seren, U., Long, Q., Nordborg, M. (2012) An efficient multi-locus mixed-model approach for genome-wide association studies in structured populations. *Nature Genetics* 44: 825-830.
- Selote, D.S., Chopra, R.K. (2004) Drought induced spikelet sterility is associated with an inefficient antioxidant defense in rice panicles. *Physiologia Plantarum* 121: 462-471.
- Sheoran, I.S., Saini, H.S. (1996) Drought-induced male sterility in rice: Changes in carbohydrate levels and enzyme activities associated with the inhibition of starch accumulation in pollen. *Sexual Plant Reproduction* 9: 161-169.
- Shi, W., Yin, X., Struik, P.C., Xie, F., Schmidt, R.C., Jagadish, K.S.V. (2016) Grain yield and quality responses of tropical hybrid rice to high night-time temperature. *Field Crops Research* 190: 18-25.
- Shomura, A., Izawa, T., Ebana, K., Ebitani, T., Kanegae, H., Konishi, S., Yano, M. (2008) Deletion in a gene associated with grain size increased yields during rice domestication. *Nature Genetics* 40: 1023-1028.
- Singh, A., Breja, P., Khurana, J.P., Khurana, P. (2016) Wheat *Brassinosteroid-Insensitive1* (*TaBRI1*) interacts with members of *TaSERK* gene family and cause early flowering and seed yield enhancement in Arabidopsis. *PLoS ONE* 11: e0153273.
- Singh, S., Mackill, D.J., and Ismail, A.M. (2009) Responses of *SUB1* rice introgression lines to submergence in the field: Yield and grain quality. *Field Crops Research* 113: 12-23.
- Singh, U., Ladha, J. K., Castillo, E. G., Punzalan, G., Tirol-Padre, A., and Duqueza, M. (1998) Genotypic variation in nitrogen use efficiency in medium and long-duration rice. *Field Crops Research* 58: 35-53.
- Slafer, G.A. (2003) Genetic basis of yield as viewed from a crop physiologist's perspective. *Annals of Applied Biology* 142: 117-128.
- Sofa, A., Dichio, B., Xiloyannis, C., Masia, A. (2004) Lipoxygenase activity and proline accumulation in leaves and roots of olive trees in response to drought stress. *Physiologia Plantarum* 121: 58-65.
- Solari, L.I., Pernice, F., DeJong, T.M. (2006) The relationship of hydraulic conductance to root system characteristics of peach (*Prunus persica*) rootstocks. *Physiologia Plantarum* 128: 324-333.

- Soltani, A., Ghassemi-Golezani, K., Khooie, F.R., and Moghaddam, M. (1999) A simple model for chickpea growth and yield. *Field Crops Research* 62: 213-224.
- Song, X.J., Huang, W., Shi, M., Zhu, M.Z., Lin, H.X. (2007) A QTL for rice grain width and weight encodes a previously unknown *RING-type E3* ubiquitin ligase. *Nature Genetics* 39: 623-630.
- Sorrells, M.E., La Rota, M., Bermudez-Kandianis, C.E., Greene, R.A., Kantety, R., Munkvold, J.D., Miftahudin Mahmoud, A., Ma, X., Gustafson, P.J., Qi, L.L., Echaliier, B., Gill, B.S., Matthews, D.E., Lazo, G.R., Chao, S., Anderson, O.D., Edwards, H., Linkiewicz, A.M., Dubcovsky, J., Akhunov, E.D., Dvorak, J., Zhang, D., Nguyen, H.T., Peng, J., Lapitan, N.L., Gonzalez-Hernandez, J.L., Anderson, J.A., Hossain, K., Kalavacharla, V., Kianian, S.F., Choi, D.W., Close, T.J., Dilbirli, M., Gill, K.S., Steber, C., Walker-Simmons, M.K., McGuire, P.E., Qualset, C.O. (2003) Comparative DNA sequence analysis of wheat and rice genomes. *Genome Research* 13: 1818-1827.
- Soundappan, I., Bennett, T., Morffy, N., Liang, Y., Stanga, J.P., Abbas, A., Leyser, O., Nelson, D.C. (2015) *SMAX1-LIKE/D53* family members enable distinct *MAX2* dependent responses to strigolactones and karrikins in Arabidopsis. *The Plant Cell* 27: 3143-3159.
- Spielmeyer, W., Ellis, M.H., Chandler, P.M. (2002) Semidwarf (*sd-1*), “green revolution” rice, contains a defective gibberellin 20-oxidase gene. *Proceedings of the National Academy of Sciences* 99: 9043-9048.
- Spindel, J., Begum, H., Akdemir, D., Virk, P., Collard, B., Redoña, E., Atlin, G., Jannink, J.L., McCouch, S.R. (2015) Genomic selection and association mapping in rice (*Oryza sativa*): Effect of trait genetic architecture, training population composition, marker number and statistical model on accuracy of rice genomic selection in elite, tropical rice breeding lines. *PLoS Genetics* 11: e1004982.
- Stahl, Y., Grabowski, S., Bleckmann, A., Kühnemuth, R., Weidtkamp-Peters, S., Pinto Karine, G., Kirschner Gwendolyn, K., Schmid Julia, B., Wink René, H., Hülsewede, A., Felekyan, S., Seidel Claus, A.M., Simon, R. (2013) Moderation of Arabidopsis root stemness by *CLAVATA1* and *ARABIDOPSIS CRINKLY4* receptor kinase complexes. *Current Biology* 23: 362-371.
- Stoop, W.A., Uphoff, N., and Kassam, A. (2002) A review of agricultural research issues raised by the system of rice intensification (SRI) from Madagascar: opportunities for improving farming systems for resource-poor farmers. *Agricultural Systems* 71: 249-274.
- Sultan, S.E. (2000) Phenotypic plasticity for plant development, function and life history. *Trends in Plant Science* 5, 537-542.
- Suralta, R.R., Inukai, Y., and Yamauchi, A. (2010) Dry matter production in relation to root plastic development, oxygen transport, and water uptake of rice under transient soil moisture stresses. *Plant and Soil* 332: 87-104.
- Suzuki, N., Rizhsky, L., Liang, H., Shuman, J., Shulaev, V., Mittler, R. (2005) Enhanced tolerance to environmental stress in transgenic plants expressing the transcriptional coactivator multiprotein bridging factor 1c. *Plant Physiology* 139: 1313-1322.
- Swamy, B.P.M., Ahmed, H.U., Henry, A., Mauleon, R., Dixit, S., Vikram, P., Tilatto, R., Verulkar, S.B., Perraju, P., Mandal, N.P., Variar, M., S.R., Chandrababu, R., Singh, O.N., Dwivedi, J.L., Das, S.P., Mishra, K.K., Yadaw, R.B., Aditya, T.L., Karmakar, B., Satoh, K., Moumeni, A., Kikuchi, S., Leung, H., Kumar, A. (2013) Genetic, physiological, and gene expression analyses reveal that multiple QTL enhance yield of rice mega-variety IR64 under drought. *PLoS ONE* 8: e62795.

- Swamy, B.P.M., Shamsudin, N.A.A., Rahman, S.N.A., Mauleon, R., Ratnam, W., Sta Cruz, M.T., Kumar, A. (2017) Association mapping of yield and yield-related traits under reproductive stage drought stress in rice (*Oryza sativa* L.). *Rice* 10: 21.
- Swamy, B.P.M., Vikram, P., Dixit, S., Ahmed, H.U., and Kumar, A. (2011) Meta-analysis of grain yield QTL identified during agricultural drought in grasses showed consensus. *BMC Genomics* 12: 319.
- Swarup, K., Benkova, E., Swarup, R., Casimiro, I., Peret, B., Yang, Y., Parry, G., Nielsen, E., De Smet, I., Vanneste, S., Levesque, M.P., Carrier, D., James, N., Calvo, V., Ljung, K., Kramer, E., Roberts, R., Graham, N., Marillonnet, S., Patel, K., Jones, J.D.G., Taylor, C.G., Schachtman, D.P., May, S., Sandberg, G., Benfey, P., Friml, J., Kerr, I., Beeckman, T., Laplaze, L., Bennett, M.J. (2008) The auxin influx carrier *LAX3* promotes lateral root emergence. *Nature Cell Biology* 10: 946-954.
- Sweeney, M., McCouch, S. (2007) The complex history of the domestication of rice. *Annals of Botany* 100: 951-957.
- Tang, L., Kim, M.D., Yang, K.S., Kwon, S.Y., Kim, S.H., Kim, J.S., Yun, D.J., Kwak, S.S., Lee, H.S. (2008) Enhanced tolerance of transgenic potato plants overexpressing nucleoside diphosphate kinase 2 against multiple environmental stresses. *Transgenic Research* 17: 705-715.
- Tang, L., Zhu, Y., Hannaway, D., Meng, Y., Liu, L., Chen, L., and Cao, W. (2009) RiceGrow: A rice growth and productivity model. *NJAS-Wageningen Journal of Life Sciences* 57: 83-92.
- Tester, M., and Langridge, P. (2010) Breeding technologies to increase crop production in a changing world. *Science* 327: 818-822.
- Thomann, A., Lechner, E., Hansen, M., Dumbliuskas, E., Parmentier, Y., Kieber, J., Scheres, B., Genschik, P. (2009) Arabidopsis *CULLIN3* genes regulate primary root growth and patterning by ethylene-dependent and-independent mechanisms. *PLoS Genetics* 5: e1000328.
- Tilman, D., Balzer, C., Hill, J., and Belfort, B.L. (2011) Global food demand and the sustainable intensification of agriculture. *Proceedings of the National Academy of Sciences* 108: 20260-20264.
- Tombesi, S., Johnson, R.S., Day, K.R., DeJong, T.M. (2010) Relationships between xylem vessel characteristics, calculated axial hydraulic conductance and size-controlling capacity of peach rootstocks. *Annals of Botany* 105: 327-331.
- Tran, T.T., Kano-Nakata, M., Suralta, R.R., Menge, D., Mitsuya, S., Inukai, Y., and Yamauchi, A. (2015) Root plasticity and its functional roles were triggered by water deficit but not by the resulting changes in the forms of soil N in rice. *Plant and Soil* 386: 65-76.
- Tuberosa, R., and Salvi, S. (2006) Genomics-based approaches to improve drought tolerance of crops. *Trends in Plant Science* 11: 405-412.
- Tyree, M.T., Ewers, F.W. (1991) The hydraulic architecture of trees and other woody plants. *New Phytologist* 119: 345-360.
- Uga, Y., Okuno, K., Yano, M. (2008) QTLs underlying natural variation in stele and xylem structures of rice root. *Breeding Science* 58: 7-14.
- Uga, Y., Sugimoto, K., Ogawa, S., Rane, J., Ishitani, M., Hara, N., Kitomi, Y., Inukai, Y., Ono, K., Kanno, N., Inoue, H., Takehisa, H., Motoyama, R., Nagamura, Y., Wu, J., Matsumoto, T., Takai, T., Okuno, K., and Yano, M. (2013) Control of root system architecture by *DEEPER ROOTING 1* increases rice yield under drought conditions. *Nature Genetics* 45: 1097-1102.
- Ullah, H., Chen, J.G., Temple, B., Boyes, D.C., Alonso, J.M., Davis, K.R., Ecker, J.R., Jones, A.M. (2003) The β -subunit of the Arabidopsis G protein negatively regulates

- auxin-induced cell division and affects multiple developmental processes. *The Plant Cell* 15: 393-409.
- Ullah, H., Chen, J.G., Young, J.C., Im, K.H., Sussman, M.R., Jones, A.M.** (2001) Modulation of cell proliferation by heterotrimeric G protein in Arabidopsis. *Science* 292: 2066-2069.
- Urano, D., Miura, K., Wu, Q., Iwasaki, Y., Jackson, D., Jones, A.M.** (2016) Plant morphology of heterotrimeric G protein mutants. *Plant and Cell Physiology* 57:437-445.
- Vatén, A., Dettmer, J., Wu, S., Stierhof, Y.D., Miyashima, S., Yadav Shri, R., Roberts Christina, J., Campilho, A., Bulone, V., Lichtenberger, R., Lehesranta, S., Mähönen Ari, P., Kim, J.Y., Jokitalo, E., Sauer, N., Scheres, B., Nakajima, K., Carlsbecker, A., Gallagher Kimberly, L., Helariutta, Y.** (2011) Callose biosynthesis regulates symplastic trafficking during root development. *Developmental Cell* 21: 1144-1155.
- Vejchasarn, P., Lynch, J.P., Brown, K.M.** (2016) Genetic variability in phosphorus responses of rice root phenotypes. *Rice* 9: 29.
- Venuprasad R, Bool ME, Quiatchon L, Cruz MS, Amante M, Atlin GN** (2012) A large-effect QTL for rice grain yield under upland drought stress on chromosome 1. *Molecular Breeding* 30: 535-547.
- Venuprasad, R., Lafitte, H.R., Atlin, G.N.** (2007) Response to direct selection for grain yield under drought stress in rice. *Crop Science* 47: 285-293.
- Venuprasad, R., Sta Cruz, M.T., Amante, M., Magbanua, R., Kumar, A., Atlin, G.N.** (2008) Response to two cycles of divergent selection for grain yield under drought stress in four rice breeding populations. *Field Crops Research* 107: 232-244.
- Venuprasad, R., Bool, M. E., Dalid, C.O., Bernier, J., Kumar, A., and Atlin, G.N.** (2009a) Genetic loci responding to two cycles of divergent selection for grain yield under drought stress in a rice breeding population. *Euphytica* 167: 261-269.
- Venuprasad, R., Dalid, C.O., Del Valle, M., Zhao, D., Espiritu, M., Sta Cruz, M.T., Amante, M., Kumar, A., and Atlin, G.N.** (2009b) Identification and characterization of large-effect quantitative trait loci for grain yield under lowland drought stress in rice using bulk-segregant analysis. *Theoretical and Applied Genetics* 120: 177-190.
- Verulkar, S.B., Mandal, N.P., Dwivedi, J.L., Singh, B.N., Sinha, P.K., Mahato, R.N., Dongre, P., Singh, O.N., Bose, L.K., Swain, P., Robin, S., Chandrababu, R., Senthil, S., Jain, A., Shashidhar, H.E., Hittalmani, S., Vera Cruz, C., Paris, T., Raman, A., Haefele, S., Serraj, R., Kumar, A.** (2010) Breeding resilient and productive genotypes adapted to drought-prone rainfed ecosystem of India. *Field Crops Research* 117: 197-208.
- Vikram, P., Swamy, B.P.M., Dixit, S., Singh, R., Singh, B.P., Miro, B., Kohli, A., Henry, A., Singh, N.K., Kumar, A.** (2015) Drought susceptibility of modern rice varieties: an effect of linkage of drought tolerance with undesirable traits. *Scientific Reports* 5: 14799.
- Vikram, P., Swamy, B.M., Dixit, S., Ahmed, H.U., Teresa Sta Cruz, M., Singh, A.K., and Kumar, A.** (2011) *qDTY1.1*, a major QTL for rice grain yield under reproductive-stage drought stress with a consistent effect in multiple elite genetic backgrounds. *BMC Genetics* 12, 89.
- Villareal, R.L., Del Toro, E., Mujeeb-Kazi, A., Rajaram, S.** (1995) The *1BL/1RS* chromosome translocation effect on yield characteristics in a *Triticum aestivum* L. cross. *Plant Breeding* 114: 497-500.
- Wan, L., Wang, X., Li, S., Hu, J., Huang, W., Zhu, Y.** (2014) Overexpression of *OsKTN80a*, a katanin P80 ortholog, caused the repressed cell elongation and stalled cell division

- mediated by microtubule apparatus defects in primary root in *Oryza sativa*. *Journal of Integrative Plant Biology* 56: 622-634.
- Wang, D., Pan, Y., Zhao, X., Zhu, L., Fu, B., Li, Z.** (2011) Genome-wide temporal-spatial gene expression profiling of drought responsiveness in rice. *BMC Genomics* 12: 1-15.
- Wang, W., Vinocur, B., Shoseyov, O., Altman, A.** (2004) Role of plant heat-shock proteins and molecular chaperones in the abiotic stress response. *Trends in Plant Science* 9: 244-252.
- Wang, X., Feng, S., Nakayama, N., Crosby, W.L., Irish, V., Deng, X.W., Wei, N.** (2003) The *COP9* signalosome interacts with *SCF(UFO)* and participates in Arabidopsis flower development. *The Plant Cell* 15: 1071-1082.
- Wassmann, R., Jagadish, S. V. K., Sumfleth, K., Pathak, H., Howell, G., Ismail, A., Serraj, R., Redoña, E., Singh, R. K., and Heuer, S.** (2009) Regional vulnerability of climate change impacts on Asian rice production and scope for adaptation. *Advances in Agronomy* 102: 91-133.
- Wasson, A.P., Richards, R.A., Chatrath, R., Misra, S.C., Prasad, S.S., Rebetzke, G.J., Kirkegaard, J.A., Christopher, J., Watt, M.** (2012) Traits and selection strategies to improve root systems and water uptake in water-limited wheat crops. *Journal of Experimental Botany* 63: 3485-3498.
- Wu, G., Lewis, D.R., Spalding, E.P.** (2007) Mutations in Arabidopsis multidrug resistance-like ABC transporters separate the roles of acropetal and basipetal auxin transport in lateral root development. *The Plant Cell* 19: 1826-1837.
- Wu, Y., Sharp, R.E., Durachko, D.M., Cosgrove, D.J.** (1996) Growth maintenance of the maize primary root at low water potentials involves increases in cell-wall extension properties, expansin activity, and wall susceptibility to expansins. *Plant Physiology* 111: 765-772.
- Wu, W., and Cheng, S.** (2014) Root genetic research, an opportunity and challenge to rice improvement. *Field Crops Research* 165: 111-124.
- Wysocka-Diller, J.W., Helariutta, Y., Fukaki, H., Malamy, J.E., Benfey, P.N.** (2000) Molecular analysis of *SCARECROW* function reveals a radial patterning mechanism common to root and shoot. *Development* 127: 595-603.
- Xiao, C., Somerville, C., Anderson, C.T.** (2014) *POLYGALACTURONASE INVOLVED IN EXPANSION1* functions in cell elongation and flower development in Arabidopsis. *The Plant Cell* 26: 1018-1035.
- Xiong, L., Wang, R.G., Mao, G., and Koczan, J.M.** (2006) Identification of drought tolerance determinants by genetic analysis of root response to drought stress and abscisic acid. *Plant Physiology* 142: 1065-1074.
- Xu, J.L., Lafitte, H.R., Gao, Y.M., Fu, B.Y., Torres, R., and Li, Z.K.** (2005) QTLs for drought escape and tolerance identified in a set of random introgression lines of rice. *Theoretical and Applied Genetics* 111: 1642-1650.
- Xu, L., and Buck-Sorlin, G.** (2016) Simulating genotype-phenotype interaction using extended functional-structural plant models: Approaches, applications and potential pitfalls. In "Crop Systems Biology: *Narrowing the gaps between crop modelling and genetics*" (X. Yin and P. C. Struik, eds.), pp. 33-53. Springer International Publishing, Cham.
- Yano, K., Yamamoto, E., Aya, K., Takeuchi, H., Lo, P.C., Hu, L., Yamasaki, M., Yoshida, S., Kitano, H., Hirano, K., Matsuoka, M.** (2016) Genome-wide association study using whole-genome sequencing rapidly identifies new genes influencing agronomic traits in rice. *Nature Genetics* 48: 927-934.

- Yao, F., Huang, J., Cui, K., Nie, L., Xiang, J., Liu, X., Wu, W., Chen, M., and Peng, S.** (2012) Agronomic performance of high-yielding rice variety grown under alternate wetting and drying irrigation. *Field Crops Research* 126: 16-22.
- Yin, X., Chasalow, S.D., Stam, P., Kropff, M.J., Dourleijn, C.J., Bos, I., Bindraban, P.S.** (2002) Use of component analysis in QTL mapping of complex crop traits: a case study on yield in barley. *Plant Breeding* 121: 314-319.
- Yin, X., Kropff, M.J., Horie, T., Nakagawa, H., Centeno, H.G.S., Zhu, D., Goudriaan, J.** (1997) A model for photothermal responses of flowering in rice I. Model description and parameterization. *Field Crops Research* 51: 189-200.
- Yin, X.** (2013) Improving ecophysiological simulation models to predict the impact of elevated atmospheric CO₂ concentration on crop productivity. *Annals of Botany* 112: 465-475.
- Yin, X., and Struik, P.C.** (2010) Modelling the crop: from system dynamics to systems biology. *Journal of Experimental Botany* 61: 2171-2183.
- Yin, X., and Struik, P.C.** (2015) Crop systems biology: Narrowing the gaps between crop modelling and genetics, Springer International Publishing, Chams.
- Yin, X., and Struik, P.C.** (2016) Crop Systems Biology: Where are we and where to go? In "Crop Systems Biology: "Narrowing the gaps between crop modelling and genetics" (X. Yin and P. C. Struik, eds.), pp. 219-227. Springer International Publishing, Cham.
- Yin, X., and Struik, P.C.** (2017) Can increased leaf photosynthesis be converted into higher crop mass production? A simulation study for rice using the crop model GECROS. *Journal of Experimental Botany* 68: 2345-2360.
- Yin, X., Chasalow, S.D., Dourleijn, C.J., Stam, P., and Kropff, M.J.** (2000) Coupling estimated effects of QTLs for physiological traits to a crop growth model: predicting yield variation among recombinant inbred lines in barley. *Heredity* 85: 539-549.
- Yin, X., Kropff, M.J., and Stam, P.** (1999) The role of ecophysiological models in QTL analysis: the example of specific leaf area in barley. *Heredity* 82: 415-421.
- Yin, X., Struik, P.C., and Kropff, M.J.** (2004) Role of crop physiology in predicting gene-to-phenotype relationships. *Trends in Plant Science* 9: 426-432.
- Yin, X., Struik, P.C., Gu, J., and Wang, H.** (2016) Modelling QTL-trait-crop relationships: Past experiences and future prospects. In "*Crop Systems Biology: Narrowing the gaps between crop modelling and genetics*" (X. Yin and P. C. Struik, eds.), pp. 193-218. Springer International Publishing, Cham.
- Yin, X., and Van Laar, H.** (2005) Crop systems dynamics: an ecophysiological simulation model for genotype-by-environment interactions, Wageningen Academic Pub.
- Yin, X., Struik, P.C., Tang, J., Qi, C., and Liu, T.** (2005) Model analysis of flowering phenology in recombinant inbred lines of barley. *Journal of Experimental Botany* 56: 959-965.
- Yin, X., Struik, P. C., van Eeuwijk, F. A., Stam, P., and Tang, J.** (2005) QTL analysis and QTL-based prediction of flowering phenology in recombinant inbred lines of barley. *Journal of Experimental Botany* 56: 967-976.
- Yoshida, S., Hasegawa, S.** (1982) The rice root system: its development and function. In: Drought resistance in crops with emphasis on rice. International Rice Research Institute, Manila, Philippines, pp 97-134.
- Yue, B., Xue, W., Xiong, L., Yu, X., Luo, L., Cui, K., Jin, D., Xing, Y., and Zhang, Q.** (2006) Genetic basis of drought resistance at reproductive stage in rice: separation of drought tolerance from drought avoidance. *Genetics* 172: 1213-1228.
- Zhang, H., Forde, B.G.** (1998) An Arabidopsis MADS box gene that controls nutrient-induced changes in root architecture. *Science* 279: 407-409.

- Zhang, Y., Xiao, Y., Du, F., Cao, L., Dong, H., Ren, H. (2011) Arabidopsis *VILLIN4* is involved in root hair growth through regulating actin organization in a Ca²⁺-dependent manner. *New Phytologist* 190: 667-682.
- Zhang, Z., Ersoz, E., Lai, C.Q., Todhunter, R.J., Tiwari, H.K., Gore, M.A., Bradbury, P.J., Yu, J., Arnett, D.K., Ordovas, J.M., Buckler, E.S. (2010) Mixed linear model approach adapted for genome-wide association studies. *Nature Genetics* 42: 355-360.
- Zhang, G.L., Chen, L.Y., Xiao, G.Y., Xiao, Y.H., Chen, X.B., and Zhang, S.T. (2009) Bulk segregant analysis to detect QTL related to heat tolerance in rice (*Oryza sativa* L.) using SSR markers. *Agricultural Sciences in China* 8: 482-487.
- Zhang, T., and Huang, Y. (2012) Impacts of climate change and inter-annual variability on cereal crops in China from 1980 to 2008. *Journal of the Science of Food and Agriculture* 92: 1643-1652.
- Zhao, C., Craig, J.C., Petzold, H.E., Dickerman, A.W., Beers, E.P. (2005) The xylem and phloem transcriptomes from secondary tissues of the Arabidopsis root-hypocotyl. *Plant Physiology* 138: 803-818.
- Zhao, Y., Xing, L., Wang, X., Hou, Y.J., Gao, J., Wang, P., Duan, C.G., Zhu, X., Zhu, J.K. (2014) The ABA receptor *PYL8* promotes lateral root growth by enhancing *MYB77*-dependent transcription of auxin-responsive genes. *Science signaling* 7: ra53-ra53.
- Zhao, K., Tung, C.W., Eizenga, G.C., Wright, M.H., Ali, M.L., Price, A.H., Norton, G.J., Islam, M.R., Reynolds, A., Mezey, J., McClung, A.M., Bustamante, C.D., and McCouch, S.R. (2011) Genome-wide association mapping reveals a rich genetic architecture of complex traits in *Oryza sativa*. *Nature Communications* 2: 467.
- Zhu, J., Kaeppeler, S.M., and Lynch, J.P. (2005a) Mapping of QTL controlling root hair length in maize (*Zea mays* L.) under phosphorus deficiency. *Plant and Soil* 270: 299-310.
- Zhu, J., Kaeppeler, S.M., and Lynch, J.P. (2005b) Mapping of QTLs for lateral root branching and length in maize (*Zea mays* L.) under differential phosphorus supply. *Theoretical and Applied Genetics* 111: 688-695.
- Zorrilla, G., Martínez, C., Berrío, L., Corredor, E., Carmona, L., Pulver, E. (2012) Improving rice production systems in Latin America and the Caribbean. In: *Eco-Efficiency: From Vision to Reality*. CIAT, Cali, Colombia, pp. 161–170.

Summary

Rice (*Oryza sativa* L.) is an important component of food security; it provides food for more than half of the world population. However, a rapidly changing climate with more frequent occurrence of water-deficit and high-temperature stress severely reduces the productivity of rice and other cereals. Among the cereals, rice is most sensitive to water-deficit stress due to its semi-aquatic adaptation: it requires 2 to 3 times more water for cultivation than other cereals. Especially, water-deficit stress occurring during the sensitive reproductive stage seriously impedes the productivity of rice. Nevertheless, stress occurring during the vegetative stage is also observed in Asia, and can also have significantly reduce final grain yield. Therefore, one of the major challenges is to improve the tolerance of rice to stress at any time during the growing period to ensure food security.

Plants have evolved specific abilities to adjust their morphology, physiology and biochemistry in response to stress a phenomenon commonly known as a phenotypic plasticity. Phenotypic plasticity is the ability of a given genotype to produce an adapted phenotype in response to changing environments. Plasticity in root morphology and anatomy is of great importance to improve the adaptation of rice to stress due to the primary role of roots in the uptake of water and nutrients. During domestication, rice has evolved a phenotypic plasticity to adapt to a wide range of moisture regimes: from traditional lowland (paddy rice) to upland/aerobic (moderately stress conditions) or even severe water-deficit stress. Nevertheless, rice is still considered to be relatively poorly adapted to water-deficit, in comparison to other dryland cereal crops, such as wheat, maize and sorghum. In addition, there is no adequate knowledge on how rice differs from dryland cereals in water-deficit stress adaptation. Therefore, in this thesis, I have studied the physiological, morphological and anatomical response or plasticity of rice genotypes well adapted to different moisture regimes (lowland, aerobic and water-deficit conditions), in comparison with that of wheat genotypes that are drought tolerant, under water-deficit stress during the vegetative stage (Chapter 2). This study allowed to demonstrate that compared with wheat, rice genotypes have a weaker morphological and anatomical plasticity in the shoot and in the root traits in response to water-deficit stress. Specifically, rice cultivars adopted a rapid water acquisition strategy through developing thinner roots under water deficit stress, whereas wheat cultivars followed a water-conserving strategy by developing thicker roots and moderate tillering. Further, a comprehensive analysis between these two divergent species made it possible to identify the functional relevance of root morphological and anatomical plasticity in water-deficit tolerance (Chapter 2). In addition,

previous studies have proven that phenotypic plasticity is under genetic control and is regulated by key environmental sensing genes. To date, very few quantitative trait loci (QTLs) regulating the phenotypic plasticity in response to water-deficit were identified in rice. Diverse rice genotypes are a pool of naturally occurring mutations, which can give fundamental insights into plant function. They are also a vital resource of novel beneficial alleles for crop plant improvement. Therefore, I have scaled the key findings from Chapter 2 up to an *indica* rice diversity panel and quantified the genotypic variation of phenotypic plasticity for physiological, morphological and root anatomical responses under water-deficit stress during the vegetative stage (Chapter 3). We then carried out a genome-wide association study (GWAS) on these traits and their plasticity, using 45,608 high-quality single nucleotide polymorphisms (SNPs). One hundred four significant loci were detected for these traits under control condition, 106 were detected under water-deficit stress, and 76 were detected for trait plasticity. The genetic basis of root morphology and anatomy was different across both water-regimes (strong QTL× Environment interactions), in line with that so many loci were detected for the plasticity of these traits. In addition, these genetic loci associated with root traits and their plasticity was associated with genes regulating biosynthesis, transport or signalling of phytohormones. Hence, genetic loci identified in Chapter 3 provide an important basis for understanding the molecular mechanism of plastic root development in response to water-deficit stress.

Rice grain yield is strongly affected by water-deficit stress occurring during the sensitive reproductive stage. So far, breeders have improved the tolerance to water-deficit stress during the reproductive stage by introgression of QTLs identified in traditional bi-parental mapping populations of rice. Although this approach has resulted in significant progress, yet many of the QTLs/genes/alleles remain hidden in the rice genetic diversity, which cannot be explored through traditional linkage analysis. Therefore, in Chapter 4, I have explored the same *indica* rice diversity panel that was used in Chapter 3, to identify those hidden QTLs/genes for grain yield and its components through a GWAS under well-watered conditions and under water-deficit stress during the reproductive stage in field experiments for two years. I have followed staggered sowing of rice genotypes to maximally synchronize their flowering and thus the phenological timing of the exposure to the water-deficit stress. One hundred two loci were detected in non-stress conditions (38 loci in 2013 and 64 loci in 2014) and 124 loci (69 loci in 2013 and 55 in 2014) in water-deficit stress. Some desynchronised flowering time strongly confounded the grain yield and its components in the data set for water-deficit stress in 2013. To minimise the confounding effect, I have carried out a statistical correction of grain yield and

yield components using days to flowering, which helped to detect 31 additional genetic loci for grain yield, its components and harvest index in 2013. In addition, most of these QTLs were specific to treatment and year, which means that there was a high QTL \times environment interaction (QEI). The QEI plays an important role in adaptation to changing environments, and is regulated by key environmental sensing genes. We identified key *a priori* candidate genes within the linkage disequilibrium block of grain yield loci regulating abiotic stress tolerant biological processes.

Grain yield is a complex trait determined by action and interaction of different component traits. A deeper understanding of how these component traits contribute to grain yield is a prerequisite for designing the future new plant type for improved grain yield under changing climatic conditions. Crop growth models are widely used to understand the complex grain yield under water-deficit stress. In Chapter 5, I have used the generic crop model, GECROS (Genotype-by-Environment interaction on CROp growth Simulator), to quantify grain yield in the *indica* rice diversity panel. The physiological component traits as model inputs included pre-flowering period (m_V), post-flowering period (m_R), photoperiod sensitivity (δ), maximum plant height (H_{\max}), single-grain weight (Sw), grain set (g_{set}), grain nitrogen concentration (n_{so}), and total crop nitrogen uptake (N_{\max}). These component traits were estimated from the control treatment in one season (2013) for an *indica* rice diversity panel consisting of 267 genotypes in Chapter 4. With these component traits, the model could account for 58% of the variation in grain yield among 267 rice genotypes under control conditions and 40% under water-deficit conditions. In addition, I have identified SNP loci associated with component traits through a GWAS in randomly selected 213 genotypes as the training datasets and the remaining 54 genotypes were used as the testing datasets. SNP-based component trait values were calculated from estimated effects of the loci, and were fed into the model. The SNP-based model could account for 37% and 29% of the yield variation under control and water-deficit conditions, respectively, in the training datasets. However, the SNP-based model could account for only 10% of the yield variation in control conditions and 15% of the yield variation under water-deficit stress in the testing datasets. The performance of the model was lower, using either original or SNP-based parameter values, when the model was used to simulate yields in an independent season (2014). Model-based sensitivity analysis ranked the relative importance of the individual SNP loci identified for component traits in determining the grain yield variation. The ranking differed greatly between control and water-deficit environments. The grain yield variation in the well-watered treatment was mainly explained by

SNP loci associated with the total crop nitrogen uptake (N_{\max}), whereas the yield variation under the water-deficit stress during the reproductive stage was explained mainly by loci associated with pre-flowering time (m_V). Further, the GECROS-based dissection approach detected more SNP loci than the analysis using yield *per se*. Virtual ideotypes based on SNPs identified by modelling had higher yield than those based on SNPs for grain yield *per se* (Chapter 5), illustrating potential values of the model-based approach in supporting marker-assisted selection.

In the general discussion (Chapter 6), I have discussed the results obtained in Chapters 2-5 based on the specific objectives designed for this thesis (Chapter 1). I have also discussed the future prospects on how to improve the integration of crop growth modelling with quantitative genetics to narrow down the genotype-by-phenotype gap. The generic GECROS model needs to be tailored to include those important morphological and physiological traits identified in Chapters 3 and 4 to more effectively explain genotype-by-environment interactions exhibited in a diversity panel of rice.

Acknowledgements

First and foremost, I should express my deepest gratitude to an anonymous private donor who provided financial support towards my PhD fellowship, and for most of the research work reported in this study. I am also indebted to the Federal Ministry for Economic Cooperation and Development, Germany, and the USAID and Bill and Melinda Gates Foundation for their partial financial support.

This thesis would not have been possible without my excellent multidisciplinary supervision team: **Dr. Krishna Jagadish, Prof. Paul C Struik, and Dr. Xinyou Yin**. I want to express my deepest gratitude to Dr. Krishna Jagadish, for selecting me as PhD candidate in “Growing Rice Like Wheat” project. Krishna, it has been honored to work with your heat stress group at IRRI. During my initial journey, I have always received very useful personal and professional guidance, constant encouragement, and unconditional support from you to finish my challenging experiments. I also really appreciate your habit to encourage students for writing scientific publications, which have not only improved my writing skills but also improved my communications skills. Paul, I have been so fortunate to have you as a promotor and thank you very much for giving me as an opportunity to pursue the doctoral degree in the Centre for Crop Systems analysis. As a promoter, your kindness always helped to lift my self-confidence, whenever I was nervous and frustrated. Xinyou, being a thesis co-promotor and daily supervisors your office was always open to discuss the ideas and organize the work. I also would also like to thank you for introducing me to the QTL-based ecophysiological modeling, which is very interesting but quite new to me.

Members from the heat stress group at IRRI also immensely contributed to smoothly finish my PhD, and without their constant support, I would not have reached this stage. So, I am grateful to all of them namely **Ancio Macahia** (we like to call him Alex), **Joel Evangelista, Allan Malabanan, Alexander Aringo, Pablo Gupit, Siena Calibo, Reneeliza Jean, Lovely lawas, Cheryl Quinones and Jacinta Evangelista**. Members of the group have been the source of friendships, and are actively collaborating and helping each other. I am especially grateful to the researcher Lovely and Cheryl, for their unconditional assistance to organize the pot weighing, and root harvesting of the greenhouse experiment. I also would like to thanks technicians team (Alex, Joel, Allan, and Siena), who constantly helped in conducting the greenhouse and field experiments. Alex, your years of experience in organizing and conducting the experiments greatly helped during my large-scale field experiments. Allan, your abilities to meticulously organize the greenhouse experiments, helped a lot to successfully finish the

challenging greenhouse experiments. Siena, I would like to thank you for constantly supervising the most difficult task of root scanning, and processing bulk of the yield and yield component samples from the field experiments. I am also thankful to **Dr. Rajeev N Bahuguna, Dr. Nicolas Mattes, Dr. David Sabella, Dr. Raju Bheemanhali, Dr. Jiang and Dr. Wanju Shi**, from whom I learnt many things and very much enjoyed scientific debate during meetings. A very special thanks to Jacinta Evangelista for managing the administrative and financial matters that have made my life so easy.

My special thanks to **Uttam Kumar** and **Umair Aslam** with whom I have shared the house at IRRI for more than two years. I am very much enjoyed preparing the food and listening bollywood songs during dinner time with lots of fun.

I am grateful to all the group members of Centre for Crop Systems Analysis for their direct or indirect support. I also would also like to thanks my Ph.D. colleagues at the Centre for Crop Systems, for their love and care during my difficult times despite my shy nature: **Gunfei Wenjing, Alejandro, Herman, Utah, Ioannis, Marcelo, Kailei, Dennis, Luuk, Martin, Ali, Shenghao, Ambra, Wanju, Cesar, Engida, Naznin, Preethi** and many more.... I wish and pray for your PhD success and future endeavors, and good luck be with you always. I also would like to express my deepest gratitude to **Sjanie, Nicole and Alex Leeuw** for handling most of the administrative issues that made my life so easy in the Netherlands. Sjanie, you are very kind and always likes to know about the different cultures. Nicole, thank you very much for your support during setting up the final layout of thesis.

I am also grateful to the other members of “Growing Rice Like Wheat” (GRLW) team for their constant support and encouragement: **Dr. Prem Bindraban, Prof. Harro Bouwmeester, Dr. Carolien Ruyter-Spira, Dr. M.S. Sheshashayee, Dr. Nataraja Karba and Dr. CG van der Linden Gerard**. My special thanks to all the PhD students of GRWL (**Wenjing, Beatriz, Giovanni, and Preethi**), with whom I have actively collaborated and shared the experiments, materials and results. One of the unique features of GRLW project was a higher level of interaction between research topics of all the PhD students, which is not often the case in academic research. I strongly believe that we will continue our teamwork in the future to “Grow Rice Like Wheat”.

I also would like to express my deepest gratitude to **Jaap, Marita, Vincent and other family members** for their hospitality, care and love. Jaap and Marita I had always enjoyed our Tuesday dinner together with playing the games.

My special thanks to my two paranympths, **Alejandro M. Sierra** and **Manjunath Prasad** for helping me to organise the defence. I am looking forward my one of the special day with you. I am also indebted to Manjunath and his family for offering me the house, and delicious homemade food during last phase of my PhD.

Finally, I would like to thank all my family members, especially my mother (**Ratnamala**) and father (**Narharirao**), and wife (**Sandhya**) for their love, care and support to move forward with my PhD. I also would like to express special thanks to my wife Sandhya for giving me the world's best gift -a baby boy! and making me as a father. I welcome my little champ (**Arjun Pandit**) to the most beautiful world with lots of love and happiness.

Niteen N. Kadam

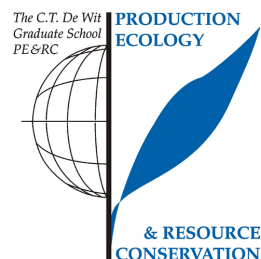
Wageningen 2018, The Netherlands

List of Publications

- Mathithumilan, Balachandran^Ψ, **Niteen N. Kadam**^Ψ, Jyoti Biradar, Sowmya H. Reddy, Mahadeva Ankaiah, Madhura J. Narayanan, Udayakumar Makarla, Paramjit Khurana, and Sheshshayee M. Sreeman. **Development and characterization of microsatellite markers for *Morus* spp. and assessment of their transferability to other closely related species.** *BMC Plant Biology* (2013): 194. DOI:10.1186/1471-2229-13-194. Ψ=First two author equal contribution.
- Niteen N. Kadam**, Gui Xiao, Reneeliza Jean Melgar, Rajeev N. Bahuguna, Cherryl Quinones, Anandhan Tamilselvan, and Pagadala Vara V. Prasad, Jagadish, Krishna S.V. **Agronomic and Physiological Responses to high temperature, drought, and elevated CO² interactions in cereals.** *Advances in Agronomy* (2014): 111-156. DOI:10.1016/B978-0-12-800131-8.00003-0.
- Niteen N. Kadam**, Xinyou Yin, Prem S. Bindraban, Paul C. Struik, and Krishna S.V. Jagadish. **Does morphological and anatomical plasticity during the vegetative stage make wheat more tolerant of water-deficit stress than rice?** *Plant Physiology* (2015): 1389-1401. DOI:10.1104/pp.114.253328.
- Niteen N. Kadam**, Anandan Tamilselven, Lovely MF Lawas, Cherryl Quinones, Rajeev N Bahuguna, Michael J Thomson, Michael Dingkhun, Raveendran Muthurajan, Paul C Struik, Xinyou Yin, and Krishna SV Jagadish **Genetic control of plasticity in root morphology and anatomy of rice in response to water-deficit.** *Plant Physiology* (2017): 2302-2315. DOI: 10.1104/pp.17.00500.

PE&RC Training and Education Statement

With the training and education activities listed below the PhD candidate has complied with the requirements set by the C.T. de Wit Graduate School for Production Ecology and Resource Conservation (PE&RC) which comprises of a minimum total of 32 ECTS (= 22 weeks of activities)



Review of literature (6 ECTS)

- Role of genomics in improvement of rice adaptation to water limited conditions

Writing of project proposal (4.5 ECTS)

- Physiological and genetic dissection of rice tolerance to water-deficit stress

Post-graduate courses (6 ECTS)

- Mixed model based QTL mapping; PE & RC (2012)
- SNP data analysis; International Rice Research Institute (IRRI), Philippines (2014)
- Rice breeding; IRRI, Philippines (2015)

Laboratory training and working visits (3 ECTS)

- Stable ¹³C isotope studies for water use efficiency in crop plants; Department of Crop Physiology, University of Agricultural Sciences, GKVK, Bangalore, India (2014)

Deficiency, refresh, brush-up courses (3.7 ECTS)

- Basic statistics; PE&RC (2015)
- Introduction to R for statistical analysis; PE&RC (2016)
- Multivariate analysis; PE&RC (2016)

Competence strengthening / skills courses (1.6 ECTS)

- Basic presentation skills; IRRI, Philippines (2014)
- Basic leadership skills; IRRI, Philippines (2014)
- Research data management; IRRI, Philippines (2014)
- Reviewing a scientific paper; PE&RC (2016)

PE&RC Annual meetings, seminars and the PE&RC weekend (0.6 ECTS)

- PE&RC Last year weekend (2016)

Discussion groups / local seminars / other scientific meetings (6 ECTS)

- CESD Division seminar; IRRI, Philippines (2013-2015)
- Thursday seminar series; IRRI, Philippines (2013-2015)

International symposia, workshops and conferences (7.1 ECTS)

- 4th International rice congress, Bangkok, Thailand (2014)
- The "Growing rice like wheat" workshop at IRRI (2015)
- Merging crop modelling and genetics; University of Florida, USA (2015)

Curriculum vitae

Niteen N. Kadam was born on 11th April 1985 in Dharasaur, a village in Maharashtra province, India. He received his primary and secondary education in India. In 2008, he obtained his Bachelor of Science (BSc) in Agriculture from Marathwada Agriculture University, Parbhani, India. In 2009, he obtained Junior Research Fellowships from the Indian Council of Agriculture Research, to pursue Master of Science (MSc) in Agriculture with specialisation in Crop Physiology at the University of Agriculture Sciences, Bangalore, India. Immediately after completion of MSc (in August 2011), he joined as a Senior Research Fellow in Crop Physiology department. In May 2012, he joined as a sandwich PhD student at the Centre for Crop Systems Analysis (CSA) at the Wageningen University & Research the Netherlands, in collaboration with International Rice Research Institute (IRRI), Philippines. This study represents his five-year of research work on physiological and genetic dissection of rice tolerance to water-deficit stress.

Funding

This work was supported by an anonymous private donor who provided the financial support, via the Wageningen University Fund. I also thank the Federal Ministry for Economic Cooperation and Development, Germany, and the USAID and Bill and Melinda Gates Foundation for their financial support towards field work at the International Rice Research Institute (IRRI) in the Philippines.

